CHEM—NUCLEAR SYSTEMS INC.

P.O. Box 1866 • Bellevue, Washington 98009 • (206) 827-0711

September 30, 1982

Mr. Charles E. MacDonald, Chief
Transportation Certification Branch
Fuel Cycle & Material Safety Division
U. S. Nuclear Regulatory Commission
Washington, D. C. 20555

Reference: Docket No. 71-6601
NRC Letter to CNSI dated 10/14/81
CNSI Letter to NRC dated 2/8/82

Dear Mr. MacDonald:

Our letter dated February 8, 1982 indicated that we would respond to your questions regarding the CNS 8-120 radioactive waste shipping cask (see NRC letter to CNSI dated 10/14/81) in the form of a completely revised Safety Analysis Report (SAR). Attached to this letter we have included:

(1) Attachment - Responses to 8-120 NRC Questions; and,

(2) A completely revised Safety Analysis Report.

In performing the extensive, in-depth analyses for the SAR, several improvements were incorporated into the design of the cask.

We have included a check in the amount of $3,500 as per 10 CFR 170.31 (11)(c) for a major amendment.

Please contact this office if you have any questions on this application.

Sincerely,

CHEM-NUCLEAR SYSTEMS, INC.

Leslie K. Poppe
Corporate Health Physicist

LKP:slj

Enclosures: 10 copies Safety Analysis Report
10 copies Drwaing C-110-E-0007, Sheets 1 & 2

RESPONSES TO 8-120 QUESTIONS

Question No. 1

The evaluation of the 30-foot drop test (Sect. 2.7.1) does not adequately demonstrate the integrity of the containment vessel. The analysis should be revised to indicate the stresses that would be present in the containment vessel and to show that these stresses are within acceptable limits to assure the integrity of the vessel. The analysis of impact effects should consider the lateral pressure of the lead against the steel shells as well as the axial stresses that would result from the steel supporting the lead. The analysis should also evaluate the effects of differential thermal expansion (axial and radial) between the lead and the steel shells. Note the statement on page 2-14 that the lead and steel are bonded together and that the steel would support the lead during impact.

Answer No. 1

The new analysis specifically addresses the concerns of this question. Full details are provided in Section 2.7.1 of the revised SAR. Maximum stress intensities throughout the cask, including the containment vessel, are shown in Tables 2.7.1-2, 2.7.1-4 and 2.7.1-6, and are shown to be below allowables, with a minimum safety factor of 1.40. In modeling the lead/steel interface, lead-to-steel bonding was not assumed to take place and, consequently, the steel does not support the lead in the axial direction. This interface was modeled by decoupling the nodes of the lead elements from the nodes of the steel elements of the axial direction, so that the lead was free to move axially with respect to the steel. However, in order to model the radial pressures exerted by the lead on the steel shells, the lead nodes were coupled radially to the steel nodes, thus transferring radial forces between the lead and the steel shells.

Because part of the loading conditions used in determining the stresses in the cask included the temperatures from the thermal analysis (Section 3.0), and the concomitant internal pressures, the stress intensities reported in the revised SAR include the effects of differential thermal expansion (both radial and axial) as well as stresses induced by thermal gradients and internal pressure.

Question No. 2

The evaluation of 30-foot end drop (Sect. 2.7.1.1) only considers slumping of the lead. The analysis should be revised to demonstrate the integrity of the containment vessel and closure under top and bottom end drop conditions.

Answer No. 2

Section 2.2.7.1.1 of the revised SAR discusses results of the 30-foot end drop. Maximum stress intensities throughout the cask, including the containment vessel and closure, are reported in Table 2.7.1-2. The stress intensities are shown to be below allowables, with a minimum factor of safety of 2.81.

Question No. 3

The analysis of the 30-foot top corner drop (Sect. 2.7.1.3) should be revised to provide the following information in connection with demonstrating that an adequate seal will be maintained under accident conditions:

a. Show that the rim which projects above the cover would deform by crushing, as was assumed in the analysis, rather than by local bending, shearing, buckling or some other mechanism which would dissipate less energy. Provide a sketch showing exactly which area of the rim is considered to be the deformed volume. Note that the shape of the deformed volume which was assumed in the analysis (i.e., solid cylindrical wedge, see sketch pg. 2-17) is not consistent with the actual geometry of the package (see Detail C, DRWG. 119-0500-E01). Therefore, it appears that the equations used to evaluate top corner impact (pgs. 2-16 and 2-17) are not valid for this purpose.

Answer No. 3-a

The overpacks in the new design prevent any contact of the cask with the impact surface. Thus no permanent deformation of the corner of the cask occurs. As a consequence of the protection afforded by the overpacks, the protruding rim which projected above the cover has been eliminated in the new design.

Question No. 3-b

b. Show that the closure design is adequate to resist the shear forces that act in the plane of the cover. The analysis (pg. A-9) apparently assumes that a portion of shear force would be reacted solely by the rim that extends above the cover. However, this does not consider that the rim, under impact forces, would deform inward and bear against the cover. Also, the cover is made of laminated plates. The revised analysis should show that the connections between the plates are adequate to transfer shear forces from one plate to another.

Answer No. 3-b

In the new design radial shear forces are reacted by a combination of bearing between the cover and the inner cask wall and by the cover bolts. The clearances around the bolts and between the cover and the inner cask wall have been designed such that radial forces which tend to drive the cask wall and the cover together are reacted by bearing between the two parts and radial forces which tend to radially separate the cask wall from the cover are borne by the cover bolts. While the cask has been designed to perform in this manner, in the actual analysis, shear forces were transmitted by coupling of the cover node to the cask body node at the bolt circle. This allowed bolt stresses to be computed based on the forces at these nodes and the bolt stress area. These analyses are discussed in Section 2.7.1.3 of the revised SAR. The new cask cover design uses two 3½-inch thick plates. The analysis treats these as two separate plates, with shear forces being transmitted only at the welds at the peripheries of the primary and secondary lids. At other locations, only forces normal to the plates are transmitted between the plates. This was accomplished by coupling nodes between the plates in the normal direction only.

Question No. 3-c

c. The revised analysis should show that an adequate seal would be maintained following the test, considering the deformation and distortion that would occur in the area of the cover and the flange.

Answer No. 3-c

The overpacks in the new design protect the cask and prevent permanent deformation in the areas of the seals. Thus, sealing capability after the drop is not altered from pre-drop conditions. Section 2.7.1.3 of the revised SAR discusses pertinent results of the stress analysis.

Question No. 3-d

d. Show that the cylindrical cask walls, and the connection between the walls and the flange, are adequate to resist the load imposed by top corner impact. This should include the lateral pressure (if any) from the lead.

Answer No. 3-d

The overpacks used in the new design reduce the loads imposed by the top corner impact. The stress analysis for this condition, discussed in Section 2.7.1.3 of the revised SAR, shows that stress intensities remain below allowables throughout the cask, with a minimum safety factor of 1.44. This stress analysis included the effects of the lateral pressure of the lead, as discussed in the response to Question No. 1, above.

Question No. 3-e

e. Revise the calculated closure bolt stress (pg. A-8) to consider the additional stresses due to pre-load and horizontal shear (if any). Note that the content weight considered in the analysis (pg. 2-25) should apparently be greater than 10,000 pounds to be consistent with the weights specified on page 2-2.

Answer No. 3-e

The results of the new bolt stress analysis are shown in Section 2.7.1.3 of the revised SAR. The maximum payload weight of 14050 pounds was used in this analysis. Because the applied load greatly exceeds the bolt preload, the preload has negligible effect on maximum bolt stresses. (Refer to Bickford, John H., An Introduction to the Design and Behavior of Bolted Joints, Marcel Dekker, Inc., 1981. See, especially, Chapter 11, Section I. A less comprehensive description of bolted joint behavior is given by Shigley, Joseph E., Mechanical Engineering Design, Third Edition, McGraw-Hill, 1977, Section 6.5, pp 240-244).

Question No. 3-f

f. Justify that it is appropriate to consider the outer edge of the cover plate to be fixed, as was done in the analysis on page A-13. Provide a free-body sketch of the cover and flange which explicitly shows how the necessary moment reaction is developed to provide fixity. Also, the analysis should be revised to consider that the cover is made of laminated plates rather than being a solid 4-inch thick plate (pg. A-14).

Answer No. 3-f

Analysis of the cover is included in the drop stress analysis discussed in Section 2.7.1.3 of the revised SAR. Edge fixity is not assumed in the new analysis. Rather, rotation of the edge is governed by the stiffness of the cask wall, to which the lid is bolted. The analysis considers the cover as laminated plates, allowing only the transmittal of normal forces between laminations, except at the peripheral welds joining the laminated plates, where shear forces, also, are transmitted.

Question No. 4

The analysis of the 30-foot bottom corner drop (Section 2.7.1.3) should be revised to provide the following information:

a. Show that the drain line (see Detail D, DRWG. 119-0500-E01) would remain sealed following a 30-foot bottom corner drop test. Note that this line is located in the region that would apparently be crushed according to the analysis on pg. 2-18.

Answer No. 4-a

The overpacks in the new design cover the drain line and prevent crushing impact, or indeed, any permanent deformation whatsoever in the area of the drain line. Thus, the sealing capability of the drain plug will remain unchanged following the drop.

Question No. 4-b

b. Provide additional narrative and sketches which clearly show the derivation of equations (10) and (11) on pg. 2-17. Also, show the equation used on that page to tabulate the values of coefficient "C".

Answer No. 4-b

Because crushing of the corner of the cask is prevented by the overpacks used in the new design, these equations are not used in the new analysis. A discussion of the corner drop analysis can be found in Section 2.7.1.3 of the revised SAR.

Question No. 4-c

c. Justify that a value of 60,000 in -lb/in^3 is appropriate for the energy absorbing constant used on pg. 2-18. This should consider the specific types of steel used to construct the cask.

Answer No. 4-c

Dynamic flow pressure is not used in the new corner drop analysis in the revised SAR. See Section 2.7.1.3.

Question No. 4-d

d. Clarify the value of kinetic energy that the cask is considered to have under 30-foot drop conditions. Note that the 60,000 pound values used on pgs. 2-18 and 2-19 do not agree with 74,000 pound weight listed on pg. 2-2.

Answer No. 4-d

The corner drop analysis in the revised SAR uses a value of kinetic energy based on the full 74,000 pound cask weight. See Section 2.7.1.3.

Question No. 4-e

e. The analysis of stresses in the plates and welds at the bottom end of the cask (pg. A-17) should be revised to include the additional stresses that would result from the axial component of the inertial force of the contents and bottom closure.

Answer No. 4-e

The inertial force at the contents and bottom closure are included in the new corner drop analysis discussed in Section 2.7.1.3 of the revised SAR.

Question No. 5

Show that the cask closure and bottom end plates are adequately designed to resist the shear forces that would act in the plane of cover under 30-foot side drop conditions. Also, show that the drain line would remain sealed following a 30-foot side drop test.

Answer No. 5

Stresses in the top and bottom closures are included in the results of the side drop analysis in the revised SAR; see Section 2.7.1.2. The overpacks in the new design serve to protect the drain line from suffering any permanent deformation from the side drop impact. Thus, sealing capacity of the drain seal is unchanged following the side drop.

Question No. 6

The revised analysis should evaluate the effects of the 40-inch puncture test considering the cask to be oriented so that the pin would impinge upon the end of the cask. The analysis should consider both the top and bottom ends. The analysis should include the effects in the local vicinity of the pin and the overall effect upon the end plates. The analysis of top end impact should include an evaluation of the pin striking the plugs located in the lid. Note that the puncture analysis (pg. 2-21) should apparently be revised to consider a weight of 74,000 pounds rather than 60,000 pounds.

Answer No. 6

A puncture analysis for end impact is included in the revised SAR in Section 2.7.2. The plugs in the lid have been eliminated from the new design. The new analysis uses the full 74,000 pound cask weight.

Question No. 7

Section 2.6.6 should be revised to explicitly demonstrate that the package meets the requirements of 10 CFR Part 71 under 1-foot drop test conditions.

Answer No. 7

Stresses for the 1-foot drop conditions have been included in Section 2.6.6 of the revised SAR.

Question No. 8

The package drawings should be revised to provide the following information:

a. The torque to which the cover bolts are tightened.

Answer No. 8-a

Cover bolt torque is now included in the package drawings, Appendix 1.3, and in Section 4.0 of the revised SAR.

Question No. 8-b

b. The method or devices used to close and seal the drain plug.

Answer No. 8-b

Drain plug sealing devices and seals are shown on the package drawings of the revised SAR, Appendix 1.3. These devices are discussed in Section 4.0 of the revised SAR.

Question No. 8-c

c. The torque to which the cover plugs are tightened and the method or devices which provide a seal at these plugs.

Answer No. 8-c

The cover plugs have been eliminated from the new design.

Question No. 8-d

d. The clearance of the closure bolts and cover which are discussed on page 2-28.

Answer No. 8-d

Dimensions for the clearances around the cover bolts and for the lid-to-cask body radial clearance are now included in the package drawings, Appendix 1.3 of the revised SAR. The impact of these clearances on bolt loads is discussed in response to question 3-b, above.

SAFETY ANALYSIS REPORT

FOR THE

CNS 8-120B SHIPPING CASK

Submitted By:

September 30, 1982

CHEM-NUCLEAR SYSTEMS, INC.
P.O. BOX 1366
BELLEVUE, WASHINGTON 98009

TABLE OF CONTENTS

TABLE OF CONTENTS

TABLE OF CONTENTS

TABLE OF CONTENTS (continued)

TABLE OF CONTENTS (continued)

LIST OF FIGURES

LIST OF TABLES

1.0 GENERAL INFORMATION

1.1 Introduction

This Safety Analysis Report describes a reusable shipping package designed to protect radioactive material from both normal conditions of transport and hypothetical accident conditions. The package is designated as the Model CNS 8-120B package.

1.2 Package Description

1.2.1 Packaging

The package consists of a steel and lead cylindrical shipping cask with a pair of circular foam-filled overpacks placed peripherally around each end. Each overpack has an external shell, fabricated from ductile low carbon steel, which allows it to undergo large deformations without fracturing. Top and bottom overpacks are connected by eight (8) one-inch ratchet binders. The volume between the inner and outer shell of the overpack is filled with a shock and thermal insulating material consisting of rigid polyurethane foam. The insulating material is poured into the cavity between the two shells and allowed to expand until the void is completely filled. It bonds to the shells which creates a unitized construction of the packaging. Properties of these materials are further described in Section 2.3

The internal cask cavity dimensions are 62 inches in diameter and 75 inches high. The cylindrical cask body is comprised of a 1-1/2 inch thick external steel shell and a 3/4 inch internal steel shell. The annular space between shells is filled with approximately 3-1/2 inch thick lead.

The base of the cask consists of two (2) 3-1/2 inch thick, flat circular steel plates.

The package Configuration is shown in Figure 1.2-1.

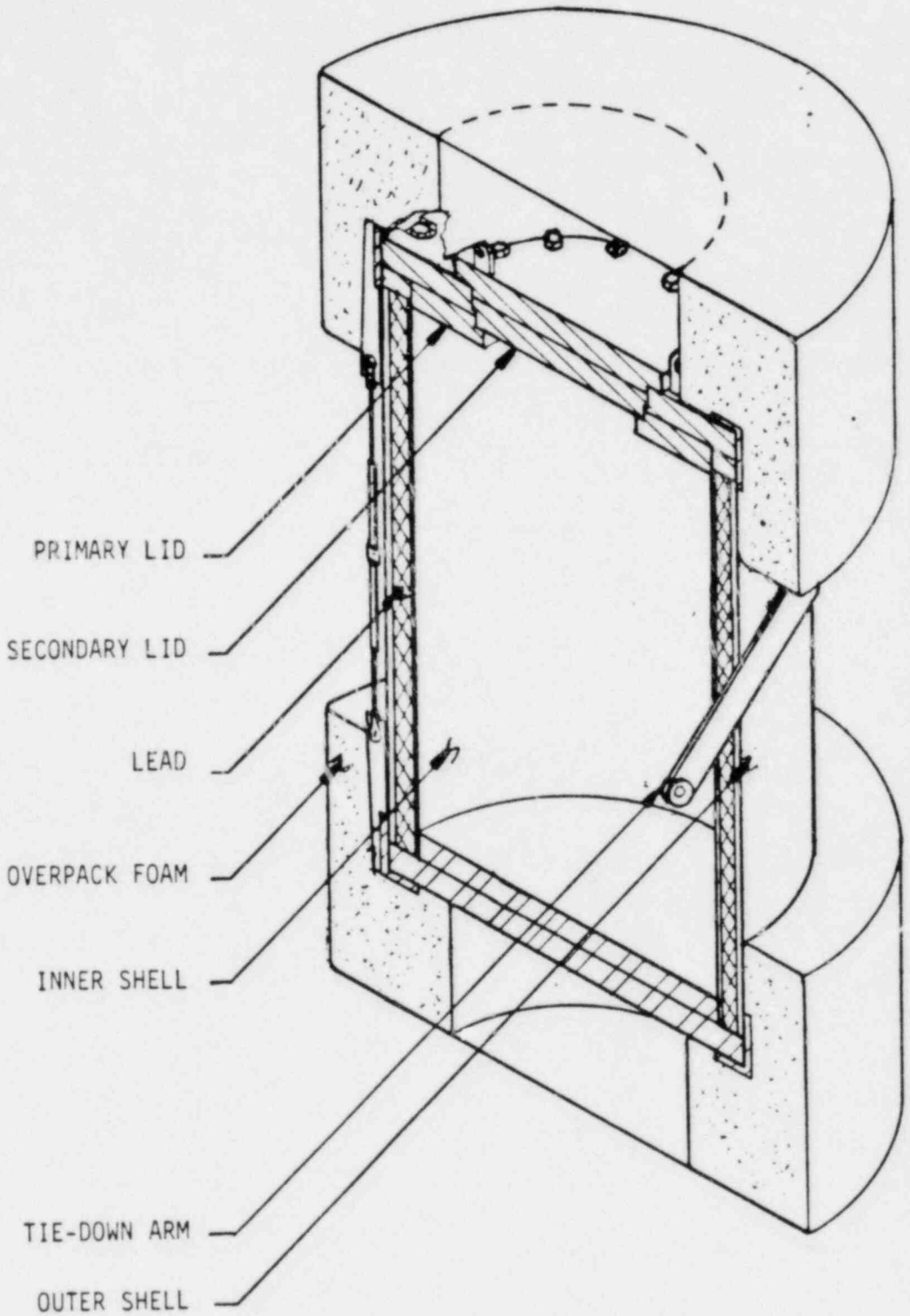

Figure 1.2-1 CASK SCHEMATIC

1.2.1 Packaging (continued)

The cask lid consists of two (2) 3-1/2 inch thick, flat circular steel plates. The lid is fastened to the cask body with thirty-two (32) 2-8 UN bolts.

A general arrangement drawing of the package is included in Appendix 1.3. It shows the package dimensions as well as all materials of construction.

1.2.1.1 Containment Vessel The containment vessel is defined as the inner steel shell of the cask body together with closure features comprised of the lower surface of the cask lid, and 32 equally spaced 2-8 UN closure bolts.

1.2.1.2 Neutron Absorbers There are no materials used as neutron absorbers or moderators in the package.

1.2.1.3 Package Weight Gross weight for the package is approximately 74000 pounds. This includes a maximum payload weight of 14050 pounds.

1.2.1.4 Receptacles There are no receptacles on this package.

1.2.1.5 Vent, Drain, Test Ports and Pressure Relief Systems Pressure test ports with manual venting features exist between the twin o-ring seals for both the primary and secondary lids. This facilitates leak testing the package in accordance with ANSI N14.5.

The drain and vent ports are provided with the same venting features for venting pressures within the containment cavity prior to lid removal, which may be generated during transport. Each port is sealed with a silicone gasket. Specification information for all seals and gaskets is contained in Chapter 4.

1.2.1.6 Lifting Devices Lifting devices are a structural part of the package. From the General Arrangement Drawing shown in Appendix 1.3, it can be seen that two removable lifting ears attached to the cylindrical cask body are provided. Three lifting lugs are also provided for removal and handling of the lid. Similarly, three lifting lugs are provided for removal and

1.2.1.6 Lifting Devices (continued)

handling of the secondary lid. Refer to Section 2.4.3 for a detailed analysis of the structural integrity of the lifting devices.

1.2.1.7 Tie-downs From the General Arrangement Drawing shown in Appendix 1.3, it can be seen that the tie-down arms are an integral part of the external cask shell. Consequently, tie-down arms are considered a structural part of the package. Refer to Section 2.4.4 for a detailed analysis of the structural integrity of the tie-down arms.

1.2.1.8 Heat Dissipation There are no special devices used for the transfer or dissipation of heat.

1.2.1.9 Coolants There are no coolants involved.

1.2.1.10 Protrusions There are no outer or inner protrusions except for the tie-down arms described above. Lifting lugs are removed prior to transport.

1.2.1.11 Shielding Cask walls provide a shield thickness of 3-1/2 inches of lead and 2-1/4 inches of steel. Cask ends provide a minimum of 7 inches of steel. The contents will be limited such that the radiological shielding provided (4.25 inches lead equivalent) will assure compliance with DOT and IAEA regulatory requirements.

1.2.2 Operational Features

Refer to the General Arrangement Drawing of the packaging in Appendix 1.3. There are no complex operational requirements associated with the package.

1.2.3 Contents of Packaging

1.2.3.1 Cask Contents The contents of the cask will consist of:

1.2.3.1 Cask Contents (continued)

(1) Greater than Type A quantities of radioactive material in the form of solids or dewatered materials in secondary containers.
(2) Greater than Type A quantities of radioactive material in the form of activated reactor components or segments of components of a nuclear power plant.
(3) That quantity of any radioactive material which does not generate spontaneously more than 100 thermal watts of radioactive decay heat.
(4) The weight of the contents in the cask cavity will be limited to 14050 lb.

1.2.3.2 Waste Forms The type and form of waste material will include:

(1) By-product material consisting of process solids or resins, either dewatered, solid, or solidified in secondary containers. (See Section 4.2.1 for specific limitations.)
(2) Neutron activated metals or metal oxides in solid form.
(3) Miscellaneous radioactive solid waste materials.

1.3 Appendix

CNS 8-120b Shipping Cask Drawing

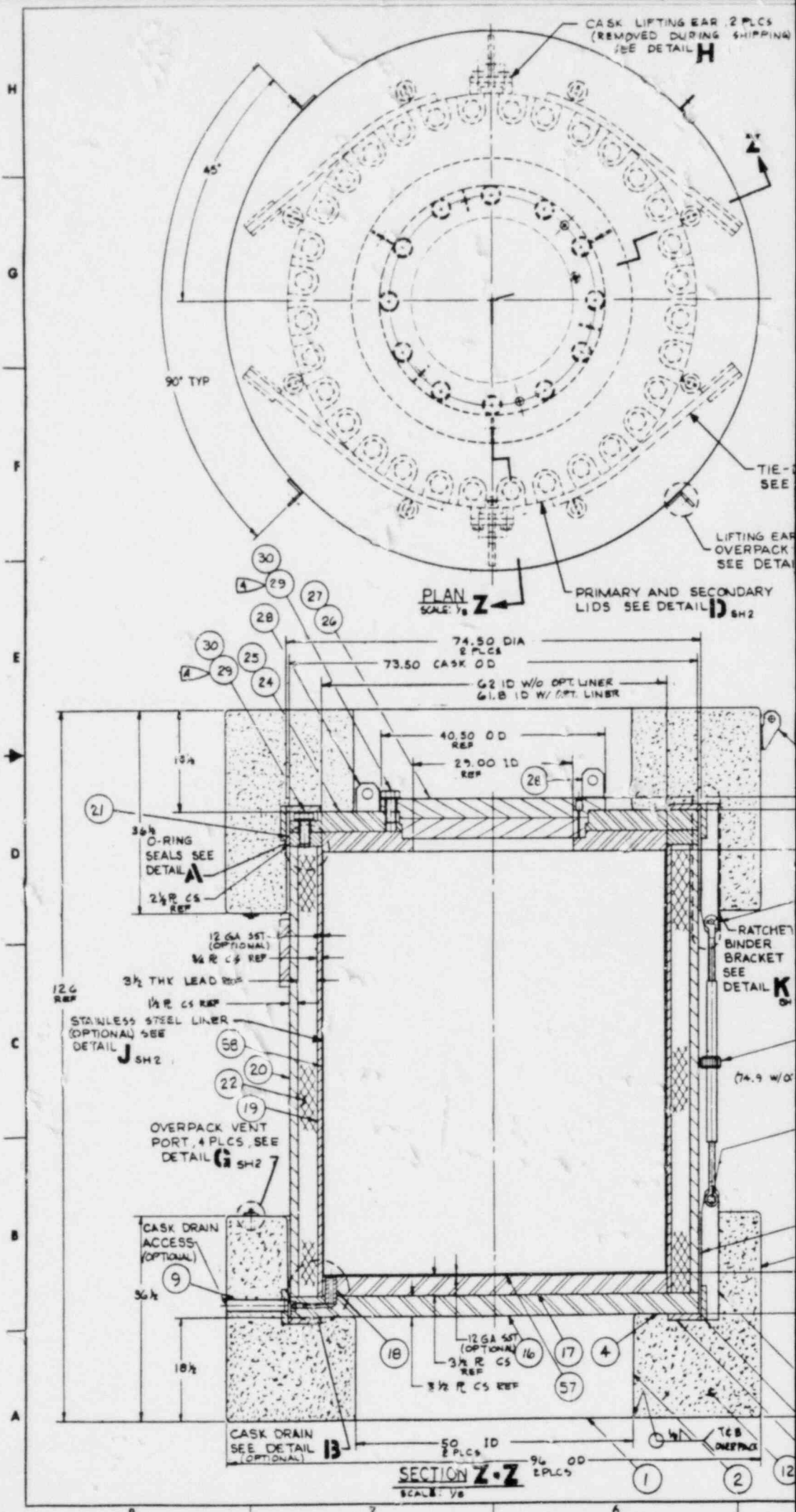
CASK LIFTING EAR, 2 PLCS (REMOVED DURING SHIPPING) SEE DETAIL H
45°
90° TYP
Z
PLAN Z
SCALE: 1/8
PRIMARY AND SECONDARY LIDS SEE DETAIL D SH2
74.50 DIA 2 PLCS
73.50 CASK OD
62 ID W/O OPT. LINER
61.8 ID W/ OPT. LINER
40.50 OD REF
29.00 ID REF
13 1/4
21
3/4 O-RING SEALS SEE DETAIL A
2 1/2 R CS REF
12 GA SST (OPTIONAL)
1/2 R CS REF
3 1/2 THK LEAD REF
1 1/2 R CS REF
STAINLESS STEEL LINER (OPTIONAL) SEE DETAIL J SH2
120 REF
58
20
22
19
OVERPACK VENT PORT, 4 PLCS, SEE DETAIL G SH2
CASK DRAIN ACCESS (OPTIONAL)
9
3/4
18 1/2
18
12 GA SST (OPTIONAL)
3 1/2 R CS REF
16
17
57
4
CASK DRAIN SEE DETAIL B (OPTIONAL)
50 ID 2 PLCS
96 OD 2 PLCS
SECTION Z-Z
SCALE: 1/8
RATCHET BINDER BRACKET SEE DETAIL K SH
TIE-
SEE
LIFTING EAR
OVERPACK
SEE DETA
1
2
8
7
6

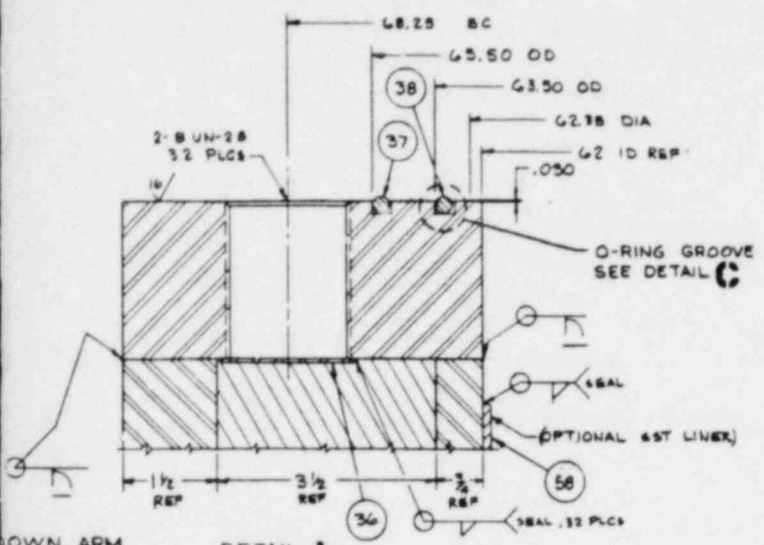

DETAIL A
SCALE: FULL

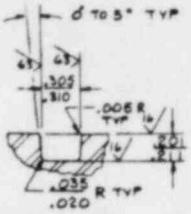

DETAIL C
SCALE: 2x
TYP 4 PLCS

NOTES:

1) WELDING SHALL BE PERFORMED BY WELDERS QUALIFIED PER ASME SECTION IX OR AWS D 1.1. WELD PROCEDURES SHALL BE SUBMITTED AND APPROVED PRIOR TO FABRICATION.
2) APPLY A LIGHT COAT OF LUBRICANT TO ALL THREADED FASTENERS. USE: MOLYKOTE, NEOLUBE OR ANTI-SIEZE.
3) USE OF CORROSION INHIBITOR ON ALL SEALING SURFACES OPTIONAL.
4) REFER TO TORQUE TABLE (SH 2) FOR RECOMMENDED BOLT TORQUES.
5) THIS DRAWING NOT TO BE USED FOR FABRICATION PURPOSES, DIMENSION SHOWN ARE FOR REFERENCE ONLY.

OWN ARM
DETAIL E SH 2

FOR
EMOVAL ONLY
F SH 2

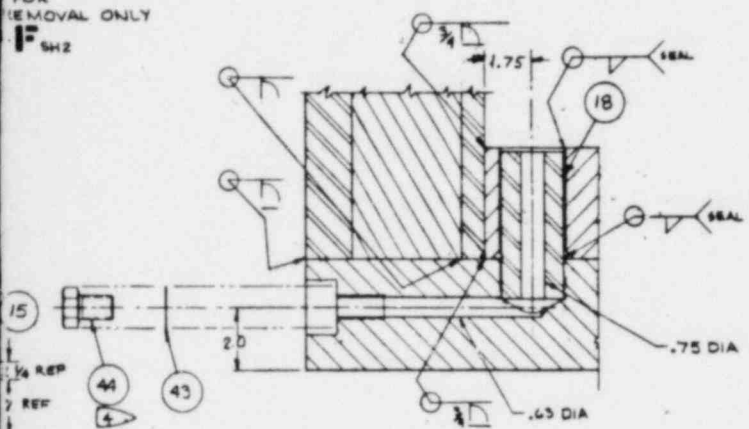

CASK DRAIN (OPTIONAL)
DETAIL B
SCALE: ½

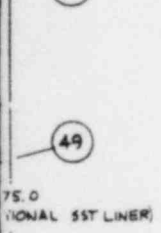

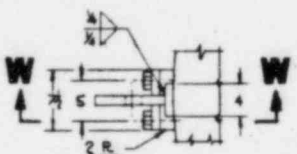

CASK LIFTING EAR
DETAIL H
SCALE: ⅛
TYP 8 PLCS

75.0
IONAL SST LINER)

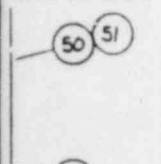

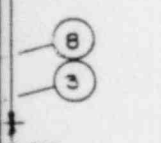

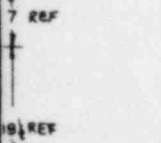

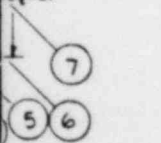

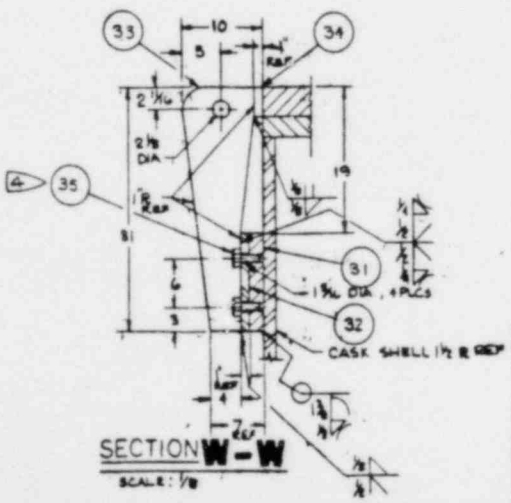

ITEM	QTY	NOMENCLATURE OR DESCRIPTION	PART NO.
59	1	PIPE PLUG, 1" NOM	ASTM-A-105
58	1	SHEET 12 GA	304 SS, ASTM-A240
57	1	SHEET 12 GA	304 SS, ASTM-A240
56	1	O-RING, ⅛ NOM.	SILICONE, S604-70
55	1	O-RING, ⅛ NOM.	SILICONE, S604-70
54	8	PLATE ⅜	ASTM-A514 OR A517
53	8	BALL LOCK PIN	
52	8	RETAINING PIN, ⅜ DIA, CARBON STEEL, SAE GRADE 5	
51	8	HVY HEX NUT, ⅜-9 UNC-2B, SELF LOCKING	
50	8	HVY HEX CAP SCREW, ⅜-9 UNC-2A x 6" LG	ASTM-A449-A
49	8	RATCHET BINDER, W.W. PATTERSON CO. TYPE J, 1" DIA. SHANK	
48	2	SEAL, ⅜ NOM. PARKER STAT-O-SEAL 600-6201-⅜	
47	2	HVY HEX CAP SCREW, ⅜-16 UNC-2A x 1" LG	ASTM-A307-A
46	1	SEAL, ½ NOM. PARKER STAT-O-SEAL 600-6201-½	
45	1	HVY HEX CAP SCREW, ½-13 UNC-2A x 1" LG	ASTM-A307-A
44	1	HVY HEX CAP SCREW, ¼-10 UNC-2A x 1" LG	ASTM-A307-A
43	1	SEAL, ¾ NOM. PARKER STAT-O-SEAL 600-6201-¾	
42	1	TUBE, ¼ OD, 1/16 WALL	ASTM-A334-GR6
41	1	ROUND BAR, 1" DIA	ASTM-A108
40	1	ROUND BAR, 1½ DIA	ASTM-A108
39	1	ROUND BAR, 1½ DIA	ASTM-A108
38	1	O-RING, ¼ NOM.	SILICONE, S604-70
37	1	O-RING, ¼ NOM.	SILICONE, S604-70
36	32	SHEET, 16 GA., 2¼ DIA	ASTM-A414-A
35	8	HVY HEX CAP SCREW, 1¼-7 UNC-2A x 2¾ LG	ASTM-A354-BD
34	2	PLATE 7"	ASTM-A516-70
33	2	PLATE 1"	ASTM-A514 OR A517
32	2	PLATE 1"	ASTM-A516-70
31	2	PLATE 2	ASTM-A516-70
30	44	FLAT WASHER, REG, 2 NOM., ¼ THK	ASTM-F436
29	44	HVY HEX CAP SCREW, 2-8 UN-2A x 4½ LG	ASTM-354-BD
28	6	PLATE ¾	ASTM-A514 OR A517
27	1	PLATE 3½	ASTM-A516-70
26	1	PLATE 3½	ASTM-A516-70
25	1	PLATE 3½	ASTM-A516-70
24	1	PLATE 3½	ASTM-A516-70
23	4	PLATE 1½	ASTM-A514 OR A517
22	A/R	LEAD, 3½ THK (POURED)	ASTM-B29
21	1	PLATE 2½	ASTM-A516-70
20	1	PLATE 1½	ASTM-A516-70
19	1	PLATE ¾	ASTM-A516-70
18	1	ROUND BAR, 2 DIA	ASTM-A108
17	1	PLATE 3½	ASTM-A516-70
16	1	PLATE 3½	ASTM-A516-70
15	4	PLATE 5/16	ASTM-A516-70
14	8	PIPE PLUG, SQR HD, 1½ NOM., PVC OR NYLON	
13	8	SHEET, 12 GA, 7" DIA	ASTM-A414-A
12	A/R	FOAM, RIGID POLYURETHANE	CNSI 1-436-112
11	8	WELDING FLANGE 1½ NOM., RYERSON PN 257	
10	2	SHEET 12 GA	ASTM-A414-A
9	1	PIPE, 2" SCH 40	ASTM-A53
8	2	SHEET 12 GA	ASTM-A414-A
7	16	PLATE ½	ASTM-A516-70
6	2	PLATE 1"	ASTM-A516-70
5	2	PLATE 1"	ASTM-A516-70
4	2	SHEET 12 GA	ASTM-A414-A
3	2	SHEET 12 GA	ASTM-A414-A
2	2	SHEET 12 GA	ASTM-A414-A
1	2	SHEET 12 GA	ASTM-A414-A

PARTS LIST

UNLESS OTHERWISE SPECIFIED DIMENSIONS ARE IN INCHES
LINEAR TOLERANCES .XX ± .01 [5]
ANGULAR TOLERANCES ± 1° [5]
MATERIAL SEE PARTS LIST
NEXT ASSEMBLY — USED ON — APPLICATION —
FINISH MACHINED SURFACE 125 [5]

CONTRACT NO.
DRAWN G JONES 8/29/82
CHECKED J. STANFORD 9-29-82
ENGINEER MIKE PRAGER 9-13-82
APPROVED [signature] 9-29-82
APPROVED [signature] 9/29/82

CHEM-NUCLEAR SYSTEMS, INC.

TITLE CNSI 8-120B SHIPPING CASK [5]

SIZE E | FSCM 54643 | DRAWING NUMBER C-110-E-0007 | REV —

SCALE NOTED | WT 59,750 LBS | SHEET 1 OF 2

5 4 3 2 1

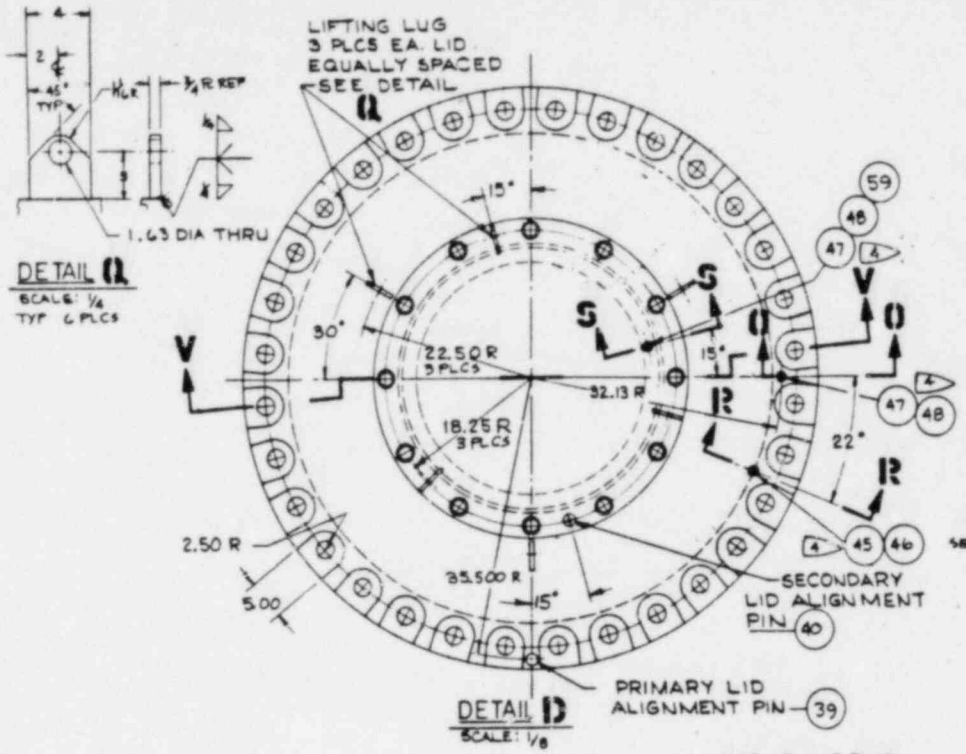

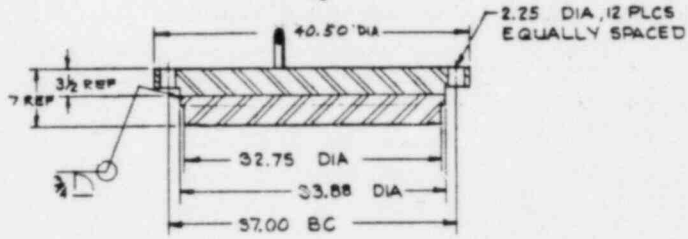

SECONDARY LID
SCALE: 1/8

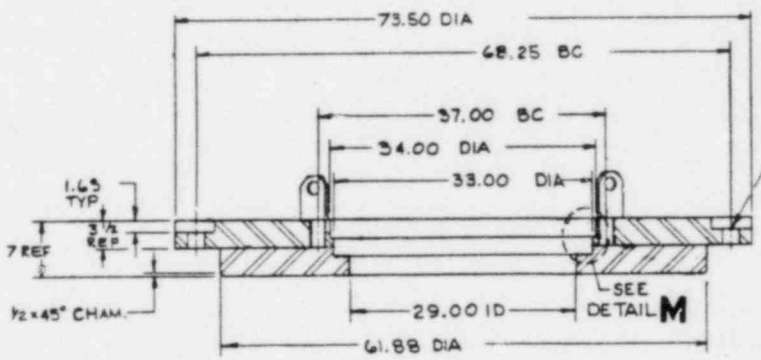

PRIMARY LID

SECTION V-V
SCALE: 1/8

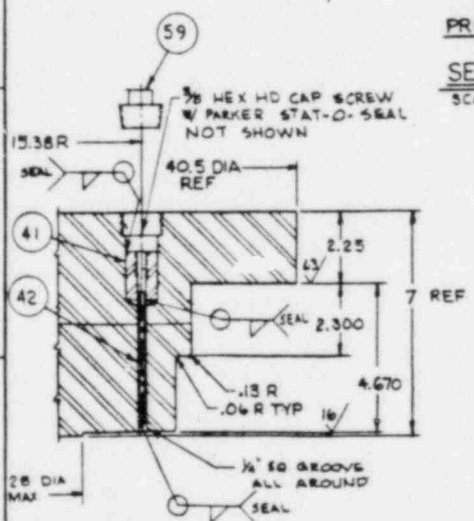

SECTION S-S
SCALE: 1/8

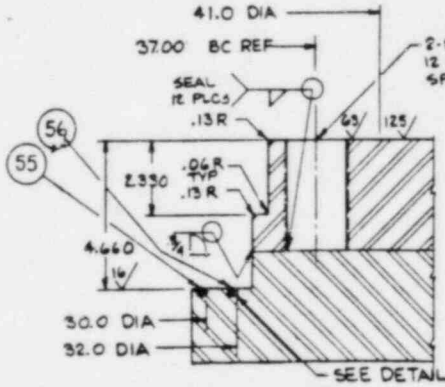

DETAIL M
SCALE: 1/2

62.63 DIA
64.00 DIA

TORQUE SPECIFICATION	
BOLT SIZE	APPLIED TORQUE LUBRICATED (FT-LB)
2-8 UN	500 ± 10%
1 1/2-7 UNC	200 ± 10%
3/8-16 UNC	80 ± 10%
1/2-13 UNC	80 ± 10%
5/8-11 UNC	12 ± 10%

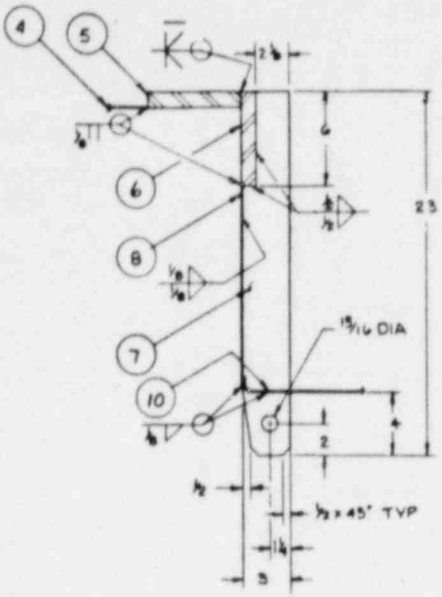

DETAIL K
SCALE: 1/4
TYP 16 PLCS

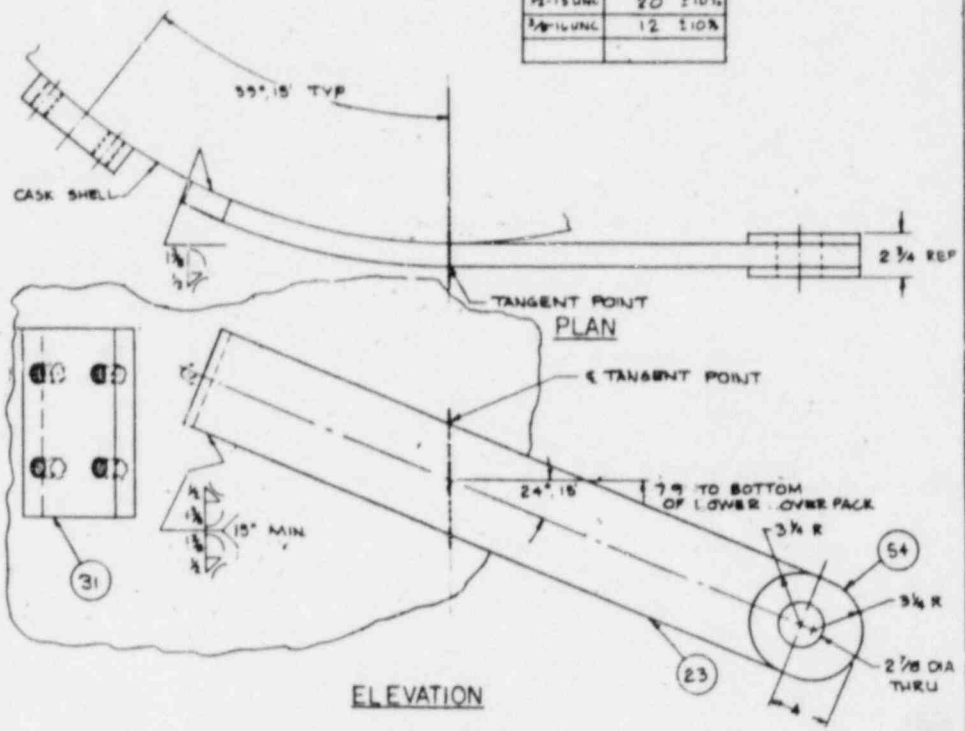

ELEVATION

DETAIL E
SCALE: 1/4
TYP 4 PLCS

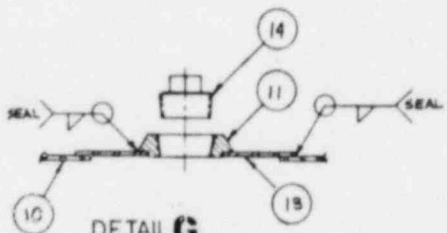

DETAIL G
SCALE: 1/2
TYP 8 PLCS

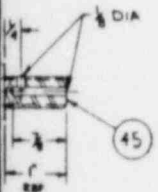

L

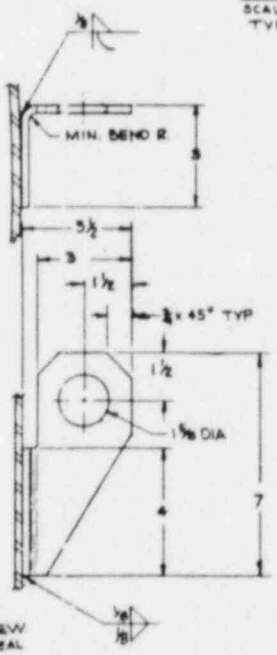

DETAIL F
SCALE: 1/2
TYP 4 PLCS

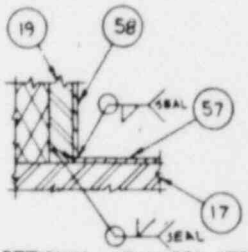

OPTIONAL STAINLESS STEEL LINER

DETAIL J
SCALE: 1/2

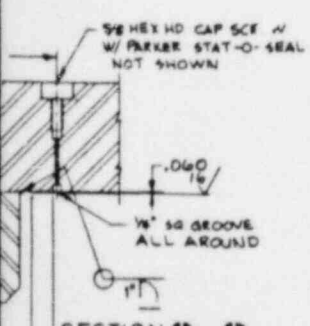

SECTION O-O
SCALE: 1/2

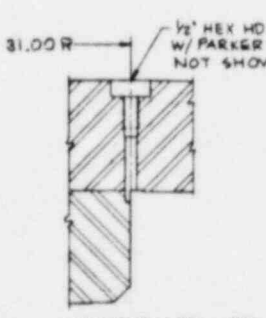

SECTION R-R
SCALE: 1/2

ITEM	QTY	CODE IDENT	NOMENCLATURE OR DESCRIPTION	PART NO.

PARTS LIST

CONTRACT NO.

CHEM-NUCLEAR SYSTEMS, INC.

G JONES 9/24/82

TITLE: CNSI 8-1208 SHIPPING CASK (5)

SIZE: E | FSCM NO. 54643 | C-110-E-0007 | REV —

SCALE: NOTE 5 | WT | SHEET 2 OF 2

2.0 STRUCTURAL EVALUATION

This chapter identifies and describes the structural design of the CNS-8-120B packaging, components, and safety systems for compliance with performance requirements of 10 CFR 71.

2.1 Structural Design

2.1.1 Discussion

The package has been designed to provide a shielded containment vessel that can withstand the Normal Conditions of Transport as well as those associated with the Hypothetical Accident Conditions.

The CNS-8-120B assembly is designed to protect the payload from the following conditions: transport environment, 30 foot drop test, 40 inch puncture test, 1475°F thermal exposure, and transfer or dissipation of any internally generated heat. The design of the package satisfies these requirements.

Principal structural elements of the system consist of:

- Containment Vessel
- Biological Shield
- Impact Limiters

These components are identified on the drawing as noted in Appendix 1.3. Their design and function in meeting the requirements of 10 CFR 71 are discussed below.

2.1.1.1 Containment Vessel The cask is comprised of inner and outer ASTM-A516, Gr 70, steel shells which envelop a lead shield, a steel base, and lid. The inner shell serves as the package containment boundary. A removable primary lid is attached to the cask body with thirty-two (32) equally-spaced 2-8 UN bolts. A secondary lid is attached to the primary lid with twelve (12) equally-spaced 2-8 UN bolts.

2.1.1.1 Containment Vessel (continued)

The lid-to-cask body and lid-to-lid interfaces each employ a pair of high temperature, solid silicone o-rings. All transport environments as well as accident conditions (i.e., 30 foot drop, 40 inch puncture test requirements, etc.) are met with impact limiters installed as discussed in Section 2.1.1.3 below. All thermal loading and dissipation requirements are met as discussed in Section 3.0.

2.1.1.2 Shielding The area between the two shells discussed in Section 2.1.1.1 is filled with lead. The lead fill is subjected to Gamma Scan inspection to assure lead integrity. The designed thickness assures that no biological hazard is presented by the package and all shielding requirements of 10 CFR 71 are met.

2.1.1.3 Impact Limiters The impact limiters (overpacks) are designed to protect the package from deformation during the 30 foot drop and to provide thermal protection during the hypothetical fire accident condition.

Their construction consists of full welded steel shells filled with foamed-in-place rigid structural polyurethane foam. The foam deforms and provides energy absorbtion during impact.

2.1.1.4 Summary Detailed discussions of all components and materials utilized in the CNS-8-120B Package including stress, thermal, and pressure calculations are contained in the applicable sections of this SAR. A drawing of the individual subassemblies and the CNS-8-120B package can be found in Appendix 1.3.

2.1.2 Design Criteria

2.1.2.1 Normal and Accident Conditions of Transport Regulatory Guide 7.6, "Design Criteria for the Structural Analysis of Shipping Cask Containment Vessels", was used in conjuction with Regulatory Guide 7.8, "Load Combinations for the Structural Analysis of Shipping Casks" to evaluate the

package according to the requirements of 10 CFR 71, Appendix A and Appendix B. Material properties used in the analysis can be found in Table 2.3-1.

(1) Containment Vessel

The containment vessel is defined to be the inside steel shell and its closures. Regulatory Guide 7.6 was used for the evaluation of the containment vessel for both the Normal Conditions of Transport and the Hypothetical Accident Conditions. Material properties used in the evaluation correspond to the design stress values, S_m and S_u, given in the ASME Code, Section III, Class 1, 1980 Edition as amended. To evaluate buckling, the value of yield stress, S_y, for the cylindrical shell is based on measured properties of the material used in the construction of the cask.

(2) Cask and Overpack

Structural evaluation of non-containment vessel items (except the external shell), such as the closures, were evaluated against yield and ultimate material properties as presented in the ASME Code, Section III, Class 1. To evaluate buckling of the external shell, the yield strength is based on measured properties of the material used in construction of the cask. For Normal Conditions of Transport, allowable stress intensities are S_m for membrane stresses and 1.5 S_m for membrane plus bending stresses. The overpack is allowed to exceed yield stress for normal conditions; hence, ultimate stress is used as the acceptance criterion. In evaluating Accident Conditions, 0.75 S_u is used to evaluate bending stress intensities and S_u is used to evaluate bending plus membrane stress intensities.

(3) Brittle Fracture

The cask is fabricated of ASTM A516, Grade 70, carbon steel. The brittle-fracture-critical carbon steel components of the package are evaluated in Paragraph. 2.6.2 per criteria set forth in NUREG/CR-1815 (UCRL-53013), Recommendations for Protecting Against Failure by Brittle Fracture in Ferritic Steel Shipping Containers up to Four Inches Thick, W.R. Holman and R.T. Langland, June 15, 1981. In the absence of definitive regulatory criteria governing use of this document, Category II criteria per this report have been employed to achieve a conservative level of safety. The rationale for this selection presumes that the higher level of safety embodied in Category I criteria is reserved for fissile and high-level waste packages.

(4) Buckling

Buckling per Regulatory Guide 7.6 is an unacceptable failure mode for the containment vessel. The intent of this guideline is to make large deformations unacceptable because they would compromise the validity of linear analysis assumptions and quasi-linear stress allowables as given in Paragraph C.6 of NRC Regulatory Guide 7.6.

The remainder of this paragraph defines techniques and criteria used in subsequent segments of this Safety Analysis Report to demonstrate that containment vessel buckling does not occur.

- Euler Column Buckling

From Reference 1, eq. 2-45, p. 104, the critical axial buckling load for a self-weight load combined with an added axial force is

$$P_{cr} = \frac{m E I}{l^2}$$

where m = tabulated function of n

$$n = \frac{4ql^3}{\pi^2 EI}$$

q = distributed axial load intensity = $2\pi Rwat$

l = half-length of cylinder

E = Young's modulus = 27.8×10^6 psi

I = $\pi R^3 t$

R = cylinder radius

t = cylinder thickness

w = weight density = 0.283 lb/in^3

a = acceleration in g's

This mode of buckling applies to the outer shell of the cask, composed of a 1 1/2-inch thick plate.

Then l = 39.25 in.

R = 36 in.

t = 1.5 in.

I = 219861 in.^{4}

q = 96.02a lb/in

And n = 3.85×10^{-7} a

For a = 135

n ≅ 0

Therefore

$$m = \frac{\pi^2}{4}$$

$$P_{cr} = 9.8 \times 10^9 \text{ lb.}$$

- Axial Stress Limits

According to Reference 2, p. 230, a thin-wall cylinder is considered "moderately long" if

$$cz > \frac{\pi^2 K_{co}}{2\sqrt{3}}$$

where c = correction factor dependent on R/t

$$Z = \frac{L^2}{Rt}\sqrt{1 - m^2}$$

K_{co} = 1 for simply supported edges (conservative)

L = length of cylinder

R = mean radius of cylinder

t = wall thickness

m = Poisson's ratio

The following two sets of shell properties correspond to the inner and outer shells of the cask:

Inner Shell	Outer Shell
t_i = 0.75 in.	t_o = 1.5 in.
R_i = 31.375 in.	R_o = 36.0 in.
L_i = 76.0 in.	L_o = 79.5 in.
m = 0.3	m = 0.3

For both shells,

$$\frac{\pi^2}{2\sqrt{3}} k_{co} = 2.849$$

Then

R_i/t_i = 41.83

R_o/t_o = 24.0

Z_i = 234

Z_o = 112

From Reference 2, Fig. 10-9, p. 230,

c_i = 0.70

c_o = 0.55

2.1.2.1 Normal and Accident Conditions of Transport (continued)

For both shells,

$$cZ > \frac{\pi^2 k_{co}}{2\sqrt{3}},$$

therefore both will be treated as moderately long cylinders.

From Baker, et. al., p. 229,

$$\sigma_e = \frac{k_c \pi^2 E}{12(1-m^2)} \left(\frac{t}{L}\right)^2$$

Where

σ_e = elastic buckling stress
E = Young's modulus
= 27.8×10^6 psi

$$k_c = \frac{4\sqrt{3}}{\pi^2} cZ$$

Then

σ_{ei} = 281353 psi
σ_{eo} = 386787 psi

- Hoop Stress Limits

From Reference 2, p. 236,

$$\sigma_e = \frac{k_p \pi^2 E}{12(1-m^2)} \left(\frac{t}{L}\right)^2$$

where k_p = function of Z (Ref. 2, Fig. 10-15, p. 237)

Then

k_{pi} = 13
K_{po} = 9

σ_{ei} = 31810 psi

σ_{eo} = 80503 psi

- Critical Buckling Stress

σ_{cr}, for each of the above cases, can be found by solving the following equation (from Ref. 2, p. 265):

$$\sigma_{cr} - \eta\sigma_e = 0$$

where η = plasticity coefficient

The plasticity coefficient, η, is defined by the following equations for the various loading conditions:

For axial stress, from Baker, et. al, p 266.

$$\eta = \frac{(E_s E_t)}{E}^{1/2}$$

For external pressure stress; from Ref. 2, p. 236

$$\eta = \frac{E_s}{E_t} \sqrt{(\frac{E_t}{E_s})^{1/2} (\frac{1}{4} + \frac{3}{4} \frac{E_t}{E_s})}$$

where:

E_t = tangent modulus = $d\sigma/d\varepsilon$
E_s = secant modulus = σ/ε
E = Young's modulus
σ = stress
ε = strain

For stresses below the proportional limit, conservatively assumed to be $0.7\sigma_y$,

$$E = E_t = E_s$$

and $\eta = 1$

For stresses above the proportional limit, stress is assumed to be a parabolic function of strain that is tangent to the elastic line at the proportional limit and has zero slope at the yield stress.

For $\sigma_y = 43.0$ ksi

and $E = 27.8 \times 10^6$ psi

then, for $0.7\sigma_y < \sigma < \sigma_y$

$$\sigma = A\varepsilon^2 + B\varepsilon + C$$

where $A = -1.4978 \times 10^{10}$

$B = 6.0233 \times 10^7$

$C = -1.7558 \times 10^4$

Using this expression for stress, the critical buckling stress equation is solved:

$$A^2 \varepsilon_{cr}^5 + 2AB\varepsilon_{cr}^4 + [2AC + B^2 - 2A^2(\tfrac{\sigma_e}{E})^2]\varepsilon_{cr}^3$$
$$+[2BC - 3AB(\tfrac{\sigma_e}{E})^2]\varepsilon_{cr}^2 + [C^2 - (\tfrac{\sigma_e}{E})^2(2AC + B^2)]\varepsilon_{cr} - BC(\tfrac{\sigma_e}{E})^2 = 0$$

Axial:

$\varepsilon_{cri} = 1.9829 \times 10^{-3}$

$\eta_i = 0.15278$

$\sigma_{cri} = 42986$ psi

$\varepsilon_{cro} = 1.9959 \times 10^{-3}$

$\eta_o = 0.11116$

$\sigma_{cro} = 42994$ psi

Hoop:

$$\varepsilon_{cri} = 1.1209 \times 10^{-3}$$
$$\eta_{cri} = .97886$$
$$\sigma_{cri} = 31138 \text{ psi}$$
$$\varepsilon_{cro} = 1.7241 \times 10^{-3}$$
$$\eta_{cro} = 0.51882$$
$$\sigma_{cro} = 41767 \text{ psi}$$

The buckling stress limits are summarized in the following table:

	Inner Shell	Outer Shell
Axial Membrane Stress Limit	42986 psi	42994 psi
Hoop Membrane Stress Limit	31138 psi	41767 psi

Evaluation of buckling of the cylindrical shells, for combined loading, is done using the technique described in Ref. 2, p. 275. Accordingly,

$$\sigma_{cr} - n\sigma_i = 0$$

where σ_{cr} = combined load critical buckling stress intensity

n = plasticity correction factor

$$= \frac{\sqrt{E_t E_s}}{E}$$

σ_i = elastic buckling stress intensity

$$= \sqrt{\sigma_a^2 + \sigma_h^2 - \sigma_a \sigma_h}$$

σ_a = elastic axial buckling stress limit

σ_h = elastic hoop buckling stress limit

2.1.2.1 Normal and Accident Conditions of Transport (continued)

Values for the inner and outer shells are as follows:

	Inner	Outer
σ_a, psi	281353	386707
σ_h, psi	31810	80503
σ_i, psi	266874	353479
η	0.1606	0.12163
σ_{cr} (combined load)	42983	42993

In evaluating stress conditions for buckling of the shells, the individual stress components will be compared to the buckling stress allowables in the hoop and axial directions. The stress intensities will be compared to the values of σ_{cr}, above, for combined loading.

2.1.2.2 Tie-downs and Lifting Devices

(1) Tie-downs

10 CFR 71, 71.31(d) paragraph (1) requires that the tie-downs be designed such that no stresses exist in any material of the package in excess of its material yield strength for the specified loading condition. Maximum package stresses and factors of safety are computed in Chapter 2.4.4.

(2) Cask and Lid Lifting Devices

10 CFR 71, 71.31(c) paragraph (1) requires that the cask lifting devices be capable of supporting three times the weight of the loaded package. Paragraph (2) requires lid lifting devices be capable of supporting three times the weight of the lid with any attachments. Both paragraphs require that no stresses be generated in any material in excess of its material yield strength.

Maximum stresses and safety factors are computed in Chapter 2.4.3. Allowable stresses and factors of safety are computed as described in Section 2.1.2.2(4).

(3) Failure of the Tie-Down and Lifting Devices

Any tie-down, cask lifting or lid lifting device must be designed such that failure of the device under excessive loads will not impair the ability of the package to meet the other requirements specified in 10 CFR 71.31 paragraphs (c)(4) and (d)(3).

Chapters 2.4.3 and 2.4.4 demonstrate that at the excessive load for which a device fails, each component of the package which is required for meeting the shielding and containment requirements before and after the normal and accident events, has had no stress generated in excess of its material yield strength. This leads one to conclude that if the remaining components have not yielded, they remain intact and undeformed and may be considered for meeting the shielding and containment requirements for normal and accident conditions.

Failure is predicted for an equivalent state of stress which produces a maximum shear stress of

$$\sigma_{failure} = \frac{F_u}{\sqrt{3}} = 0.58\ F_u \qquad (1)$$

where F_u = Material's ultimate tensile strength.

(1)

2.1.2.2 Tie-downs and Lifting Devices (continued)

(4) Allowable Stresses - Tie-Downs and Lifting Devices

Maximum shear stresses (one-half the stress intensity) are computed for the required loading condition and compared to the allowable shear yield stresses. Allowable shear yield stresses are determined as follows:

- Base-Metal

The allowable shear yield stresses for all base metals are determined from "Maximum Shear Failure Theory" (ref. 2, p.212, Table 9.1, case 3) which says that, "two states of stress are equivalent if their maximum shear stresses are equal." This is represented by

$$\sigma_{\text{shear yield}} = \frac{F_y}{2} \geq \frac{\sigma_{p1} - \sigma_{p2}}{2}$$

where F_y is the yield stress as determined for a specimen loaded in axial tension only. Allowable yield stress for all base metals may be found in Table 2.3-1.

The theory is conservative for ductile materials because the shear yield stress as determined from a tension test (pure shear) is greater than one half the tensile yield stress as determined for a specimen loaded in axial tension only (reference 5, p.416.)

The factors of safety are determined as:

$$\text{F.S.} = \left[\frac{\sigma_{\text{shear allowable(membrane + bending)}}}{\sigma_{\text{shear max.}}} \right]$$

Factors of Safety greater than 1.0 are acceptable.

- Weld Metal

All welds are sized such that the effective weld throat, for both full and partial penetration welds, maintains a stress area greater than or equal to the effective base metal stress area.

AWS D1.1 Table 8.4.1 defines the allowable shear stress weld stress, regardless of direction of loading, as:

$$\sigma_{weld} \leq 0.3\ F_u$$

where F_u = minimum ultimate tensile strength (ksi).

For 70 series welding wire, this gives an allowable stress of:

$$\sigma_{weld} = 0.3(70) = 21.0 \text{ ksi}$$

In satisfying the allowable stress criterion for the base metal, weld stresses are inherently satisfied. This is because the effective stress areas for the welds are greater than or equal to those for the base metals and the minimum allowable shear stress for all base metals is less than the allowable weld stresses. This is illustrated as follows:

For any load P:

$$\sigma_{base\ metal} = \frac{P}{A_{base\ metal}} \leq \frac{F_y}{2} = 19 \text{ ksi}$$

where F_y = 38 ksi for A516-70 steel

Therefore:

$$\sigma_{weld} \leq \frac{P}{A_{base\ metal}} \leq 19 \text{ ksi} < 21.0 \text{ ksi}$$

because $A_{weld} \geq A_{base\ metal}$

2.1.2.2 Tie-downs and Lifting Devices (continued)

In addition, all welds are inspected by non-destructive testing methods to verify sound deposition of weld material and verification of weld integrity.

2.2 Weights and Center of Gravity

The center of gravity of the package is located at the geometric center of the package.

Weight breakdown is as follows:

Cask Body	44830
Lids (primary and secondary)	7320
Overpacks	7500
Overpack Binders (8)	300
Net Package	59950 lbs.
Payload	14050
TOTAL GROSS PACKAGE WEIGHT:	74000 lbs.

2.3 Mechanical Properties of Materials

The package is fabricated from carbon steel, lead, and structural foam. Drawing C-110-E-0007, Appendix 1.3, defines the specific material used for each item of the package. Table 2.3-1 presents material properties used throughout the analyses and references the sources of these data.

Material	Grade or Type	Temp °F	Strength (ksi)			Young's Modulus (10^6psi)(4)	Coefficient of Thermal Expansion (10^{-6}in/in/°F)(5)
			Yield (1)	Ult. (2)	Allow. (3)		
ASTM A516 Plate (Inner and outer shells lids, base plates and overpack plates)	70	70	38 (6)	70	23.3	27.9	6.50
		100	38 (6)	↑	23.3		6.67
		200	34.6(6)	|	23.1	27.7	6.87
		300	33.7	|	22.5	27.4	7.07
		400	32.6	|	21.7	27.0	7.25
		500	30.7	↓ 70	20.5	26.4	
ASTM A414 Sheet (overpack shell)	C	100			13.7		6.50
		200			↑		6.67
		300	30	55	| (7)	29.9	6.87
		400	(7)	(7)	|		7.07
		500			↓ 13.7		7.25
ASTM A514 or ASTM A517 (Tie-down arms, lifting ears and lugs)	-	70	100	110	-	29.9	6.41 (10)
	-	70	100	115	-	29.9	6.41.(10)
ASTM B29 Lead	C	70	5 Dynamic Compression Minimum (8)	-	-	2.0 (8)	16.3
ASTM A354 2-8UN (Lid closure bolts)	BD	70	130 (9)	150 (9)	-	29.9	6.5
ASTM A354 1¼-7UNC (Lifting ear bolts)	BD	70	130 (9)	150 (9)	-	29.9	6.5
ASTM A307 (Drain plug bolt) (Vent/test plug bolt)	A	70	-	60 (9)	-	29.9	6.5

References for Table 2.3-1:

(1) ASME Code, Section III, Appendices, Table I-2.1

(2) ASME Code, Section III, Appendices, Table I-3.1

(3) ASME Code, Section III, Appendices, Table I-1.1

(4) ASME Code, Section III, Appendices, Table I-6.0

(5) ASME Code, Section III, Appendices, Table I-5.0, Coefficient B

(6) For inner and outer cask cylindrical shells, minimum measured yield stress is used:

T, °F	Yield Stress (ksi)
70	45.0
100	45.0
300	41.0

(7) ASME Code, Section III, Appendices, Table I-7.1

(8) Cask Designer's Guide, ORNL-NSIC-68

(9) ASTM Specification

(10) ASME Code, Section III, Appendices, Table I-5.0, Coefficient A.

2.3 Mechanical Properites of Materials (continued)

The material used in construction of the inner and outer skins of the cask shell is tested for a minimum yield strength of 45 ksi at normal temperature (70°F). To determine the corresponding yield stress at other temperatures, this measured value is multiplied by a stress ratio based on values given in the ASME Code, Section III, Class 1. This stress ratio is the ratio between the ASME tabulated values of yield stress at the temperature of interest and the yield stress at normal temperature, for ASTM A516, Gr.70, steel.

The energy absorbing overpacks are constructed of rigid, self-extinguishing, polyurethane foam, foamed-in-place. Figure 2.3-1 represents the stress-strain curve for the foam used for this package.

Foam samples will be taken during the actual foaming process and tested in accordance with CNSI specification 1-436-112 which includes the ASTM specification for testing.

2.4 General Standards for All Packages

This section demonstrates that the general standards and loading conditions for all packages are met.

2.4.1 Chemical and Galvanic Reactions

The materials from which the packaging is fabricated (steel, lead, and polyurethane foam) along with the contents of the package will not cause significant chemical, galvanic, or other reaction in air, nitrogen, or water atmospheres.

2.4.2 Positive Closure

The positive closure system has been previously described in Section 1.2.1.

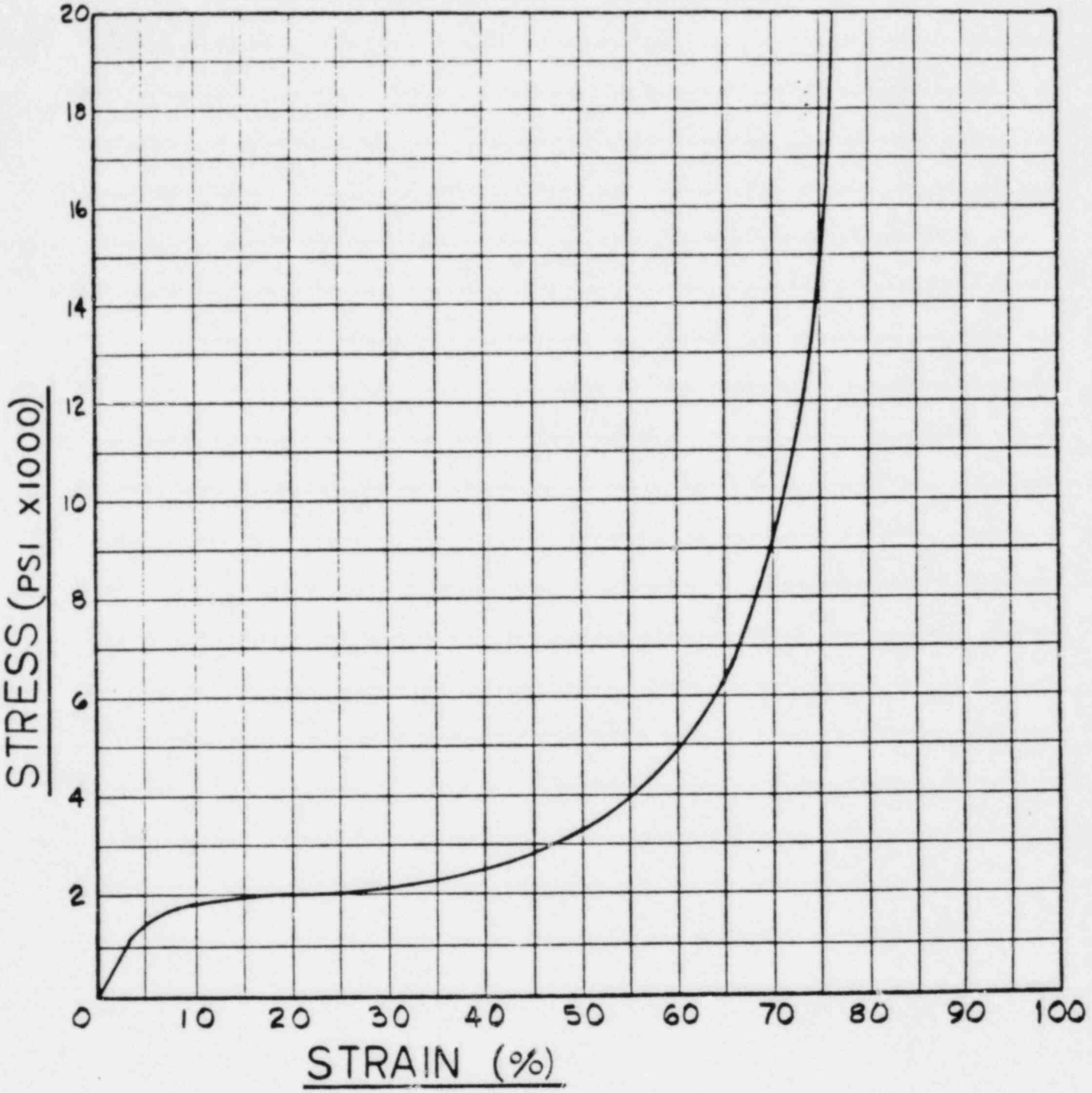

COMPRESSIVE STRESS vs STRAIN

MATERIAL : CNSI SPEC 1-436-112

Figure 2.3-1

2.4.3 Lifting Devices

The cask is provided with two removable lifting ears, attached to the side of the cask, by which the cask and load can be lifted. The primary and secondary lids are furnished with three lifting lugs by which the lids may be removed from the cask.

The load requirements for lifting devices are defined in 10 CFR 71, Subpart C, Para 71.31 as, ". . . capable of supporting three times the weight . . . without generating stresses in any material of the packaging in excess of its yield strength."

2.4.3.1 Cask Lifting Ears

(1) Cask Lifting Ear Stress Summary

The results of the cask lifting ear stress analyses are summarized as follows:

Location	Max. Shear Stress Memb.+ Bending(psi)	Factor of Safety
Bolt	34322	1.89
Mounting plate (weld)	1864	10.19
Lifting ear plate (weld)	8327	2.28
Tearout	46758	1.07
Threads (cask)	362	52.52

As determined in Section 2.4.3.1 (3), the vertical load for computing the above safety factors is:

$$P = 99750 \text{ lbs.}$$

The detailed stress analyses for each component listed above may be found in subsequent paragraphs.

2.4.3.1 Cask Lifting Ears (continued)

(2) Failure of the Cask Lifting Ears Under Excessive Loads

Since failure will first occur in the region of the smallest factor of safety, the cask lifting ear will fail by eye tearout at a load which produces a maximum shear stress of:

$$\sigma_{failure} = \frac{F_u}{\sqrt{3}} = 66395 \text{ psi (see Section 2.1.2.2)}$$

where F_u = 115000 psi so as to give a conservative value of the maximum shear stress for either ASTM A517 or A514 steel.

The failure load can then be computed as:

$$P_{failure} = \frac{P(\sigma_{failure})}{\sigma_{actual}} = \frac{99750(66395)}{46758} = 141642 \text{ lbs.}$$

where σ_{actual} = stress in the component with the minimum factor of safety.

Should the failure load inadvertently develop, the corresponding stresses in other parts of the ear would be:

Location	σ_{shear} (psi)	Allowable stress (psi)
Bolt	46736	52500
Mounting plate (weld)	2647	19000
Lifting ear plate (weld)	11824	19000
Threads (cask)	514	19000

Since the load which causes failure of the lifting ear does not generate stresses in excess of any other material's yield strength, it can be concluded that the remaining components remain intact and undeformed, and may be so considered for meeting the normal and accident shielding and containment requirements.

2.4.3.1 Cask Lifting Ears (continued)

(3) Bolt Stresses

The cask lifting ears can be used only with the overpacks removed. Therefore, the total lifted weight is:

$$W = 74000 - 7500 = 66500 \text{ lbs.}$$

For three times the weight of the cask, the vertical ear load is:

$$P_V = \frac{3W}{2 \text{ ears}} = \frac{3(66500)}{2 \text{ ears}}$$

$$= 99750 \text{ lb/ear}$$

The equations of equilibrium for the lifting ear shown in Figure 2.4.3-1, are:

Summation of Forces:

$$\text{Horizontal: } F + P_H - R_T = 0$$

$$\text{Vertical: } P_V - V = 0$$

Summation of Moments about point O:

$$25F + 2.688\, P_H - 5\, P_V + 2V = 0$$

Given:

$$P_V = 99750 \text{ lb.}$$

$$P_H = \frac{P_V}{\tan 60^\circ} = 57591 \text{ lb.}$$

Then: $V = 99750$ lb.

$$F = (1/25)(5P_V - 2.688\, P_H - 2V)$$

$$= 5778 \text{ lb.}$$

$$R_T = 63369 \text{ lb.}$$

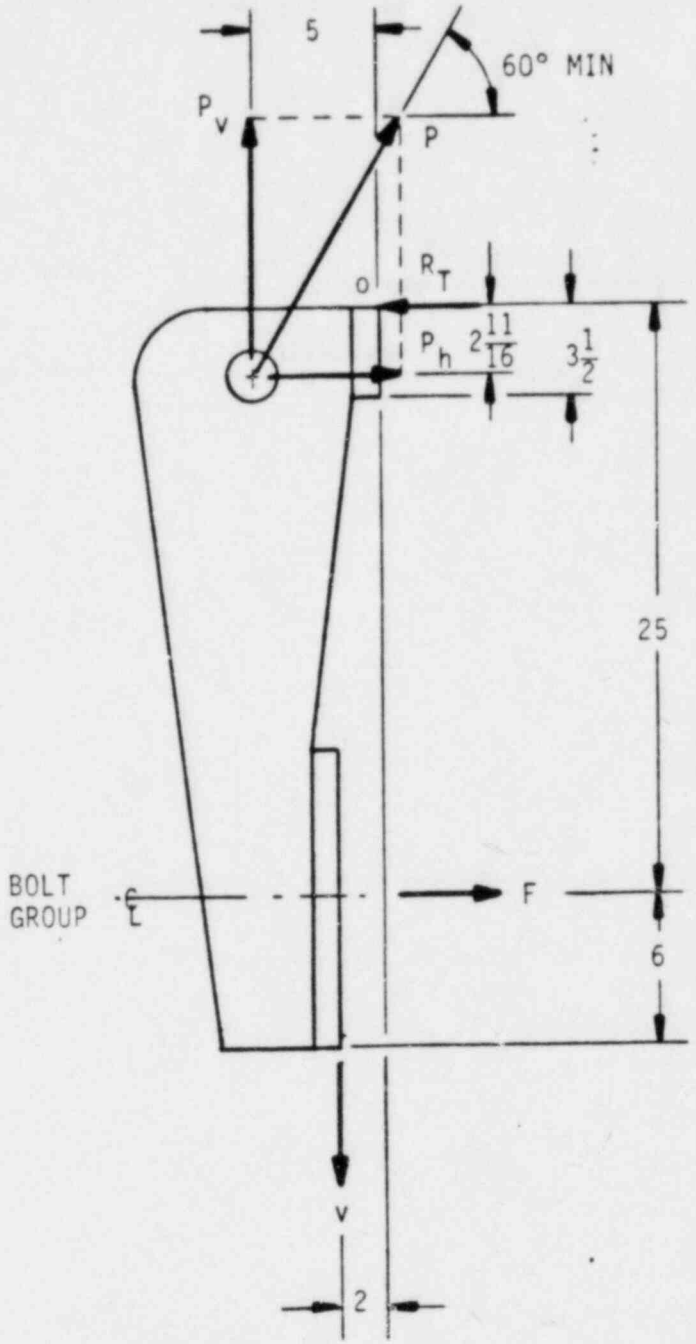

P = Lifting force on ear
F = Tensile force on bolts
V = Shear force on bolts
R_T = Reaction force against top of cask with lid in place.

Figure 2.4.3-1 LIFTING EAR FREEBODY DIAGRAM

2.4.3.1 Cask Lifting Ears (continued)

Each lifting ear is attached to the cask, as shown in Figure 2.4.3-2, using four 1-1/4 - 7 UNC-2A, 2-3/4 inch long ASTM A354 Grade BD hex head bolts. The stress area for each bolt is 0.969 in^2.

The shear force, V, will be carried by four bolts, so the nominal shear stress in the bolts is:

$$\sigma_{snom} = \frac{99750}{4(0.969)} = 25735 \text{ psi}$$

The maximum shear stress in the bolts will be four-thirds the nominal shear stress, so

$$\sigma_s = \frac{4}{3}(25735) = 34314 \text{ psi}$$

The tensile force, F, will be carried by the four bolts. The resulting tensile stress will be

$$\sigma_t = \frac{F}{4(0.969)}$$
$$= 1491 \text{ psi}$$

The maximumm principal stresses in the bolt are found by:

$$\sigma_p = \frac{\sigma_t}{2} \pm \sqrt{\left(\frac{\sigma_t}{2}\right)^2 + \sigma_s^2}$$

Thus

$$\sigma_{p1} = 35067 \text{ psi}$$

$$\sigma_{p2} = -33576 \text{ psi}$$

The maximum shear stress is given by:

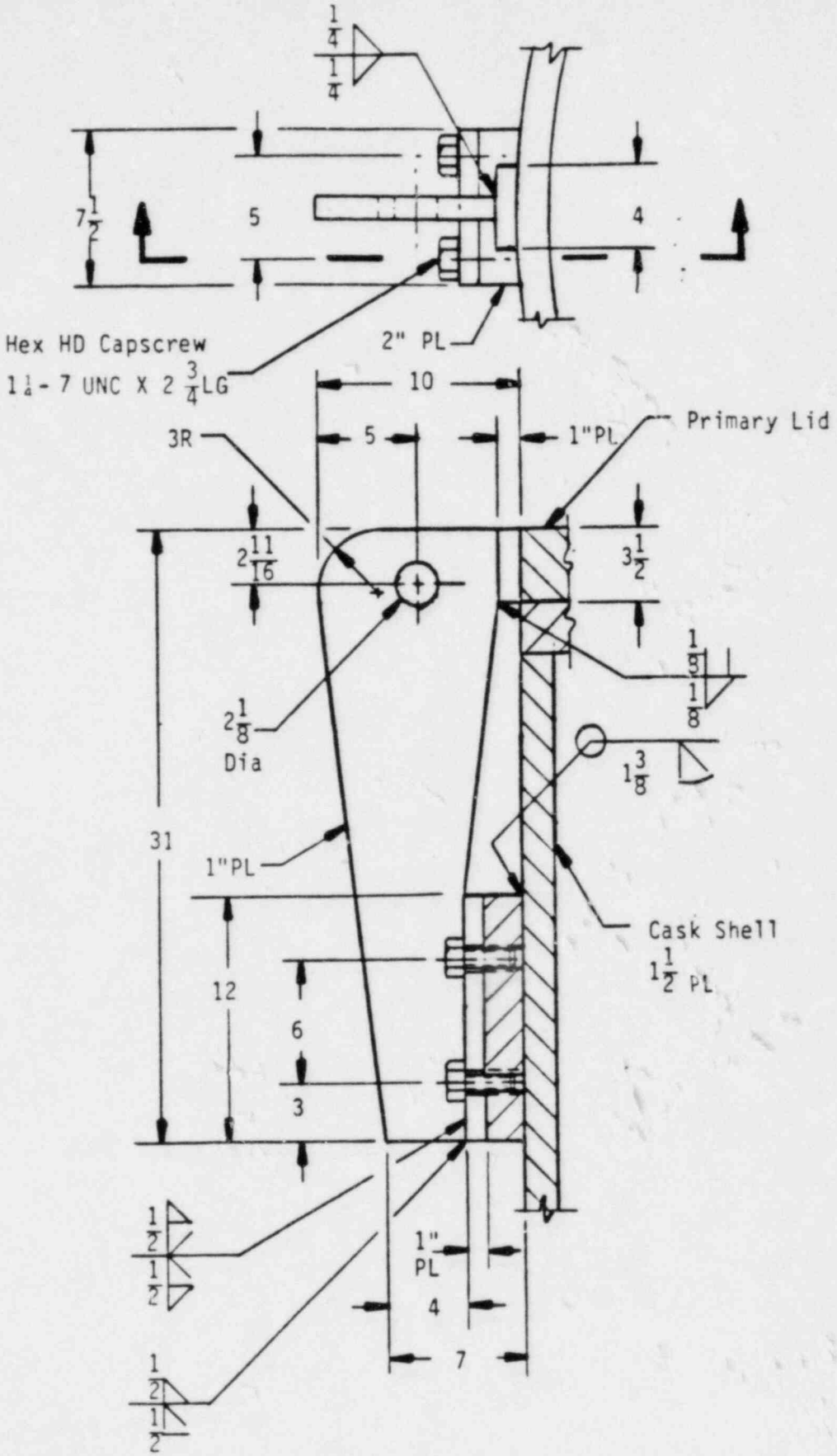

Figure 2.4.3-2 CASK LIFTING EAR

$$\sigma_{smax} = \frac{\sigma_{p1} - \sigma_{p2}}{2}$$

$$= 34322 \text{ psi}$$

The factor of safety for the bolts is:

$$F.S. = \frac{\sigma_{allow}}{\sigma_{actual}} = \frac{(0.5)(\sigma_{yield})}{\sigma_{actual}}$$

$$= \frac{(0.5)(130000)}{34322}$$

$$= 1.89$$

(4) Lifting Ear Mounting Plate Weld Stresses

The stresses in the welds attaching the lifting ear mounting plate to the cask outer shell are found by applying the bolt shear and tensile forces to the weld around the perimeter of the plate. The shear stress in the weld due to the shear force is given by

$$\sigma_{sv} = \frac{V}{A_w}$$

where A_w = effective weld area

$= 2(b+L)(t)(1.0)$

b = plate width = 7.5 in.

L = plate length = 12 in.

t = weld leg dimension = 1.375 in.

V = shear force = 99750 lb.

σ_{sv} = 1860 psi

The shear stress in the weld due to the tensile force is given by:

$$\sigma_{st} = \frac{F}{A_w}$$

where A_w = weld area as defined above

F = tensile force = 5778 lb.

2.4.3.1 Cask Lifting Ears (continued)

$$\sigma_{st} = 106 \text{ psi}$$

The maximum shear stress is given by:

$$\sigma_{smax} = \sqrt{\sigma_{sv}^2 + \sigma_{st}^2}$$

$$= 1864 \text{ psi}$$

This corresponds to a factor of safety for the welds of:

$$F.S. = \frac{\sigma_{allow}}{\sigma_{actual}} = \frac{19000}{1864}$$

$$F.S. = 10.19$$

(5) Outstanding Lifting Ear Plate Weld Stresses

The outstanding lifting ear plate is attached to the lower flush plate with a vertical double vee weld, as shown in Figure 2.4.3-2.

The shear stress in the weld due to the shear force is given by:

$$\sigma_{sv} = \frac{V}{A_w}$$

where A_w = effective weld area = 2tL
t = weld leg dimension = 0.5 in
L = plate length = 12.0 in
V = shear force = 99750 lb.

$$\sigma_{sv} = 8313 \text{ psi.}$$

The shear stress in the weld due to the tensile force is found from

$$\sigma_{st} = \frac{F}{A_w}$$

where A_w = effective weld area as defined above
F = tensile force = 5778 lb.

2.4.3.1 Cask Lifting Ears (continued)

$$\sigma_{st} = 481.5 \text{ psi.}$$

The maximum shear stress is given by:

$$\sigma_{smax} = \sqrt{\sigma_{sv}^2 + \sigma_{st}^2}$$

$$= 8327 \text{ psi}$$

This corresponds to a factor of safety for the welds of:

$$F.S. = \frac{\sigma_{allow}}{\sigma_{actual}} = \frac{19000}{8327}$$

$$F.S. = 2.28$$

(6) Cask Lifting Ear Eye Tearout Stresses

The critical tearout area for the cask lifing ear is determined from Figure 2.4.3-2 as:

$$A_{tearout} = [2(t)(d)]$$

where t = section thickness = 1.0 in.
d = tearout distance = 1.6 in.

$$A_{tearout} = 3.20 \text{ in}^2$$

As previously determined, the vertical force applied to the cask lifting ear is 99750 lbs. This results in a nominal tearout stress of:

$$\sigma_{shear} = \frac{P}{A_{tearout}} = \frac{99750}{3.20} = 31172 \text{ psi}$$

The maximum tearout stress is 1.5 times the nominal, or

$$\sigma_{tearout} = 1.5(31172) = 46758 \text{ psi}$$

The maximum shear stress theory predicts an allowable stress of:

$$\sigma_{allowable} = 0.5\ S_y = (0.5)(100000) = 50000 \text{ psi}$$

This corresponds to a factor of safety of:

$$F.S. = \frac{\sigma_{allowable}}{\sigma_{actual}} = \frac{50000 \text{ psi}}{46758 \text{ psi}} = 1.07$$

(7) Threads - Cask Metal

Because the cask material is weaker than the bolt material, failure will occur at the root of the cask material threads. From ref. 6, pp. 272-273, the equations for shear area and the length of thread engagement required to develop full strength of the threads are:

$$A_{TS} = (\pi)(n)(L_e)(D_{min})\left[\frac{1}{2n} + 0.57735\,(D_{min} - E_{nmax})\right]$$

$$L_e = \frac{S_{st}(2A_s)}{(S_{nt})(\pi)(n)(D_{min})\left[(1/2n) + 0.57735(D_{min} - E_{nmax})\right]}$$

where:

D_{min} = Min. O.D. of bolt, in.
= 1.25 in.

E_{nmax} = Max. P.D. of cask threads, in.
= 1.157 in.

S_{st} = Tensile strength of bolt material, psi
= 150000 psi

n = Threads per inch
= 7.0 threads/in

A_s = Stress area of bolt threads, in^2
= 0.969 in^2

S_{nt} = Tensile strength of cask material, psi
= 70000 psi

A_{TS} = Shear area at root of cask threads, $in.^2$

L_e = Length of thread engagement required to develop full strength, in.

$$L_e = \frac{(150000)(2)(0.969)}{\pi(70000)(7)(1.25)\left[1/14 + 0.57735(1.25 - 1.157)\right]}$$

L_e = 1.21 in. deep

2.4.3.1 Cask Lifting Ears (continued)

$$A_{TS} = (\pi)(n)(L_e)(D_{min})[1/2n + 0.57735(D_{min} - E_{nmax})]$$

$$A_{TS} = 4.16 \text{ in}^2$$

From Section 2.4.3.1(3), the bolt tension was determined as 1505 psi

resulting in a shear stress at the threads of:

$$\sigma_{thread\ shear} = \frac{F_{bolt}}{A_{ts}} = \frac{1505}{4.16}$$

$$= 362 \text{ psi}$$

The allowable shear stress is $(0.5)(S_y)$, where the yield stress for the cask body material is 38000 psi.

$$\sigma_{allowable} = (0.5)(38000) = 19000 \text{ psi}$$

The associated factor of safety is:

$$F.S. = \frac{\sigma_{allowable}}{\sigma_{actual}} = \frac{19000}{362} = 52.52$$

2.4.3.2 Primary and Secondary Lid Lifting Lugs The primary and secondary lifting lugs have the same design and are illustrated in Figures 2.4.3-3 and 2.4.3-4. They are sized such that the combined weight of the primary and secondary lids may be lifted from either the secondary lift lugs or the primary lift lugs.

10 CFR 71, subpart 71.31, paragraph C2, states that for a "system of lifting devices which is a structural part only of the lid, the system shall be capable of supporting three times the weight of the lid and any attachments without generating stress in any material of the lid in excess of its yield strength."

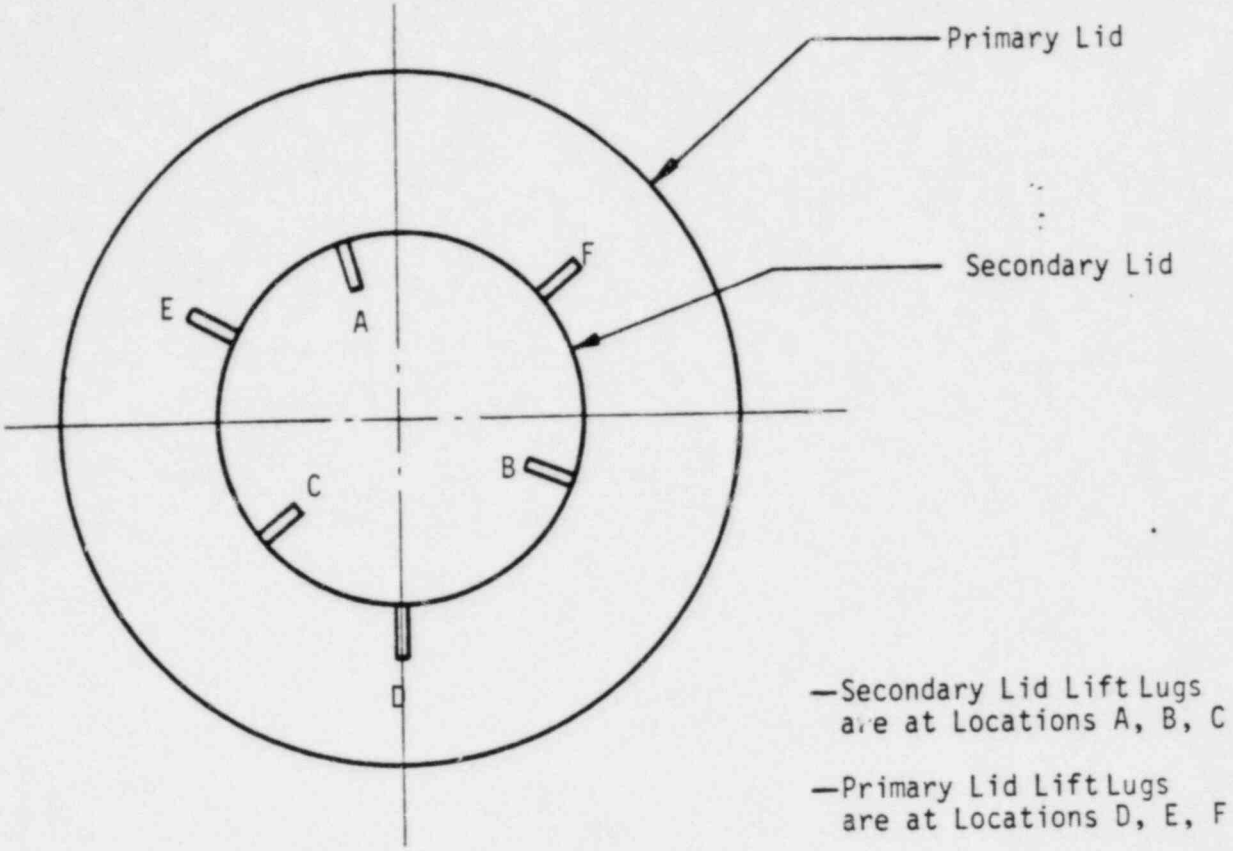

Figure 2.4.3.-3 PRIMARY/SECONDARY LID LIFTING LUG ORIENTATION

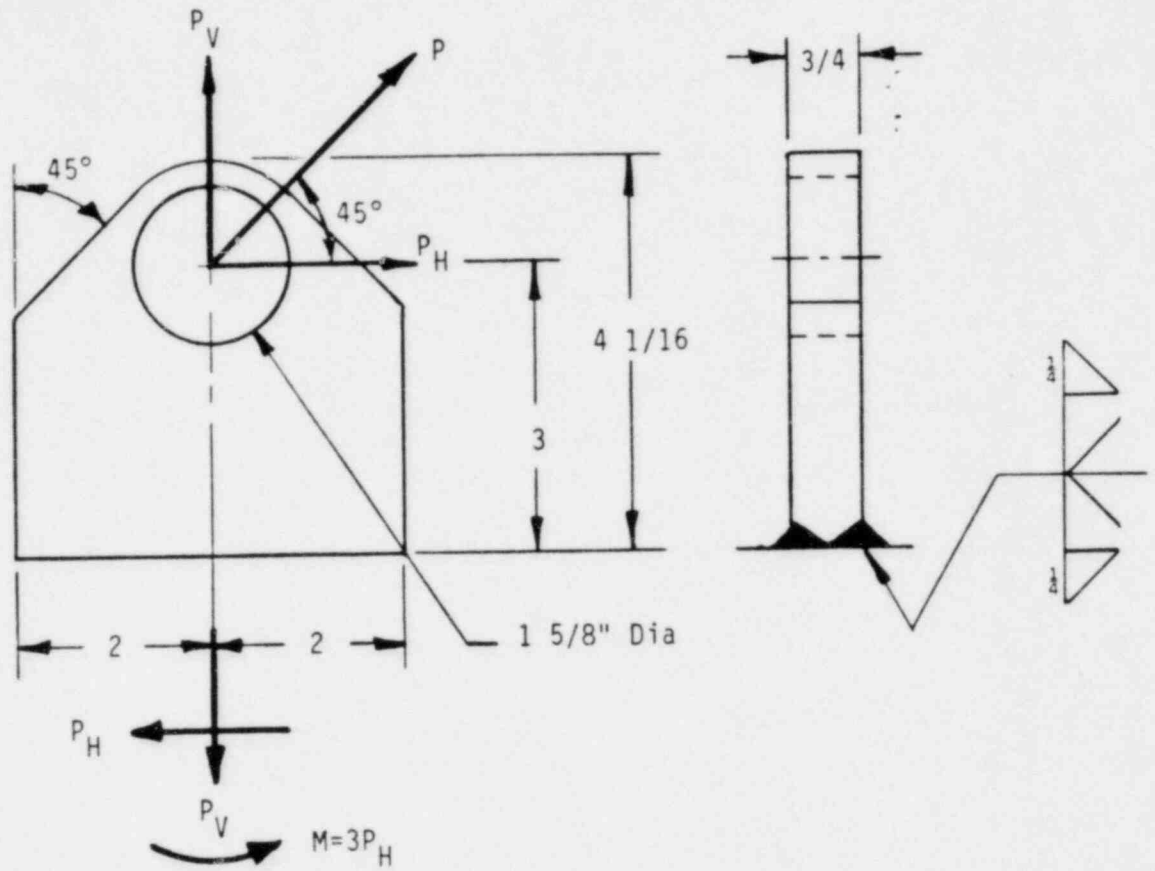

Figure 2.4.3-4 FREEBODY DIAGRAM OF LID LIFTING LUG

(1) Primary and Secondary Lid Lifting Lug Stress Summary

The results of the lifting lug stress analyses are summarized as follows:

Location	Max. Shear Stress Memb.+ Bending (psi)	Factor of Safety
Base	7643	2.49
Tearout	45670	1.10
Lifting hole midplane	11810	4.23

As determined in Section 2.4.3.2 (3), the load for computing the above safety factors is:

$$P = 10352 \text{ lbs.}$$

The detailed stress analyses for each component listed above may be found in subsequent paragraphs.

(2) Failure of the Lid Lifting Lugs Under Excessive Loads

Since failure will first occur in the region of the smallest factor of safety, the lid lifting lugs will fail by eye tearout at a load which produces a maximum shear stress of:

$$\sigma_{failure} = \frac{F_u}{\sqrt{3}} = 66395 \text{ psi (see Section 2.1.2.2)}$$

where $F_u = 115000$ psi.

The failure load can then be computed as:

$$P_{failure} = \frac{P(\sigma_{failure})}{\sigma_{actual}} = \frac{10352(66395)}{45670} = 15050 \text{ lbs.}$$

2.4.3.2 Primary and Secondary Lid Lifting Lugs (continued)

Where P = three times the actual load per lug

σ_{actual} = the stress of the component with the lowest factor of safety.

Should the failure load inadvertently develop, the corresponding stresses in other parts of the lug would be:

Location	σ_{shear} (psi)	Allowable yield stress (psi)
Base	15714	19000
Pinhole midplane	24281	50000

Since the load which causes failure of the lifting lugs does not generate stresses in excess of any other material's yield strength, it can be concluded that remaining components of the lid remain intact and undeformed and may be so considered for meeting the normal and accident shielding and containment requirements.

(3) Weight Analysis

Weights of the primary and secondary lids are as follows:

Primary lid (including bolts)	5180 lb.
Secondary lid	2140 lb
Total lid weight	7320 lbs

The effective weight to be lifted be each lug, P_v from Figure 2.4.3-4, is therefore determined as:

$$P_v = \frac{3(7320)}{3 \text{ lugs}} = 7320 \text{ lbs.}$$

The total load per lug is determined as:

$$P = \frac{P_v}{\cos 45^\circ} = \frac{7320}{0.707} = 10352 \text{ lbs.}$$

This results in a shear force of:

$$P_H = P\cos 45° = 10352(0.707) = 7320 \text{ lbs.}$$

(4) Base Stresses

The tensile stress at the bottom of the lifting lug as shown on figure 2.4.3-4 is:

$$\sigma_{tens} = \frac{P_V}{A_b}$$

where A_b = base area = (w)(t), in^2.
w = lug width = 4 in.
t = lug thickness = 0.75 in
P_V = vertical reaction = 7320 lbs.

$$\sigma_{tens} = \frac{7320}{3} = 2440 \text{ psi}$$

The bending stress, maximum at the bottom outer edge of each lug, is:

$$\sigma_b = Mc/I$$

where M = bending moment = 21960 in-lb
c = distance to neutral axis = 2 in.

I = moment of inertia = $\frac{(b)(h)^3}{12}$
b = lug thickness = 0.75 in.
h = lug height = 4 in.

$$\sigma_b = 10980 \text{ psi}$$

At the outer edge of the lift ear, the bending stress will add to the tensile stress to produce a total tensile stress of:

2.4.3.2 Primary and Secondary Lid Lifting Lugs (continued)

$$\sigma_{total} = \sigma_{bending} + \sigma_{tens}$$
$$= 10980 + 2440$$
$$= 13420 \text{ psi}$$

The nominal shear stress at the bottom of the lift ear is:

$$\sigma_v = \frac{P_H}{A_b}$$

where P_H = shear force = 7320 lbs.
A_b = base area = 3 in^2
σ_v = 2440 psi

The maximum shear stress is 1.5 times the nominal, or

$$\sigma_{shear} = 1.5(2440 \text{ psi}) = 3660 \text{ psi}$$

The effects of the shear and total tensile stresses are combined to form the principal stresses for the lifting ears as follows:

$$\sigma_{p1}, \sigma_{p2} = \frac{\sigma_{total}}{2} \pm \left(\left(\frac{\sigma_{total}}{2}\right)^2 + (\sigma_{shear})^2\right)^{1/2}$$

Thus,

$$\sigma_{p1} = 14353 \text{ psi}$$
$$\sigma_{p2} = -933 \text{ psi}$$

The maximum shear stress will be:

$$\sigma_{max\ shear} = \frac{\sigma_{p1} - \sigma_{p2}}{2} = 7643 \text{ psi}$$

The maximum shear stress theory will be used to determine the allowable shear stress. Therefore:

$$\sigma_{allowable} = (0.5)(S_{yield}) = (0.5)(38{,}000) = 19{,}000 \text{ psi}$$

The factor of safety will be:

$$F.S. = \frac{\sigma_{allowable}}{\sigma_{actual}} = \frac{19000}{7643} = 2.49$$

(5) Lifting Lug Tearout Stress Analysis

The critical section for lifting lug tearout was determined to be as shown in Figure 2.4.3-5. Numerically, this area is:

$$A_{shear} = 2(L)(t)$$

where: L = length of tearout section = 0.23 in.
t = section thickness = 0.75 in.

$$A_{shear} = 0.34 \text{ in}^2$$

As previously determined in Section 2.4.3.2(3), the total cable force is 10352 lbs. This results in a shear stress due to tearout of:

$$\sigma_{shear} = \frac{P}{A_{shear}} = \frac{10352}{0.34} = 30447 \text{ psi}$$

The maximum shear stress is 1.5 times the nominal, or

$$\sigma_{smax} = 1.5(30447) = 45670 \text{ psi.}$$

The maximum shear stress theory predicts an allowable shear stress of:

$$\sigma_{allowable} = 0.5\ S_y = 0.5(100000) = 50000 \text{ psi}$$

This translates into a factor of safety of:

$$F.S. = \frac{\sigma_{allow}}{\sigma_{shear}} = \frac{50000}{45670} = 1.10$$

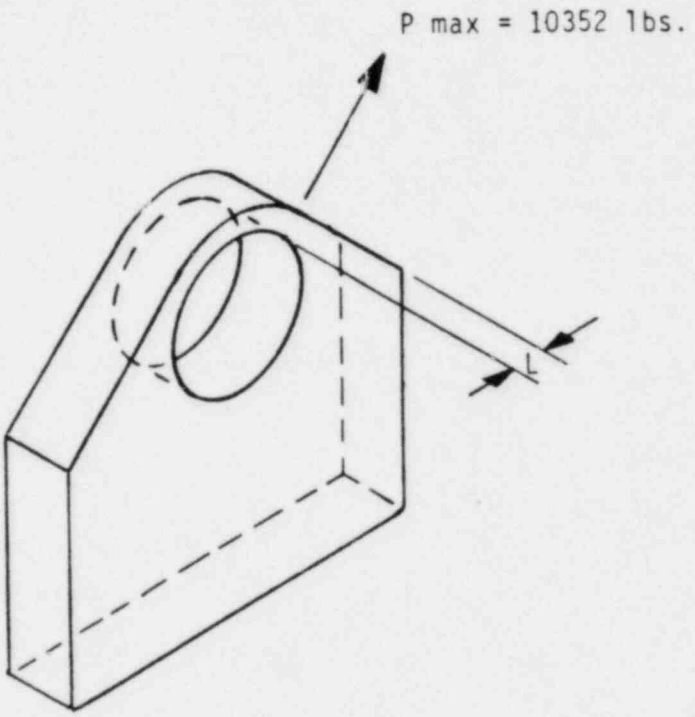

Figure 2.4.3-5 LIFTING LUG EYE TEAROUT AREA

(6) Lifting Lug Stress Analysis at Pin Hole

The maximum tensile stress in the lifting lug occurs in the section of least cross-sectional area, as shown in Figure 2.4.3.-6. Numerically, this area is found to be:

$$A = (W-D)(t)$$

where W = width of lifting lug at hole centerline = 2.94 in.
D = diameter of hole = 1.63 in.
t = plate thickness = 0.75 in.

$$A = 0.98 \text{ in}^2$$

From Section 2.4.3.2(3), the shear and tensile forces were determined as:

$$P_H = P_V = 7320 \text{ lbs.}$$

This translates into a nominal shear and tensile stress of:

$$\sigma_{ns}, \sigma_t = F/A = 7320/0.98 = 7469 \text{ psi}$$

The maximum shear stress is 1.5 times the nominal, or

$$\sigma_{shear} = 1.5\ (7469) = 11204 \text{ psi}$$

Combining the effects of the shear and tensile stresses to form the principal stresses yields:

$$\sigma_{p1}, \sigma_{p2} = \frac{\sigma t}{2} \pm \left[\left(\frac{\sigma t}{2}\right)^2 + \sigma_{shear}^2\right]^{1/2}$$

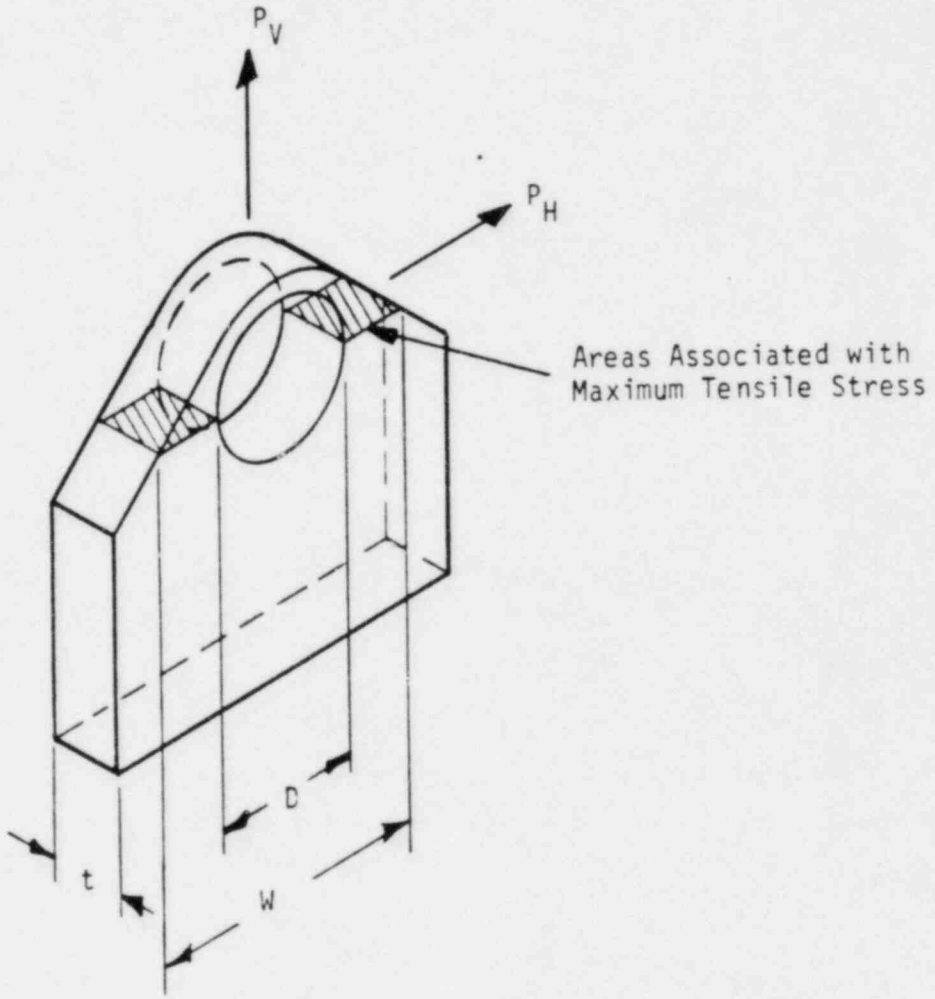

Figure 2.4.3-6 LIFTING LUG NET TENSILE AREA

2.4.3.2 Primary and Secondary Lid Lifting Lugs (continued)

Thus,

$$\sigma_{p1} = 15545 \text{ psi}$$
$$\sigma_{p2} = -8076 \text{ psi}$$

The maximum shear stress is found to be:

$$\sigma_{max} = \frac{\sigma_{p1} - \sigma_{p2}}{2} = 11810 \text{ psi}$$

The maximum shear stress theory predicts an allowable shear stress of:

$$\sigma_{allow} = 0.5\ S_y = 0.5(100000) = 50000 \text{ psi}$$

This translates into a factor of safety of:

$$F.S. = \frac{\sigma_{allow}}{\sigma_{max}} = \frac{50000}{11810} = 4.23$$

2.4.4 Tie-down Devices

The tie-down system for transporting the package is designed in accordance with the loading conditions defined in 10 CFR 71, Paragraph 71.31 (a) (1). This load condition is defined as follows: ". . . The system shall be capable of withstanding, without generating stress in any material of the package in excess of its yield strength, a static force applied to the center of gravity of the package having a vertical component of two times the weight of the package with its contents, a horizontal component along the direction in which the vehicle travels of 10 times the weight of the package with its contents and a horizontal component in the transverse direction of 5 times the weight of the package with its contents."

In addition, the tie-downs are designed such that failure of the tie-down device under excessive load will not impair the ability of the package to meet the other requirements of 10 CFR 71.

The cask lifting ears are removed and the primary and secondary lid lifting lugs covered during transport to prevent them from being used for tie-down purposes.

2.4.4.1 Description of the Tie-down Device The package has been provided with two 1-1/2" thick steel plates (tie-down arms) which are welded to the external shell of the cask body. The steel plates are used for tying the package down. They project outward from the cask in four directions so as to allow specially designed rigging components to be connected to the ends of the tie-down arms. Four shear blocks prevent movement of the base of the package.

The geometric configuration of the tie-down system was selected such that:

(1) The resultant tie-down arm tensile loads are tangent to the cask surface in order to minimize the effects of out-of-plane stresses in the cask shell. (See Figure 2.4.4-1 for determination of the tie-down geometry).
(2) The shear block loads are transferred to the cask surface via compression in the lower overpack.

2.4.4.2 Tie-down Forces The analytic model for determining the loads required to prevent rotation and translation of the package due to the applied loads is shown in Figure 2.4.4-2. The shear block forces at the bottom of the package are initially represented by the orthogonal components of a single force vector, S, occuring at some angle, θ. This base shear resultant is later transformed into individual shear block loads for evaluation of overpack and cask stresses.

The six equations of equilibrium for the freebody diagrams of Figure 2.4.4-2 yield the following for the six unknowns:

$$\Sigma F_x = 0$$

$$\frac{-59}{102.34} T_1 + \frac{59}{102.34} T_2 + \frac{59}{102.34} T_3 - S\sin\theta = 5(74) = 370$$

$$\Sigma F_y = 0$$

$$\frac{72.3}{102.34} T_1 + \frac{72.3}{102.34} T_2 - \frac{72.3}{102.34} T_3 + S\cos\theta = 10(74) = 740$$

$$\Sigma F_z = 0$$

$$\frac{42}{102.34} T_1 + \frac{42}{102.34} T_2 + \frac{42}{102.34} T_3 - V = 2(74) = 148$$

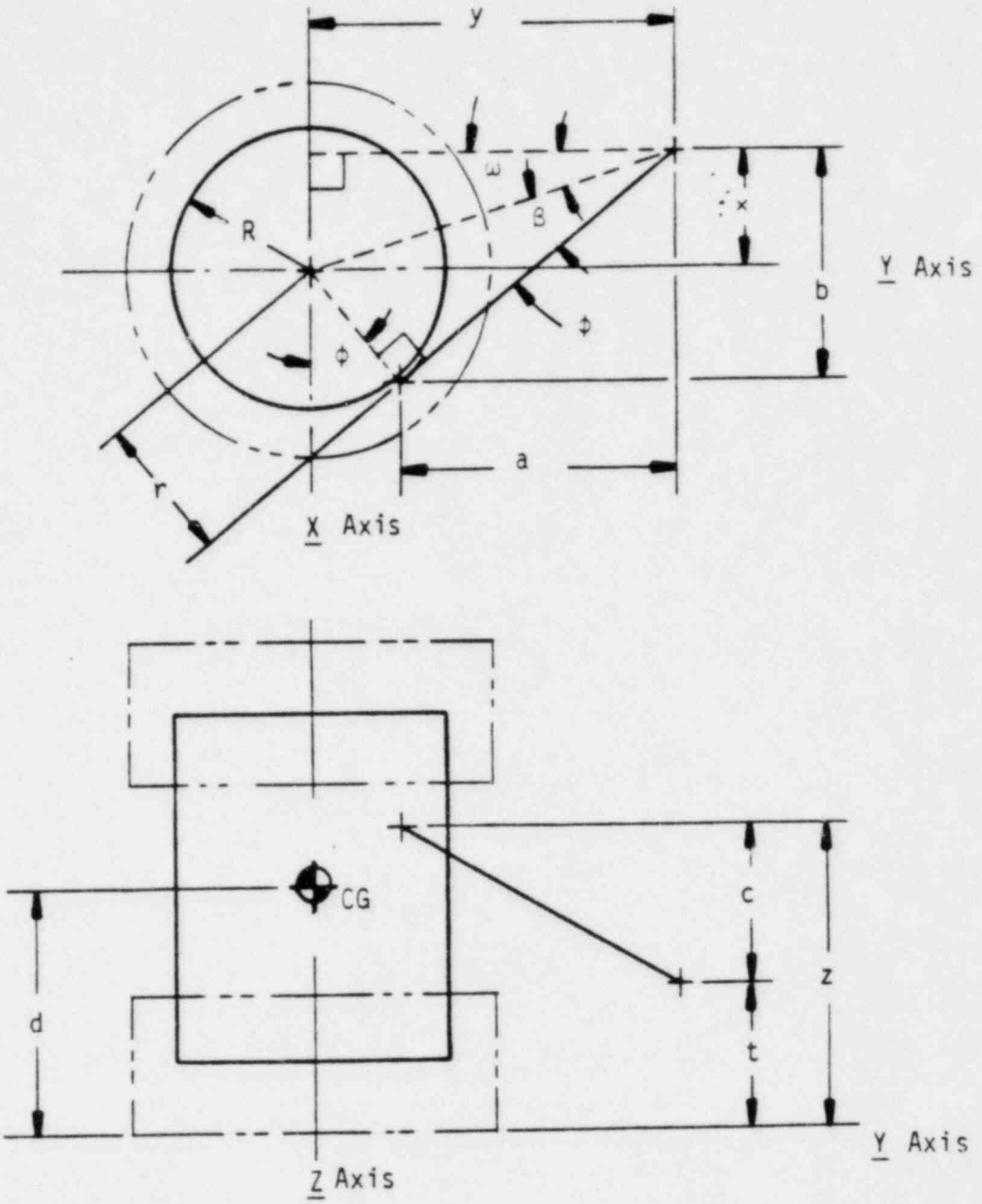

R = 36.75 = CASK RADIUS
r = 37.5 = R+ TANGENT OFFSET
d = 62.5 = CASK C.G. ELEV.
t = 37.0 = TRAILER EAR ELEV.
x = 30.0 = Y AXIS OFFSET
y = 96.0 = $\overline{X}$ AXIS OFFSET
z = 79.0 = $\overline{C}$ASK TANGENT ELEV.
$\omega = 17.35° = ATN\ (x/y)$
$\beta = 21.89° = ASN\ [r/(y/\cos\omega)]$
$\phi = 39.25° = \omega + \beta$
a = 72.27 = $y - r\sin\phi$
b = 59.04 = $x + r\cos\phi$
c = 42.0 = z - t
L = 102.34 = $(a^2 + b^2 + c^2)^{\frac{1}{2}}$

Figure 2.4.4-1 TIE-DOWN ARM GEOMETRY

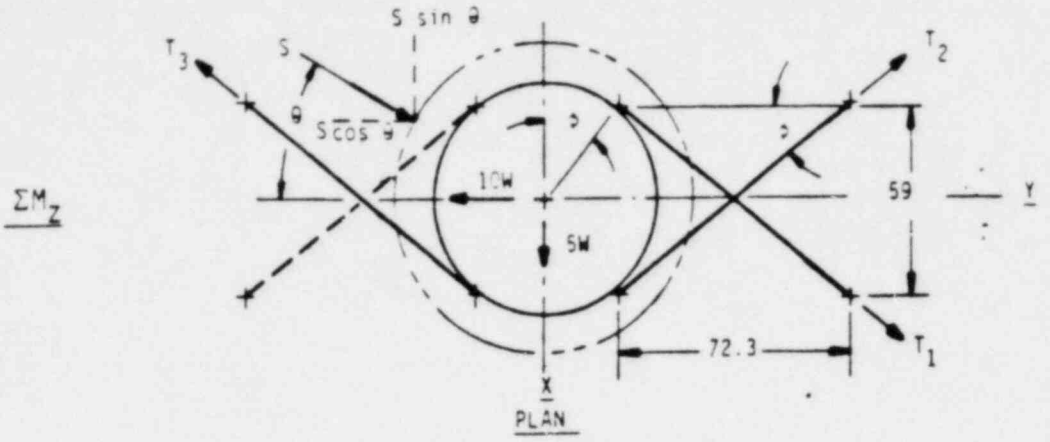

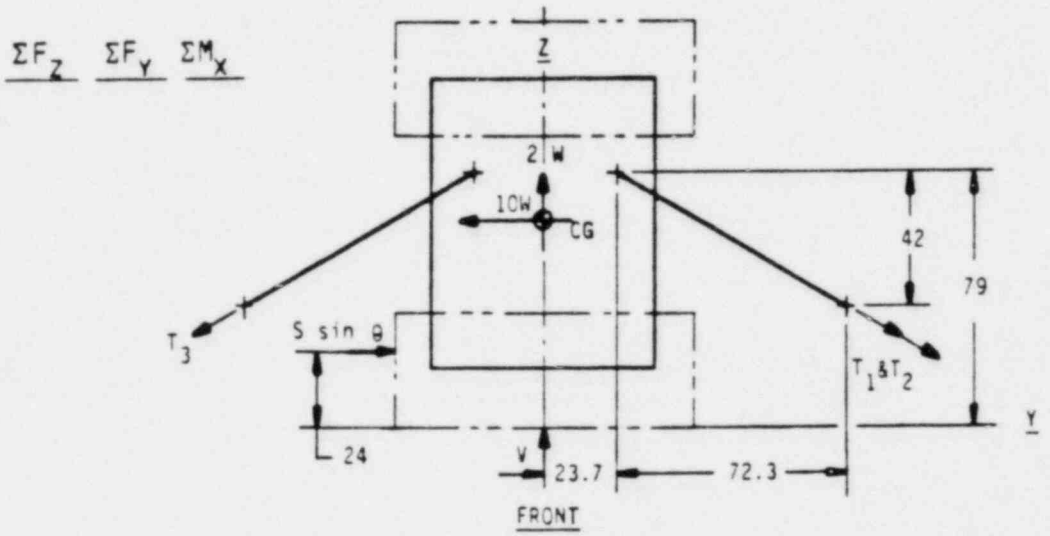

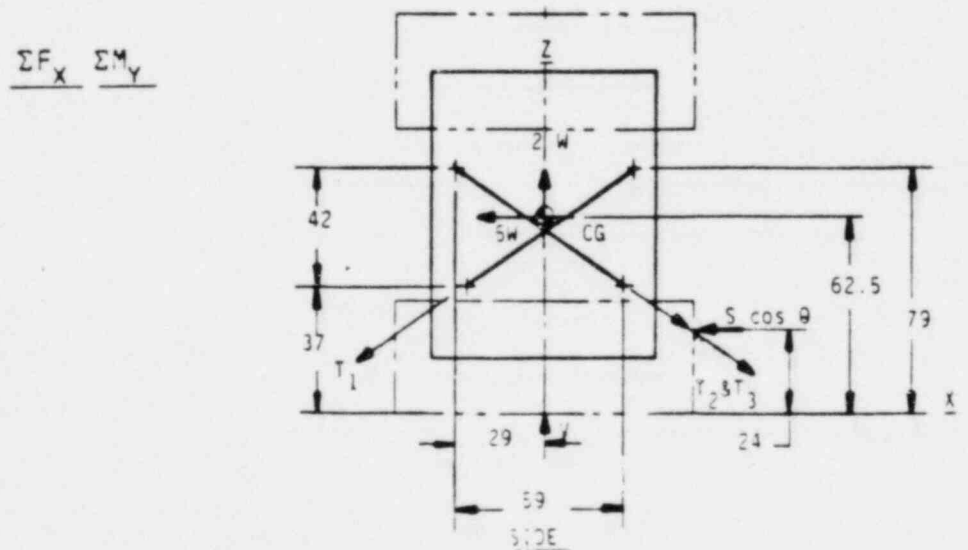

Figure 2.4.4-2 TIE-DOWN FREEBODY DIAGRAMS

2.4.4.2 Tie-down Forces (continued)

$$\Sigma M_x = 0$$

$$\left[\frac{42}{102.34}(23.73) + \frac{72.3}{102.34}(79)\right] T_1 + \left[\frac{42}{102.34}(23.73) + \frac{72.3}{102.34}(79)\right] T_2$$

$$-\left[\frac{42}{102.34}(23.73) + \frac{72.3}{102.34}(79)\right] T_3 + S\cos\theta\,(24) = 10(74)(62.5) = 46250$$

$$\Sigma M_y = 0$$

$$\left[\frac{42}{102.34}(29.04) - \frac{59}{102.34}(79)\right] T_1 + \left[\frac{59}{102.34}(79) - \frac{42}{102.34}(29.04)\right] T_2$$

$$+\left[\frac{59}{102.34}(79) - \frac{42}{102.34}(29.04)\right] T_3 - S\sin\theta\,(24) = 5(74)(62.5) = 23125$$

$$\Sigma M_z = 0$$

$$\left[\frac{(59^2 + 72.3^2)^{1/2}}{102.34}(37.5)\right] T_1 - \left[\frac{(59^2 + 72.3^2)^{1/2}}{102.34}(37.5)\right] T_2$$

$$+\left[\frac{(59^2 + 72.3^2)}{102.34}(37.5)\right] T_3 = 0$$

In matrix notation the equations appear as:

$$\begin{bmatrix} -0.577 & 0.577 & 0.577 & -1 & 0 & 0 \\ 0.706 & 0.706 & -0.706 & 0 & 1 & 0 \\ 0.410 & 0.410 & 0.410 & 0 & 0 & -1 \\ 65.528 & 65.528 & -65.528 & 0 & 24 & 0 \\ -33.657 & 33.657 & 33.657 & -24 & 0 & 0 \\ 34.197 & -34.197 & 34.197 & 0 & 0 & 0 \end{bmatrix} \times \begin{bmatrix} T_1 \\ T_2 \\ T_3 \\ S\sin\theta \\ S\cos\theta \\ V \end{bmatrix} = \begin{bmatrix} 370 \\ 740 \\ 148 \\ 46250 \\ 23125 \\ 0 \end{bmatrix}$$

Simultaneous solution of the six equations yields the following:

T_1 = 293.24 kips
T_2 = 652.75 kips
T_3 = 359.51 kips
$S\sin\theta$ = 44.81 kips

2.4.4.2 Tie-down Forces (continued)

$S\cos\theta = 325.82$ kips

$V = 387.76$ kips

The base shear resultant and the angle at which it occurs are determined as follows:

$$\theta = \tan^{-1}\frac{S\sin\theta}{S\cos\theta} = 7.83°$$

$$S = \frac{S\sin\theta}{\sin\theta} = 328.69 \text{ kips}$$

The individual shear block loads are determined by solving the equilibrium equations for the freebody diagram of Figure 2.4.4-3.

$\Sigma Fx = 0$:

$$(S_2 - S_1)\sin 38° = 44.81 \text{ kips}$$

$\Sigma Fy = 0$:

$$(S_1 + S_2)\cos 38° = 325.82 \text{ kips}$$

Simultaneous solution of the two equations yields:

$S_1 = 170.40$ kips

$S_2 = 243.13$ kips

2.4.4.3 Package Stress Results

The results of the tie-down stress analysis are summarized as follows:

	Max Shear Stress Memb. + Bending(psi)	Factor of Safety
Cask Lid	1868	10.17
Exterior Cask Shell	12400	1.53
Cask Bottom	1243	15.28
Lid Bolts	22795	2.85
Tie Down Arms**	66949	1.49
Lower Overpack*	1017	1.78
Tearout	46315	1.08

2.4.4.3 Package Stress Results (continued)

The above factors of safety correspond to a maximum applied load of P = 652750 lbs. and were computed using the tie-down stress analysis failure criteria described in Section 2.1.2.2(3).

Detailed analyses for each of the above stresses may be found in subsequent sections.

(1) Failure of the Cask Tie-down Arms Under Excessive Loads

Since failure will first occur in the region of the smallest factor of safety, the tie-down arms will fail by edge tearout at a load which produces a maximum shear stress of:

$$\sigma_{failure} = \frac{F_u}{\sqrt{3}} = 66395 \text{ psi (see Section 2.1.2.2)}$$

where F_u = 115000 psi so as to give a conservative value of the maximum shear stress for either ASTM A517 or A514 steel.

The failure load can then be computed as:

$$P_{failure} = \frac{P(\sigma_{failure})}{\sigma_{actual}} = \frac{(652750)(66395)}{46315} = 935752 \text{ lbs.}$$

where P = Maximum tie-down arm load = 652750

σ_{actual} = stress of the component with the lowest factor of safety.

Should the failure load inadvertently develop, the corresponding stresses in other parts of the tie-down arm would be:

---

* Compression Stress

** Tension Stress

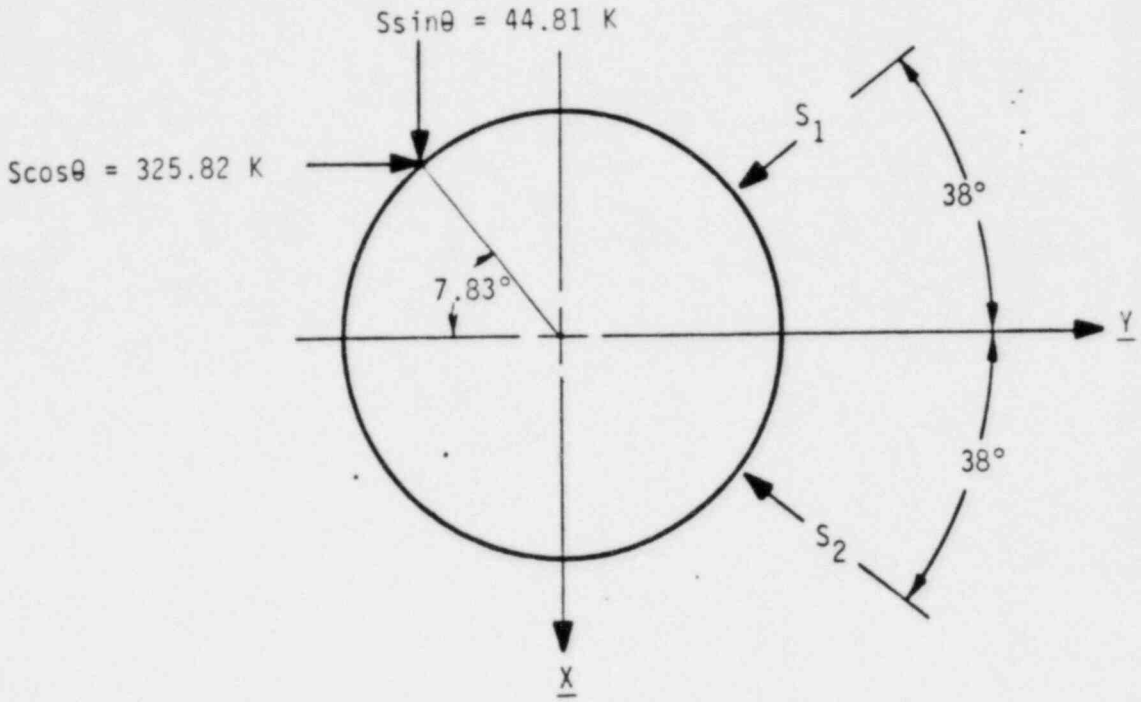

Figure 2.4.4-3 INDIVIDUAL SHEAR BLOCK LOADS

2.4.4.3 Package Stress Results (continued)

Location	σ_{shear} (psi)	Allowable yield stress(psi)
Cask Lid	2678	19000
Exterior Cask Shell	17776	19000
Cask Bottom	1782	19000
Lid Bolts	32678	65000
Tie-down Arms	95975	100000
Lower Overpack	1458	1500

Since the load which causes failure of the tie-down arm does not generate stresses in any material of the cask in excess of its material yield strength, it can be concluded that the cask remains intact and undeformed and may be so considered for meeting the normal and accident shielding and containment requirements.

2.4.4.4 Cask Stress Analysis A finite element stress analysis was performed using STARDYNE to determine stresses in the cask due to the tie-down loading requirements of 10 CFR 71 paragraph 71-31 (d)(1). A description of STARDYNE may be found in Appendix 2.10.5. Because of the non-axisymmetric loading condition, the cask structure was modeled using a 3-D finite element model. The geometric representation of the finite element model relative to the actual cask structure is shown in Figure 2.4.4-4. The finite element model of the cask is described in Figures 2.4.4-5 through 2.4.4-13.

(1) Finite Element Model-Applied Loads

The tie-down arm loads determined in Section 2.4.4.2 were applied to the finite element model as shown on Figure 2.4.4-8. The vertical base reaction, as determined in Section 2.4.4.2, was applied as a pressure to the exterior quad plate elements of the cask bottom. This was conservative in the sense that the pressure applied by the bottom inner surface of the lower overpack was not distributed over the total available area as shown in Figure 2.4.4-14.

The total area of quad plate elements 613 through 644 was determined as 2093.84 in^2.

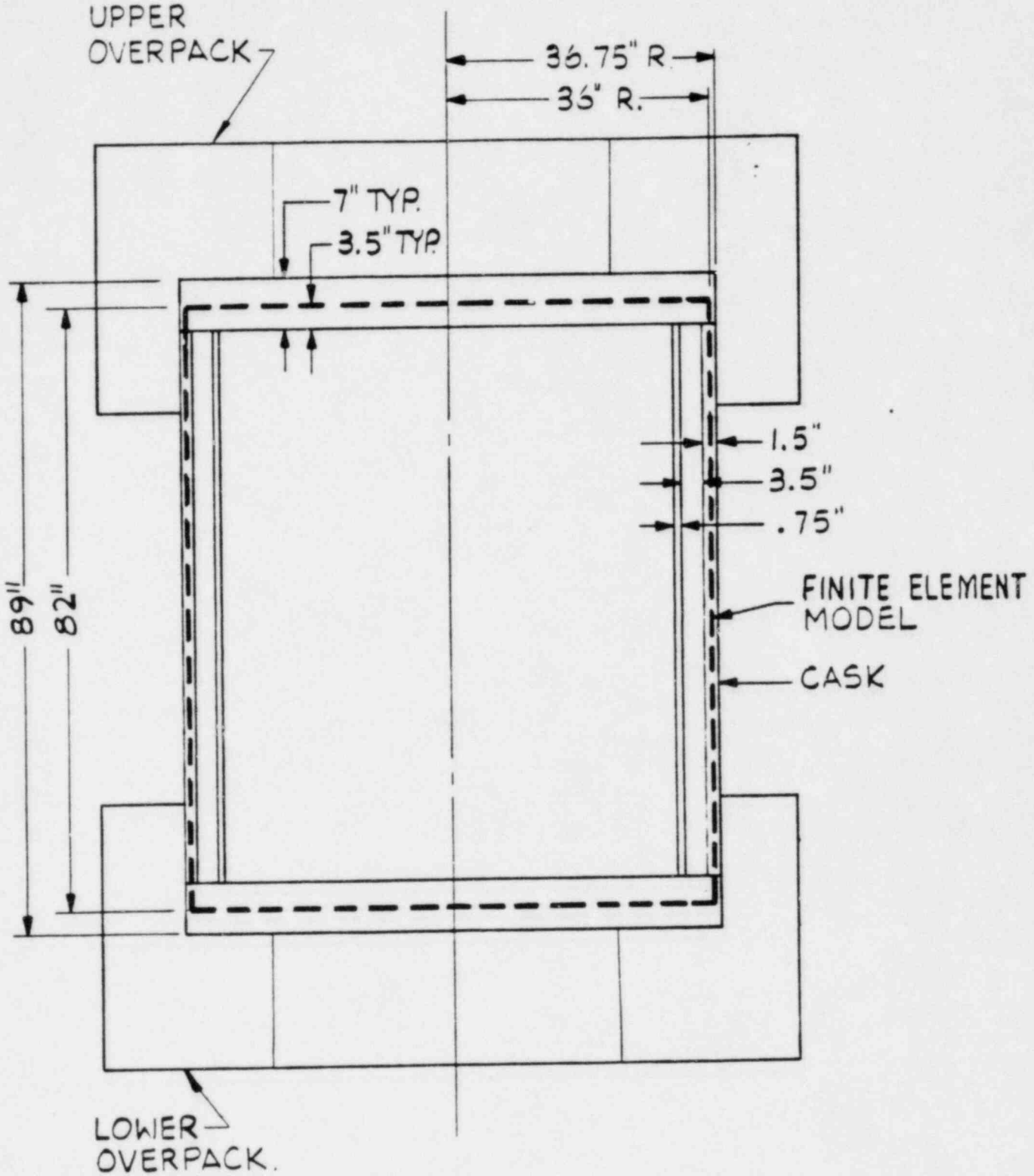

Figure 2.4.4-4—CASK MODEL—GEOMETRIC IDEALIZATION

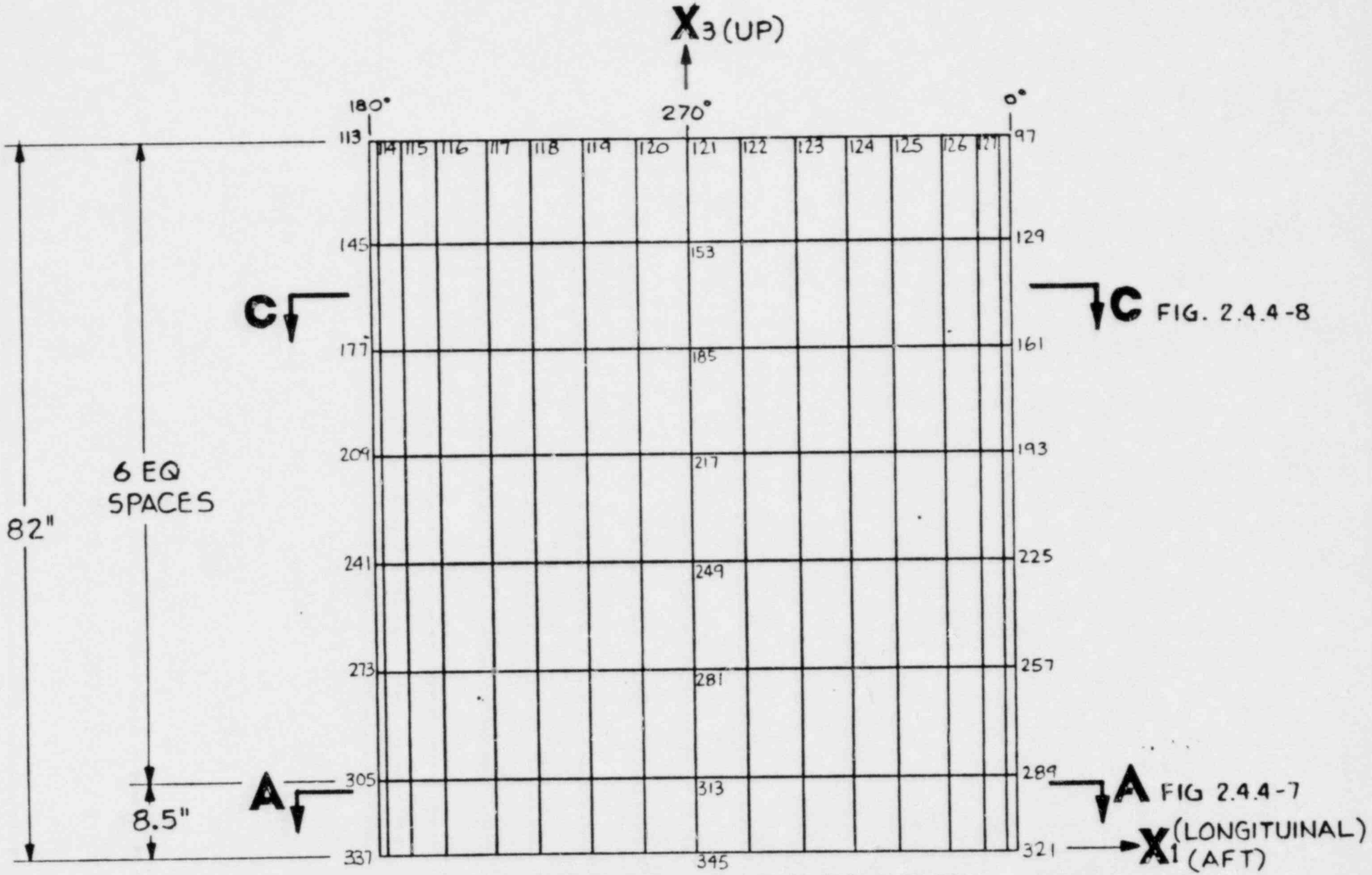

Figure 2.4.4-5 ELEVATION OF MODEL—LKG INB'D FROM LEFT SIDE

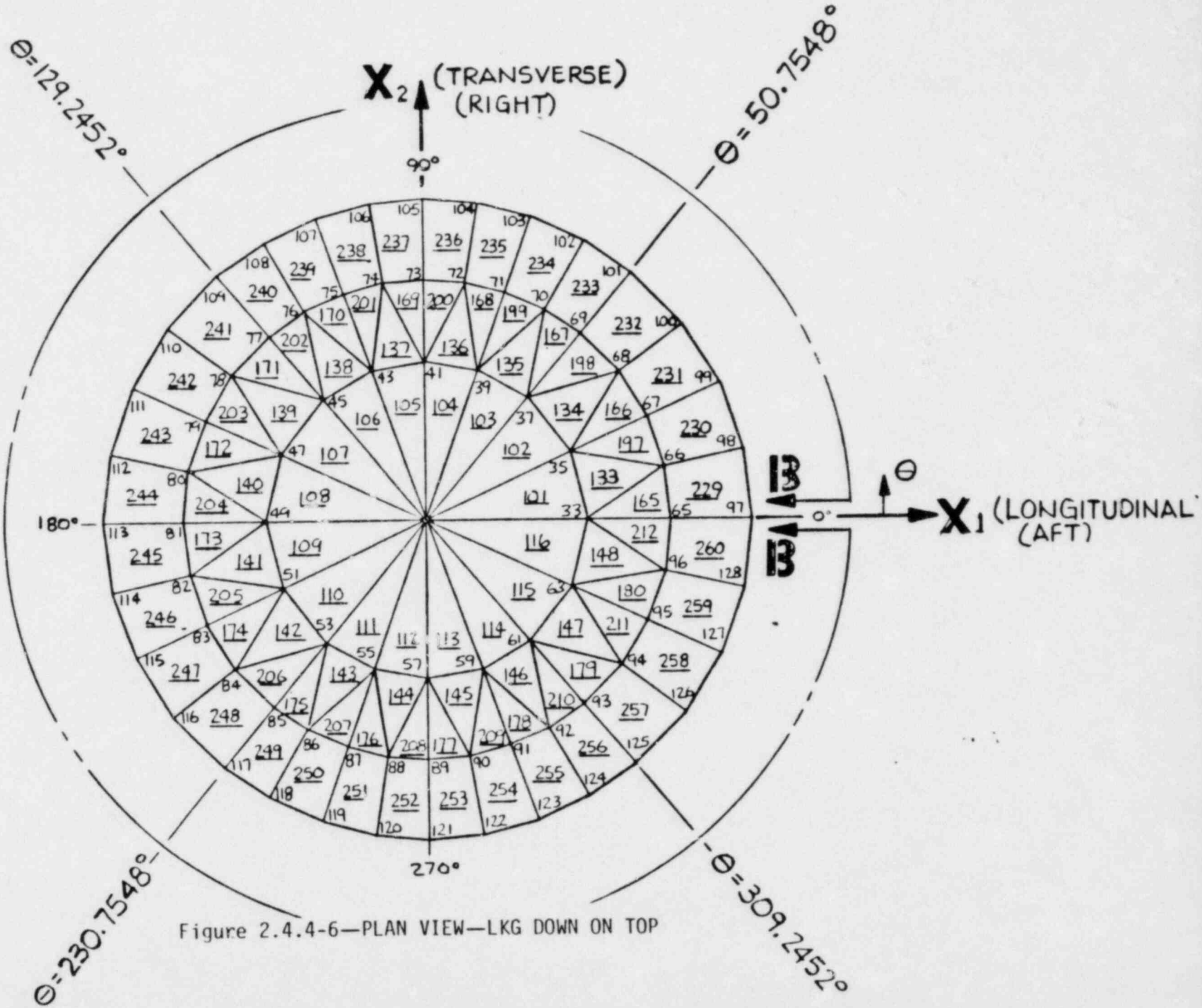

Figure 2.4.4-6—PLAN VIEW—LKG DOWN ON TOP

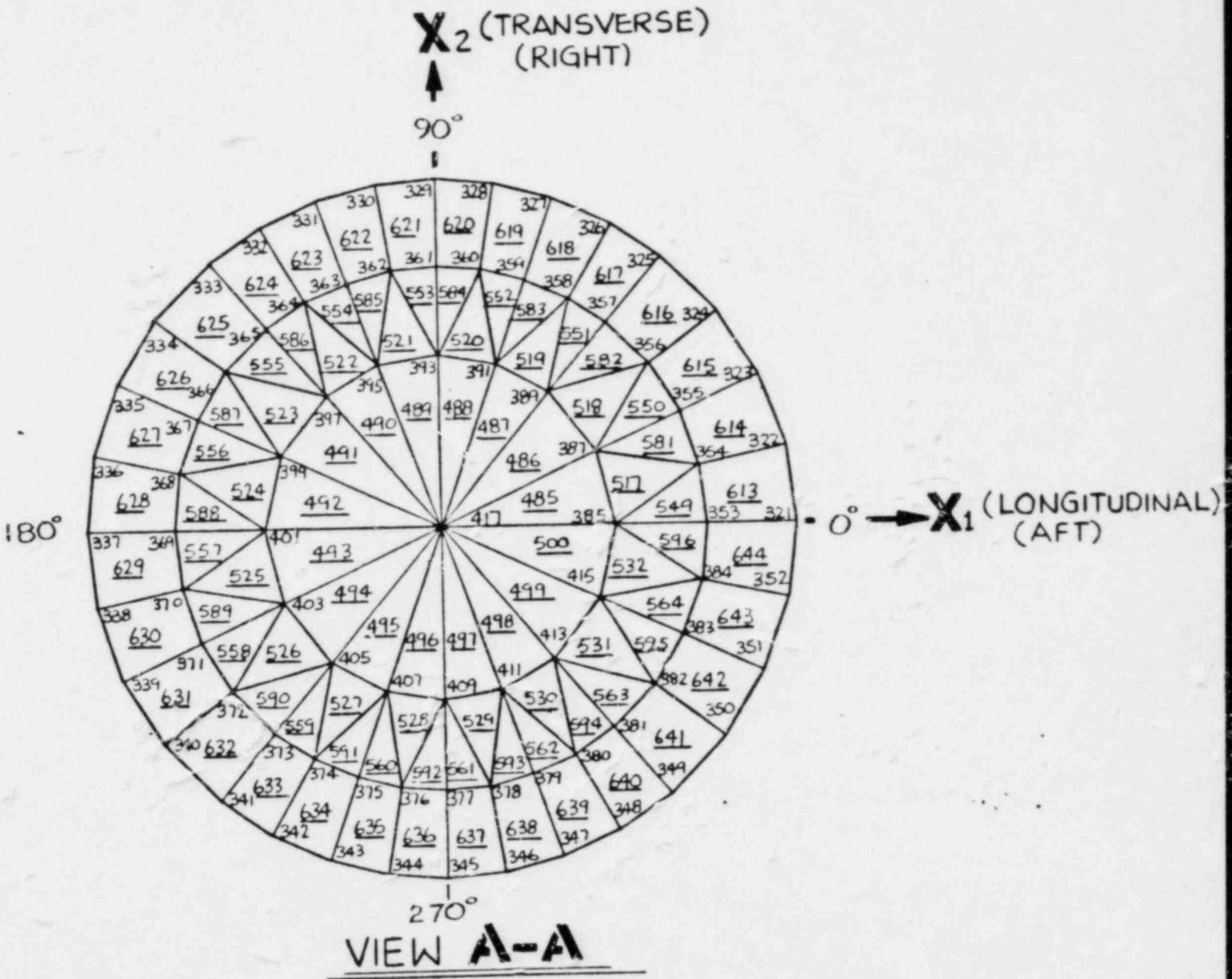

Figure 2.4.4-7—PLAN VIEW—LKG DOWN AT BASE

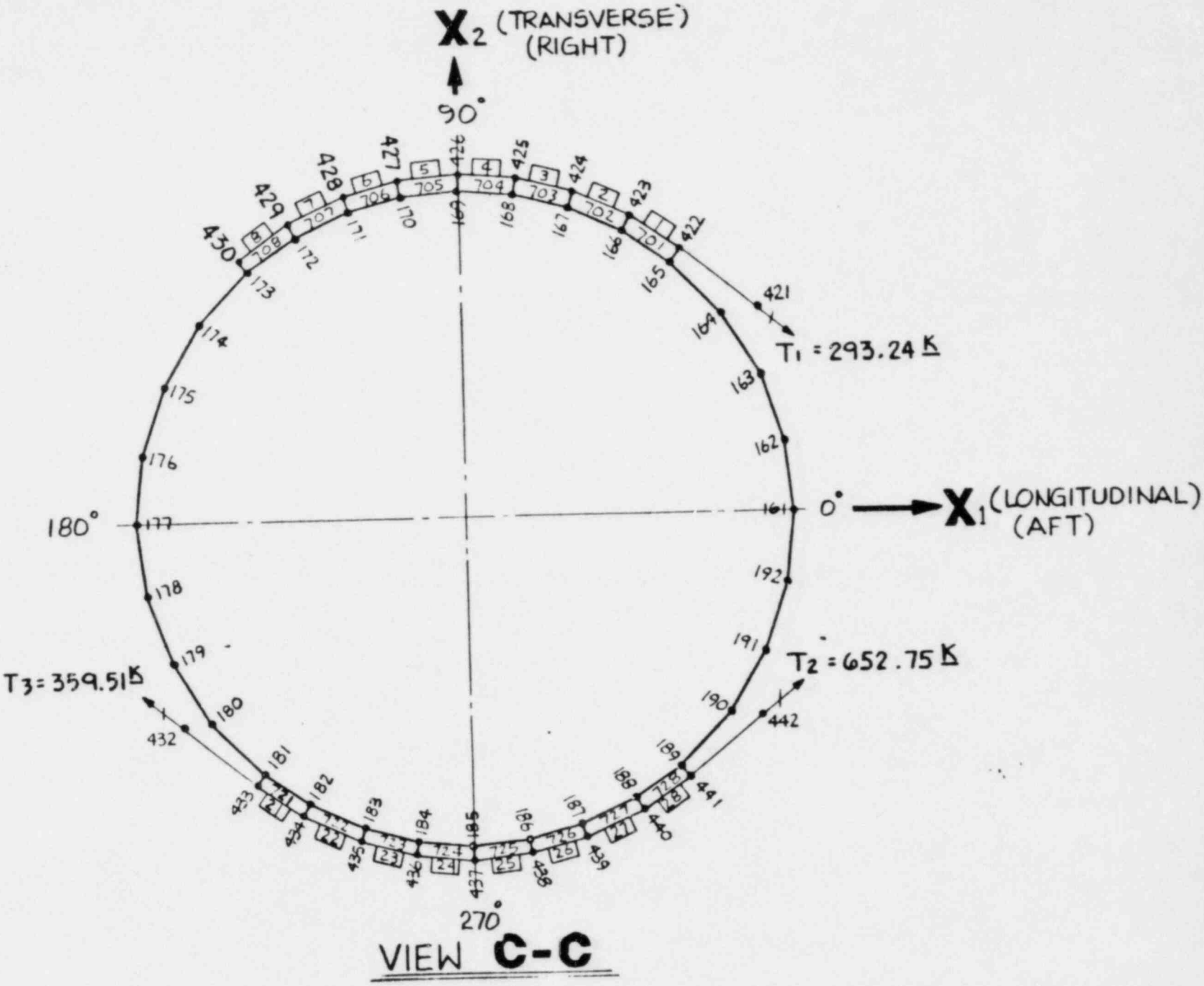

Figure 2.4.4-8—PLAN VIEW—LKG DOWN AT CABLE ATTACHMENT LOCATION

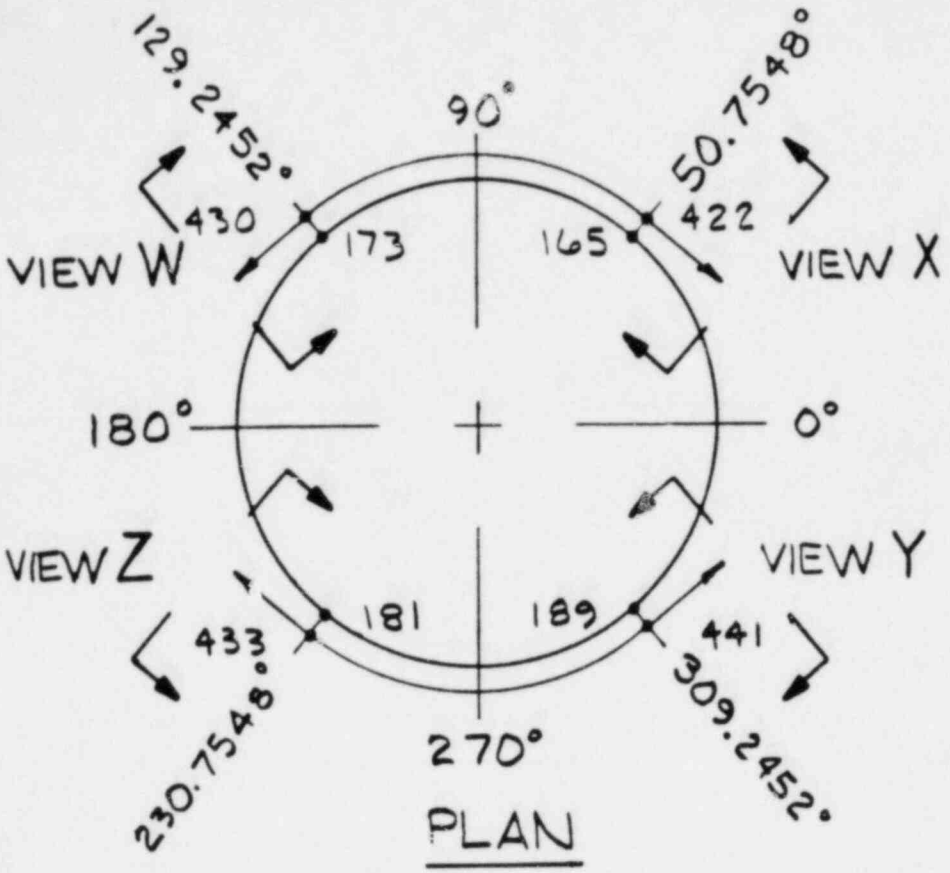

PLAN

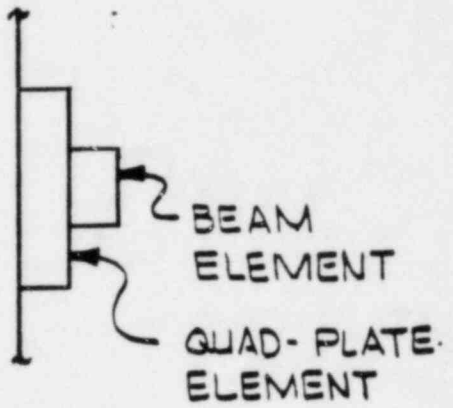

ELEMENT KEY

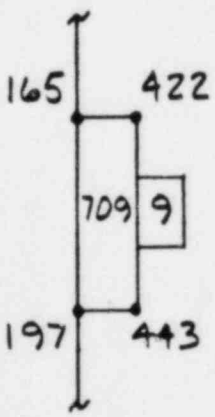

VIEW X
50.7548°

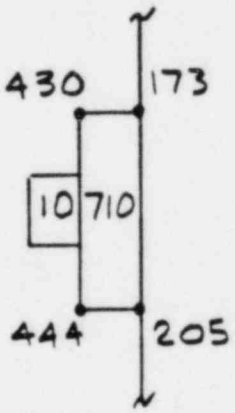

VIEW W
129.2452°

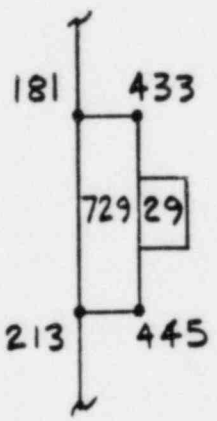

VIEW Z
230.7548°

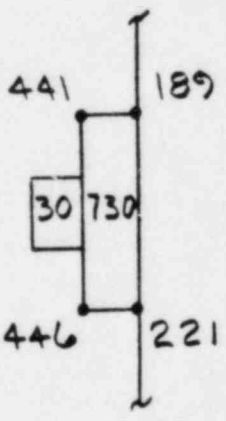

VIEW Y
309.2452°

Figure 2.4.4-9 TIE-DOWN ARM ORIENTATION

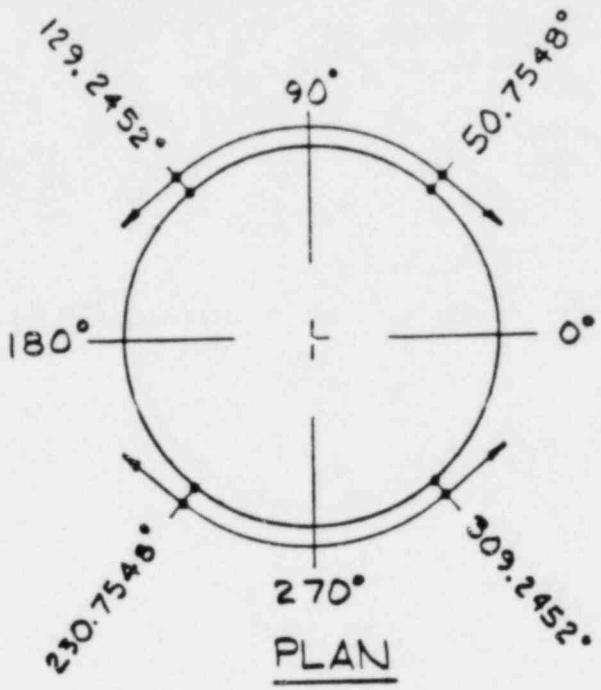

PLAN

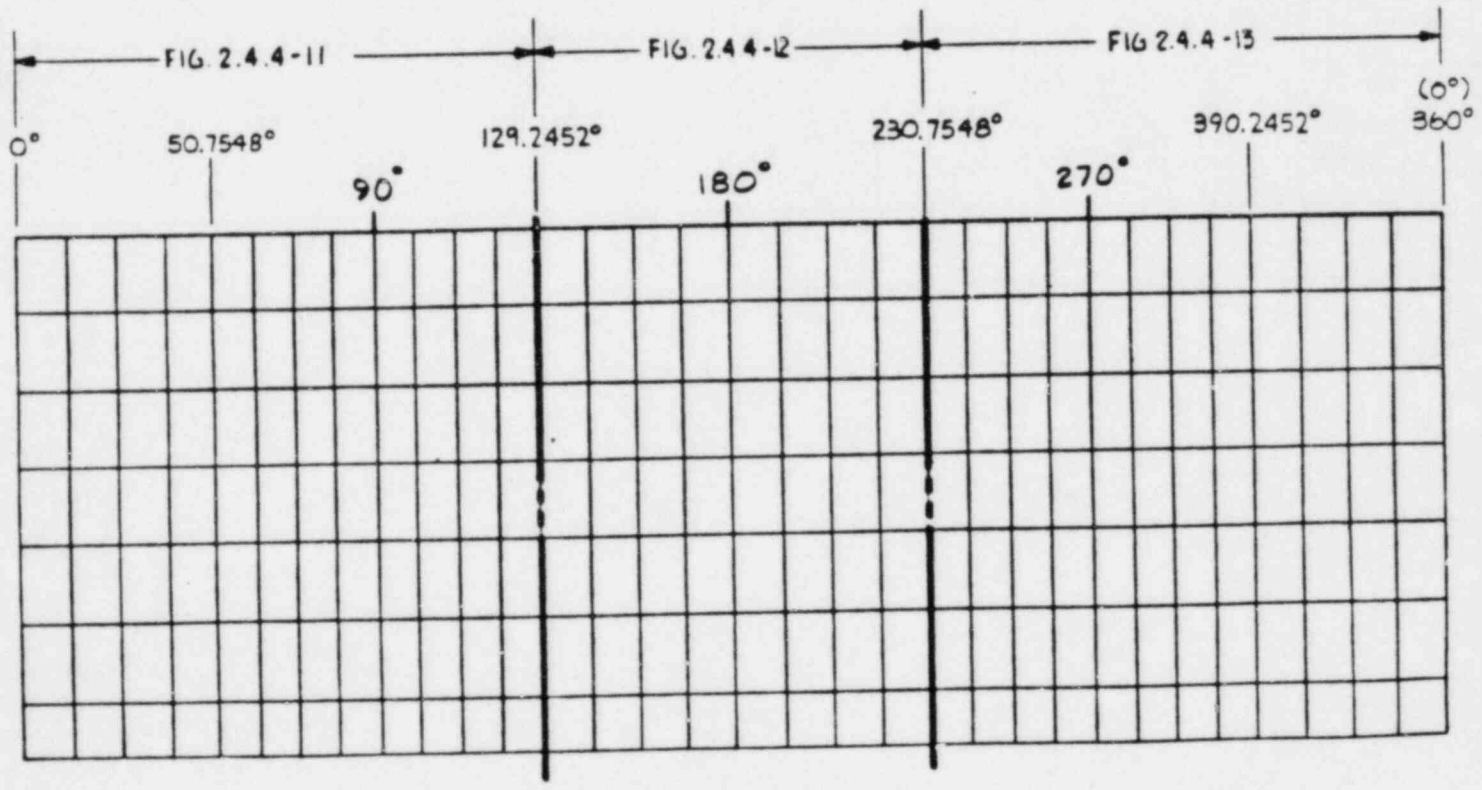

VIEW 13-13

Figure 2.4.4-10—SIDE VIEW—LKG INBOARD AT UNWRAPPED SHELL

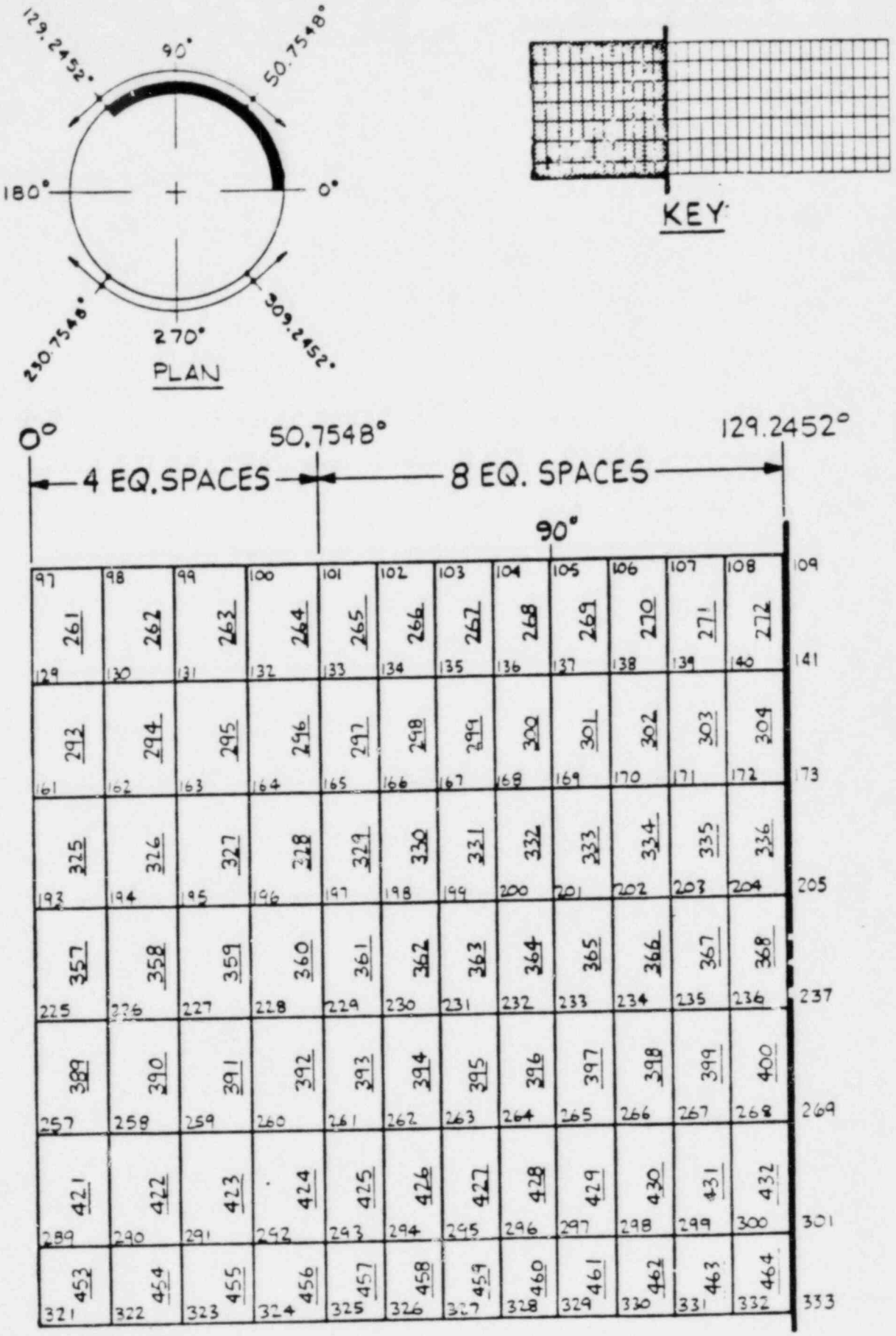

Figure 2.4.4-11—UNWRAPPED SHELL—SECTION I

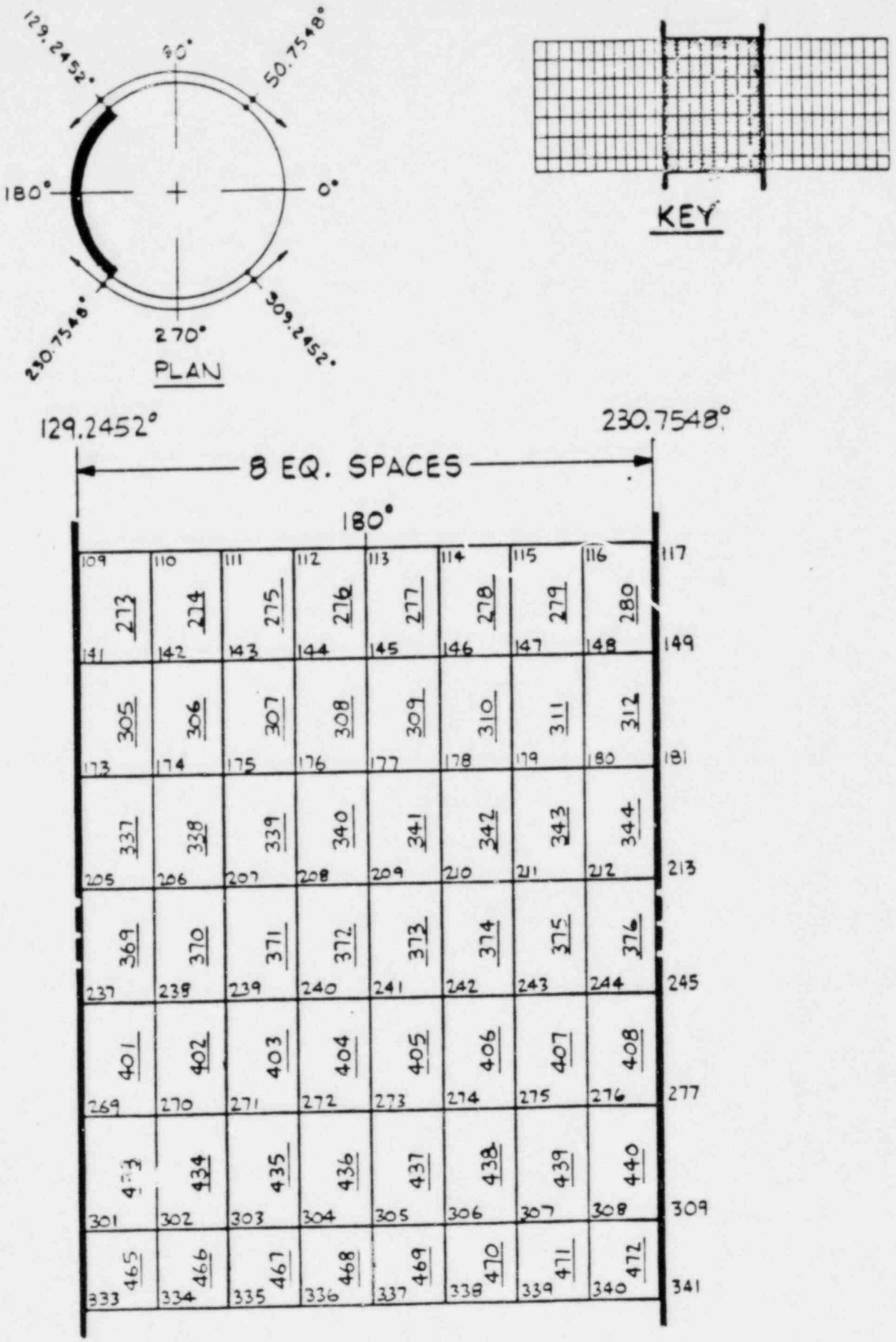

Figure 2.4.4-12—UNWRAPPED SHELL—SECTION II

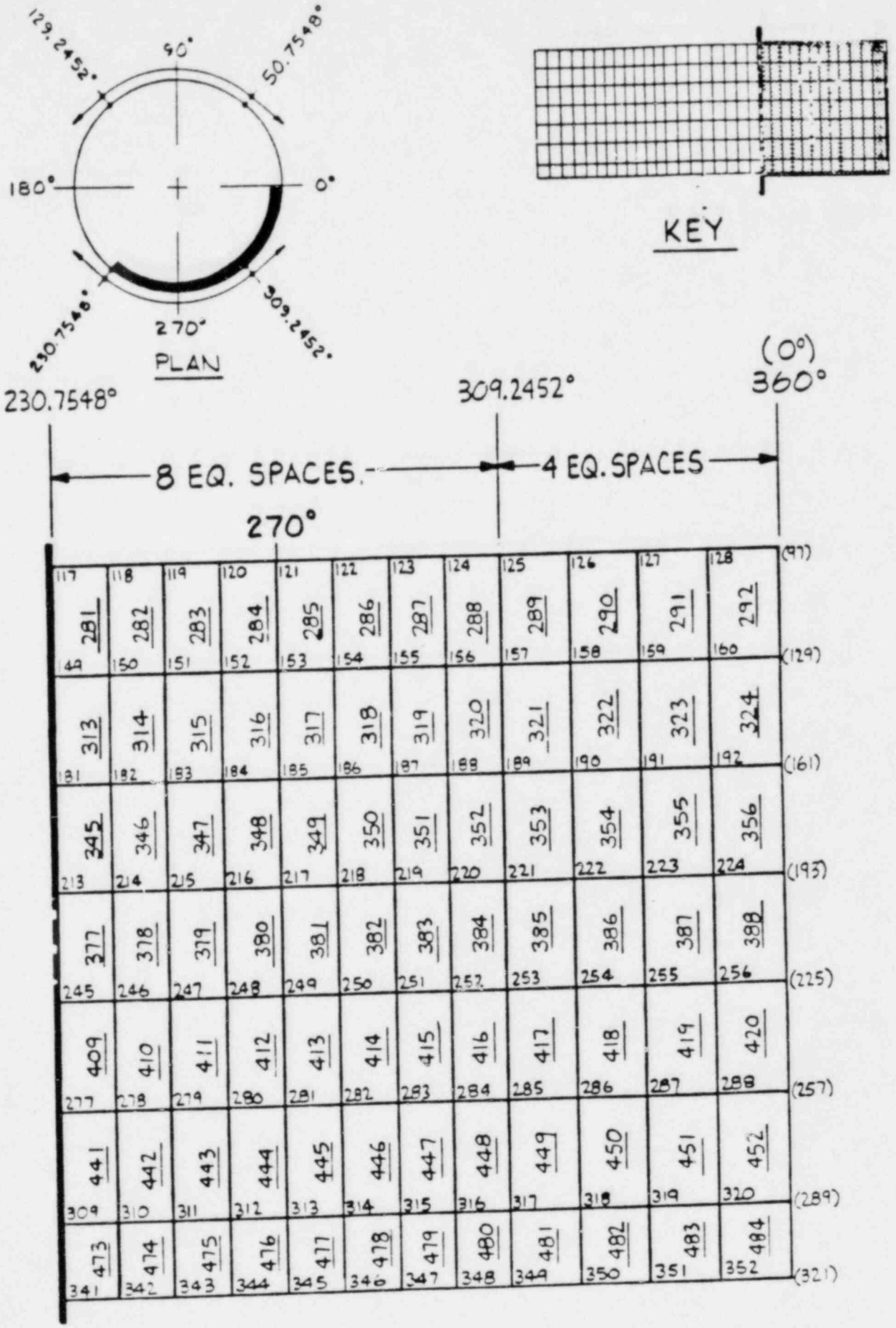

Figure 2.4.4-13—UNWRAPPED SHELL—SECTION III

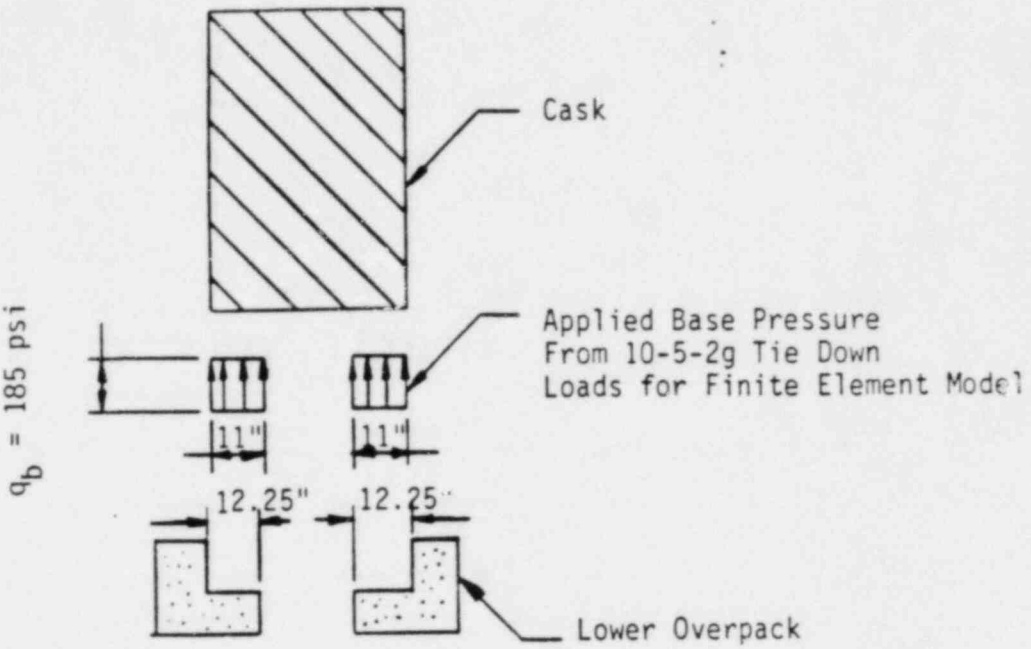

Figure 2.4.4-14—PRESSURE DISTRIBUTION OF BOTTOM OVERPACK

2.4.4.4 Cask Stress Analysis (continued)

The applied plate pressure is therefore:

$$q_b = \frac{V}{2093.84} = \frac{387765}{2093.84} = 185 \text{ psi}$$

The individual shear block loads (k_1, R_2 on Figure 2.4.4-15) were applied to the cask as nodal forces (R_3, R_4, R_5, R_6) near the contact surface between the shear block and the cask. The nodal forces were assumed to be normal to the cask surface and uniform along the circumference. They were determined by solving the following equilibrium equations written for the freebody diagrams of Figure 2.4.4-15 (a-c).

From Figure 2.4.4-15a,

$$\Sigma F_x = 0 \quad (\cos 50.7548 + \cos 38.0661 + \cos 25.3774)\, k_1 + (\cos 50.7548 + \cos 38.0661 + \cos 25.3774)\, k_2 = 325618$$

$$\Sigma F_y = 0 \quad (\sin 50.7548 + \sin 38.0661 + \sin 25.3774)\, R_1 - (\sin 50.7548 + \sin 38.0661 + \sin 25.3774)\, R_2 = 44812$$

Simultaneous solution of these equations shows:

$R_1 = 82433$ lbs.
$R_2 = 57800$ lbs.

Applying equilibrium conditions to Figure 2.4.4-15c yields:

$$\Sigma F = 0 \quad F_1 + F_2 = P$$
$$\Sigma M = 0 \quad P(6) = F_2\,(8.5)$$

Thus,

$F_1 = 0.294\ P$
$F_2 = 0.706\ P$

The individual shear block loads, R_1 and R_2, were resolved into nodal forces, R_3 through R_6, as shown in Figure 2.4.4-15 b,c. Solving for these nodal forces yields:

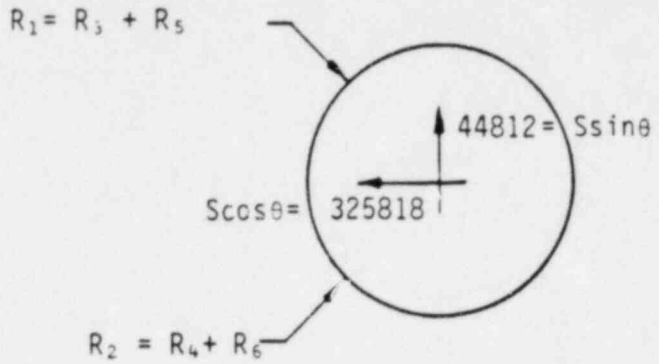

(a)

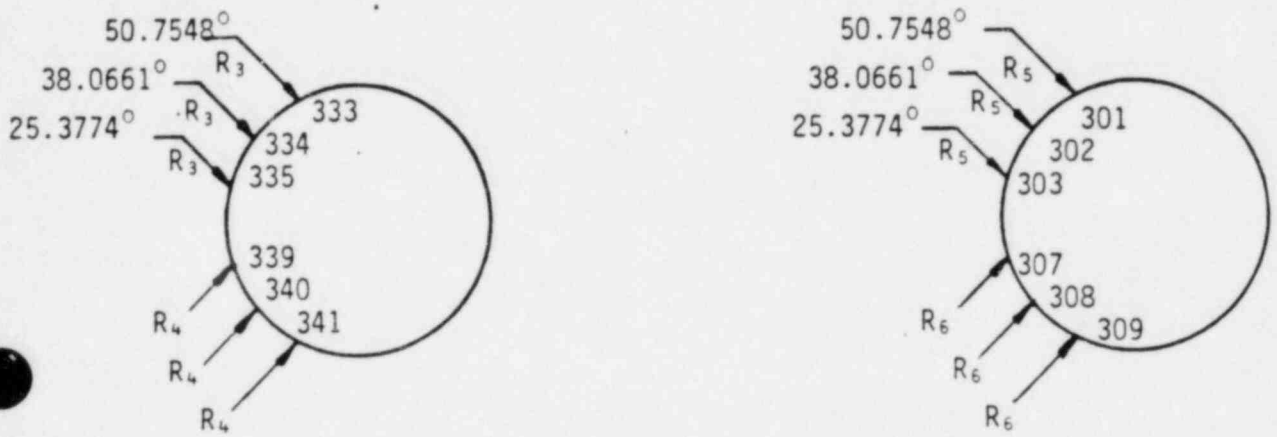

(b)

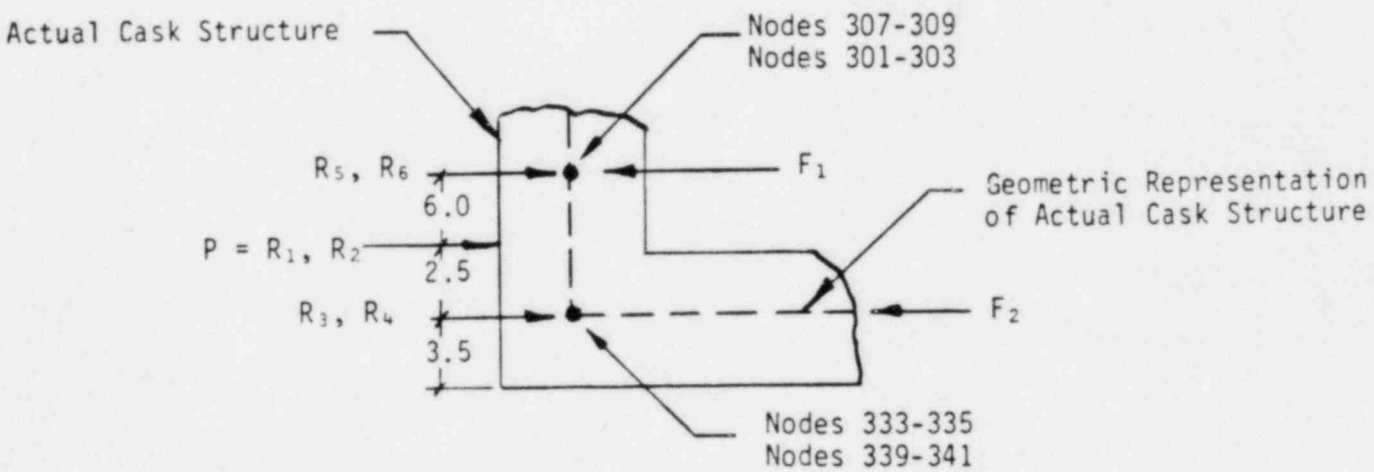

(c)

Figure 2.4.4-15—FREEBODY DIAGRAMS NODAL SHEAR BLOCK LOADS

2.4.4.4 Cask Stress Analysis (continued)

R_3 = 58188 lbs.

R_4 = 40800 lbs.

R_5 = 24245 lbs.

R_6 = 17000 lbs.

(2) Evaluation of Cask Stresses

The input and output for the STARDYNE, Finite Element Stress Analysis may be found on microfiche in Appendix 2.10.5.

The stress results are summarized as follows:

	Max Shear Stress (Memb. + Bending)	Element Number	Factor of Safety
Cask Lid	1868 psi	257	10.17
Exterior Cask Shell	12,400 psi	353	1.53
Cask Bottom	1243 psi	627	15.28

The factors of safety are determined as:

$$F.S. = \left[\frac{\sigma_{\text{shear allowable(membrane + bending)}}}{\sigma_{\text{shear max.}}}\right]$$

where: $\sigma_{\text{shear allowable}} = \frac{Fy}{2} = \frac{38}{2} = 19$ ksi for A516 Gr 70.

2.4.4.5 Lid Bolt Stress Analysis

(1) Lid Bolt Stresses

The cask lid is held in place by 32 ASTM A354 Grade BD 2-8 UN x 4-1/2" bolts, equally spaced around the cask perimeter.

During the 10-5-2 g loading, forces are generated in the lid bolts.

The forces consist of direct bolt tension and bolt shear. In addition, the lid bolts experience a tension due to a prying action bending moment which exists between the side wall of the cask and the cask lid. These forces and moments vary in magnitude and direction around the circumference of the cask, and were determined from the results of the cask finite element stress analysis outlined in Section 2.4.4.5(2).

The maximum lid bolt loads were determined in Section 2.4.4.5(2), and are shown in Figure 2.4.4-16(a) as follows:

V_x = 45955 lb.
V_y = 7423 lb.
V_z = 10605 lb.
M = -28280 in-lb.

- Shear Stress

Since both V_x and V_y act in the plane of the cask lid, they combine to form a resultant shear force on the bolts.

$$F_{shear} = \sqrt{(V_x)^2 + (V_y)^2}$$

$$= \sqrt{(45955)^2 + (-7423)^2}$$

$$= 46550 \text{ lb}$$

Net bolt area for the 2" - 8 UN x 4-1/2" bolts is 2.77 in^2.

This yields a nominal shear stress of:

$$\sigma_{nominal} = \frac{F_{shear}}{A_{bolt}}$$

$$= \frac{46550 \text{ lb}}{2.77 \text{ in}^2}$$

$$= 16805 \text{ psi}$$

2.4.4.5 Lid Bolt Stress Analysis (continued)

The maximum shear stress is found at the center of the bolt cross section and is 4/3 x the nominal shear stress.

$$\sigma_s = 4/3(16805) = 22407 \text{ psi}$$

The effects of this stress are evaluated when combined with the tensile bolt stresses computed in the next section.

- Tension Stress

The edge moment, M, produces a tensile stress on the bolt and an area of compressive contact pressure on the outside edge of the lid as shown in Figure 2.4.4-16a. The maximum bolt tension caused by the prying action moment occurs when the applied moment creates a compressive contact pressure on the outer edge of the lid.

Applying equilibrium conditions to Figure 2.4.4-16a yields:

$$\Sigma F = 0 \qquad T_2 = (1/2)zbl \qquad \text{Equation I}$$

where:

z = compressive contact pressure, psi
b = width of edge section under influence of the bolt, in.
l = length of edge section under influence of the compressive contact pressure, in.
T_2 = bolt tensile force, lbs.

$$\Sigma M = 0$$

$$-M = T_2(L - l/3) \qquad \text{Equation II}$$

where:

M = edge moment, in-lb.
L = length from edge to bolt, in.

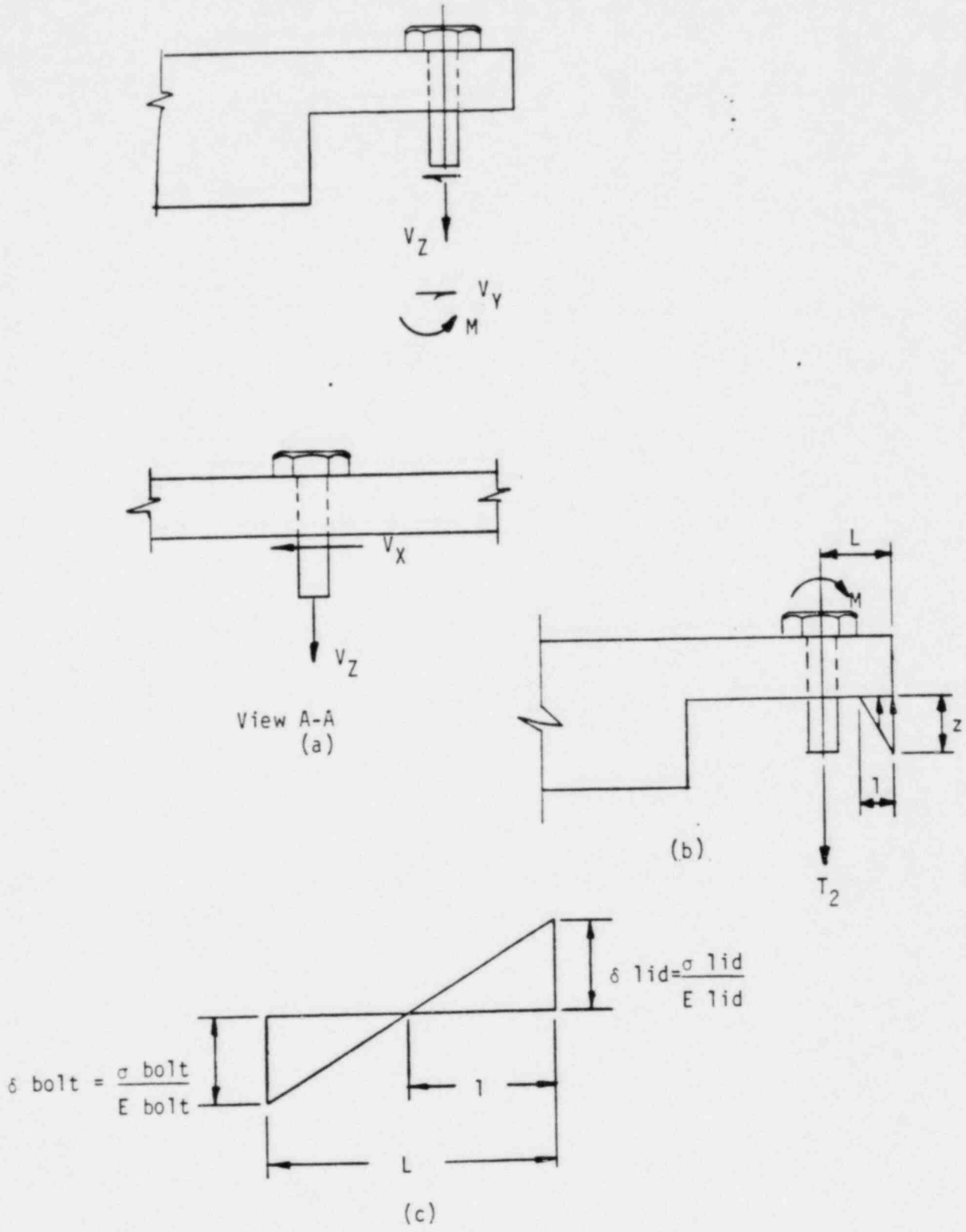

Figure 2.4.4-16 BOLT FREEBODY DIAGRAM AND DEFLECTION DISTRIBUTION

Condition of Compatibility - The deflection analysis assumes that all plane sections remain plane, and that the deflection of the bolt will be proportional to deflection of the lid.

$$\frac{\delta_{bolt}}{\delta_{lid}} = \frac{\left(\frac{\sigma_{bolt}}{E_{bolt}}\right)}{\left(\frac{z}{E_{A516}}\right)}$$

From the bolt and lid deflections shown in Figure 2.4.4-16(b),

$$\frac{\delta_{bolt}}{\delta_{lid}} = \frac{L-l}{l}$$

Therefore,

$$T_2 l = A_{bolt}\, z(L-l)(1.07) \qquad \text{Equation III}$$

Equations,(I), (II), and (III) contain three unknowns: T_2, z, and l.

Substituting equation (I) into equation (II) yields:

$$z = \frac{-2M}{(bl(L-l/3)} \qquad \text{Equation IV}$$

Similarly, substituting equation (I) into equation (III), given:

$$A_{bolt} = 2.77 \text{ in}^2$$
$$E_{A516\text{-}70} = 27.9\text{x}10^6 \text{ psi}$$
$$E_{bolt} = 29.9\text{x}10^6 \text{ psi}$$
$$L = 2.62 \text{ in.}$$
$$b = 7.06 \text{ in}$$

$$(1/2)zbl^2 = A_{bolt}\, z\, (L-l)(1.07)$$

$$3.531^2 + 2.961 - 7.76 = 0$$

$$l = 1.12 \text{ in.}$$

2.4.4.5 Lid Bolt Stress Analysis (continued)

Using equation (IV), the contact pressure is found as:

$$z = \frac{-2h_1}{b_1(L-1/3)} = \frac{-(2)(-28280)}{(7.06)(1.12)(2.62 - 1.12/3)}$$

$$z = 3183 \text{ lb/in}^2$$

Solving equation (I) for the bolt load yields:

$$T_2 = (1/2)zb_1 = \frac{(3183)(7.06)(1.12)}{2}$$

$$T_2 = 12587 \text{ lb.}$$

This tensile bolt load will add directly to the tensile force, V_z, to produce the total bolt load,

$$F_{total} = 12587 + 10605$$
$$= 23192 \text{ lb.}$$

This yields a bolt tensile stress of:

$$\sigma_{tens} = \frac{F_{total}}{A_{bolt}} = \frac{23192}{2.77}$$

$$\sigma_{tens} = 8372 \text{ psi}$$

- Combined Stress

Combining the tensile bolt stress and the resultant shear stress to obtain the principal stresses and the maximum shear stress:

$$\sigma_{p1}, \sigma_{p2} = \sigma_{tens}/2 \pm ((\sigma_{tens}/2)^2 + (\sigma_s)^2)^{1/2}$$

$$\sigma_{p1} = 26981 \text{ psi}$$
$$\sigma_{p2} = -18609 \text{ psi}$$

$$\sigma_{max\ shear} = \frac{\sigma_{p1} - \sigma_{p2}}{2} = 22795 \text{ psi}$$

2.4.4.5 Lid Bolt Stress Analysis (continued)

According to ASTM specificaton A-354, the yield strength for grade BD 2"-8 UN bolts is 130000 psi. Therefore:

$$\sigma_{allowable} = (0.5)(\sigma_{yield}) = (0.5)(130000) = 65000 \text{ psi}$$

The associated factor of safety is

$$F.S. = \frac{\sigma_{allowable}}{\sigma_{actual}} = \frac{65000}{22795} = 2.85$$

(2) Analytic Method for Determining Lid Bolt Loads

Since the lid bolts were not specifically modelled in the finite element geometry, the lid bolt loads (forces and moments) were not directly available from the finite element cask stress analysis output. The method used for determining these loads is described in the following paragraphs.

A typical section of the finite element model where the outside edge of the cask lid joins the cask side wall is shown in Figure 2.4.4-17a.

The global corner forces for each of the four plates at the adjoining node is shown in Figure 2.4.4-17(b). Numerical values of these corner forces were extracted from the finite element analysis output (Table 2.4.4-1) for each node along the outer edge of the lid (nodes 97 through 128).

The global corner forces were added as shown in Figure 2.4.4-17(c). Numerical values for these resultants, Px, Py, Pz, Mx, My, and Mz, are given in Table 2.4.4-2.

2.4.4.5 Lid Bolt Stress Analysis (continued)

The global corner force sums of Figure 2.4.4-17(c) were rotated into a local (edge) coordinate system for each node as shown in Figure 2.4.4-18(a). P'x, P'y, P'z, M'x, M'y and M'z are given in Table 2.4.4-3 and represent the unbalanced nodal loads which must be transmitted from the upper side of the cask body to the lid via the joint continuity provided by the lid bolts. M'y and M'z were found to be zero in the local (edge) coordinate system.

Since the nodes along the outer edge of the lid do not coincide with the bolt locations, the loads of Figure 2.4.4-18(a) were first converted into loads per inch of lid circumference, (lb/in and in-lb/in) as shown in Figure 2.4.4-18(b). Numerical values for q_x, q_y, q_z and qm_x are given in Table 2.4.4-3 and plotted with respect to circumferential position in Figure 2.4.4-19.

Peak edge loads were found from Figure 2.4.4-19 to be:

q_{px} = 6500 lb/in
q_{py} = 1050 lb/in
q_{pz} = 1500 lb/in
q_{pmx} = -4000 in-lbs/in

Even though these peak loads occur at different circumferential positions, they were conservatively assumed to occur simultaneously for determining the maximum lid bolt loads.

The maximum bolt load was determined by multiplying the peak edge loads by the circumferential spacing between bolts as shown on figure 2.4.4-20. Since the 32 bolts are equally spaced around the lid circumference, the spacing between the bolts is:

$l = 2\pi r/32$ bolts = 7.07 in.

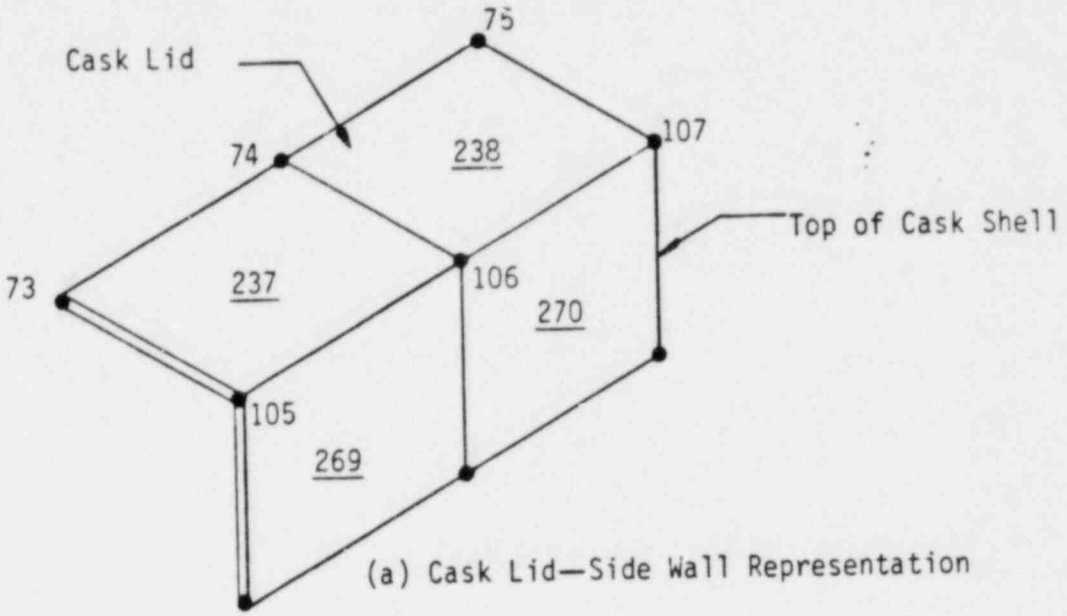

(a) Cask Lid—Side Wall Representation

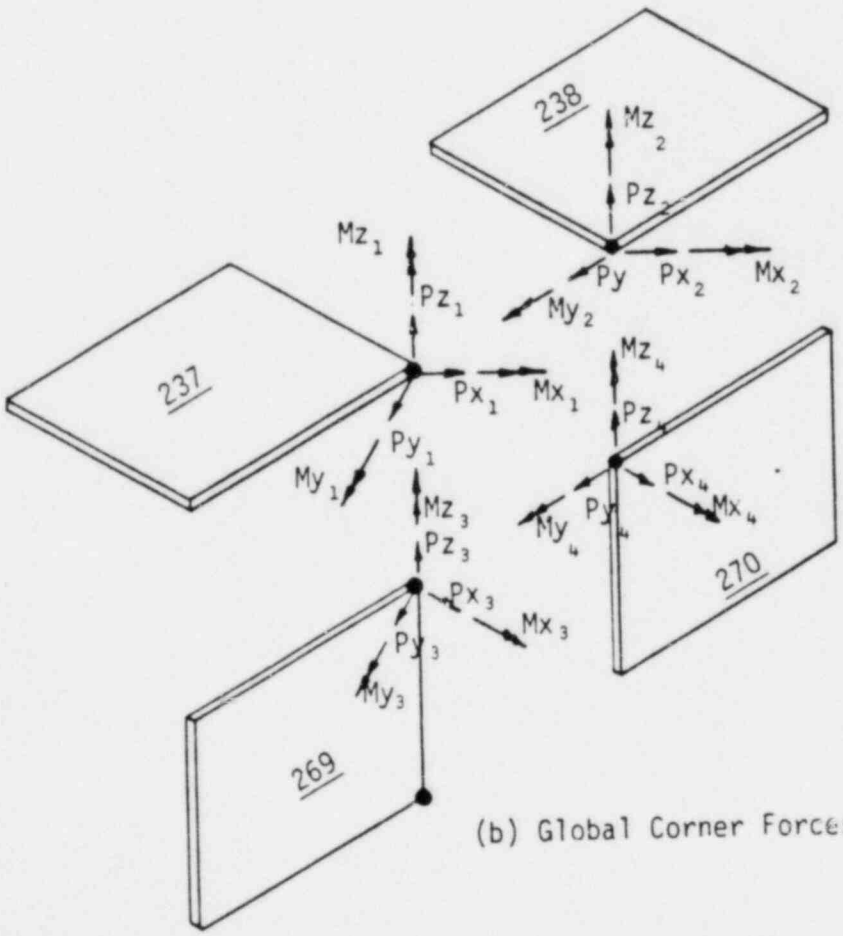

(b) Global Corner Forces at Edge of Lid

Figure 2.4.4-17

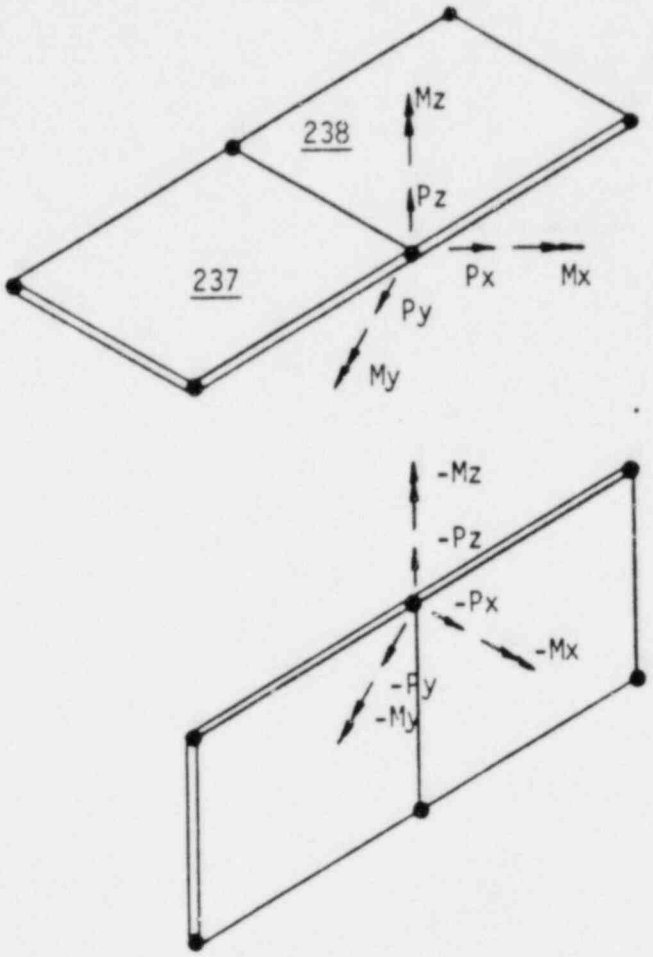

$$Px = Px_1 + Px_2 = -(Px_3 + Px_4)$$
$$Py = Py_1 + Py_2 = -(Py_3 + Py_4)$$
$$Pz = Pz_1 + Pz_2 = -(Pz_3 + Pz_4)$$
$$Mx = Mx_1 + Mx_2 = -(Mx_3 + Mx_4)$$
$$My = My_1 + My_2 = -(My_3 + My_4)$$
$$Mz = Mz_1 + Mz_2 = -(Mz_3 + Mz_4)$$

(c) Global Corner Force Sums at Edge of Lid

Figure 2.4.4-17

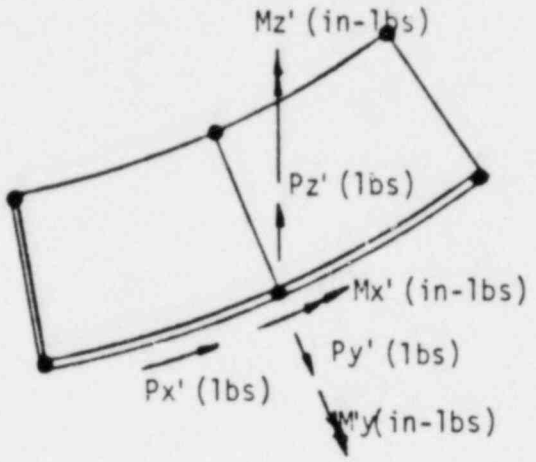

(a) Corner Force Sums—Local Edge Coordinate System

$q_x = \frac{Px}{L}$ (lbs/in) $\quad q_{mx} = \frac{Mx}{L}$ $(\frac{\text{in-lbs}}{\text{in}})$

$q_y = \frac{Py}{L}$ (lbs/in) $\quad q_{my} = \frac{My}{L} = 0$

$q_z = \frac{Pz}{L}$ (lbs/in) $\quad q_{mz} = \frac{Mz}{L} = 0$

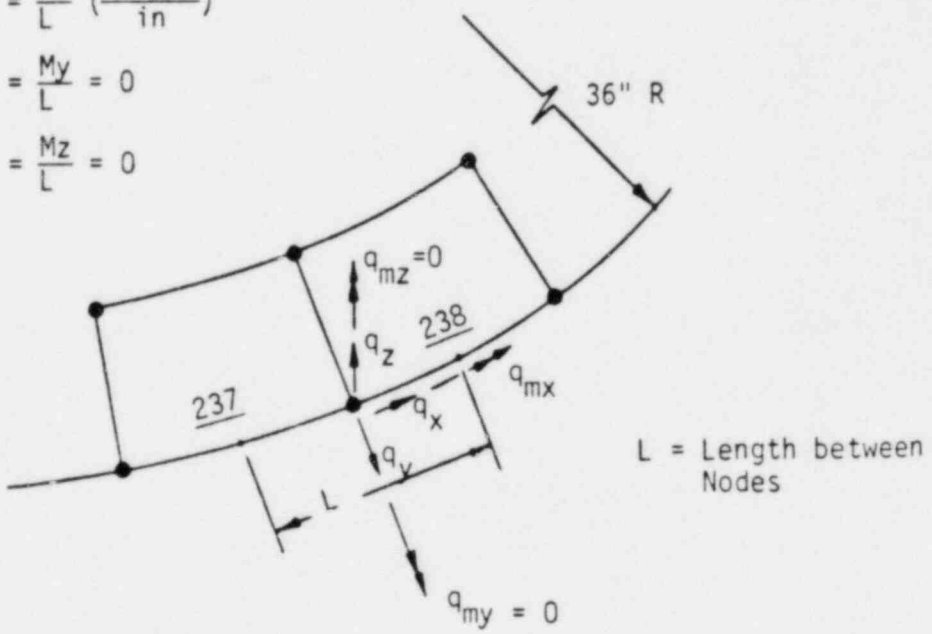

(b) Lid Edge Loads per Inch of Lid Circumference—
Local Edge Coordinate System

Figure 2.4.4-18

MODEL DESCRIPTION... CHEM NUCLEAR RADIATION CASK

CORNER FORCE TABLE:

NODE NO	PLATE NO	CORNER NO	CONDITION NUMBER	GLOBAL CORNER FORCES PX (LB)	PY (LB)	PZ (LB)	MX (IN-LB)	MY (IN-LB)	MZ (IN-LB)
65	229	1	1	539.09	44101.00	-5324.00	48987.00	4752.90	0.00
65	260	4	1	-3246.00	-44261.00	3713.00	-44816.00	8105.40	0.00
66	229	4	1	-4654.20	-36233.00	7405.40	-29017.00	698.44	0.00
66	230	1	1	-483.76	41804.00	-7308.30	32477.00	3077.70	0.00
67	230	4	1	-7465.40	-26220.00	9104.70	-12722.00	-1787.60	0.00
67	231	1	1	188.05	36306.00	-8239.30	17809.00	-2152.80	0.00
68	231	4	1	-13213.00	-16953.00	9749.70	3112.90	-820.60	0.00
68	232	1	1	1537.20	29733.00	-6522.20	6939.10	-10811.00	0.00
69	232	4	1	-18240.00	-10694.00	7610.80	15765.00	3693.90	0.00
69	233	1	1	8167.90	19132.00	-4534.70	509.58	-19678.00	0.00
70	233	4	1	-22087.00	-7412.30	5160.40	14040.00	6839.20	0.00
70	234	1	1	11669.00	14258.00	-1825.90	2024.10	-20019.00	0.00
71	234	4	1	-24534.00	-5556.00	2246.50	12729.00	6321.30	0.00
71	235	1	1	16524.00	9518.10	622.08	5862.60	-16059.00	0.00
72	235	4	1	-26559.00	-3905.70	-146.09	8847.70	407.42	0.00
72	236	1	1	20398.00	6506.10	2129.60	7386.10	-7686.30	0.00
73	236	4	1	-26399.00	-3273.90	-1656.30	6317.40	-6879.30	0.00
73	237	1	1	23155.00	4287.30	3609.10	5332.30	4906.20	0.00

Table 2.4.4-1

MODEL DESCRIPTION... CHEM NUCLEAR RADIATION CASK

CORNER FORCE TABLE:

NODE NO	PLATE NO	CORNER NO	CONDITION NUMBER	GLOBAL CORNER FORCES PX (LB)	PY (LB)	PZ (LB)	MX (IN-LB)	MY (IN-LB)	MZ (IN-LB)
74	237	4	1	-24402.00	-2152.70	-2942.70	7626.40	-11471.00	0.00
74	238	1	1	23542.00	3404.30	3204.00	1238.30	12070.00	0.00
75	238	4	1	-20653.00	-880.94	-2397.90	9703.40	-13366.00	0.00
75	239	1	1	22456.00	2361.40	3666.60	-4603.70	15993.00	0.00
76	239	4	1	-16359.00	1591.40	-2768.90	11136.00	-7747.70	0.00
76	240	1	1	19550.00	1317.20	3057.70	-6666.30	14432.00	0.00
77	240	4	1	-11982.00	4673.20	-1936.70	11621.00	-2588.40	0.00
77	241	1	1	17038.00	-21.98	3546.30	-5083.50	12931.00	0.00
78	241	4	1	-6871.40	10384.00	-2221.80	7701.20	5152.60	0.00
78	242	1	1	12114.00	-3982.10	4693.70	-3452.20	8561.70	0.00
79	242	4	1	-3917.40	15656.00	-3404.50	6430.30	8223.80	0.00
79	243	1	1	7853.10	-9526.00	5125.80	-1063.40	5227.00	0.00
80	243	4	1	-2174.30	19697.00	-3772.00	14304.00	4420.80	0.00
80	244	1	1	5058.40	-16043.00	6395.80	-9747.10	3698.90	0.00
81	244	4	1	-1232.60	21955.00	-4724.00	27629.00	1369.50	0.00
81	245	1	1	2975.20	-21945.00	4691.40	-23390.00	-2241.60	0.00
82	245	4	1	1822.80	20728.00	-2421.00	44695.00	3472.10	0.00
82	246	1	1	1795.70	-25521.00	597.26	-36771.00	-14712.00	0.00

Table 2.4.4-1

MODEL DESCRIPTION... CHEM NUCLEAR RADIATION CASK

CORNER FORCE TABLE:

NODE NO	PLATE NO	CORNER NO	CONDITION NUMBER	GLOBAL CORNER FORCES PX (LB)	PY (LB)	PZ (LB)	MX (IN-LB)	MY (IN-LB)	MZ (IN-LB)
83	246	4	1	7051.30	16842.00	2135.90	49189.00	11480.00	0.00
83	247	1	1	-1397.20	-26054.00	-3626.60	-41044.00	-26462.00	0.00
84	247	4	1	16207.00	11166.00	6469.00	33272.00	15790.00	0.00
84	248	1	1	-6478.40	-24002.00	-8068.80	-29882.00	-24011.00	0.00
85	248	4	1	26769.00	6206.10	10366.00	13406.00	12897.00	0.00
85	249	1	1	-18092.00	-14915.00	-9434.80	-17277.00	-11849.00	0.00
86	249	4	1	35548.00	3017.10	10583.00	1588.20	5464.59	0.00
86	250	1	1	-26902.00	-9779.70	-9101.00	-12613.00	-2103.80	0.00
87	250	4	1	42737.00	930.45	9738.40	-6761.10	-4623.60	0.00
87	251	1	1	-37275.00	-3905.80	-7345.40	-10656.00	8455.70	0.00
88	251	4	1	47513.00	-1652.10	7435.90	-10965.00	-15676.00	0.00
88	252	1	1	-46208.00	23.84	-4729.70	-11199.00	16331.00	0.00
89	252	4	1	47902.00	-3750.30	4489.10	-12694.00	-25680.00	0.00
89	253	1	1	-51026.00	3367.20	-1021.20	-13916.00	23731.00	0.00
90	253	4	1	42501.00	-8164.60	586.28	-10745.00	-35502.00	0.00
90	254	1	1	-50594.00	5222.10	3833.50	-18823.00	28274.00	0.00
91	254	4	1	33572.00	-13798.00	-4083.80	-6582.70	-38071.00	0.00

Table 2.4.4-1

MODEL DESCRIPTION... CHEM NUCLEAR RADIATION CASK

CORNER FORCE TABLE:

NODE NO	PLATE NO	CORNER NO	CONDITION NUMBER	GLOBAL CORNER FORCES PX (LB)	PY (LB)	PZ (LB)	MX (IN-LB)	MY (IN-LB)	MZ (IN-LB)
91	255	1	1	-45062.00	8400.50	8105.40	-24364.00	27122.00	0.00
92	255	4	1	22718.00	-21926.00	-7959.60	-3209.60	-26191.00	0.00
92	256	1	1	-38456.00	11274.00	12502.00	-19586.00	16201.00	0.00
93	256	4	1	14798.00	-28869.00	-11866.00	-5694.30	-11262.00	0.00
93	257	1	1	-28425.00	16380.00	14353.00	-8244.60	4182.70	0.00
94	257	4	1	1653.60	-42948.00	-12322.00	-28293.00	17166.00	0.00
94	258	1	1	-17789.00	23631.00	11610.00	25502.00	-7575.10	0.00
95	258	4	1	-1880.00	-46466.00	-8578.00	-51422.00	31432.00	0.00
95	259	1	1	-7139.40	33092.00	6351.50	59488.00	-7707.80	0.00
96	259	4	1	-4029.00	-47604.00	-3202.60	-54269.00	21546.00	0.00
96	260	1	1	-1858.80	40583.00	-1043.50	63072.00	1078.10	0.00
97	229	2	1	3174.60	44805.00	8495.60	44026.00	-6833.60	0.00
97	260	3	1	-274.74	-50925.00	-8250.80	-43868.00	-12246.00	0.00
98	229	3	1	940.50	-52674.00	-10577.00	-21024.00	-16735.00	0.00
98	230	2	1	5158.80	31124.00	9186.90	23882.00	4844.60	0.00
99	230	3	1	2790.30	-46707.00	-10983.00	-4243.10	-13319.00	0.00
99	231	2	1	10916.00	18099.00	10240.00	7566.70	6779.00	0.00
100	231	3	1	2109.00	-37453.00	-11750.00	12333.00	2015.20	0.00

Table 2.4.4-1

MODEL DESCRIPTION... CHEM NUCLEAR RADIATION CASK

CORNER FORCE TABLE:

NODE NO	PLATE NO	CORNER NO	CONDITION NUMBER	GLOBAL CORNER FORCES PX (LB)	PY (LB)	PZ (LB)	MX (IN-LB)	MY (IN-LB)	MZ (IN-LB)
100	232	2	1	16766.00	10500.00	7704.60	-11596.00	-2571.80	0.00
101	232	3	1	-63.08	-29539.00	-8793.30	16214.00	19792.00	0.00
101	233	2	1	24020.00	5118.70	2124.70	-20346.00	-16327.00	0.00
102	233	3	1	-10101.00	-16838.00	-2750.50	8234.10	20576.00	0.00
102	234	2	1	27535.00	3372.40	-168.13	-16152.00	-16144.00	0.00
103	234	3	1	-14670.00	-12075.00	-252.46	2085.70	20243.00	0.00
103	235	2	1	31320.00	2179.90	-4182.60	-11770.00	-16866.00	0.00
104	235	3	1	-21286.00	-7792.30	3706.60	-3647.10	9290.70	0.00
104	236	2	1	32510.00	2236.20	-5847.20	-5931.50	-7726.90	0.00
105	236	3	1	-26509.00	-5468.40	5373.90	-4866.20	-4505.00	0.00
105	237	2	1	30379.00	2561.10	-5372.00	-2763.80	4402.90	0.00
106	237	3	1	-29132.00	-4695.70	4705.60	-1463.00	-14168.00	0.00
106	238	2	1	25716.00	2092.00	-3563.20	-3344.60	13239.00	0.00
107	238	3	1	-28606.00	-4615.40	2757.10	2848.60	-16935.00	0.00
107	239	2	1	19724.00	233.45	-1507.40	-5263.60	15997.00	0.00
108	239	3	1	-25821.00	-4186.30	609.72	4675.80	-13571.00	0.00
108	240	2	1	13774.00	-3110.90	-154.52	-5555.50	13025.00	0.00

Table 2.4.4-1

MODEL DESCRIPTION... CHEM NUCLEAR RADIATION CASK

CORNER FORCE TABLE:

NODE NO	PLATE NO	CORNER NO	CONDITION NUMBER	GLOBAL CORNER FORCES PX (LB)	PY (LB)	PZ (LB)	MX (IN-LB)	MY (IN-LB)	MZ (IN-LB)
109	240	3	1	-21342.00	-2879.60	-966.50	3312.40	-7057.00	0.00
109	241	2	1	7034.70	-9227.90	-43.54	-3648.50	6740.30	0.00
110	241	3	1	-17201.00	-1134.30	-1281.00	-3735.40	116.42	0.00
110	242	2	1	2907.60	-15893.00	-2071.80	3545.30	-372.84	0.00
111	242	3	1	-11104.00	4218.90	782.54	-8483.80	1369.20	0.00
111	243	2	1	1011.70	-22000.00	-5965.90	8905.10	-609.79	0.00
112	243	3	1	-6690.40	11829.00	4612.10	-775.72	-753.82	0.00
112	244	2	1	541.02	-26369.00	-9476.80	1982.70	5536.00	0.00
113	244	3	1	-4366.80	20457.00	7805.00	19952.00	3358.40	0.00
113	245	2	1	-494.98	-26933.00	-9477.20	-19790.00	9048.40	0.00
114	245	3	1	-4303.00	28151.00	7206.70	42177.00	19555.00	0.00
114	246	2	1	-4242.30	-22912.00	-3524.20	-46699.00	966.98	0.00
115	246	3	1	-4604.70	31590.00	791.04	44783.00	37497.00	0.00
115	247	2	1	-12144.00	-15523.00	5798.80	-55716.00	-14650.00	0.00
116	247	3	1	-2666.10	30411.00	-8641.30	22010.00	36216.00	0.00
116	248	2	1	-22925.00	-8626.20	11149.00	-35054.00	-20057.00	0.00
117	248	3	1	2634.30	26422.00	-13446.00	443.54	16282.00	0.00
117	249	2	1	-36935.00	-1369.10	10229.00	-7046.90	-10856.00	0.00

Table 2.4.4-1

MODEL DESCRIPTION... CHEM NUCLEAR RADIATION CASK

CORNER FORCE TABLE:

NODE NO	PLATE NO	CORNER NO	CONDITION NUMBER	GLOBAL CORNER FORCES PX (LB)	PY (LB)	PZ (LB)	MX (IN-LB)	MY (IN-LB)	MZ (IN-LB)
118	249	3	1	19480.00	13266.00	-11377.00	-1033.30	4753.10	0.00
118	250	2	1	-47888.00	2042.20	11079.00	3355.20	-6370.60	0.00
119	250	3	1	32053.00	6807.10	-11716.00	-2748.50	-11205.00	0.00
119	251	2	1	-58431.00	4475.30	8545.40	12853.00	7341.50	0.00
120	251	3	1	48193.00	1082.60	-8636.00	2399.20	-20464.00	0.00
120	252	2	1	-62506.00	5065.60	6797.30	14895.00	17272.00	0.00
121	252	3	1	60813.00	-1339.10	-6556.60	9795.90	-29473.00	0.00
121	253	2	1	-57278.00	6231.80	4364.40	12104.00	29369.00	0.00
122	253	3	1	65803.00	-1434.40	-3929.50	19195.00	-39205.00	0.00
122	254	2	1	-44301.00	10445.00	-1153.30	2932.50	43040.00	0.00
123	254	3	1	61324.00	-1869.50	1403.60	27426.00	-41303.00	0.00
123	255	2	1	-27659.00	18532.00	-10198.00	-9919.10	47648.00	0.00
124	255	3	1	50003.00	-5006.10	10052.00	24416.00	-23772.00	0.00
124	256	2	1	-16481.00	26395.00	-13705.00	-14857.00	29383.00	0.00
125	256	3	1	40139.00	-8799.80	13069.00	17273.00	-13209.00	0.00
125	257	2	1	3714.10	46203.00	-21990.00	-19796.00	11168.00	0.00
126	257	3	1	23057.00	-19635.00	19960.00	-25771.00	16838.00	0.00
126	258	2	1	7174.30	51626.00	-18334.00	12120.00	-33403.00	0.00

Table 2.4.4-1

MODEL DESCRIPTION... CHEM NUCLEAR RADIATION CASK

CORNER FORCE TABLE:

NODE NO	PLATE NO	CORNER NO	CONDITION NUMBER	GLOBAL CORNER FORCES PX (LB)	PY (LB)	PZ (LB)	MX (IN-LB)	MY (IN-LB)	MZ (IN-LB)
127	258	3	1	12494.00	-28791.00	15303.00	-70011.00	22390.00	0.00
127	259	2	1	7981.80	56204.00	-4531.70	56388.00	-50566.00	0.00
128	259	1	1	3186.70	-41693.00	1382.80	-70125.00	3248.80	0.00
128	260	4	1	5379.60	54603.00	5581.20	64015.00	-30572.00	0.00

Table 2.4.4-1

MODEL DESCRIPTION... CHEM NUCLEAR RADIATION CASK

SUMMED CORNER FORCES TABLE:

		----- GLOBAL CORNER FORCE SUMS -----					
NODE NO	CONDITION NUMBER	PX (LB)	PY (LB)	PZ (LB)	MX (IN-LB)	MY (IN-LB)	MZ (IN-LB)
65	1	-2706.91	-160.00	-1611.00	4171.00	12858.30	0.00
66	1	-5137.96	5571.00	97.10	3460.00	3776.14	0.00
67	1	-7277.35	10086.00	865.40	5087.00	-3940.40	0.00
68	1	-11675.80	12780.00	3227.50	10052.00	-11631.60	0.00
69	1	-10072.10	8438.00	3076.10	16274.58	-15984.10	0.00
70	1	-10418.00	6845.70	334.50	16064.10	-13179.80	0.00
71	1	-8010.00	3962.10	2868.58	18591.60	-9737.70	0.00
72	1	-6161.00	2600.40	1983.51	16233.80	-7278.88	0.00
73	1	-3244.00	1013.40	1952.80	11649.70	-1973.10	0.00
74	1	-860.00	1251.60	261.30	8864.70	599.00	0.00
75	1	1803.00	1480.46	1268.70	5099.70	2627.00	0.00
76	1	3191.00	2908.60	288.80	4469.70	6684.30	0.00
77	1	5056.00	4651.22	1609.60	6537.50	10342.60	0.00
78	1	5242.60	6401.90	2471.90	4249.00	13714.30	0.00
79	1	3935.70	6130.00	1721.30	5366.90	13450.80	0.00
80	1	2884.10	3654.00	2623.80	4556.90	8119.70	0.00
81	1	1742.60	10.00	-32.60	4239.00	-872.10	0.00
82	1	3618.50	-4793.00	-1823.74	7924.00	-11239.90	0.00
83	1	5654.10	-9212.00	-1490.70	8145.00	-14982.00	0.00
84	1	9728.60	-12836.00	-1599.80	3390.00	-8221.00	0.00
85	1	8677.00	-8708.90	931.20	-3871.00	1048.00	0.00
86	1	8646.00	-6762.60	1482.00	-11024.80	3360.70	0.00

Table 2.4.4-2

MODEL DESCRIPTION... CHEM NUCLEAR RADIATION CASK

SUMMED CORNER FORCES TABLE:

		----- GLOBAL CORNER FORCE SUMS -----					
NODE NO	CONDITION NUMBER	PX (LB)	PY (LB)	PZ (LB)	MX (IN-LB)	MY (IN-LB)	MZ (IN-LB)
87	1	5462.00	-2975.35	2393.00	-17417.10	3832.10	0.00
88	1	1305.00	-1628.26	2706.20	-22164.00	655.00	0.00
89	1	-3124.00	-383.10	3467.90	-26610.00	-1949.00	0.00
90	1	-8093.00	-2942.50	4419.78	-29568.00	-7228.00	0.00
91	1	-11490.00	-5397.50	4021.60	-30946.70	-10949.00	0.00
92	1	-15738.00	-10652.00	4542.40	-22795.60	-9990.00	0.00
93	1	-13627.00	-12489.00	2487.00	-13938.90	-7079.30	0.00
94	1	-16135.40	-19317.00	-712.00	-2791.00	9590.90	0.00
95	1	-9019.40	-13374.00	-2226.50	8066.00	23724.20	0.00
96	1	-5887.80	-7021.00	-4246.10	8803.00	22624.10	0.00
97	1	2899.86	-6120.00	244.80	158.00	-19079.60	0.00
98	1	6099.30	-21550.00	-1390.10	2858.00	-11890.40	0.00
99	1	13706.30	-28608.00	-743.00	3323.60	-6540.00	0.00
100	1	18875.00	-26953.00	-4045.40	737.00	-556.60	0.00
101	1	23956.92	-24420.30	-6668.60	-4132.00	3465.00	0.00
102	1	17434.00	-13465.60	-2918.63	-7917.90	4432.00	0.00
103	1	16650.00	-9895.10	-4435.06	-9684.30	3377.00	0.00
104	1	11224.00	-5556.10	-2140.60	-9578.60	1563.80	0.00
105	1	3870.00	-2907.30	1.90	-7630.00	-102.10	0.00
106	1	-3416.00	-2603.70	1142.40	-4807.60	-929.00	0.00
107	1	-8882.00	-4381.95	1249.70	-2415.00	-938.00	0.00
108	1	-12047.00	-7297.20	455.20	-879.70	-546.00	0.00

Table 2.4.4-2

MODEL DESCRIPTION... CHEM NUCLEAR RADIATION CASK

SUMMED CORNER FORCES TABLE:

		----- GLOBAL CORNER FORCE SUMS -----					
NODE NO	CONDITION NUMBER	PX (LB)	PY (LB)	PZ (LB)	MX (IN-LB)	MY (IN-LB)	MZ (IN-LB)
109	1	-14307.30	-12107.50	-1010.04	-336.10	-316.70	0.00
110	1	-14293.40	-17027.30	-3352.80	-190.10	-256.42	0.00
111	1	-10092.30	-17781.10	-5183.36	421.30	759.41	0.00
112	1	-6149.38	-14540.00	-4864.70	1206.98	4782.18	0.00
113	1	-4861.78	-6476.00	-1672.20	162.00	12406.80	0.00
114	1	-8545.30	5239.00	3682.50	-4522.00	20521.98	0.00
115	1	-16748.70	16067.00	6589.84	-10933.00	22847.00	0.00
116	1	-25591.10	21784.80	2507.70	-13044.00	16159.00	0.00
117	1	-34300.70	25052.90	-3217.00	-6603.36	5426.00	0.00
118	1	-28408.00	15308.20	-298.00	2321.90	-1617.50	0.00
119	1	-26378.00	11282.40	-3170.60	10104.50	-3863.50	0.00
120	1	-14313.00	6148.20	-1838.70	17294.20	-3192.00	0.00
121	1	3535.00	4892.70	-2192.20	21899.90	-104.00	0.00
122	1	21502.00	9010.60	-5082.80	22127.50	3835.00	0.00
123	1	33665.00	16662.50	-8794.40	17506.90	6345.00	0.00
124	1	33522.00	21388.90	-3653.00	9559.00	5611.00	0.00
125	1	43853.10	37403.20	-8921.00	-2523.00	+2041.00	0.00
126	1	30231.30	31991.00	1626.00	-13651.00	-16565.00	0.00
127	1	20475.80	27413.00	10771.30	-13623.00	-28176.00	0.00
128	1	8566.30	12910.00	6964.00	-6110.00	-27323.20	0.00

Table 2.4.4-2

MODEL DESCRIPTION... CHEM NUCLEAR RADIATION CASK
PANEL SERIES..... 229 THRU 260

SUMMED AND ROTATED CORNER FORCES PLUS RUNNING LOADS TABLE:

FOR EDGE..... 97 98 99 100 101 102 103 104 105 106 107 108 109 110 111 112 113 114 115
115 117 118 119 120 121 122 123 124 125 126 127 128

PANEL EDGE FORCES IN (EDGE) COORDINATE SYSTE

NODE NO	EDGE FORCE TRIAD JA NO	JB NO	JC NO	COND NO	PX (LB)	QX (LB/IN)	PY (LB)	QY (LB/IN)	PZ (LB)	QZ (LB/IN)	MX IN-LB
97	128	98	65	1	-6120.	-769.	-2900.	-364.	245.	31.	-19080.
98	97	99	65	1	-22363.	-2811.	-1217.	-153.	-1390.	-175.	-12228.
99	98	100	65	1	-31722.	-3987.	-123.	-15.	-743.	-93.	-7333.
100	99	101	65	1	-32858.	-4130.	1758.	221.	-4045.	-508.	-893.
101	100	102	65	1	-34086.	-4830.	2901.	411.	-6669.	-945.	5392.
102	101	103	65	1	-21801.	-3541.	3160.	513.	-2919.	-474.	9074.
103	102	104	65	1	-19006.	-3087.	3729.	606.	-4435.	-720.	10256.
104	103	105	65	1	-12007.	-1950.	3562.	579.	-2141.	-348.	9705.
105	104	106	65	1	-3870.	-629.	2907.	472.	2.	0.	7630.
106	105	107	65	1	3810.	619.	1984.	322.	1142.	186.	4896.
107	106	108	65	1	9838.	1598.	1145.	186.	1250.	203.	2590.
108	107	109	65	1	14078.	2286.	435.	71.	455.	74.	1034.
109	108	110	65	1	18742.	2656.	-145.	-21.	-1010.	-143.	461.
110	109	111	65	1	22218.	2793.	-755.	-95.	-3353.	-421.	319.
111	110	112	65	1	20391.	2563.	-1498.	-188.	-5183.	-651.	-867.
112	111	113	65	1	15536.	1953.	-2805.	-353.	-4865.	-611.	-4931.
113	112	114	65	1	6476.	814.	-4862.	-611.	-1672.	-210.	-12407.
114	113	115	65	1	-6988.	-878.	-7186.	-903.	3683.	463.	-21014.
115	114	116	65	1	-21695.	-2727.	-8247.	-1036.	6590.	828.	-25328.

Table 2.4.4-3

MODEL DES[illegible]TION... CHEM NUCLEAR RADIATION CASK
PANEL SERIES..... 229 THRU 260

SUMMED AND ROTATED CORNER FORCES PLUS RUNNING LOADS TABLE:

FOR EDGE..... 97 98 99 100 101 102 103 104 105 106 107 108 109 110 111 112 113 114 115
116 117 118 119 120 121 122 123 124 125 126 127 128

EDGE FORCE TRIAD				PANEL EDGE FORCES IN (EDGE) COORDINATE SYSTEM							
NODE NO	JA NO	JB NO	JC NO	COND NO	PX (LB)	QX (LB/IN)	PY (LB)	QY (LB/IN)	PZ (LB)	QZ (LB/IN)	MX IN-LB	QMX INLB/IN
116	115	117	65	1	-32930.	-4139.	-6716.	-844.	2508.	315.	-20765.	-2610.
117	116	118	65	1	-42342.	-6000.	-3362.	-476.	-3217.	-456.	-8545.	-1211.
118	117	119	65	1	-32264.	-5240.	-628.	-102.	-298.	-48.	2817.	458.
119	118	120	65	1	-28635.	-4651.	1769.	287.	-3171.	-515.	10815.	1757.
120	119	121	65	1	-15151.	-2461.	3619.	588.	-1839.	-299.	17585.	2856.
121	120	122	65	1	3535.	574.	4893.	795.	-2192.	-356.	21900.	3557.
122	121	123	65	1	22723.	3691.	5215.	847.	-5083.	-826.	22457.	3647.
123	122	124	65	1	37306.	6059.	4389.	713.	-8794.	-1428.	18621.	3024.
124	123	125	65	1	39706.	6449.	2155.	350.	-3653.	-593.	11083.	1800.
125	124	126	65	1	57637.	8168.	-224.	-32.	-8921.	-1264.	-3244.	-460.
126	125	127	65	1	43826.	5508.	-4076.	-512.	1626.	204.	-21458.	-2697.
127	126	128	65	1	33543.	4216.	-6751.	-849.	10771.	1354.	-31296.	-3933.
128	127	97	65	1	14476.	1819.	-5521.	-694.	6964.	875.	-27998.	-3519.

Table 2.4.4-3

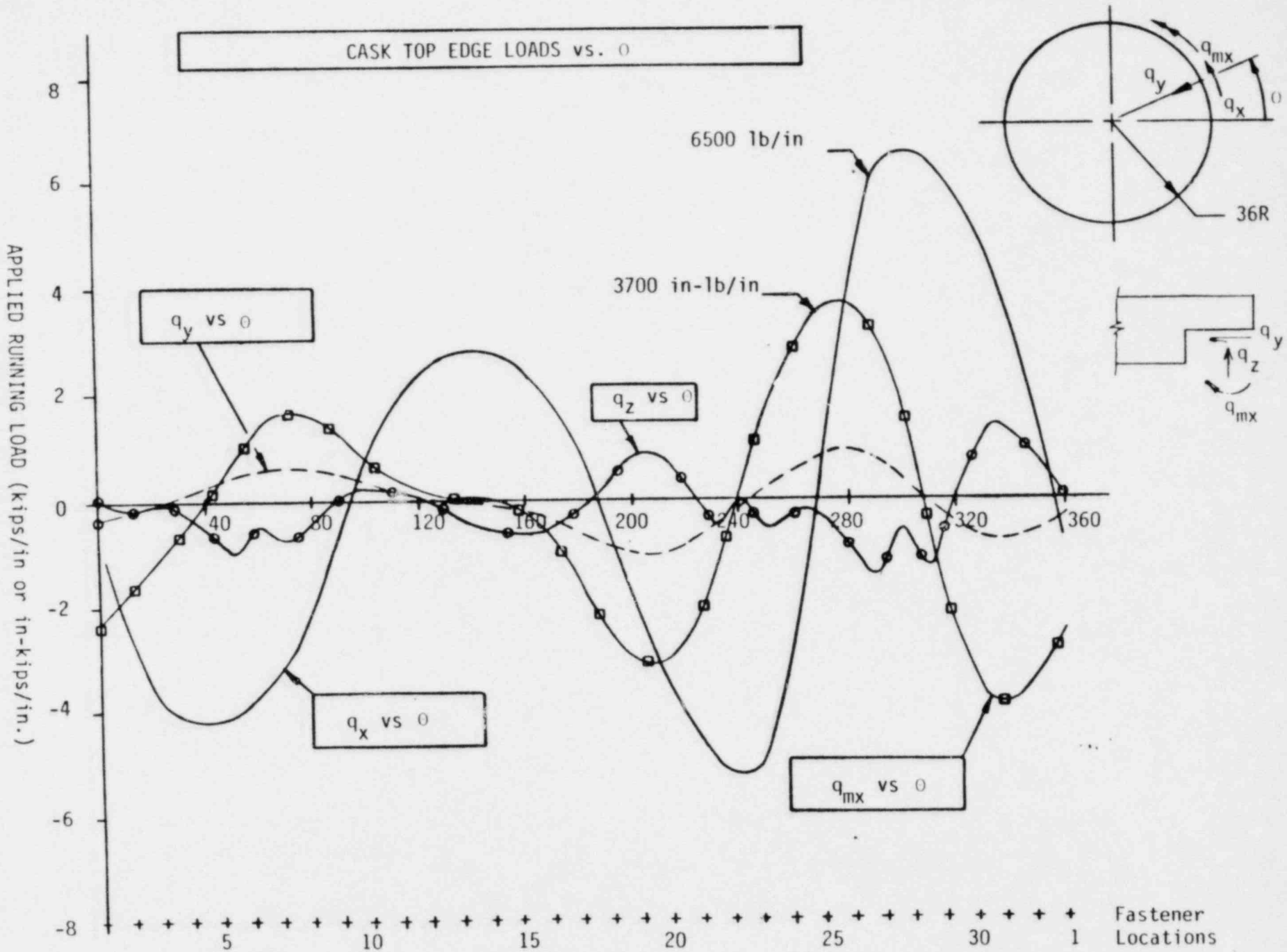

Figure 2.4.4-19

2.4.4.5 Lid Bolt Stress Analysis (continued)

Therefore the maximum lid bolt loads shown on Figure 2.4.4-20, are:

V_x = 6500(7.07) = 45955 lbs.
V_y = 1050 (7.07) = 7423 lbs.
V_z = 1500 (7.07) = 10605 lbs.
M = -4000 (7.07) = -28280 in-lbs.

Lid bolt stresses are determined in Section 2.4.4.5(1)

2.4.4.6 Tie-down Arm Stress Analysis The tie-down arm is welded to the outer cask shell as shown in Figure 2.4.4-21(a) and (b).

The maximum tie-down arm load of 652750 lbs. was determined in Section 2.4.4.2.

Stresses for the tie-down arm and it's connection to the exterior cask shell are determined as follows:

(1) Tension on Net Section at Hole

$$A_{net} = (6.5 - 2.875)\ 2.75 = 9.97\ in^2$$

$$\sigma_t = \frac{652750}{9.97} = 65480\ psi$$

$\sigma_{allow} = F_y$ = 100000 psi (tension only - A517 or A514 steel. See table 2.3-1)

Therefore:

$$F.S. = \frac{\sigma_{allow}}{\sigma_t} = \frac{100000}{65480} = 1.53$$

(2) Contact Bearing at Lifting Hole

$$A_{brg} = 2.75(2.75) = 7.56\ in^2$$

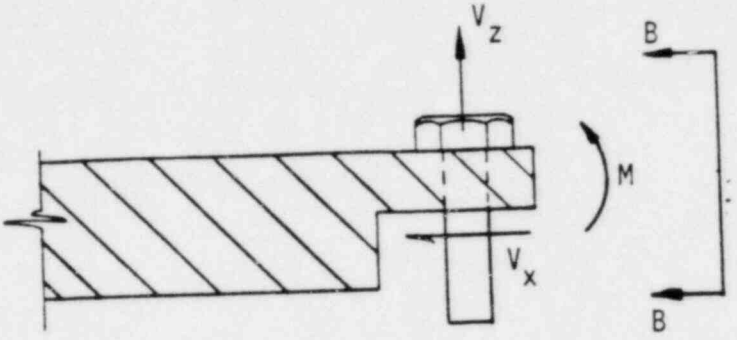

Section A-A

l = circumferential spacing between bolts (in.)

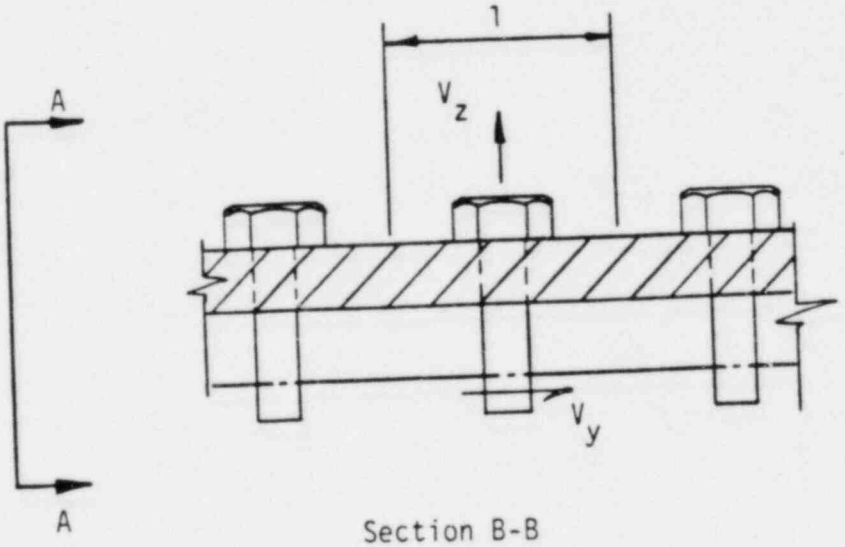

$V_x = q_{px} \times l$

$V_y = q_{py} \times l$

$V_z = q_{pz} \times l$

$M = q_{mx} \times l$

Section B-B

Figure 2.4.4-20 MAXIMUM LID BOLT LOADS

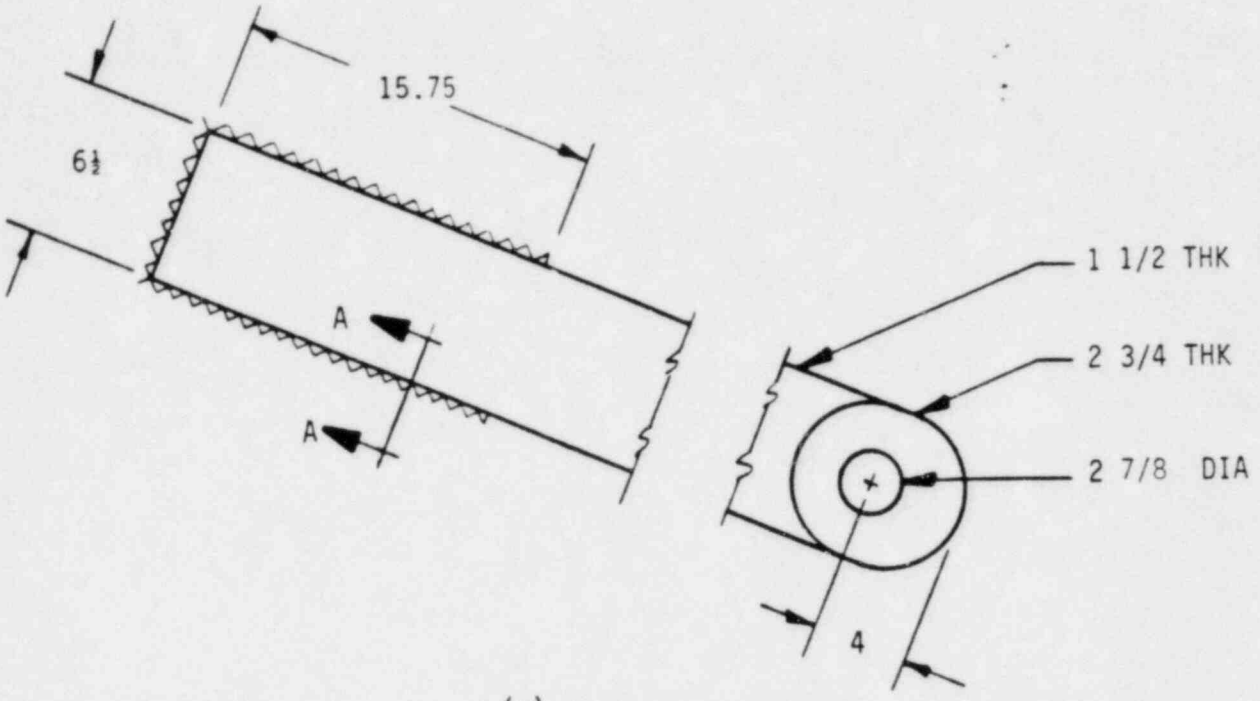

(a)

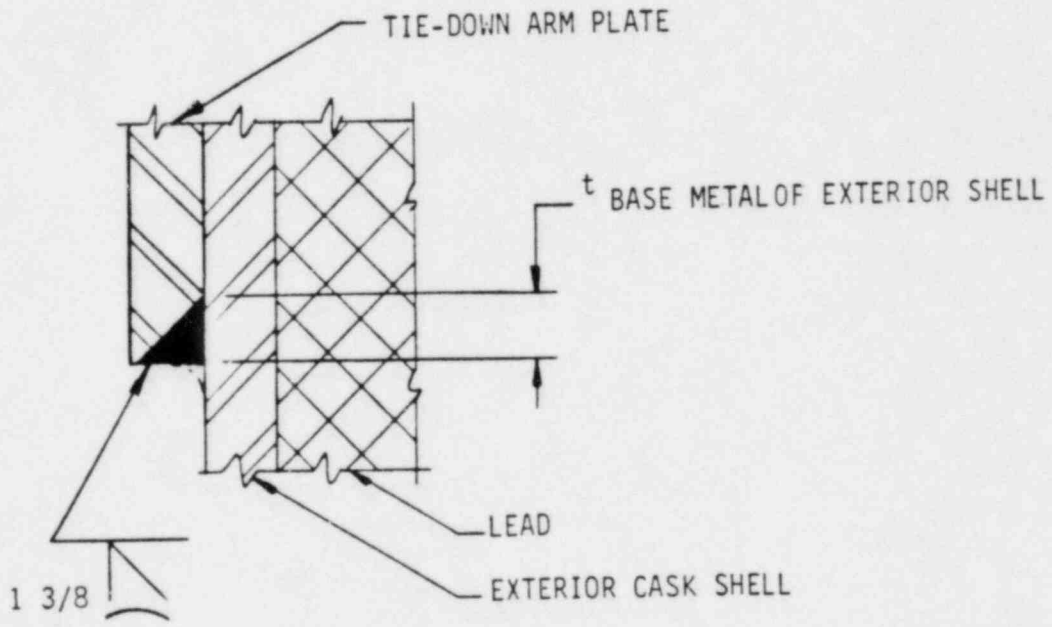

SECTION A-A

(b)

Figure 2.4.4.-21 CASK TIE-DOWN ARM

2.4.4.6 Tie-down Arm Stress Analysis (continued)

$$\sigma = \frac{652750}{7.56} = 86343 \text{ psi}$$

$$\sigma_{allow} = 1.35 F_y = 1.35(100000) = 135000 \text{ psi}$$

(contact bearing)

Therefore:

$$F.S. = \frac{\sigma_{allow}}{\sigma} = \frac{135000}{86343} = 1.56$$

(3) Arm Tension

$$A_{arm} = 1.5(6.5) = 9.75 \text{ in}^2$$

$$\sigma_t = \frac{652750}{9.75} = 66949 \text{ psi}$$

$$\sigma_{allow} = F_y = 100000 \text{ psi (tension only)}$$

Therefore:

$$F.S. = \frac{\sigma_{allow}}{\sigma_t} = \frac{100000}{66949} = 1.49$$

(4) Edge Tearout

$$A = (4-1.4375)(2.75)2 = 14.09 \text{ in}^2$$

$$\sigma = \frac{652750}{14.09} = 46315 \text{ psi (shear)}$$

$$\sigma_{allow} = \frac{F_y}{2} = \frac{100000}{2} = 50000 \text{ psi (shear)}$$

Therefore:

$$F.S. = \frac{\sigma_{allow}}{\sigma} = \frac{50000}{46315} = 1.08$$

2.4.4.6 Tie-down Arm Stress Analysis (continued)

(5) Weld Stresses

Weld stresses are determined for the material with the lowest yield strength (exterior cask shell). The effective weld shear area from Figure 2.4.4-21(a) and (b) is determined as:

$$A_{weld} = (6.5 + 2\ (15.75))\ 1.375 = 52.25\ in^2$$

$$\sigma = \frac{652750}{52.25} = 12492\ psi$$

$$\sigma_{allow} = \frac{F_y}{2} = \frac{38000}{2} = 19000\ psi$$

Therefore:

$$F.S. = \frac{\sigma_{allow}}{\sigma} = \frac{19000}{12492} = 1.52$$

2.4.4.7 Overpack Stress Analysis

(1) Vertical Loads

The bearing pressure on the annular land of the lower overpack was computed in Section 2.4.4.4(1) to be 185 psi. The allowable compressive stress for the foam in the overpacks, as shown in Figure 2.3-1, is 1500 psi. Therefore,

$$F.S. = \frac{\sigma_{allowable}}{\sigma_{actual}} = \frac{1500}{185} = 8.1$$

(2) Lateral Loads

The maximum force experienced by the shear block is 243.13 kips, as determined in Section 2.4.4.2.

2.4.4.7 Overpack Stress Analysis (continued)

The shear block has a circumferential width of 24.0 inches (ref. Figure 2.4.4-22), and a height of 12.0 inches. This produces

$$A_{block} = (24)(12) = 288 \text{ in}^2$$

The compressive stress in the overpack foam is:

$$\sigma_{block} = \frac{F_{shear\ block}}{A_{block}} = \frac{243130}{288} = 844.2 \text{ psi}$$

Comparing this with allowable stress of 1500 psi for the foam produces:

$$F.S. = \frac{\sigma_{allowable}}{\sigma_{actual}} = \frac{1500}{844.2} = 1.78$$

2.5 Standards for Type "B" and Large Quantity Packaging

10 CFR 71, Para. 71.32 defines additional structural standards to be applied to Type B and large quantity packaging. These standards consist of "load resistance" and "external pressure".

2.5.1 Load Resistance

"Regarded as a simple beam supported at its ends along any major axis, packaging shall be capable of withstanding a static load normal to and uniformly distributed along its length equal to 5 times its fully loaded weight. . ."

$$\sigma_t = \frac{Mc}{I}$$

where $M = \frac{Wl}{8}$

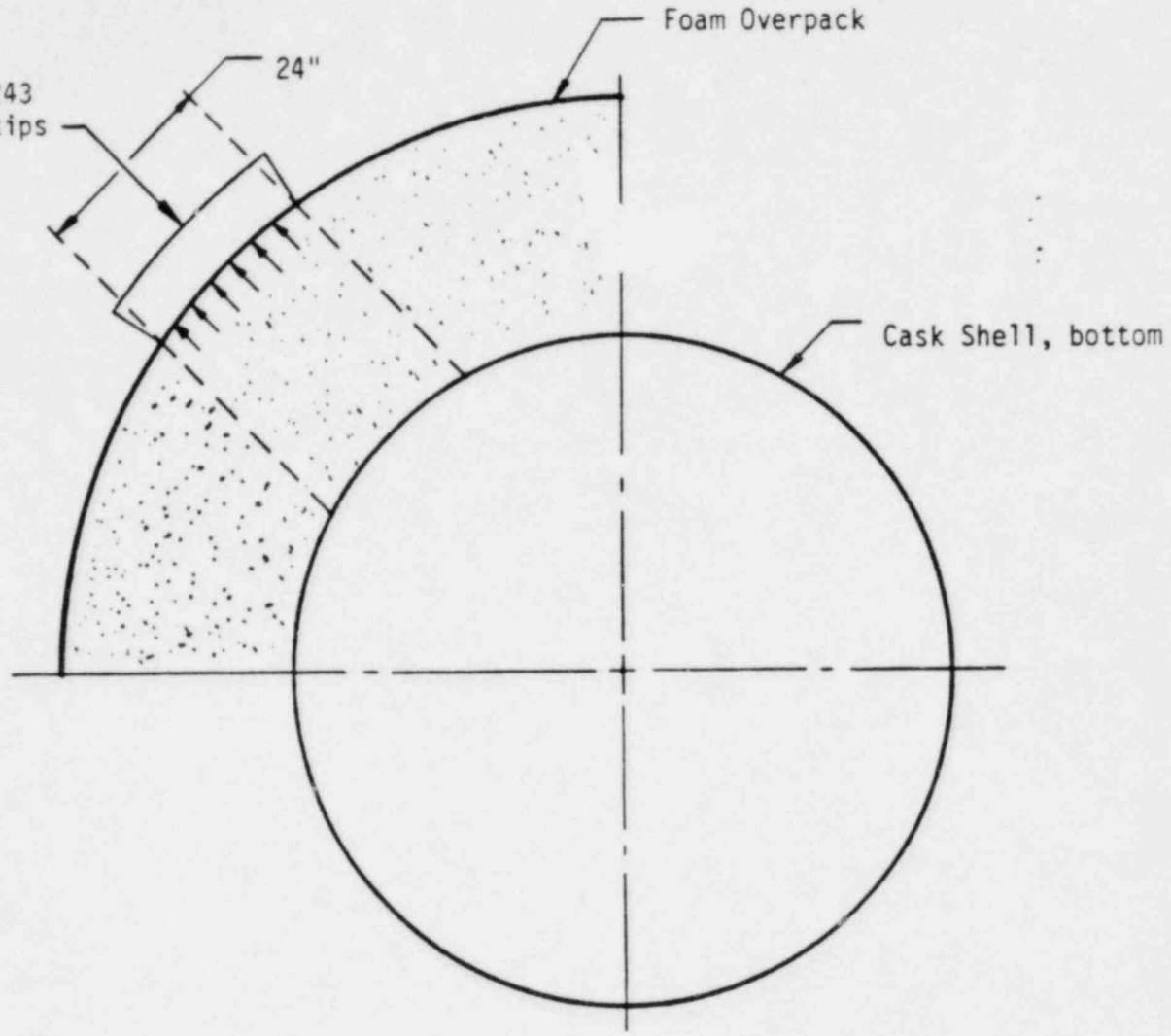

Figure 2.4.4.-22—BOTTOM OVERPACK AND SHEAR BLOCK REACTIONS

2.5.1 Load Resistance (continued)

Assume the outer shell alone supports this load.

l = Total length of cask = 89.0 in.

c = Cask shell radius = 36.75 in.

d_o = 73.5 in.

d_i = 72.0 in.

$$I = \frac{\pi}{64} [d_o^4 - d_i^4]$$

$$= 1.134 \times 10^5 \text{ in}^4$$

$$M = \frac{(5)(74000)(89)}{8} = 4.116 \times 10^6 \text{ in-lb.}$$

$$\sigma_t = \frac{(4.116 \times 10^6)(36.75)}{1.134 \times 10^5}$$

$$= 1334 \text{ psi}$$

Safety Factor = 34650/1334 = 26.0

2.5.2 External Pressure

The requirement for external pressure is that the cask must be able to withstand an external pressure of 25 psig without loss of contents. It has been conservatively assumed that only the 3.5 inch end plates and the outermost 1.5 inch steel plate cylinder are effective in resisting the external pressure.

2.5.2.1 Bottom End Plate(1)

$$\sigma_t = \frac{3}{32} \left(\frac{D}{t}\right)^2 P(3+\nu)$$

D = Diameter = 73.5 inches

(1) Ref. 3, p. 363, Table 24, case 10a

P = 25 psig

t = 3.50 inches

ν = 0.30

σ = 3411 psi

Safety Factor = 34650/3411 = 10.2

2.5.2.2 Cylindrical Shell - Buckling[1]

$$P_c = \frac{0.8E\frac{t}{r}}{1+\frac{1}{2}\left(\frac{\pi r}{nl}\right)^2}\left\{\frac{1}{n^2\left[1+\left(\frac{nl}{\pi r}\right)^2\right]^2}+\frac{n^2t^2}{12r^2(1-\nu^2)}\left[1+\left(\frac{\pi r}{nl}\right)^2\right]^2\right\} \quad (1)$$

n = buckling mode number

E = Modulus of Elasticity = 27.9×10^6 psi

ν = 0.3

$r = \frac{1}{4}(73.5 + 72.0) = 36.375$ in.

t = 1.50 in.

l = 89 in.

The minimum critical pressure occurs at n = 4

and P_c = 3131 psi

Safety Factor = 3131/25 = 125

2.5.2.3 Primary Lid

$$\sigma_1 = \frac{6}{t^2}\left(\frac{Pr_2^3(1-\nu^2)}{r_1}\right)\frac{1-\frac{1-\nu}{4}\left[1-\left(\frac{r_1}{r_2}\right)^4\right]-\left(\frac{r_1}{r_2}\right)^2\left[1+(1+\nu)\ln\left(\frac{r_2}{r_1}\right)\right]}{2\left(1-\nu^2\right)\left(\frac{r_2}{r_1}-\frac{r_1}{r_2}\right)} \quad (2)$$

$$\sigma_2 = \frac{6}{t^2}\left(\frac{wr_2^2(1-\nu^2)}{r_1}\right)\frac{2\frac{r_1}{r_2}\quad\frac{1+\nu}{2}\ln\left(\frac{r_2}{r_1}\right)+\frac{1-\nu}{4}\left[1-\left(\frac{r_1}{r_2}\right)^2\right]}{(1-\nu^2)\left(\frac{r_2}{r_1}-\frac{r_1}{r_2}\right)} \quad (3)$$

$\sigma = \sigma_1 + \sigma_2$

(1) Ref. 3, p. 556, Table 35, case 20

(2) Ref. 3, p.339, Table 24, case 2a

(3) Ref. 3, p.334, Table 24, case 1a

2.5.2.3 Primary Lid (continued)

where $\nu = 0.3$

$t = 3.5$ in.

$P = 25$ psi

$r_1 = 16.5$ in.

$r_2 = 36.75$ in.

$w = \frac{1}{2} Pr_1 = 206.25$ lb/in

and $\sigma_1 = 4357$ psi

$\sigma_2 = 2757$ psi

$\sigma = 7114$ psi

Safety Factor = 34650/7114 = 4.9

2.5.2.4 Secondary Lid[1]

$$\sigma = \frac{3}{8} \left(\frac{r_1}{t}\right)^2 P (3+\nu)$$

$r_1 = 16.5$ in.

$t = 3.5$ in.

$P = 25$ psi

$\nu = 0.3$

$\sigma = 687$ psi

Safety Factor = 34650/687 = 50

2.5.2.5 Cylindrical Shell - Maximum Stress

For external pressure $\sigma = \frac{Pr}{t}$

$= \frac{(25)(36.375)}{1.5} = 606$ psi

Safety Factor = 23100/606 = 38

2.6 Normal Conditions of Transport

The package has been designed, constructed, and the contents limited (as described in Section 1.2.3), such that the performance requirements specified in 10 CFR 71.35 will be met when the package is subjected to the normal conditions of transport specified in Appendix A of 10 CFR 71. The ability of the package to satisfactorily withstand the normal conditions of transport has been assessed as described below:

(1) Ref. 3, p.363, Table 24, case 10a

2.6.1 Heat

A detailed thermal analysis for normal conditions of transport can be found in Section 3.4. The analysis used an internal heat load of 100 watts.

The maximum cavity temperature was found to be 177°F assuming 130°F ambient air and full insolation. This is the maximum package temperature. These temperatures will have no detrimental effects on the package.

2.6.1.1 Summary of Pressures and Temperatures From Sections 3.4.2 and 3.4.4, it was found that the maximum temperatures and pressure are:

Pressure:

P_{max} = 6.7 psig

Temperatures:

Outer Surface 177°F

Containment Cavity 177°F

2.6.1.2 Differential Thermal Expansion From the summary temperatures shown in Section 2.6.1.1 and Section 3.1, it can be seen that the temperature variations between the external shell and the inner containment vessel are less than one Fahrenheit degree.

Since lead bonding is not present, fabrication stresses are minimized because of the short term creep properties of lead. Therefore, a stress-free temperature of 70°F was assumed.

The analysis of package stresses due to differential thermal expansion has been performed using an axisymmetric finite element model, Figure 2.6.1-1. The same model is used for computing cask stresses throughout Sections 2.6 and 2.7 of this report. This ANSYS finite element model is described fully in Appendix 2.10.3.

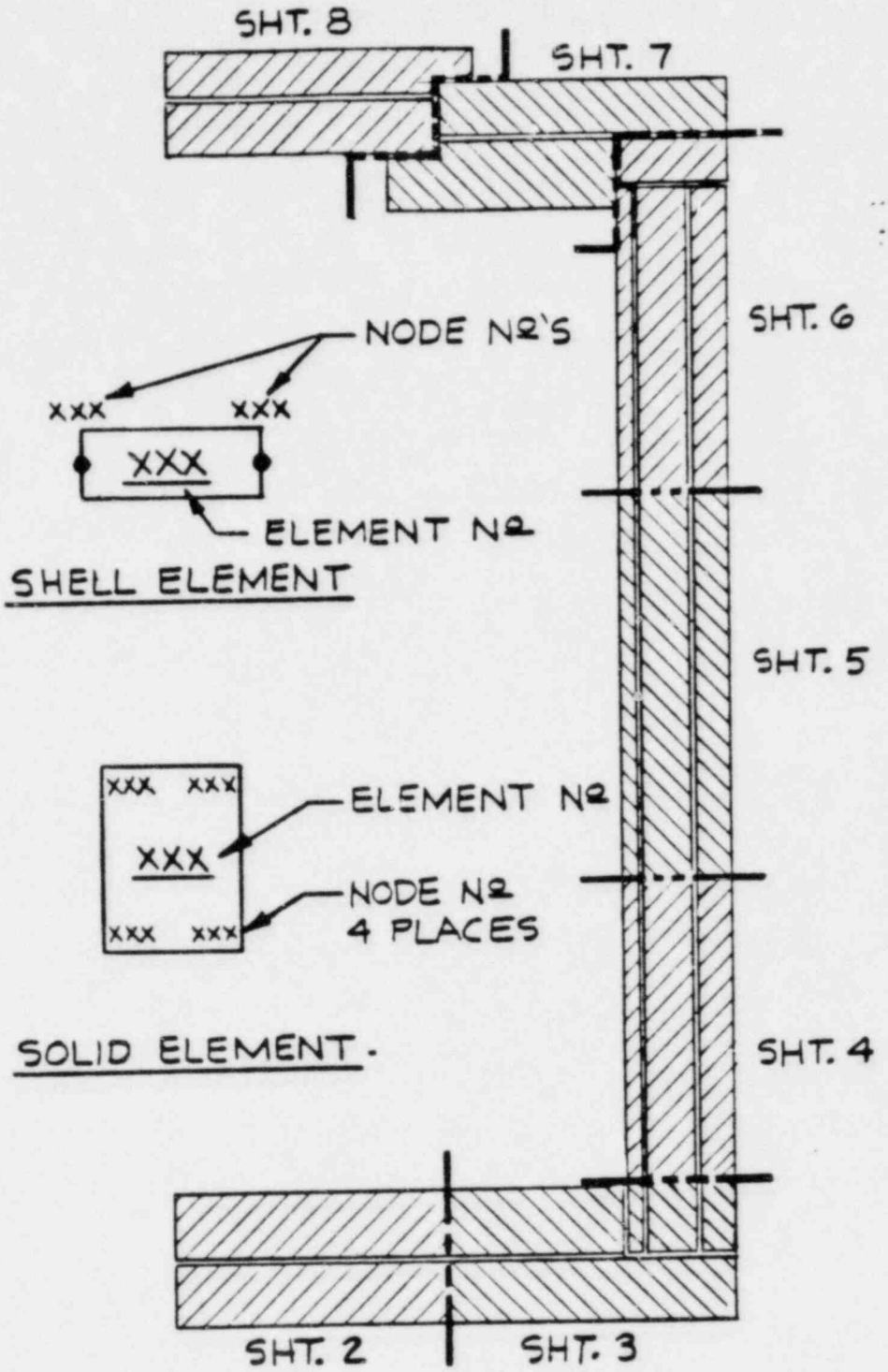

KEY

8-120 FINITE ELEMENT MODEL

Figure 2.6.1-1

SHT. 1 OF 8

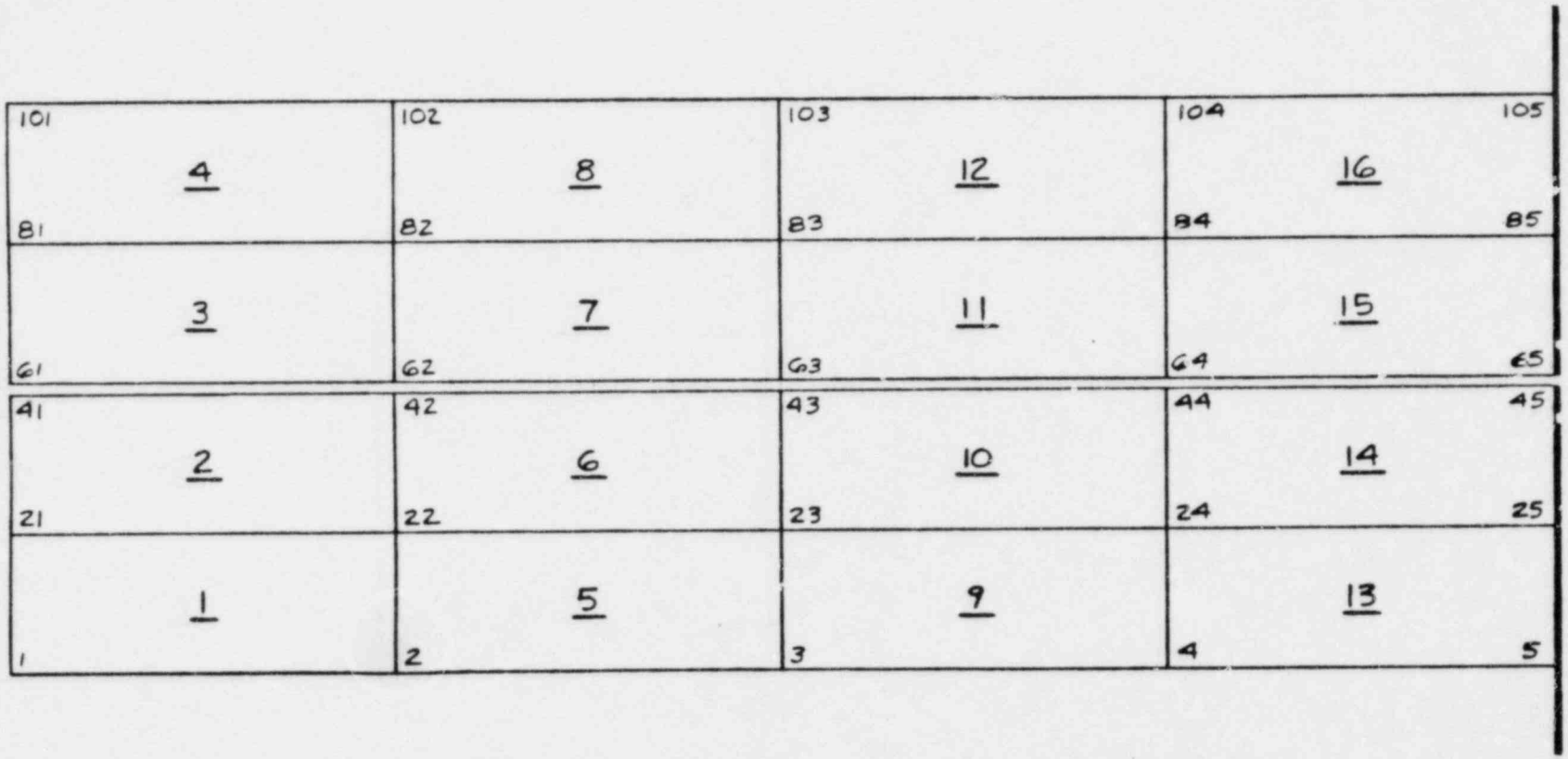

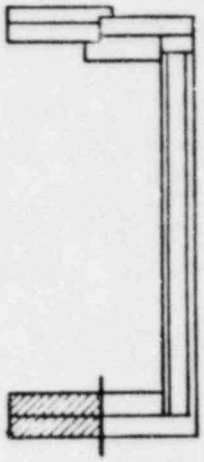

KEY

Figure 2.6.1-1

SHT. 2 OF 8

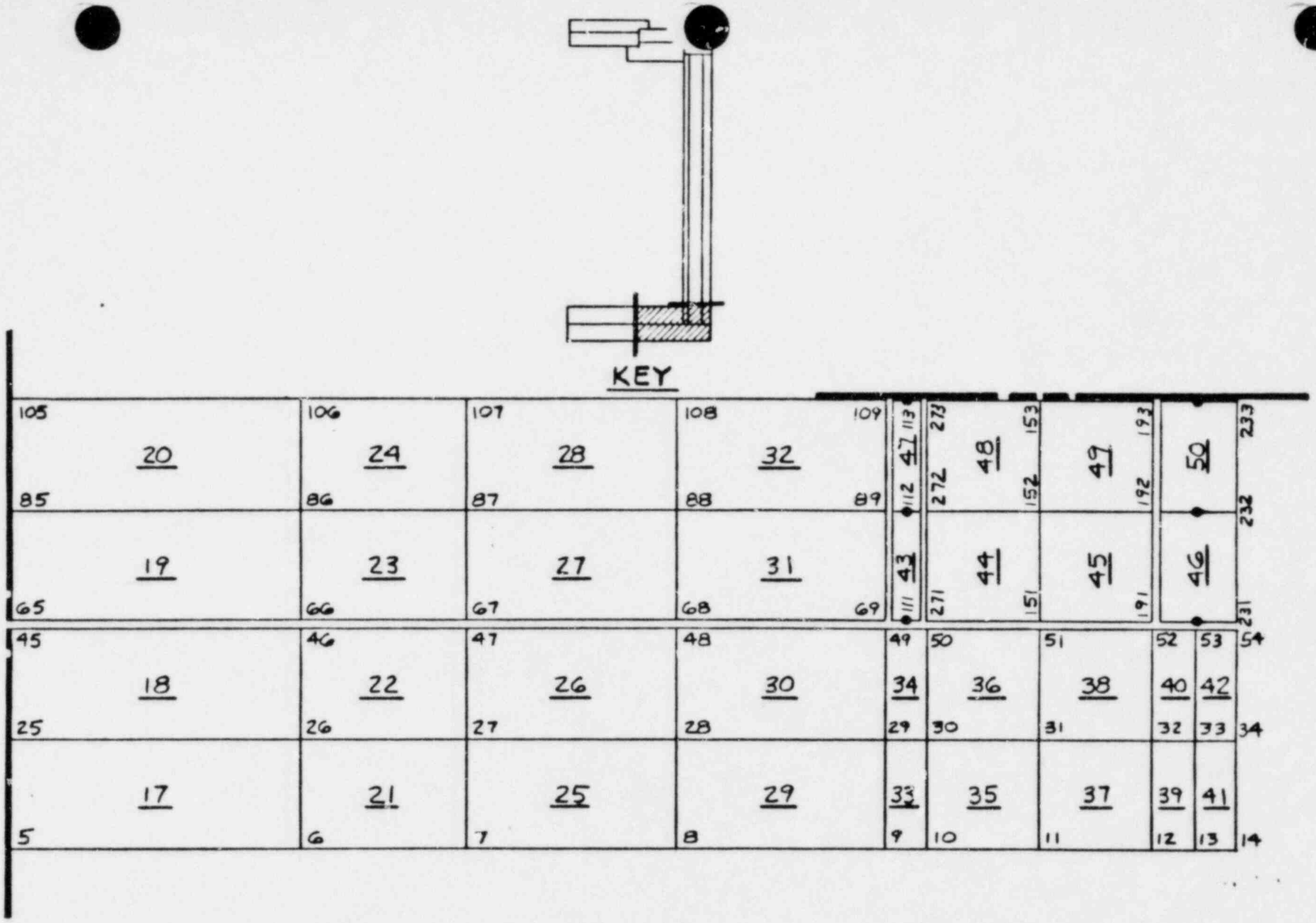

Figure 2.6.1-1

SHT. 3 OF 8

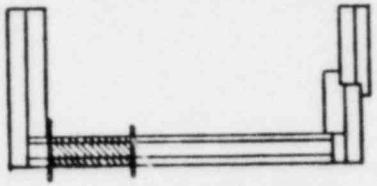

KEY

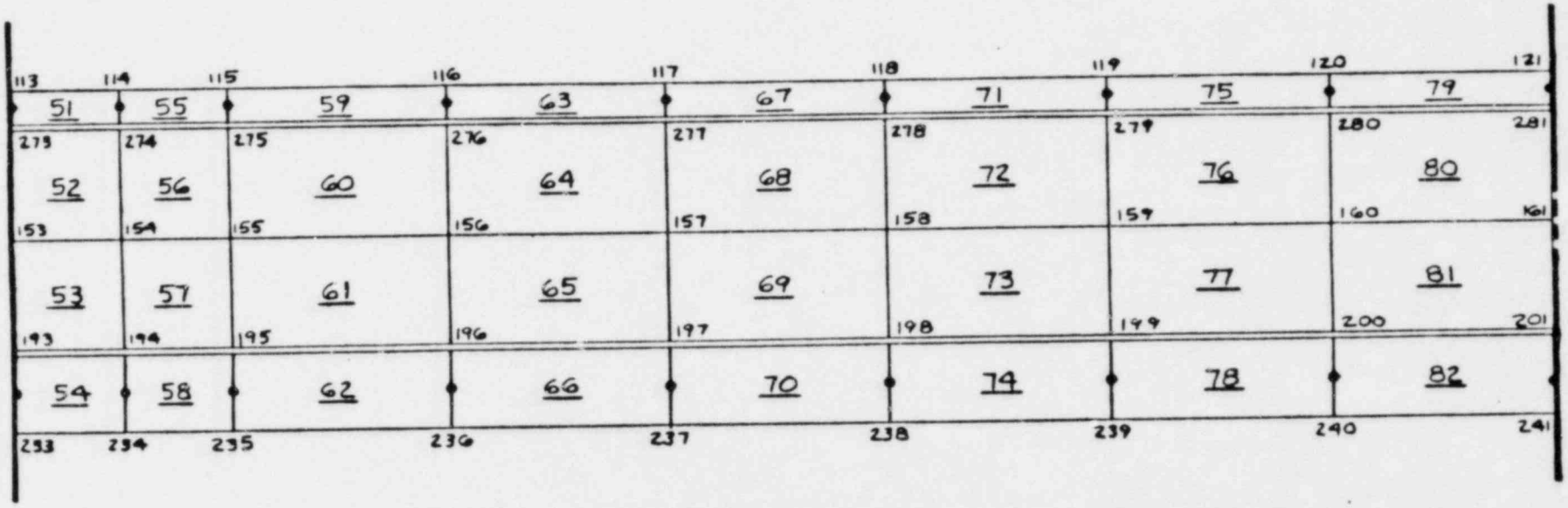

Figure 2.6.1-1

SHT. 4 OF 8

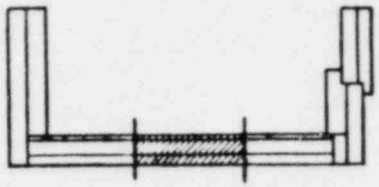

KEY

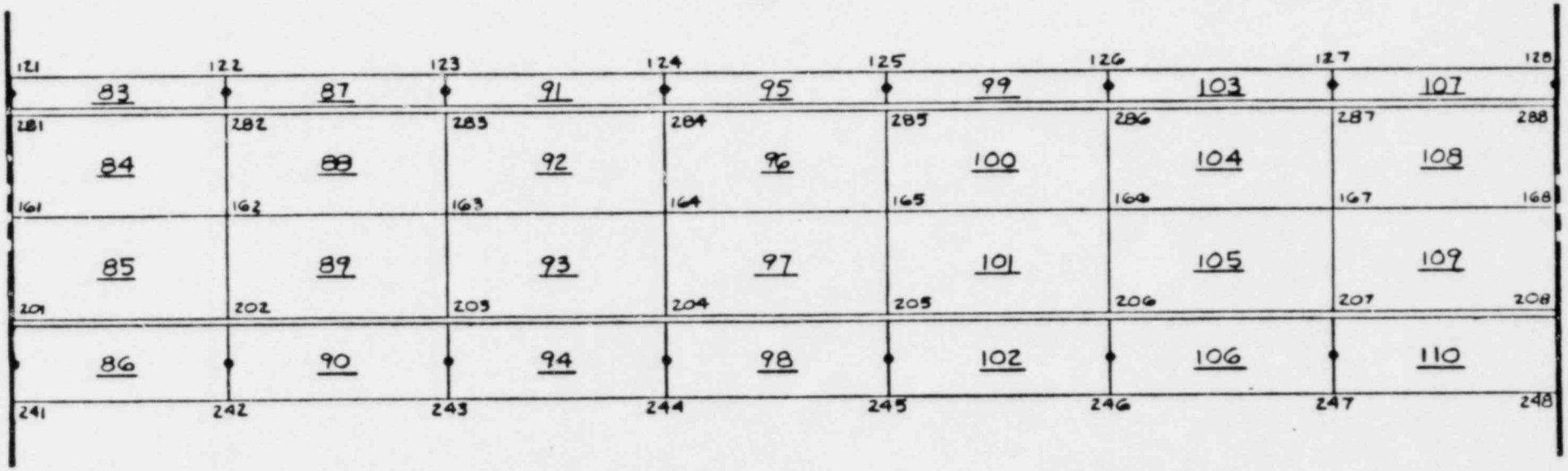

Figure 2.6.1-1

SHT. 5 OF 8

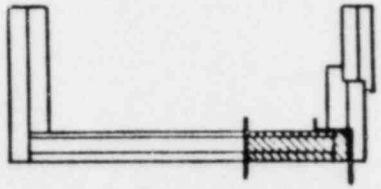

KEY

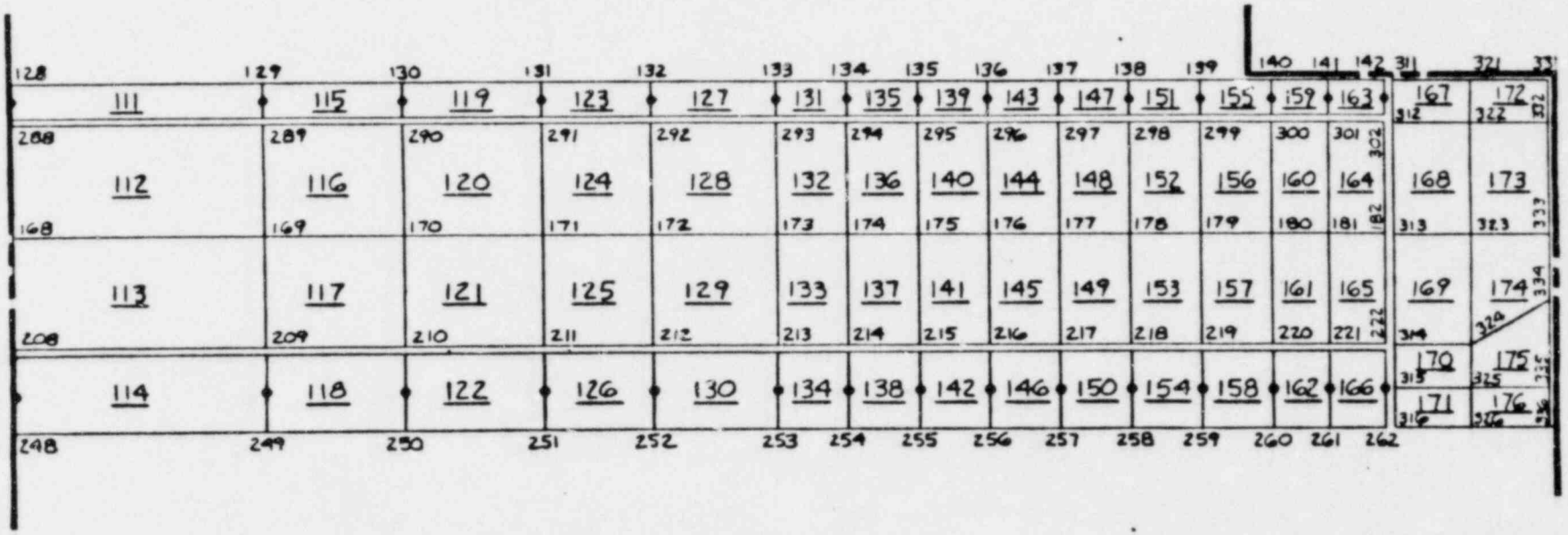

Figure 2.6.1-1

SHT. 6 OF 8

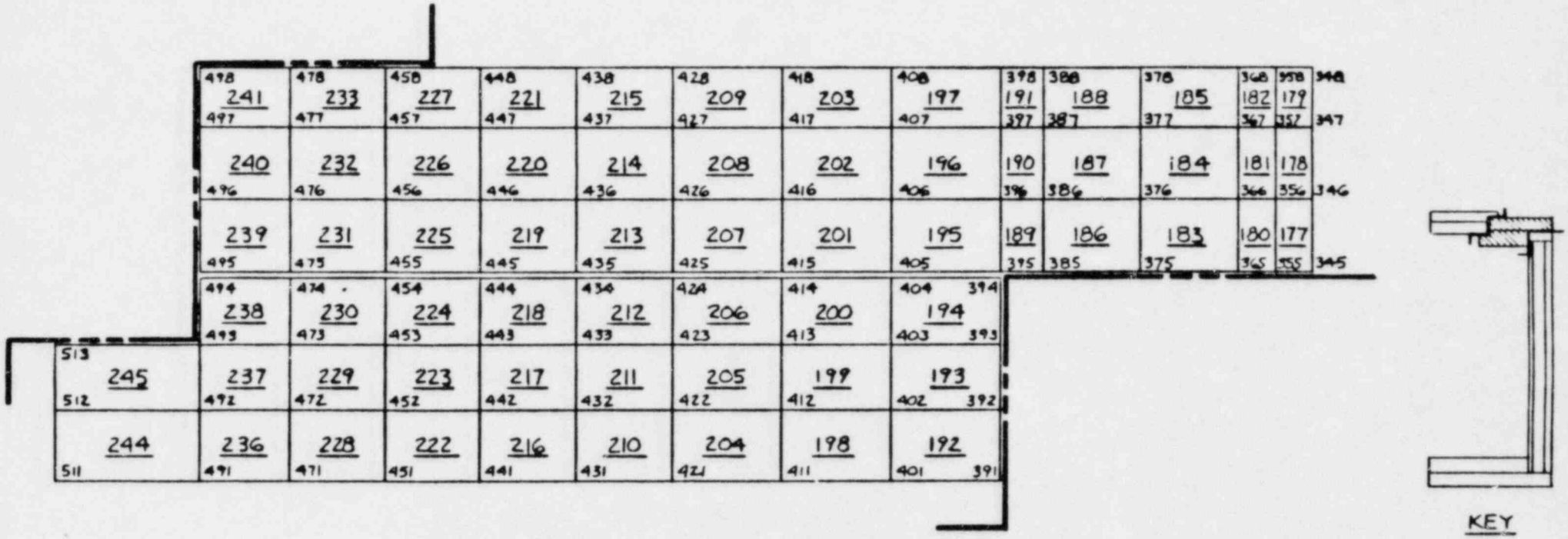

SHT. 7 OF 8

Figure 2.6.1-1

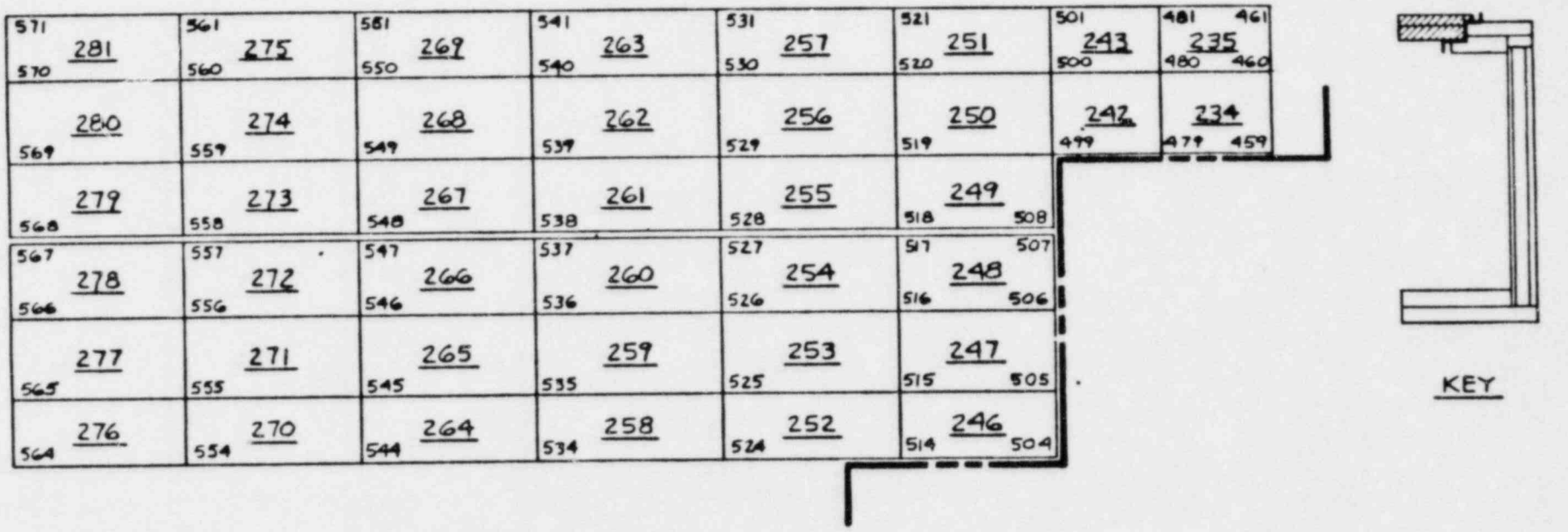

Figure 2.6.1-1

SHT. 8 OF 8

2.6.1.2 Differential Thermal Expansion (continued)

The referenced figure completely describes model geometry. All material properties of the model are taken directly from Table 2.3-1 for steel, ASTM A516 Gr70, and lead. To represent the unbonded lead, the lead elements were decoupled from the steel shells in the axial direction. This assures that shear forces are not transmitted between the steel shells and the lead, yet permits proper treatment of direct radial forces between the steel shells and the lead due to differential thermal expansion effects.

A stress analysis was made using combined temperature and pressure loads. This analysis evaluated stresses in the cask due to temperature gradients and differential thermal expansion along with stresses due to the thermally - induced internal pressure.

Stress intensities throughout the cask are well below allowables under these conditions, as shown in Table 2.6.1-1. The maximum stress intensity is seen to occur in the inner shell near the upper end, where the maximum stress intensity is 16362 psi in element 159. This is the area with the lowest factor of safety, 2.12.

A plot of the elastically deformed cask is shown in Figure 2.6.1-2. For clarity, the deformations are greatly exaggerated. The maximum deformation is 0.042 inch.

2.6.1.3 Stress Calculations The complete stress analysis for combined loads was discussed in Section 2.6.1.2.

2.6.1.4 Comparison with Allowable Stresses The comparison with allowable stresses was discussed in Section 2.6.1.2.

2.6.2 Cold

The materials of construction for the packaging, including the lead, carbon steel, overpack and the seals themselves are not significantly affected by an ambient temeprature of -40°F.

ELEMENT TYPE	STRESS TYPE (σ allow) (psi)		BASE PLATES		CASK BODY							PRIMARY LID		SECONDARY LID	
			INNER	OUTER	LOWER INNER	LOWER OUTER	MID INNER	MID OUTER	UPPER INNER	UPPER OUTER	BOLT RING	INNER	OUTER	INNER	OUTER
SHELL ELEMENT . STIF61	MEMBRANE (23100)	ELEMENT			51	62	95	118	159	126					
		VALUE (psi)			4369	6427	4360	6166	4407	6054					
	MEMBRANE + BENDING (34650)	ELEMENT			51	50	119	118	159	158					
		VALUE (psi)			6777	12034	4619	6315	16362	9844					
SOLID ELEMENT . STIF25	MEMBRANE (23100)	ELEMENT	3-4	39-40							167-172	237	187	247	250
		VALUE (psi)	1554	7489							5310	590	1196	219	644
	MEMBRANE + BENDING (34650)	ELEMENT	4	34							169	204	191	276	242
		VALUE (psi)	2787	9289							3424	1096	1214	479	1126

LOADING: 130° F Ambient + Pressure + 100 W Payload

Maximum Stress Intensities in Cask Regions

Table 2.6.1-1

STEP 1 ITER 1 TIME .00 .0421

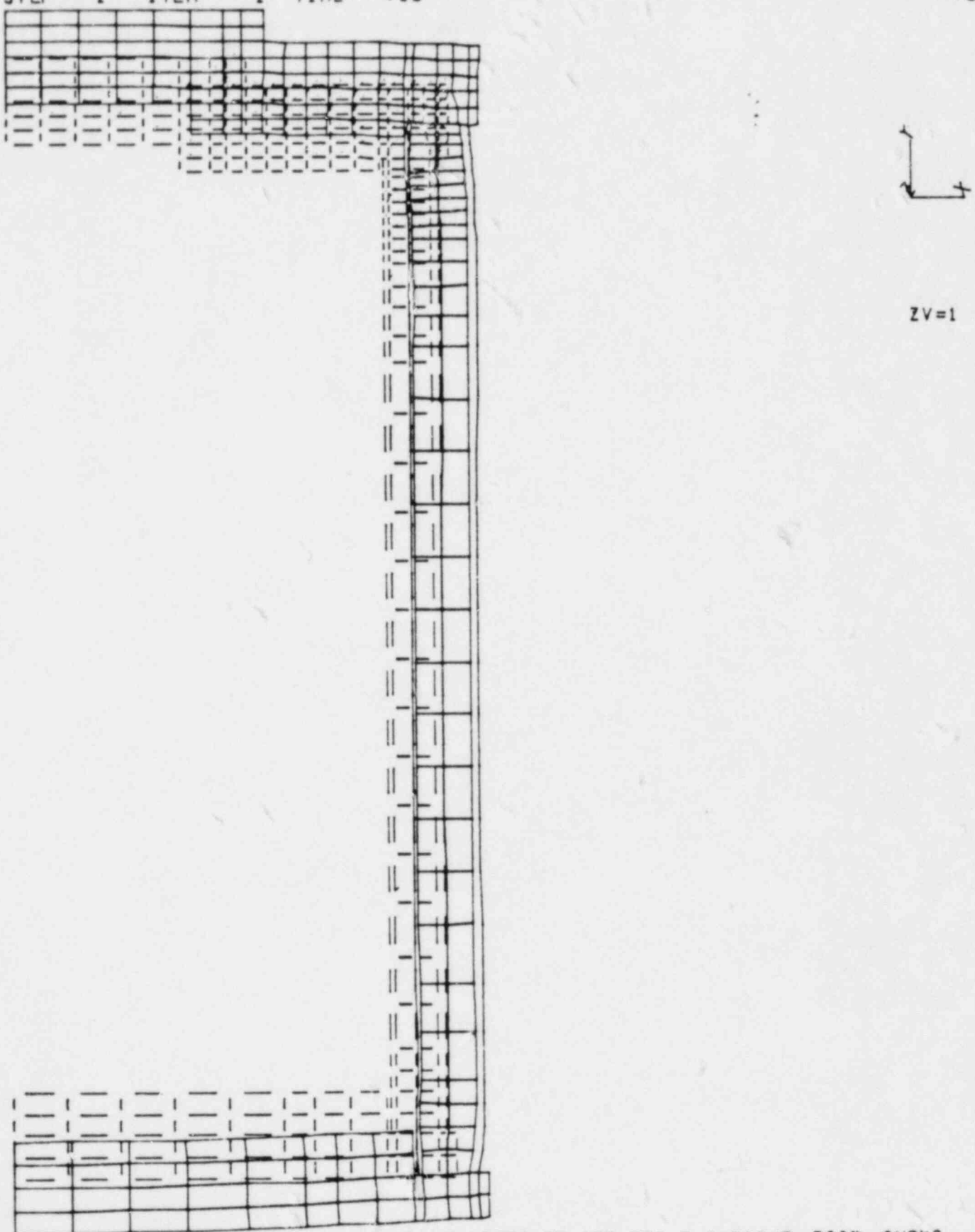

ZV=1

2D STATIC ANALYSIS, THERMAL AND PRESSURE LOADS AT 130 DEG F AMBIENT DISP ANSYS 1

Figure 2.6.1-2

2.6.2 Cold (continued)

The cask must be able to resist brittle fracture failure under normal conditions of transport and hypothetical accident conditions at temperatures as low as -20°F per NRC Regulatory guide 7.8. Fracture-critical parts of the cask include the 1-1/2 inch thick outer shell, the 3-1/2 inch thick end plates and lids, and the 3/4 inch thick steel inner shell. Note that according to NuReg/CR-1875 (UCRL-53013), the bolts are not fracture-critical because they are part of a redundant system.

Fracture toughness, then, is of concern only for the outer shell, inner shell, and the end plates, which are made from ASTM A516 grade 70 carbon steel. For compliance with Category II fracture toughness requirements of NuReg/CR-1875, the nil ductility transition temperature (T_{NDT}) of this steel must be less than the value determined by the equation:

$$T_{NDT} = LST - A$$

where: LST = Lowest Service Temperature (= -20°F)
A = Value from Figure 2.6.2-1.

Entering the figure, the following values may be determined:

Thickness	A	T_{NDT}
1-1/2	-20	0°F
3-1/2	+5	-25°F
3/4	-20	0°F

Therefore, the nil ductility transition temperatures must be less than -20°F for the outer and inner shells, and -25°F for the end plates.

By definition, the NDT temperature is that temperature at which material has 40,000 psi $(in)^{1/2}$ of dynamic fracture toughness. The corresponding required Charpy V-notch test energy can be calculated by the following equation from UCRL-53013:

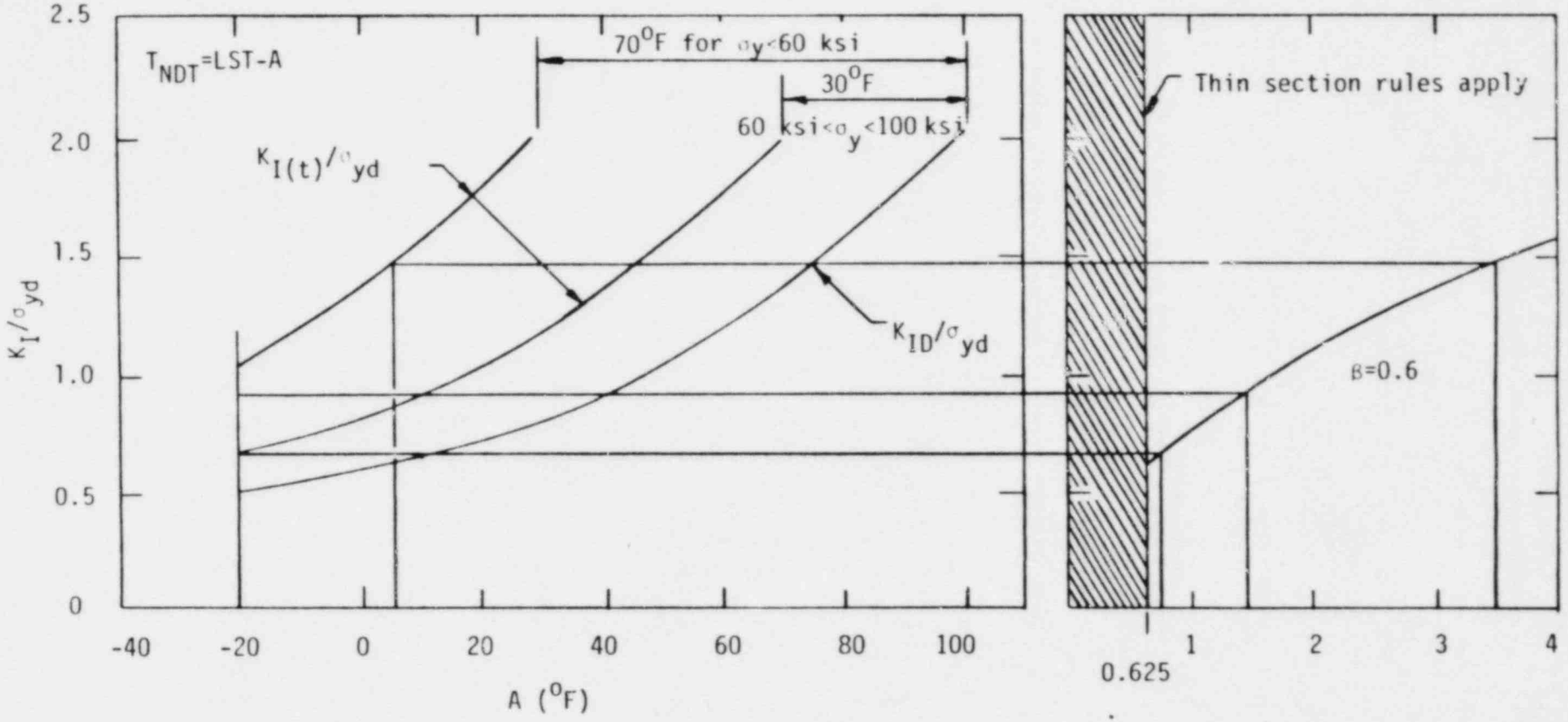

DESIGN CHART FOR CATEGORY II FRACTURE CRITICAL COMPONENTS (FROM UCRL-53013)

Figure 2.6.2-1

2.6.2 Cold (continued)

$$k_{ID}^{\ 2} = 5(C_v)\ E$$

$$C_v = \frac{(40000)^2}{5(29\times10^6)} = 11.0 \text{ ft.-lb.}$$

The C_v value specified for both the end plates and the outer shell is at least 12 ft-lb and the average of 3 test specimens is at least 15 ft-lbs at -40°F, 15° below the lowest required NDT temperature. Therefore, the design is sufficiently ductile, over the lowest service temperature range, to prevent brittle failure of the cask containment.

2.6.3 Pressure

The containment vessel has been designed as a pressure containment vessel for pressure well in excess of the 0.5 atmosphere referenced in 10 CFR 71, Appendix A.3.

By inspection and comparison to the analysis shown in Section 2.6.1, the package can resist an internal pressure of 0.5 atmosphere without resulting in change to its structural integrity.

2.6.4 Vibration

The package is an improved lineal descendent of a proven cask with well over ten years of operational use in a transport environment. This experience demonstrates that vibrations normally incident to transport will have no effect upon the package.

2.6.5 Water Spray

Not applicable, since the package exterior is constructed of steel.

2.6.6 Free Drop

The package weight of 74000 pounds means that the package must be able to survive a one-foot free fall drop onto a flat, unyielding surface without reducing its effectiveness in withstanding subsequent accident conditions. Using the techniques described in Appendix 2.10.1, the maximum accelerations experienced by the package for a one-foot drop have been calculated to be those shown below:

Condition	Acceleration (g's)
End	46.4
Side	24.6
Corner	8.5

The stresses resulting from these loads have been found as a percentage of those calculated for the 30-foot drop conditions based on the ratios of peak accelerations. These stresses are summarized in the following sections.

2.6.6.1 End Drop The ratio of stresses for the one-foot drop compared to the 30-foot drop is 46.4/135.3 = 0.343. Maximum stress intensities are summarized in Table 2.6.6-1.
Stress intensities throughout the package are well below allowables. The maximum stress intensity, 7742 psi, occurs in the bolt ring. This is also the area with the lowest factor of safety:

$$F.S. = \frac{23100}{5985} = 3.86$$

2.6.6.2 Side Drop The ratio of stresses for the one-foot drop compared to the 30-foot drop is:

$$\frac{24.6}{108.3} = 0.227$$

Maximum stress intensities are summarized in Table 2.6.6-2.

ELEMENT TYPE	STRESS TYPE (σ_{allow}) (psi)		BASE PLATES		CASK BODY							PRIMARY LID		SECONDARY LID	
			INNER	OUTER	LOWER INNER	LOWER OUTER	MID INNER	MID OUTER	UPPER INNER	UPPER OUTER	BOLT RING	INNER	OUTER	INNER	OUTER
Shell Element STIF61	Membrane (23100)	Element			55	58	119	122	155	134					
		Value (psi)			2408	2329	3120	3882	3263	4091					
	Membrane + Bending (34650)	Element			51	54	119	122	135	158					
		Value (psi)			3420	3556	3130	3913	3627	5949					
Solid Element STIF25	Membrane (23100)	Element	31-32	35-36							167-172	199	190	253	242-243
		Value (psi)	1458	1339							5985	2215	1838	456	1037
	Membrane + Bending (34650)	Element	31	1							167	210	189	276	242
		Value (psi)	4546	3617							7742	2885	3795	1082	1523

LOADING: 100°F Ambient + Pressure + 1-Foot Side Drop + 100W Payload

Maximum Stress Intensities in Cask Regions

Table 2.6.6-1

ELEMENT TYPE	STRESS TYPE (σ_{allow}) (psi)		BASE PLATES		CASK BODY							PRIMARY LID		SECONDARY LID	
			INNER	OUTER	LOWER INNER	LOWER OUTER	MID INNER	MID OUTER	UPPER INNER	UPPER OUTER	BOLT RING	INNER	OUTER	INNER	OUTER
Shell Element STIF61	Membrane (23100)	Element			59	62	119	106	135	138					
		Value (psi)			5088	2711	3482	2987	6615	5821					
	Membrane + Bending (34650)	Element			47	50	119	110	139	138					
		Value (psi)			10596	6491	4351	5252	7850	9038					
Solid Element STIF25	Membrane (23100)	Element	31-32	39-40							167-172	199	181	253	250
		Value (psi)	3321	3651							4632	2001	5245	648	3517
	Membrane + Bending (34650)	Element	32	40							169	194	186	248	242
		Value (psi)	5151	4411							3380	3968	11378	1902	7377

LOADING: 100°F Ambient + Pressure + 1-Foot End Drop + 100W Payload

Maximum Stress Intensities in Cask Regions

Table 2.6.6-2

2.6.6.2 Side Drop (continued)

Stress intensities throughout the cask remain well below allowables during the side drop. The highest stress intensity is 11378 psi at the bolt in the primary lid. The minimum factor of safety, 3.05, occurs in the same area.

2.6.6.3 Corner Drop The ratio of stresses for the one-foot drop compared to the 30-foot drop is found as:

$$\frac{8.5}{76.1} = 0.112$$

Maximum stress intensities are summarized in Table 2.6.6-3.

Stress intensities are well below allowables throughout the cask. The highest stress intensity, 5412 psi, occurs at the center of the secondary lid. This corresponds to the minimum factor of safety,

$$F.S. = \frac{34650}{5412} = 6.4$$

2.6.7 Corner Drop

Not applicable, since the package weighs more than 110 lbs.

2.6.8 Penetration

Impact energies resulting from a 13 pound rod dropping from a height of 40 inches will have no significant effect on the exterior of the package. The overpack fully protects both ends of the cask leaving only the central body exposed. The cask body is manufactured from 1-1/2 inch thick steel plate and backed with over 3 inches of lead. The ends are 7-inch thick steel. No valves, valve covers or fragile protrusions exist.

2.6.9 Compression

Not applicable since the package weighs more than 10,000 lbs.

ELEMENT TYPE	STRESS TYPE (σ_{allow}) (psi)		BASE PLATES		CASK BODY							PRIMARY LID		SECONDARY LID	
			INNER	OUTER	LOWER INNER	LOWER OUTER	MID INNER	MID OUTER	UPPER INNER	UPPER OUTER	BOLT RING	INNER	OUTER	INNER	OUTER
Shell Element STIF61	Membrane (23100)	Element			63	62	115	118	123	126					
		Value (psi)			571	887	2483	2568	2270	2431					
	Membrane + Bending (34650)	Element			51	54	115	118	159	126					
		Value (psi)			736	1319	2737	3012	3979	2609					
Solid Element STIF25	Membrane (23100)	Element	31-32	1-2							167-172	229	178	277	280
		Value (psi)	429	699							2278	784	2160	1679	2310
	Membrane + Bending (34650)	Element	4	1							167	238	185	276	281
		Value (psi)	1244	1750							4246	1656	2405	2070	5412

LOADING: 100°F Ambient + Pressure + 1-Foot Corner Drop + 100W Payload

Maximum Stress Intensities in Cask Regions

Table 2.6.6-3

2.6.10 Conclusions

From the above assessment, under normal conditons of transport, the package complies with the five criteria set forth in Section 71.35 of 10 CFR 71, as follows:

- There will be no release of radioactive material from the containment vessel.
- The effectiveness of the packaging will not be reduced.
- There will be no mixture of gases or vapors in the package which could, through any credible increase in pressure or an explosion, significantly reduce the effectiveness of the package.
- Radioactive contamination of the liquid or gaseous primary coolant will not exceed the limits specified in 10 CFR 71 Section 71.35. (This requirement is not applicable since no coolants are involved.)
- There will be no loss of coolant. (This requirement is not applicable since no coolants are involved.)

2.7 Hypothetical Accident Conditions

The package has been designed and the contents limited such that the performance requirements specified in 10 CFR 71.36 will be met if the package is subjected to the hypothetical accident conditions specified in Appendix B of 10 CFR 71.

To demonstrate the structural integrity of the cask and its ability to withstand accident conditions, a set of comprehensive loading, stress and deflection analyses have been made, addressing each of the specified accident conditions. For the 30-foot drop analyses, loads were derived by computing energy absorption of the foam overpacks and the distribution of stresses over the outer cask surface due to the overpacks. For the fire accident conditions, temperatures throughout the cask were computed using a lumped-parameter finite difference model of the cask. These loads were applied to an ANSYS finite element model in order to find stresses and deflections in the cask. Full descriptions of these analyses are contained in Appendix 2.10.1.

2.7.1 Free Drop

Appendix B of 10 CFR 71 requires that the package survive a 30 foot drop onto a flat essentially unyielding surface. The analytical methods used to demonstrate this capability closely parallel the techniques used for past Type B packages. Analytical techniques are completely described in Appendix Section 2.10.2.

As described in Section 1.2, the package features circular energy absorbing overpacks surrounding each end of the cask body. These overpacks are designed to minimize damage to the cask body from 30 foot drops at any orientation onto an unyielding surface. The analyses described in this section demonstrate that these overpacks function as designed; the cask body experiences no damage and incurs no stresses in excess of allowable levels. This behavior under 30 foot drop conditions assures the complete effectiveness of the cask closure features essential for preservation of package containment integrity.

Using the methods of Appendix 2.10.1.1., three drop conditions for the package have been evaluated, i.e., end, corner, and side. Analytical values of stress and deflection are combined with appropriate analytical values due to temperature and pressure. These combined results are then compared with applicable criteria to demonstrate compliance of the package with requirements for hypothetical accident conditions.

2.7.1.1 Free Drop Impact, End Drop Of all the potential orientation angles, the end drop produces the largest package deceleration forces. This produces the worst case loading for lead slump.

For a thirty foot end impact drop, deformation of the overpack amounted to 3.61 inches. This prediction employed the end drop analysis, described in Appendix 2.10.2.1, and the energy absorbing foam properties of Figure 2.3-1. Results of the analysis are shown in Table 2.7.1-1. A peak deceleration of 135.3g was calculated.

```
          END DROP ANALYSIS
                  C A S K   G E O M E T R Y
     CASK ID B-120       D                          G= 386.4      (IN/SEC**2)
                         -  (REV)      -
)))))) PACKAGE                 (USES CORRECTION FACTOR TABLE  STANDARD      )

        WEIGHT                (LB)    W    74000
        OUTER DIAMETER        (IN)    POD  73.5
        LENGTH                (IN)    LC   89
        DROP HEIGHT           (FT)    H    30
        CG (CASK BTM)         (IN)    LCG  44.5
        MOMENT INERTIA                ICG                (LB SEC**2 INCHES)
)) OVP MATERIALS TOP  CNSI_1-436-112-25          BTM  CNSI_1-436-112-25
                              REF   UPPER          LOWER
        INNER DIAMETER        OID   50             50              (ALL VALUES IN
        OUTER DIAMETER        OOD   96             96               INCHES)
        INNER THICKNESS       LI    18.5           18.5
        OUTER THICKNESS       LO    36.5           36.5


     C A S K   D R O P   R E S U L T S                  82/09/01     13 47 18
           END DROP ANALYSIS                           METHOD 2
-------------------------------------------------------------------------------
     CASK B-120       D     OVERPACK CNSI_1-436-112-25          UPPER
          ============       ==========================
     ALPHA
                ITERATION   TIME      DEFLECTION  ACC      FORCE       E(ABS)
     PROJECTION    20          .0121      3.607   -135.3   4541697.    26913800.
     OVERPACK                                              5543567.


                          CORRECTION FACTORS
       1   1          1          1          1          1
       6   1          1          1          1          1
      11   1          1          1          1          1


     TO SEE DETAILS OF SPECIFIC ITERATIONS, ENTER
      THEIR NUMBERS (4 AT A TIME)
```

Table 2.7.1-1

2.7.1.1 Free Drop Impact, End Drop (continued)

Detailed cask stress calculations were made using the cask finite element model discussed in Section 2.6.1. See Figure 2.6.1-1. The stresses associated with an end impact deceleration of 135.3g's were combined with maximum normal temperature and pressure stresses, as outlined in NRC Regulatory Guide 7.8. Maximum stress intensities are summarized in Table 2.7.1-2.

Stress intensities throughout the cask are well below allowables, with the maximum stress intensity of 22575 psi occurring in the bolt ring at element 167. This is also the area with the minimum factor of safety, 2.81, due to membrane stress.

The minimum factor of safety for buckling occurs in element 127, where the axial membrane stress is -8183 psi and the hoop membrane stress is 1346 psi. These are combined, according to the techniques described in Section 2.1.2.1, to yield a buckling stress intensity of 9529 psi. Thus, the factor of safety for buckling is

$$F.S. = \frac{42983}{9529} = 4.51$$

For considering Euler buckling, the axial force is due to the inertia of the cask end plus one overpack. The weight of these two items is 11070 lb. (see Section 2.2). Thus, the inertial load will be (135.3)(11070) = 1.5×10^6 lb. This is less than the critical load of 9.8×10^9 lb. (see Section 2.1.2.1, Euler Column Buckling), therefore, the cask will not fail by column buckling.

A plot of the elastically deformed cask is shown in Figure 2.7.1-1. For clarity, the deformations are greatly exaggerated. The maximum deformation is 0.077 inch.

ELEMENT TYPE	STRESS TYPE (σ allow) (psi)		BASE PLATES		CASK BODY							PRIMARY LID		SECONDARY LID	
			INNER	OUTER	LOWER INNER	LOWER OUTER	MID INNER	MID OUTER	UPPER INNER	UPPER OUTER	BOLT RING	INNER	OUTER	INNER	OUTER
SHELL ELEMENT STIF61	MEMBRANE (49000)	ELEMENT			55	58	119	122	155	134					
		VALUE (psi)			7022	6778	9097	11319	9514	11930					
	MEMBRANE + BENDING (70000)	ELEMENT			51	54	119	122	135	158					
		VALUE (psi)			9972	10370	9126	11409	10576	17346					
SOLID ELEMENT STIF25	MEMBRANE (49000)	ELEMENT	31-32	35-36							167-172	199	190	253	242-243
		VALUE (psi)	4252	3904							17453	6458	5359	1329	3025
	MEMBRANE + BENDING (70000)	ELEMENT	31	1							167	210	189	276	242
		VALUE (psi)	13256	10547							22575	8413	11065	3155	4440

LOADING: 100°F Ambient + Pressure + 30-Foot End Drop + 100W Payload

Maximum Stress Intensities in Cask Regions

Table 2.7.1-2

8/3/82. 16.9 3 D2.

STEP 1 ITER 1 TIME 1.00 .07729

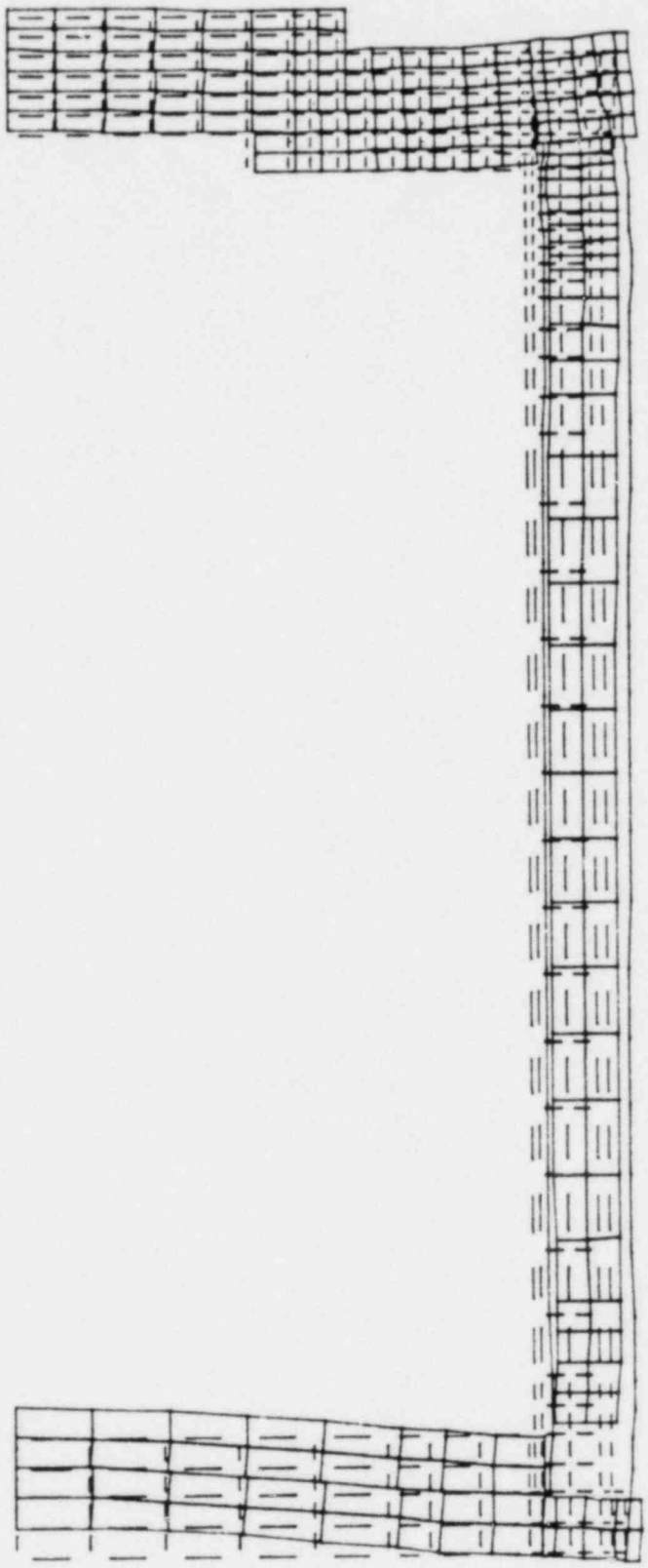

ZV=1

8-120 LINEAR STATIC ANALYSIS, END DROP, TOP DOWN DISP ANSYS 1

Figure 2.7.1-1

(1) Lead Slump

Historically, lead slump in shipping casks due to the 30-foot drop accident condition has been analyzed using an equation presented by L.B. Shappert in ORNL-NSIC-68, "Cask Designers Guide," as follows:

$$\Delta h = \frac{RWH}{\pi(R^2-r^2)(t_s\sigma_s+R\sigma_{Pb})} \qquad (1)$$

where Δh = change in height of lead (i.e., lead slump) (in.)
R = radius of outer steel shell of cask (in.)
W = total weight of cask (lb.)
H = drop height (in.)
r = radius of inner steel shell of cask (in.)
t_s = thickness of outer steel shell of cask (in.)
σ_s = yield strength of outer steel shell of cask (psi)
σ_{Pb} = dynamic flow pressure of lead (psi)

The development of this equation was presented by B.B. Klima, L.B. Shappert and W.C.T. Stoddart in ORNL-TM-1312, Vol. 6, "Structural Analysis of Shipping Casks, Vol. 6 - Impact Testing of a Long Cylindrical Lead-Shielded Cask Model." The basic approach used in their analysis of lead slump was to equate the kinetic energy of the falling cask to the strain energy required to cause lead slump. The strain energy of lead slump was composed of two parts: that energy required to deform the lead and that energy required to deform the outer steel shell of the cask to provide a volume into which the lead could flow.

In computing this energy balance, it is important to note that Klima, et. al., used the entire weight of the cask in computing the kinetic energy to be dissipated by the straining of the lead. Implicit in this method is the assumption that the non-lead components of the cask (e.g., steel shells and end closures, and the payload) can somehow transfer their kinetic energy to the lead, or that these components represent a negligible part of the kinetic energy, compared to the

lead. This is not generally a reasonable assumption. Nevertheless, two comparisons of lead slump predicted by the equation were made with measured values obtained by dropping scale model casks. These comparisons showed that the predicted lead slump was 80-85 per cent of the measured values. Based on these comparisons, the conclusion was drawn that the equation gave a reasonable prediction of lead slump. If the more reasonable assumption is made that only the kinetic energy of the lead is to be used in computing lead slump, in comparison with the same two tests, the equation predicts lead slump to be 60-65 per cent of the measured values. These are not acceptably close enough to the measured values to be considered adequate predictions of lead slump. Thus, the equation historically used to predict lead slump is unacceptable because of erroneous assumptions made in its derivation. Even if these assumptions are corrected, it is still unacceptable due to lack of agreement with test values. While the equation was known not to apply to casks with energy absorbers, it has, in the past, been used to predict an upper bound worst case lead slump for casks so equipped. The equation is not even adequate for that purpose, and, for the reasons outlined above, this equation is not used to predict lead slump in the CNS 8-120B cask. Instead, lead slump is derived directly from the finite element model used to compute stresses and deflections in the cask for the end drop analysis. From that analysis, lead slump is predicted to be 0.10 inch. This agrees well with test results of other type B packages using foam overpacks, in which no measurable lead slump was found. No bonding was assumed between the lead and the steel shells in evaluating lead slump.

2.7.1.2 Free Drop Impact, Side Drop Behavior of the overpacks during side drop conditions has been evaluated using the analysis described in Appendix 2.10.1.1. Results are shown in Table 2.7.1-3. A peak acceleration of 108.3g was calculated.

```
                    C A S K   G E O M E T R Y
     CASK ID B-120       D                              G= 386.4      (IN/SEC**2)
                         -  (REV)        -
))))))) PACKAGE                  (USES CORRECTION FACTOR TABLE  STANDARD       )

          WEIGHT              (LB)    W    74000
          OUTER DIAMETER      (IN)    POD  73.5
          LENGTH              (IN)    LC   89
          DROP HEIGHT         (FT)    H    30
          CG (CASK BTM)       (IN)    LCG  44.5
          MOMENT INERTIA              ICG                (LB SEC**2 INCHES)
)) OVP MATERIALS TOP: CNSI_1-436-112-25                   BTM  CNSI_1-436-112-25
                          REF   UPPER          LOWER
          INNER DIAMETER  DID   50             50                (ALL VALUES IN
          OUTER DIAMETER  DOD   96             96                 INCHES)
          INNER THICKNESS L1    18.5           18.5
          OUTER THICKNESS LO    36.5           36.5


     C A S K   D R O P   R E S U L T S                    82/09/01    13 53 23
     SIDE DROP                                           METHOD 2
-------------------------------------------------------------------------------
     CASK B-120       D     OVERPACK CNSI_1-436-112-25
       ===========          ========================

     ALPHA
                 ITERATION   TIME      DEFLECTION  ACC      FORCE       E(ABS)
TOP                  57        .0198      6.397    -108.3   4045224.   13557266.
BOTTOM                                     6.397    -108.3   4045224.   13557257.
COMBINED                                             -108.3   8090448.   27114525.

                         CORRECTION FACTORS
          1   1          1          1          1          1
          6   1          1          1          1          1
         11   1          1          1          1          1


     TO SEE DETAILS OF SPECIFIC ITERATIONS, ENTER
      THEIR NUMBERS (4 AT A TIME)
```

Table 2.7.1-3

2.7.1.2 Free Drop Impact, Side Drop (continued)

Detailed cask stress analysis was performed using the finite element model described in Section 2.6.1.2. See Figure 2.6.1-1. The stresses associated with the 30-foot side drop were combined with normal thermal and pressure stresses. Maximum stress intensities are summarized in Table 2.7.1-4.

Stress intensities are well below allowables throughout the cask during the 30-foot side drop. The highest stress intensity, 50125 psi, occurs in element 183 at the bolt in the primary lid. This is also the area having the minimum factor of safety, 1.40. This high stress intensity is due to a radial compressive stress which is developed because of the radial coupling of the lid to the bolt ring at the bolt location (Nodes 334 and 365). This was done in order to determine bolt forces and, hence, bolt stresses. However, this results in unrealistically high stresses in the lid because the lid and bolt design are such that radial compressive forces will be reacted by bearing between the cask wall and the lower plate of the lid. Actual stresses in this area of the cask will be substantially lower (below yield) than this analysis indicates.

A plot of the deformed cask is shown in Figure 2.7.1-2. For clarity, the deformations are greatly exaggerated. The maximum deformation is 0.064 inch.

(1) Side Drop, Lid Bolt Forces

The loads required to hold the primary and secondary lids in place were computed using the ANSYS stress analysis model. The forces of the bolts were computed in the axial (tensile), radial (shear) and hoop (shear) directions. The lids and bolts are designed so that radial "compressive" forces are reacted by bearing between the primary lid and the cask body and between the secondary lid and the primary lid. Because of this, only radial "tensile" forces are used in computing bolt stresses. Radial "compressive" forces are those which tend to drive the bolted parts together in the radial direction, while radial "tensile" forces are those which tend to separate the bolted parts in the radial direction. These forces were converted to coordinate stresses by dividing by the bolt stress area (2.77 in^2 for 2-8 UN bolts). Principal stresses and stress intensities were then computed based on these coordinate stresses.

ELEMENT TYPE	STRESS TYPE (σ allow) (psi)		BASE PLATES		CASK BODY							PRIMARY LID		SECONDARY LID	
			INNER	OUTER	LOWER INNER	LOWER OUTER	MID INNER	MID OUTER	UPPER INNER	UPPER OUTER	BOLT RING	INNER	OUTER	INNER	OUTER
SHELL ELEMENT STIF61	MEMBRANE (49000)	ELEMENT			59	62	119	106	135	138					
		VALUE (psi)			22400	11933	15331	13151	29124	25628					
	MEMBRANE + BENDING (70000)	ELEMENT			47	50	119	110	139	138					
		VALUE (psi)			46647	28575	19154	23123	34558	39788					
SOLID ELEMENT STIF25	MEMBRANE (49000)	ELEMENT	31-32	39-40							167-172	199	181	253	250
		VALUE (psi)	14621	16072							20392	8809	23091	2855	15482
	MEMBRANE + BENDING (70000)	ELEMENT	32	40							169	194	186	248	242
		VALUE (psi)	22679	19420							14882	17471	50125	8375	32476

LOADING: 100°F Ambient + Pressure + 30-Foot Side Drop + 100W Payload

Maximum Stress Intensities in Cask Regions

Table 2.7.1-4

8/3/82 17.3 3 D2

STEP 1 ITER 1 TIME 1.00 .06361

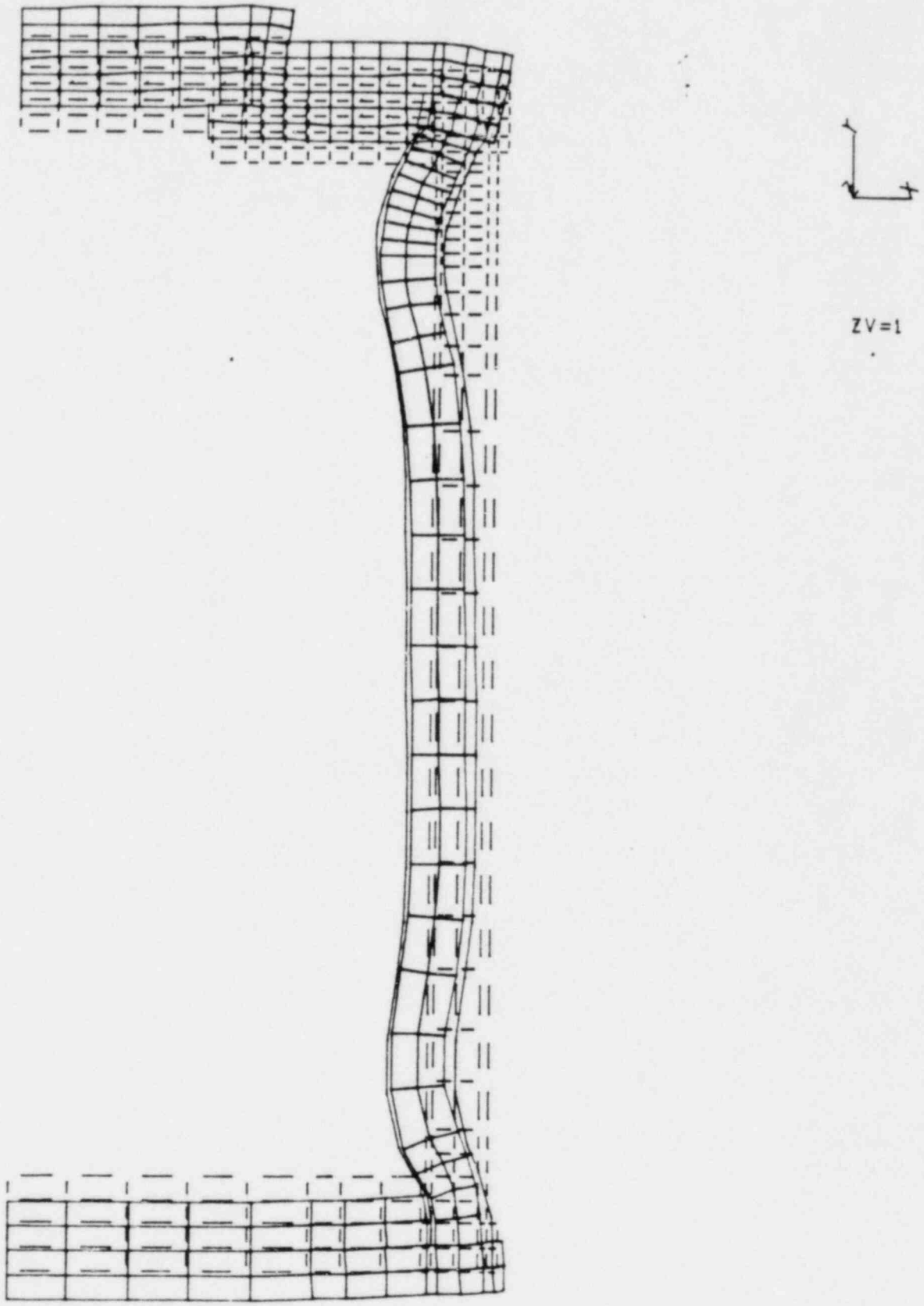

8-120 STATIC ANALYSIS, SIDE DROP DISP ANSYS 1

Figure 2.7.1-2

2.7.1.2 Free Drop Impact, Side Drop (continued)

The resulting stress intensities, as functions of angular position of the bolts, are shown in Figures 2.7.1-3 and 2.7.1-4 for the primary bolts and secondary bolts, respectively. The angular position is measured around the circumference of the cask with zero degrees corresponding to the vertical downward direction. The highest stress intensity was found to be 123 ksi, and the resultant safety factor, based on yield, is

$$F.S. = \frac{130}{123} = 1.06$$

2.7.1.3 Free Drop Impact, Corner Drop An energy balance analysis, described in Appendix 2.10.1, was used to predict loads on the cask during the corner drop. The angle of the cask with respect to the impact surface was chosen so that the center of pressure at full deformation was directly beneath the cask center of gravity. Because none of the drop energy is converted to rotational energy of the cask, this is the worst case. Results of the analysis are shown in Table 2.7.1-5. Peak acceleration was calculated to be 76.1g's at a deformation of 15.39 inches.

A detailed cask stress analysis was performed using the finite element model described in Section 2.6.1.2. See Figure 2.6.1-1. The stresses associated with a corner drop acceleration of 76.1g's were combined with normal thermal and pressure stresses, as outlined in NRC Regulatory Guide 7.8. Maximum stress intensities are summarized in Table 2.7.1-6.

Stresses in the cask are well below allowables during the 30-foot corner drop. The highest stress, 48449 psi, occurs in element 281 at the center of the secondary lid. The minimum factor of safety occurs in this area and is equal to 1.44.

Buckling was evaluated according to the techniques described in Section 2.1.2.1. The minimum factor of safety for buckling was found to occur in the inner shell near the bolting ring, at element 163. The axial membrane stress was -27030 psi and the hoop membrane stress was 7857 psi. The corresponding buckling stress intensity is 27030 psi, and the minimum factor of safety is

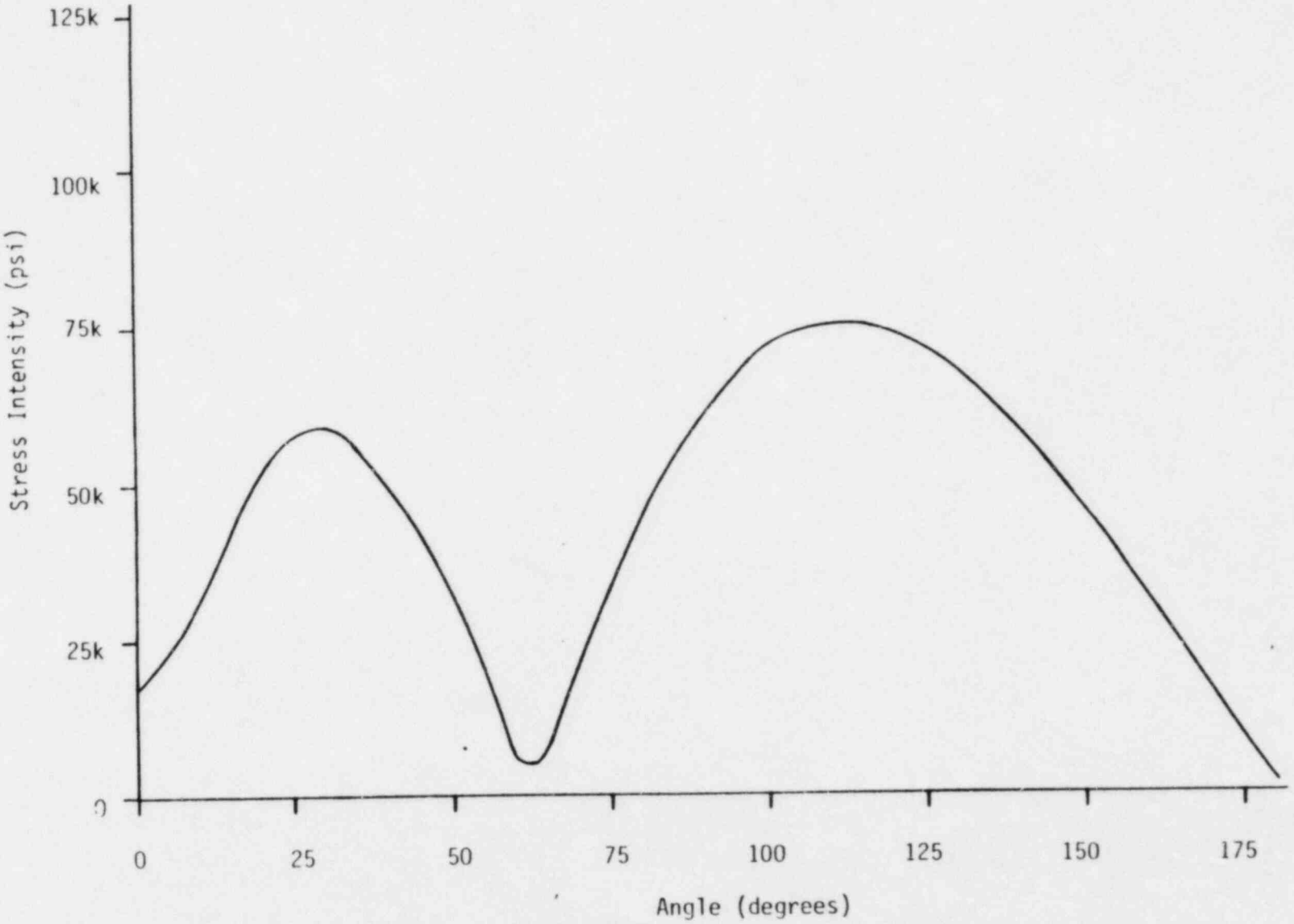

Figure 2.7.1-3 PRIMARY LID BOLT STRESS INTENSITY FOR SIDE DROP

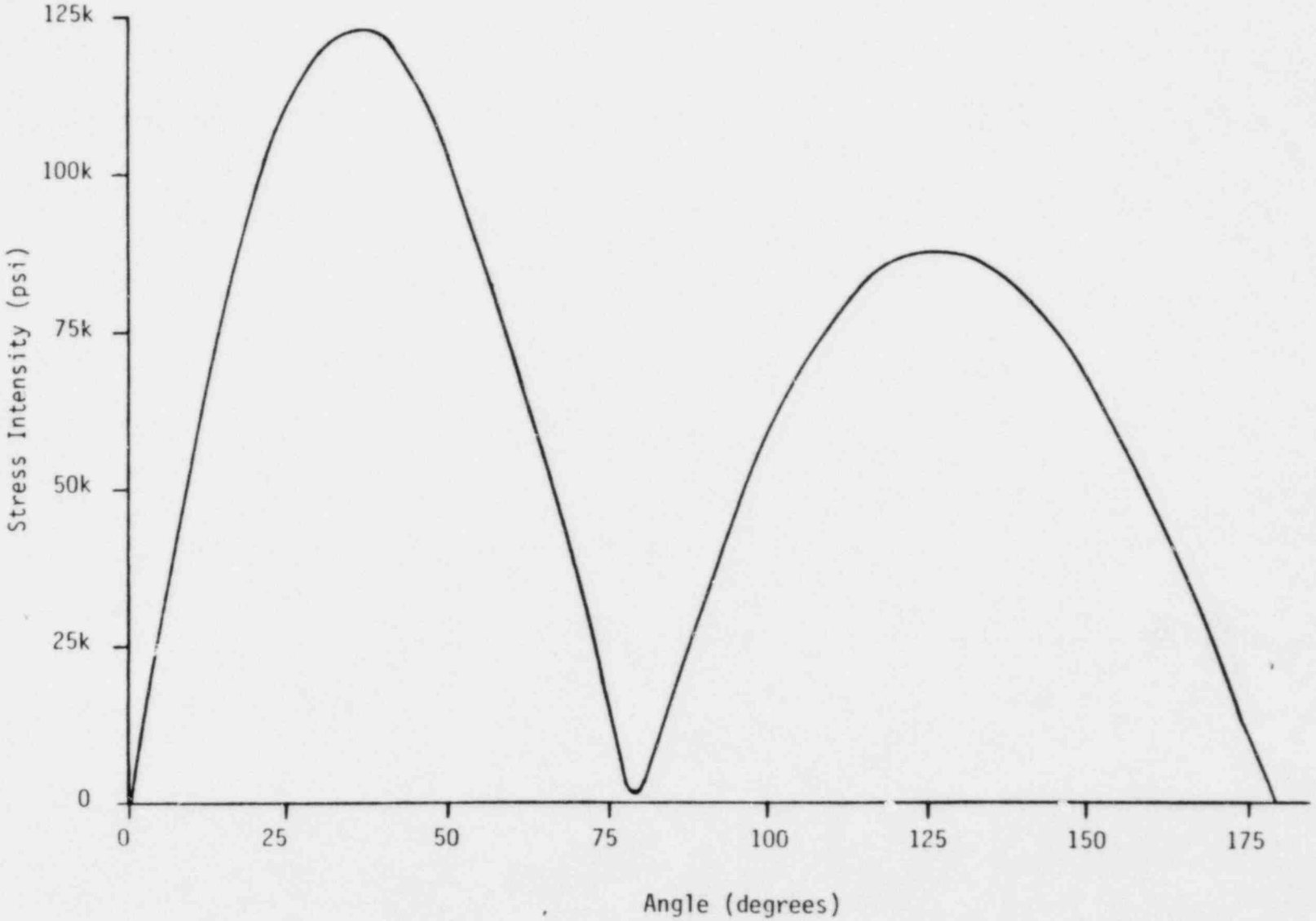

Figure 2.7.1-4 SECONDARY LID BOLT STRESS INTENSITY FOR SIDE DROP

```
                    C A S K   G E O M E T R Y
    CASK ID B-120       D                          G= 386.4      (IN/SEC**2)
                        -  (REV)       -
)))))))) PACKAGE                (USES CORRECTION FACTOR TABLE: STANDARD       )

        WEIGHT              (LB)   W    74000          .
        OUTER DIAMETER      (IN)   POD  73.5
        LENGTH              (IN)   LC   89
        DROP HEIGHT         (FT)   H    30
        CG (CASK BTM)       (IN)   LCG  44.5
        MOMENT INERTIA             ICG                (LB SEC**2 INCHES)
)) OVP MATERIALS TOP: CNSI_1-436-112-25          BTM: CNSI_1-436-112-25
                           REF   UPPER          LOWER
        INNER DIAMETER     OID   50             5                (ALL VALUES IN
        OUTER DIAMETER     OOD   96             96                INCHES)
        INNER THICKNESS    LI    18.5           18.5
        OUTER THICKNESS    LO    36.5           36.5


    C A S K   D R O P   R E S U L T S:                 82/09/08    16:38:05
    CORNER DROP                                       METHOD 2
-------------------------------------------------------------------------------
    CASK B-120       D    OVERPACK CNSI_1-436-112-25
         ============        ========================
    ALPHA:  149.20
              ITERATION    TIME      DEFLECTION  ACC       FORCE       E(ABS)
  TOP DOWN        71          .0401     15.393    -76.1    5704910.    27777556.


                        CORRECTION FACTORS
      1:  1          1          1          1          1
      6:  1          1          1          1          1
     11:  1          1          1          1          1

    TO SEE DETAILS OF SPECIFIC ITERATIONS, ENTER
     THEIR NUMBERS (4 AT A TIME):
```

Table 2.7.1-5

ELEMENT TYPE	STRESS TYPE (σ allow) (psi)		BASE PLATES		CASK BODY							PRIMARY LID		SECONDARY LID	
			INNER	OUTER	LOWER INNER	LOWER OUTER	MID INNER	MID OUTER	UPPER INNER	UPPER OUTER	BOLT RING	INNER	OUTER	INNER	OUTER
SHELL ELEMENT STIF61	MEMBRANE (49000)	ELEMENT			63	62	115	118	123	126					
		VALUE (psi)			5112	7938	22229	22988	20321	21769					
	MEMBRANE + BENDING (70000)	ELEMENT			51	54	115	118	159	126					
		VALUE (psi)			6587	11809	24501	26969	35628	23361					
SOLID ELEMENT STIF25	MEMBRANE (49000)	ELEMENT	31-32	1-2							167-172	229	178	277	280
		VALUE (psi)	3840	6262							20392	7021	19338	15028	20680
	MEMBRANE + BENDING (70000)	ELEMENT	4	1							167	238	185	276	281
		VALUE (psi)	11134	15667							38015	14829	21531	18529	48449

LOADING: 100°F Ambient + Pressure + 30-Foot Corner Drop + 100W Payload

Maximum Stress Intensities in Cask Regions

Table 2.7.1-6

2.7.1.3 Corner Drop (continued)

$$F.S. = \frac{42943}{27030} = 1.59$$

A plot of the deformed cask is shown in Figure 2.7.1-5. For clarity, the deformations are greatly exaggerated. The maximum deformation is 0.042 inch.

(1) Corner Drop, Lid Bolt Forces

The loads required to hold the primary and secondary lids in place were computed using the ANSYS stress analysis model. The forces of the bolts were computed in the axial (tensile), radial (shear) and hoop (shear) directions. The lids and bolts are designed so that radial "compressive" forces are reacted by bearing between the primary lid and the cask body and between the secondary lid and the primary lid. Because of this, only radial "tensile" forces are used in computing bolt stress. Radial "compressive" forces are those which tend to drive the bolted parts together in the radial direction, while radial "tensile" forces are those which tend to separate the bolted parts in the radial direction. These forces were converted to coordinate stresses by dividing by the bolt stress area (2.77 in^2 for 2-8 UN bolts). Principal stresses and stress intensities were then computed based on these coordinate stresses. The resulting stress intensities, as functions of angular position of the bolts, are shown in Figures 2.7.1-6 and 2.7.1-7 for the primary bolts and secondary bolts, respectively. The angular position is measured around the circumference of the cask with zero degrees corresponding to the vertical downward direction. The highest stress intensity was found to be 113 ksi, and the resultant safety factor, based on yield, is

$$F.S. = \frac{130}{113} = 1.15$$

As a rough check on these calculations, a second calculation of lid bolt forces was performed, as outlined below.

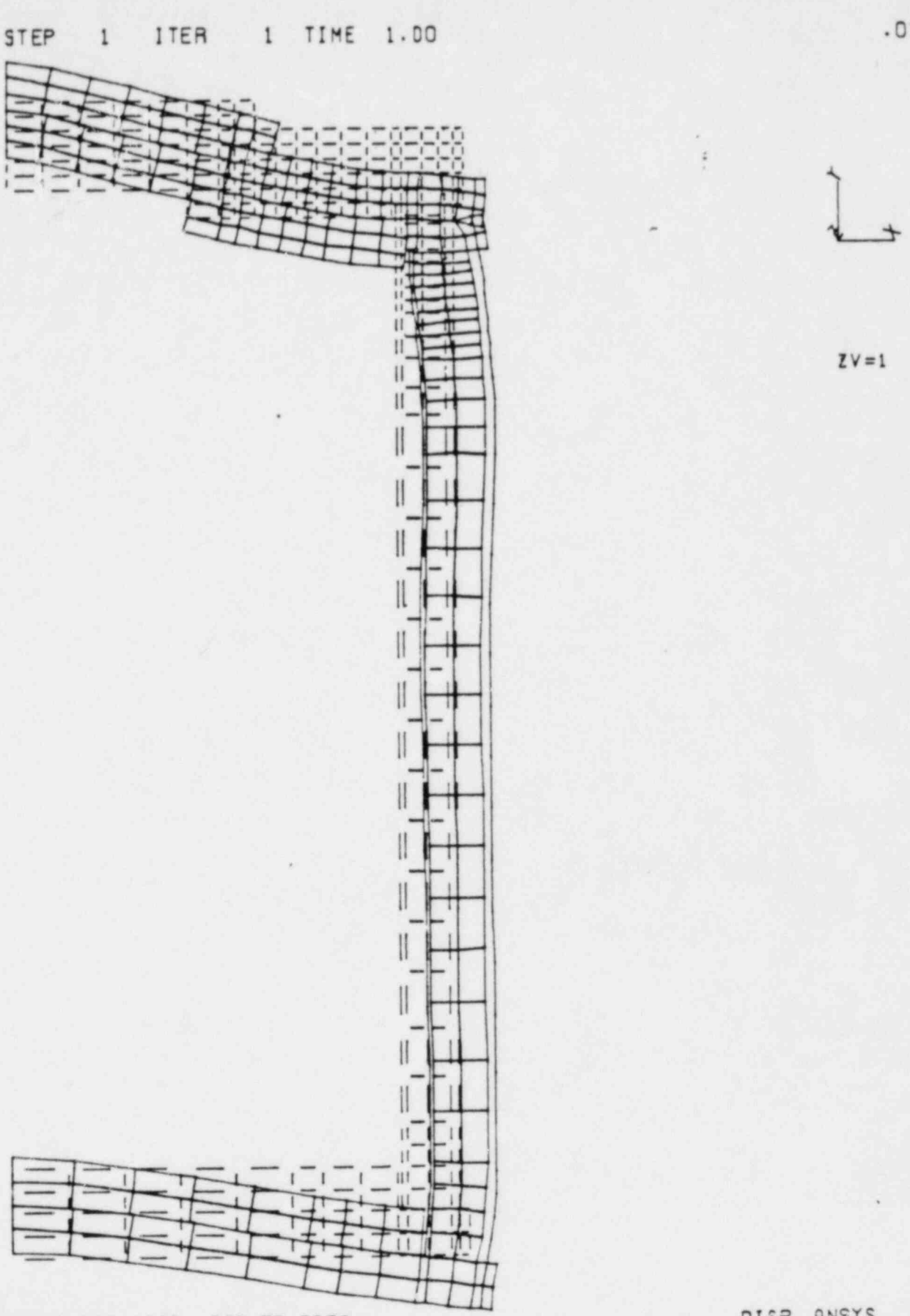
8/3/82 17.4 3 D2
STEP 1 ITER 1 TIME 1.00
.03676
ZV=1
8-120 STATIC ANALYSIS, CORNER DROP
DISP ANSYS 1

Figure 2.7.1-5

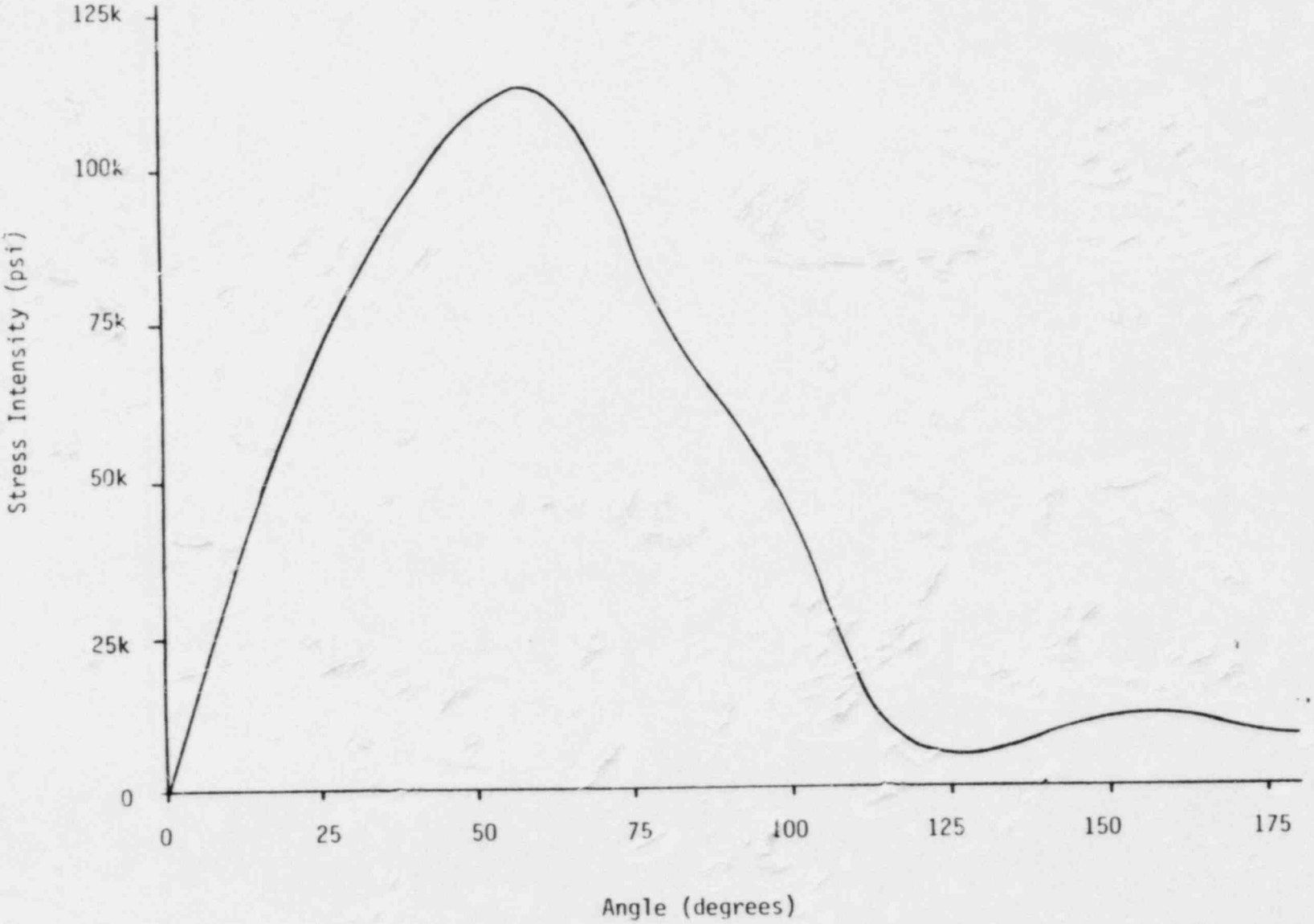

Figure 2.7.1-6 PRIMARY LID BOLT STRESS INTENSITY FOR CORNER DROP

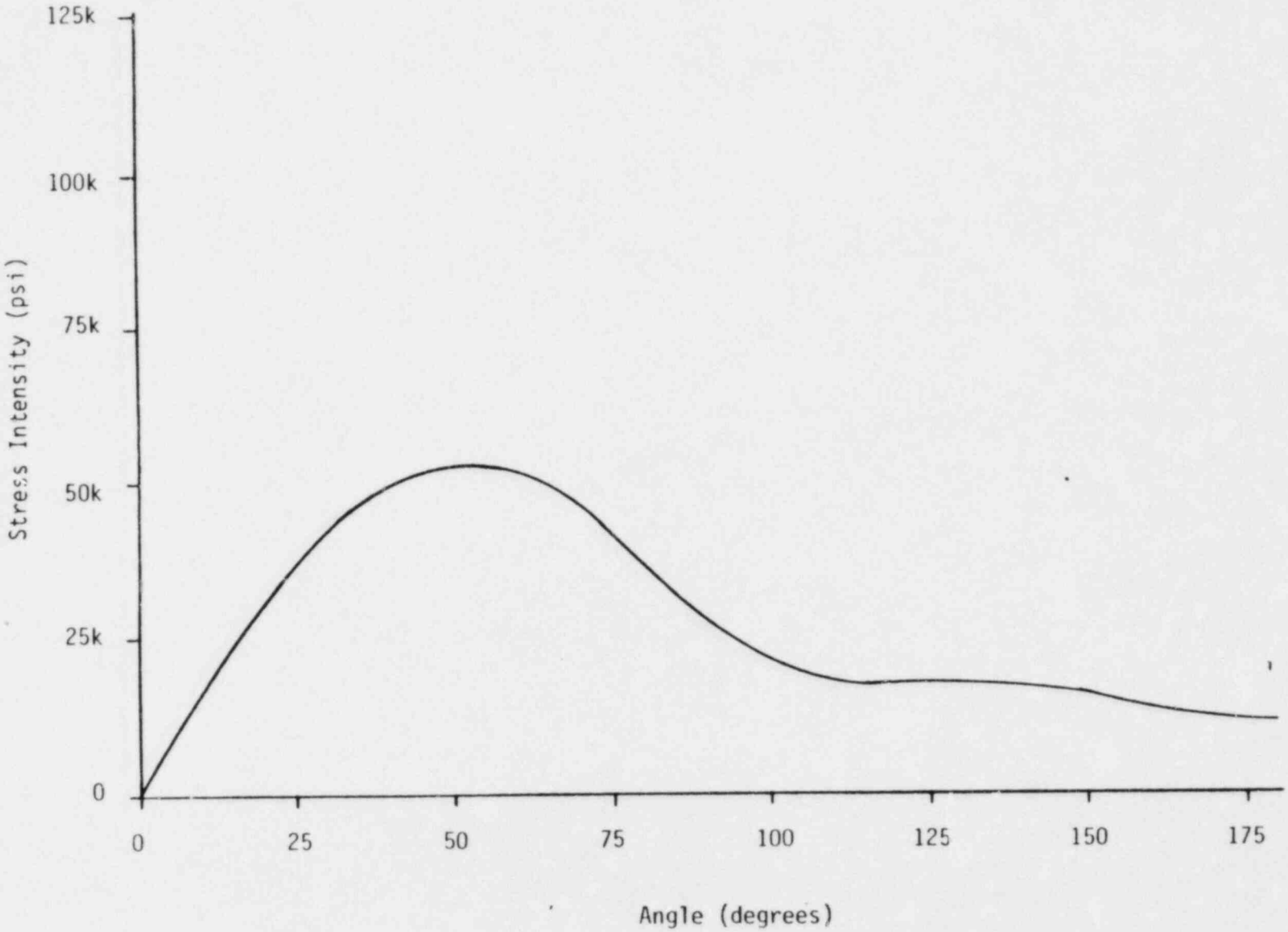

Figure 2.7.1-7 SECONDARY LID BOLT STRESS INTENSITY FOR CORNER DROP

2.7.1.3 Corner Drop (continued)

Assume the cask is to be dropped at an angle such that the cask CG is above the impact point. Then forces on the lid (except bolt forces) will be as shown schematically in Figure 2.7.1-8.

Symbols used are defined as follows:

α = angle of cask with horizontal

F_p = total inertial force of payload in axial direction (distributed over lid area)

F_c = total cask inertial load in axial direction (distributed as a ring load at the lid circumference)

F_I = impact load

F_L = total lid inertial load (distributed over lid volume)

For the purpose of determining lid bolt forces, the cask inertial force, F_c, can be conservatively neglected. F_c tends to reduce the bolt tensile loads, therefore neglecting it will result in higher bolt loads than if the effects of F_c are considered.

Due to the manner in which loads are applied to the lid, the lid will tend to rotate about the impact point. If the lid were to rotate as a rigid body, bolts near the point of impact would experience little or no tensile force, but, as the bolts get further from the point of impact, the tensile force in the bolts will increase. Thus, one might take bolt forces to be proportional to distance from the impact point. However, there is a second effect at work here. Refer to Figure 2.7.1-9.

As distance from the impact point increases, the width of plate which must be supported by each bolt changes. First the plate width increases to a maximum equal to one-half the diameter of the lid and then decreases to a minimum at the side opposite the impact point. Because the loads imposed on the bolts are inertial, they are proportional to lid area. If one assumes that the area of plate to be supported by each bolt is proportional to the width of plate to be

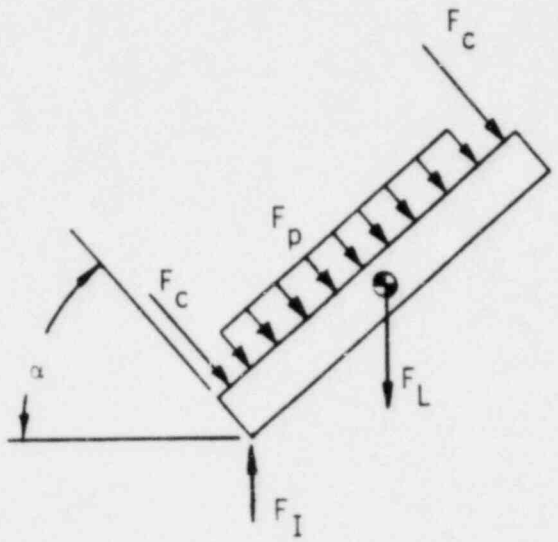

Figure 2.7.1-8 SIDE VIEW OF LID FOR CORNER DROP

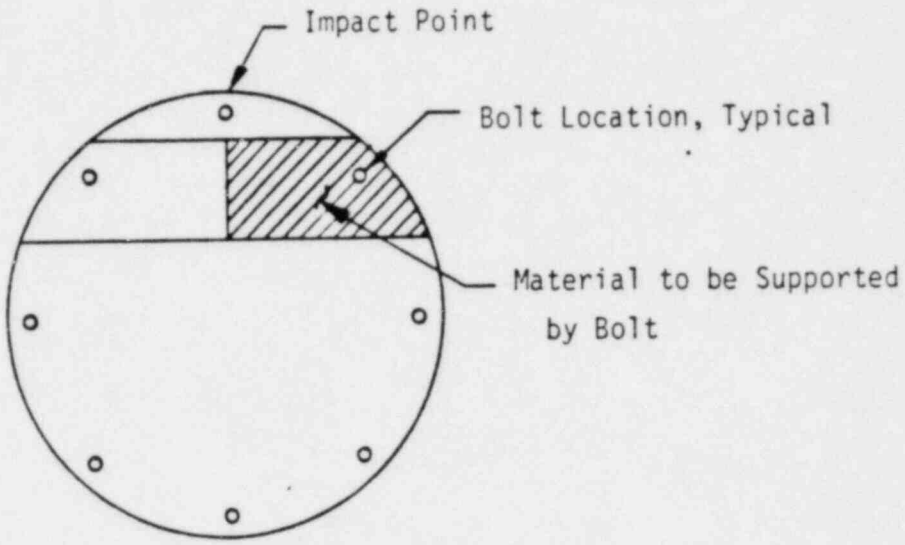

Figure 2.7.1-9 END VIEW OF LID FOR CORNER IMPACT

supported by each bolt, then bolt forces are proportional to plate width at each bolt location.

These two effects, distance from impact point and plate width, can be combined by taking the load on each bolt to be proportional to distance times width.

The expression for this proportionality factor will now be derived for a lid having n bolts, where n is an even integer.

Refer to Figure 2.7.1-10. For n bolts evenly spaced, the angle between adjacent bolts is:

$$\beta = \frac{2\pi}{n}$$

Then, the angular location of bolt i is

$$\theta_i = (i-1)\beta \qquad 1 \leq i \leq (n/2) + 1$$

Note that, due to considerations of symmetry, only bolts having $0 \leq \theta \leq \pi$ are considered. In computing bolt forces, this will be compensated by multiplying the appropriate terms by two in order to account for the opposite bolts.

For bolt i:

$$x'_i = R\cos(\theta_i - \pi/2)$$
$$= R\sin\theta_i$$
$$y'_i = R\sin(\theta_i - \pi/2)$$
$$= -R\cos\theta_i$$
$$\Delta_i = \sqrt{R_0^2 - Y_i^2} - X_i$$
$$= \sqrt{R_0^2 - R^2\cos^2\theta_i} - R\sin\theta_i$$

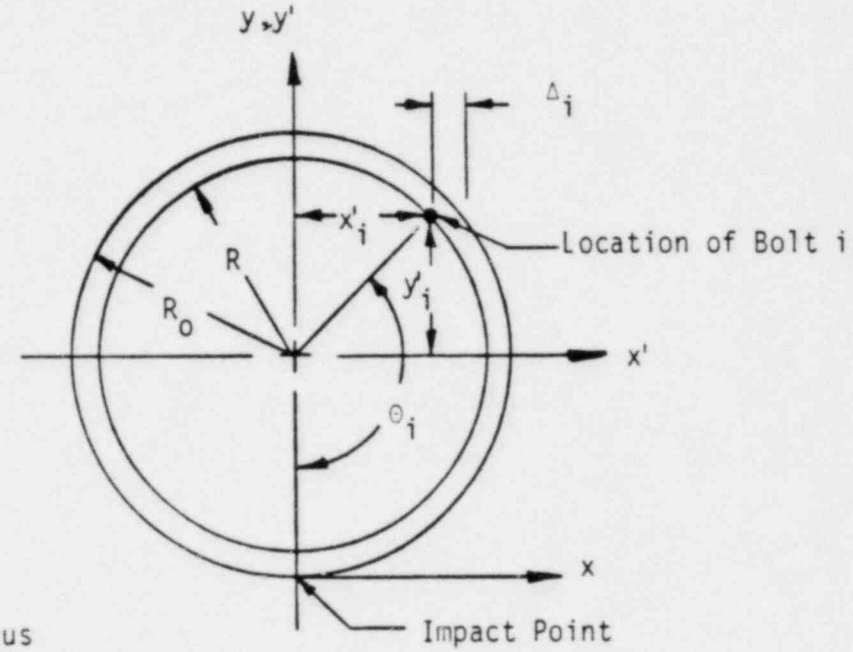

R=Bolt Circle Radius

R_o=Lid Radius

Figure 2.7.1-10 LID BOLT LOCATION GEOMETRY

2.7.1.3 Corner Drop (continued)

To translate to a coordinate system with origin at the point of impact

$$x = x'$$

$$y = y' + R_o$$

Then

$$x_i = R\sin\theta_i$$

$$y_i = R_o - R\cos\theta_i$$

$$\Delta_i = \sqrt{R_b^2 - R^2\cos^2\theta_i} - R\sin\theta_i$$

The weighting factor for a given bolt is

$$k_i = y_i\,(x_i + \Delta_i)$$

$$= (k_o - R\cos\theta_i)\,\sqrt{R_b^2 - R^2\cos^2\theta_i}$$

$$= \left[R_o - R\cos[(i-1)\,2\pi/n]\right]\sqrt{k_b^2 - k^2\cos^2[(i-1,\,2\pi/n]}$$

for $1 \leq i \leq (n/2) + 1$

The force on bolt "i" is given by

$$F_i = k_i\,F_n$$

where

F_n = a nominal bolt force

By force balance,

$$\sum_{i=1}^{n} F_i = F_T$$

where F_T = total applied lid force

$= F_L \sin\alpha + F_p$ (Refer to Fig. 2.7.1-8)

However

$$\sum_{i=1}^{n} F_i = F_n[k_1 + k_{n/2+1} + 2\sum_{i=2}^{n/2} k_i]$$

Then

$$F_n = \frac{F_T}{k_2 + k_{n/2+1} + 2\sum_{i=2}^{n/2} k_i}$$

2.7.1.3 Corner Drop (continued)

The maximum bolt force will correspond to the maximum k and

$$F_{max} = k_{max} F_n$$

This is the maximum tensile force in the lid bolts and will result in a tensile bolt stress. The maximum bolt stress will be a result of this force plus the shear force in the bolts. If it is conservatively assumed that the bolts resist the shearing forces between the lid and cask body, then the shearing force in each bolt, assuming the force is evenly divided amongst the bolts, is

$$F_s = \frac{W_c(a)\cos\alpha}{n}$$

where

W_c = total weight of cask minus weight of lid and one overpack
a = acceleration in g's (vertical)
α = angle of cask to horizontal (Ref. to Fig. 2.7.1-8)
n = number of lid bolts

This bolt shear force will result in a bolt shear stress which must be considered in conjunction with the tensile stress previously computed to determine the principal stresses and stress intensity in the bolt.

The following values apply to the 8-120B primary lid bolts:

n = 32 bolts
R_o = 36.75 in.
R = 34.125 in.
α = 34°
F_L = 7420 lb. x 76.1 g's = 564662 lb.
F_p = 14050sinα x 76.1 g's = 597892 lb.

2.7.1.3 Corner Drop (continued)

Then the values of k are as follows:

i	k	i	k
1	35.80	10	1568.83
2	49.79	11	1711.01
3	98.62	12	1753.83
4	195.63	13	1687.49
5	349.80	14	1521.01
6	560.10	15	1289.32
7	813.82	16	1065.78
8	1087.60	17	966.73
9	1350.56		

and

$$k_i + k_{17} + 2 \sum_{L=2}^{16} k_i = 31209$$

$$k_{max} = 1753.83$$

$$F_T = 564662\sin(34°) + 597892$$

$$= 9.14 \times 10^5 \text{ lb.}$$

So that

$$F_n = \frac{9.14 \times 10^5}{31209}$$

$$= 29.29$$

Then

$$F_{max} = (29.29)(1753.83)$$

$$= 51363 \text{ lb.}$$

Also,

$$W_c = 74000 - 7320 - 3750$$

$$= 62930 \text{ lb.}$$

2.7.1.3 Corner Drop (continued)

and

$$F_s = \frac{(62930)(76.1)\cos 34^\circ}{32}$$

$$= 124070 \text{ lb.}$$

For a 2-6 UN bolt, $A_s = 2.77 \text{ in}^2$, therefore

$$\sigma = \frac{51363}{2.77} = 18543 \text{ psi}$$

$$\sigma_{shear} = \frac{124070}{2.77} = 44791 \text{ psi}$$

The corresponding principal stresses are

$$\sigma_1 = 55 \text{ ksi}$$

$$\sigma_2 = -36.5 \text{ ksi}$$

$$\sigma_3 = 0$$

and the stress intensity,

$$SI = 55 + 36.5 = 91.5 \text{ ksi}$$

Therefore

$$\text{Safety Factor} = \frac{130}{91.5} = 1.42$$

Using two different analytical techniques, it has been shown that stresses in the lid bolts will remain below yield during the 30-foot corner drop accident conditions.

2.7.1.4 Oblique Drop Figure 2.7.1-11 illustrates the position of the package at the beginning of the oblique drop. An analysis of oblique drops is presented in Appendix 2.10.1.4. The analysis indicates that for a package with a diameter approximately equal to its length, there is no slapdown effect. That is, the impact is not more severe than a side drop.

Since the diameter of the package impact limiter is 96 inches and the overall package height is 126 inches, the oblique drop is not more severe than the side drop, as shown in the oblique analysis.

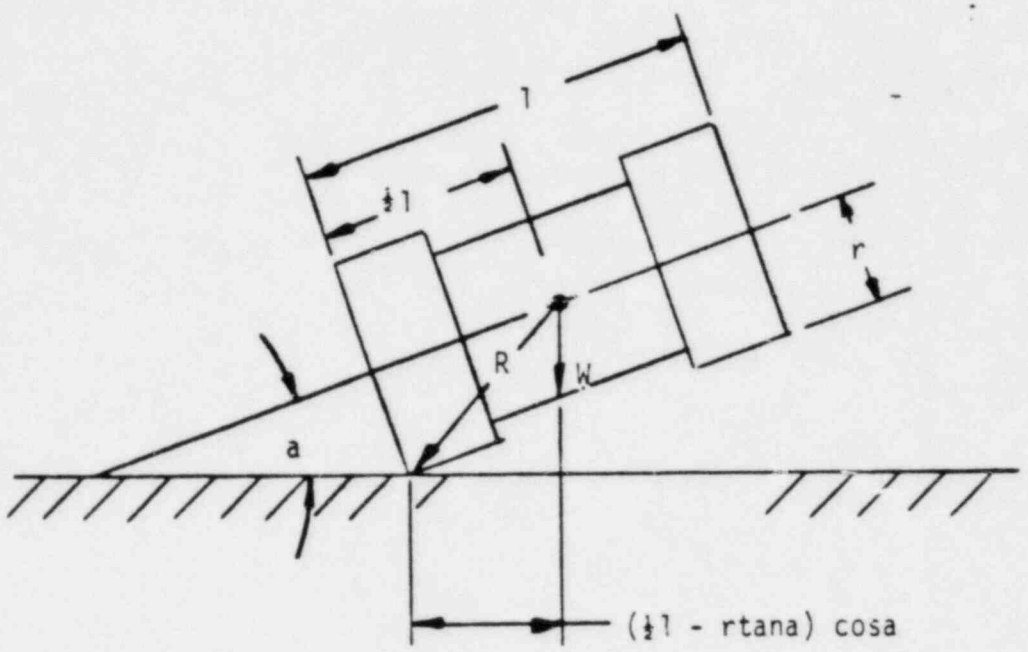

Figure 2.7.1-11 CASK ORIENTED FOR OBLIQUE DROP

2.7.2 Puncture

The Nelms[1] puncture relation is given as:

$$t = (W/S)^{0.71}$$

where: t = shell thickness = 1-1/2 inches
W = cask weight, lbs.
S = ultimate tensile strength of outer shell
= 70000 psi

The package weight causing puncture is:

$$W = St^{1.4}$$

The corresponding weight to cause puncture of the 1-1/2 inch outer shell is:

$$W_s = (70000)(1.5)^{1.4} = 123488 \text{ lbs.}$$

The actual package weight is 74000 lbs; therefore, the factor of safety for puncture resistance on an energy basis is:

$$F.S. = \frac{123488}{74000} = 1.67$$

When the package impacts the puncture pin, the force imposed upon the package is estimated as:

$$F_I = k_s A_I$$

k_s = Dynamic flow pressure of steel = 45,000 psi[2]

R_c = Pin diameter = 6.0 inches

$$A_I = \frac{\pi}{4} (R_c)^2 = \frac{\pi}{4} (6.0)^2 = 28.27 \text{ in.}^2$$

(1) Shappert, L.B., "Cask Designers Guide", ORNL-NSIC-68, Page 18.
(2) Shappert, L.B., "Cask Designers Guide", ORNL-NSIC-68, Page 64.

2.7.2 Puncture (continued)

$$F_I = (45000)(28.27)$$
$$= 1.272 \times 10^6 \text{ lbs.}$$

This force induces a moment at the midsection of the package. The moment is estimated as:

$$M = \frac{FI}{8} = \frac{(1.272 \times 10^6)(89)}{8} = 14.2 \times 10^6 \text{ in-lb.}$$

Using the section properties from Section 2.5.1 to calculate stresses gives a bending stress of:

$$\sigma_b = \frac{Mc}{I} = \frac{(1.42 \times 10^7)(36.75)}{1.134 \times 10^5}$$
$$\sigma_b = \pm 4602 \text{ psi}$$

Conservatively assuming that the compressive and tensile stresses occur at the same location, the stress intensity is 9204 psi and the factor of safety is:

$$F.S. = \frac{70}{9.2} = 7.6$$

To evaluate the ability of the cask to withstand puncture from a 40-inch end drop onto a 6-inch diameter pin, the end of the cask will be treated as two simply supported plates with a central load. Since the end is comprised of two 3.5-inch thick plates which must have identical deflections, the energy of the drop will be divided evenly between the two plates.

Ref. 4, p. 415 gives the following equation for the deflection of a centrally loaded circular plate:

$$\frac{w_o}{h} + A\left(\frac{w_o}{h}\right)^3 = B\left(\frac{Pa^2}{Eh^4}\right)$$

where:

w_o = deflection at center of plate, in.
h = plate thickness, in.
P = central load, lb.
E = elastic modulus, psi

2.7.2 Puncture (continued)

a = plate radius, in.

$A = 0.272$

$B = 0.552$ } for simply supported plate, Ref. 4, p.416

The deformation energy can be found from

$$u = \int_0^{\delta} P dw_0$$

$$= \frac{Eh^4}{Ba^2}\left[\frac{\delta^2}{2h} + \frac{A\delta^4}{4h^3}\right]$$

This can be equated to the drop energy, WH/2, to find the central deflection:

$$\delta^2 = \frac{-\frac{1}{h} + \sqrt{\frac{1}{h^2} + \frac{Aba^2}{Eh^7}\frac{WH}{2}}}{\frac{A}{2h^3}}$$

Ref. 4, p.415, gives the following equations for the maximum membrane and membrane-plus-bending stresses:

membrane:

$$\sigma_1 = \alpha E \delta^2/a^2$$

membrane-plus-bending:

$$\sigma_2 = \beta E \delta h/a^2$$

For

$h = 3.5$ in.

$E = 29 \times 10^6$ psi

$a = 31$ in.

$W = 74000$ lbs.

$H = 40$ in.

$\alpha = 0.407$

$\beta = 0.606$ } Ref. 4, p.416

2.7.2 Puncture (continued)

Then

δ = 0.793 in.

σ_1 = 7728 psi

σ_2 = 50771 psi

The minimum factor of safety is

$$F.S. = \frac{70000}{50771} = 1.38$$

2.7.3 Thermal

2.7.3.1 Summary of Pressures and Temperatures

The maximum temperatures and pressures resulting from the hypothetical accident conditions, presented in Section 3.5.3 and 3.5.4, are summarized below:

(1) Maximum Containment Vessel Pressure = 19.2 psig

(2) Temperatures:

Cavity (Inner Shell)	= 360°F
Outer Surface	= 492°F
Lead Shield	= 359°F
Seal Area:	
Primary Lid	= 178°F
Secondary Lid	= 224°F

2.7.3.2 Differential Thermal Expansion Differential thermal expansion between the two shells of the cask and the lead shield, along with temperature gradients in the cask, produce significant stresses. Stresses have been assessed by use of the finite element models discussed in Section 2.6.1; see Figure 2.6.1-1.

2.7.3.3 Stress Calculation Stress calculations for pressure and thermal loads were performed using the conditions summarized in Section 2.7.3.1.

2.7.3.4 Comparison with Allowable Stresses The results of the stress analysis are summarized in Table 2.7.3-1. All stress intensities throughout the cask remain well below allowables during the fire accident. The highest stress intensity occurs in the inner shell near the top, where the stress intensity reaches 47385 psi. This corresponds to a factor of safety of 1.46, which is the lowest value for this load condition.

A plot of the deformed cask geometry is shown in Figure 2.7.3-1. For clarity the deformations are greatly exaggerated. The maximum deformation is 0.166 inch.

2.7.4 Water Immersion

Not applicable, since no fissile materials are to be carried in the cask.

2.7.5 Summary of Damage

The structural integrity of the Model CNS-8-120b Package has been verified for hypothetical accident conditions.

Damage to the package that results from the hypothetical accident condition is:

(1) Impact limiters crush during the 30 foot drop condition. Cask stresses are less than those prescribed by NRC Regulatory Guide 7.6.

(2) Small local deformations to the external shell may result during the 40 inch puncture condition. There will be no loss of shielding and the containment vessel will not be deformed.

(3) Presence of the overpacks limits temperatures in the containment vessel walls to less than 360°F. and internal pressures to 19.2 psig. Geometry and temperature integrity of the seals are maintained.

Element Type	Stess Type (σ allow) (psi)		Base Plates		Cask Body							Primary Lid		Secondary Lid	
			Inner	Outer	Lower Inner	Lower Outer	Mid Inner	Mid Outer	Upper Inner	Upper Outer	Bolt Ring	Inner	Outer	Inner	Outer
Shell Element · STIF61	Membrane (49000)	Element			59	46	91	122	159	126					
		Value (psi)			24121	16736	29374	12394	24185	13666					
	Membrane + Bending (70000)	Element			59	66	91	122	159	126					
		Value (psi)			31306	22476	30180	19269	47385	22218					
Solid Element · STIF25	Membrane (49000)	Element	27-28	33-34							167-172	244-245	181	277	250
		Value (psi)	26295	29632							26000	10543	15423	15796	11366
	Membrane + Bending (70000)	Element	23	25							167	236	191	270	242
		Value (psi)	22025	41455							20066	12549	20939	10008	20768

LOADING: Thermal Accident: ½ hour after start of fire
Includes 100W payload & internal pressure
Maximum stress intensities in cask regions

Table 2.7.3-1

STEP 1 ITER 1 TIME .00 .166

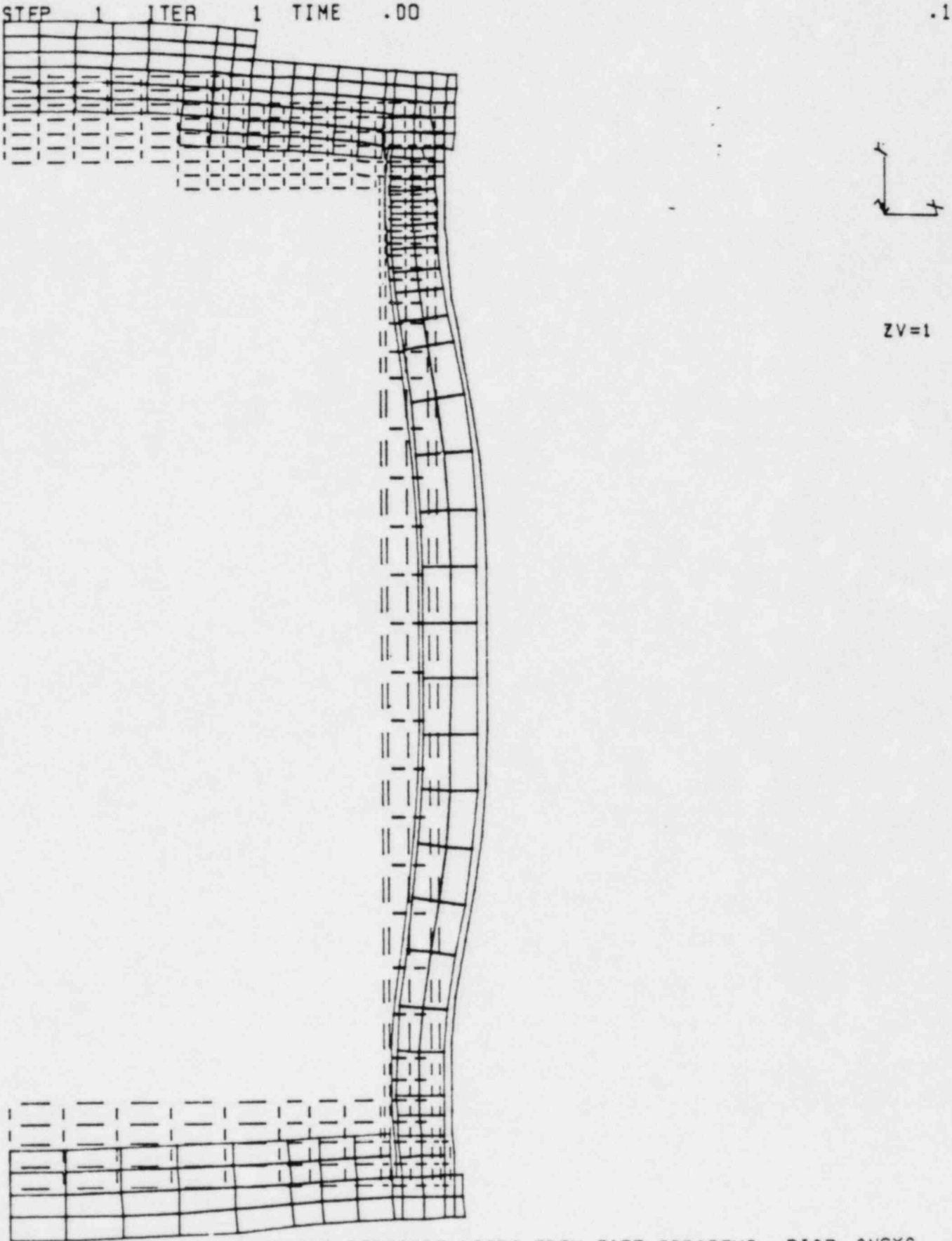

Figure 2.7.3-1

2.8 Special Form

Not applicable since no special form is claimed.

2.9 Fuel Rods

Not applicable, since fuel rods will not be part of package contents.

2.10 Appendix

2.10.1 Analytical Methods

This section briefly documents the analytical methods used to demonstrate compliance of the package with applicable provisions of 10 CFR 71 under normal and accident conditions. 2.10.1.1 deals with the calculation of forces imposed upon the package when subjected to drop events. 2.10.1.2 discusses the verification of the analyses described in the first subsection. 2.10.1.3 describes the ANSYS finite element analysis employed for detailed evaluation of package stresses under normal and accident conditions. 2.10.1.4 contains an analysis showing that the side drop is worse than an oblique drop for this cask. 2.10.1.5 presents the results of the thermal analysis for a 100°F ambient condition.

2.10.1.1 Overpack Deformation Behavior The package is protected by foam-filled energy absorbing end buffers, called overpacks. For purposes of analysis, the overpacks are assumed to absorb, in plastic deformation of foam, the potential energy of the drop event. That is, the analyses assume that none of the drop potential energy is transferred to kinetic or strain energy of the target (the "unyielding surface" assumption of 10 CRF 71) nor strain energy in the package body itself.

There are three orientations of the package with respect to the impact surface where an evaluation is made of impact forces and stresses. These three orientations are:

- End Drop - on the circular end surface of the overpack.
- Side Drop - on the cylindrical side surface of the overpacks.
- Corner Drop - with package center of gravity directly above the center of pressure of the fully-deformed overpack.

2.10.1.1 Overpack Deformation Behavior (continued)

For these three orientations, the prediction of overpack behavior can be approached from straightforward energy balance principles:

$$E = W(h + \delta) = \int_0^{\delta} F_x \, dx \qquad \text{Equation I}$$

Where: W = Package weight

h = Drop height

δ = Maximum overpack deformation

F_x = Force imposed upon target and package by the overpack at the deflection equal to x.

The left-hand term represents the potential energy of the drop. The right hand term represents the strain energy of the deformed overpack.

Each of these three orientations is treated by an individual analysis reflecting the differing geometric characteristics of each event. All three employ common energy balance techniques to assess maximum overpack deformations, along with a common description of the crushable energy absorbing foam.

This foam exhibits a stress-strain plateau of nearly constant stress up to a total strain of 40-60 percent. Above this strain value, pronounced strain-hardening effects commence, reflecting the collapse or consolidation of the foam cells. Accordingly, a tabular definition of foam stress-strain relations is employed in each of the three analyses. This tabular definition is taken directly from measured properties and accurately reflects the strain hardening behavior of the foam up to strains of 75-80 percent.

This discussion of these three analyses proceeds from the geometrically simple (end drop) to the most complex (corner drop).

(1) End Drop

The force produced by the overpack is

2.10.1.1 Overpack Deformation Behavior (continued)

$$F = \sum_i A_i \, \sigma(\varepsilon_i) \qquad \text{Equation II}$$

where A_i = the area of a given region of the overpack (e.g., that region which is beneath the cask, or, that annular region which is outside the cask)

$\sigma(\varepsilon_i)$ = the foam crush stress at strain ε_i

ε_i = the strain corresponding to area A_i

= x/l_i

x = deformation

l_i = undeformed length of overpack region corresponding to area A_i

The end drop analysis performs the calculations described by equations (I) and (II) by making incremental changes in the deflection until the energy balance of equation (I) is satisfied. At this point the results are printed in terms of deflection, force, acceleration, and elapsed time. Elapsed time is computed based on the following equations:

$$\Delta KE = 1/2 \; m \; (\Delta v)^2$$

where ΔKE = kinetic energy increment

= strain energy increment of deformation of overpack

m = total cask mass

Δv = velocity increment

and $F \, \Delta t = m \, \Delta v$

where F = total force applied to cask

Δt = time increment

Total elapsed time for the impact is then the sum of Δt for all deflection increments.

(2) Side Drop

The side drop analysis differs from the end drop solution only in the fact that both deformation and strain vary from point, to point and that the total force at a given crush depth must be found by geometric integration over these points. The details on this geometry are found in Figure 2.10.1-1. For each incremental deformation value, the force is found as:

$$F = 4 \sum_{i} l_i \int_{o}^{x_{max}} \sigma(\varepsilon_x)\, dx$$

where: l_i = effective length of an overpack for region i

$$x_{max} = [r_3^2 - (r_3 - \delta)^2]^{1/2}$$

$\sigma(\varepsilon_x)$= tabular definition of foam stress-strain properties

ε_x = the foam strain at location x

The computation of strain for each region of the overpack (i.e., various "backed" and "unbacked" regions) is calculated as

$$\varepsilon_x = \frac{\text{Crush Depth}}{\text{Original Thickness}}$$

In general, the expression for ε_x varies with the region under consideration and is a function of x.

(3) Corner Drop

The corner drop analysis is like the side drop analysis except that a two-dimensional geometric integration is required to assess the overpack crush force at each deformation. A detailed explanation follows.

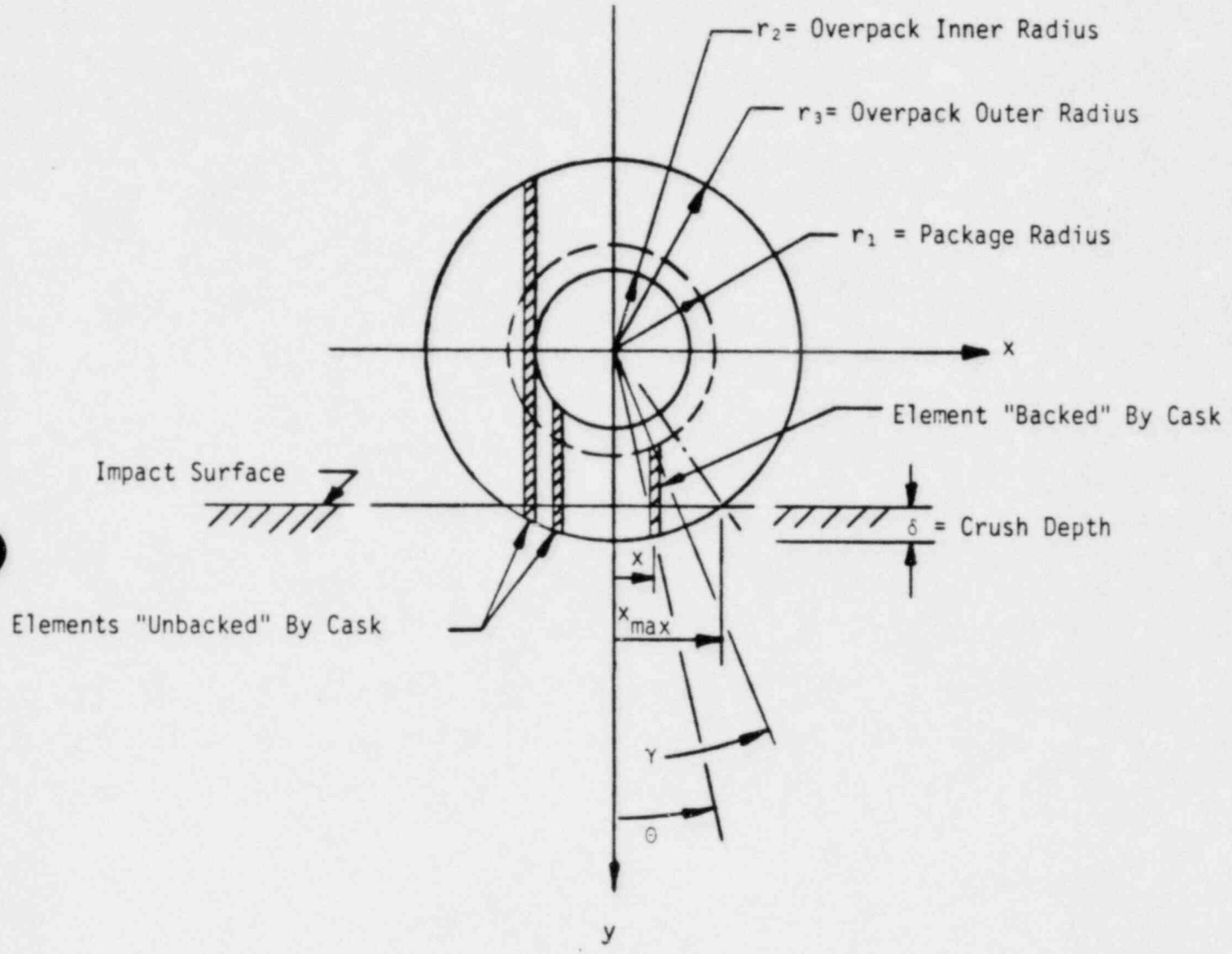

Figure 2.10.1-1 SIDE DROP GEOMETRY

The corner drop analysis treats the corner impact of a cylindrical package upon an unyielding surface. The package itself consists of a cylindrical payload portion surrounded by a larger cylindrical volume composed of a crushable media. The analysis was developed specifically to address problems of large deformations of this crushable media and to analyze geometries where the cylindrical overpack envelope possesses axisymmetric cylindrical voids (e.g. does not completely cover the cylindrical ends of the payload package).

The large deformation behavior of the crushable media is accommodated by determining the actual strain of the crushable media at a point. This strain is used to determine the corresponding stress from the tabular definition of media stress-strain characteristics. The total crush force is found by a double integration over the contact area of the crush plane.

Strain energy absorbed by the crushable media is determined by integrating the crush force and its associated deformation. The package is assumed to be at "rest" when the computed strain energy value equals the applied drop energy.

The geometric calculations for the contact surface and the associated strains are carried out using the (x_{CG}, y_{CG}, z_{CG}) coordinate system in which the x-y plane is projected onto the crush plane. See Figure 2.10.1-2. The crush plane itself represents a segment of an ellipse. The contact area is this ellipse segment, provided no cylindrical end void exists. When a cylindrical end void exists, the contact area of the crush plane is reduced by the removal of a second elliptical region associated with the projection of this void into the contact plane.

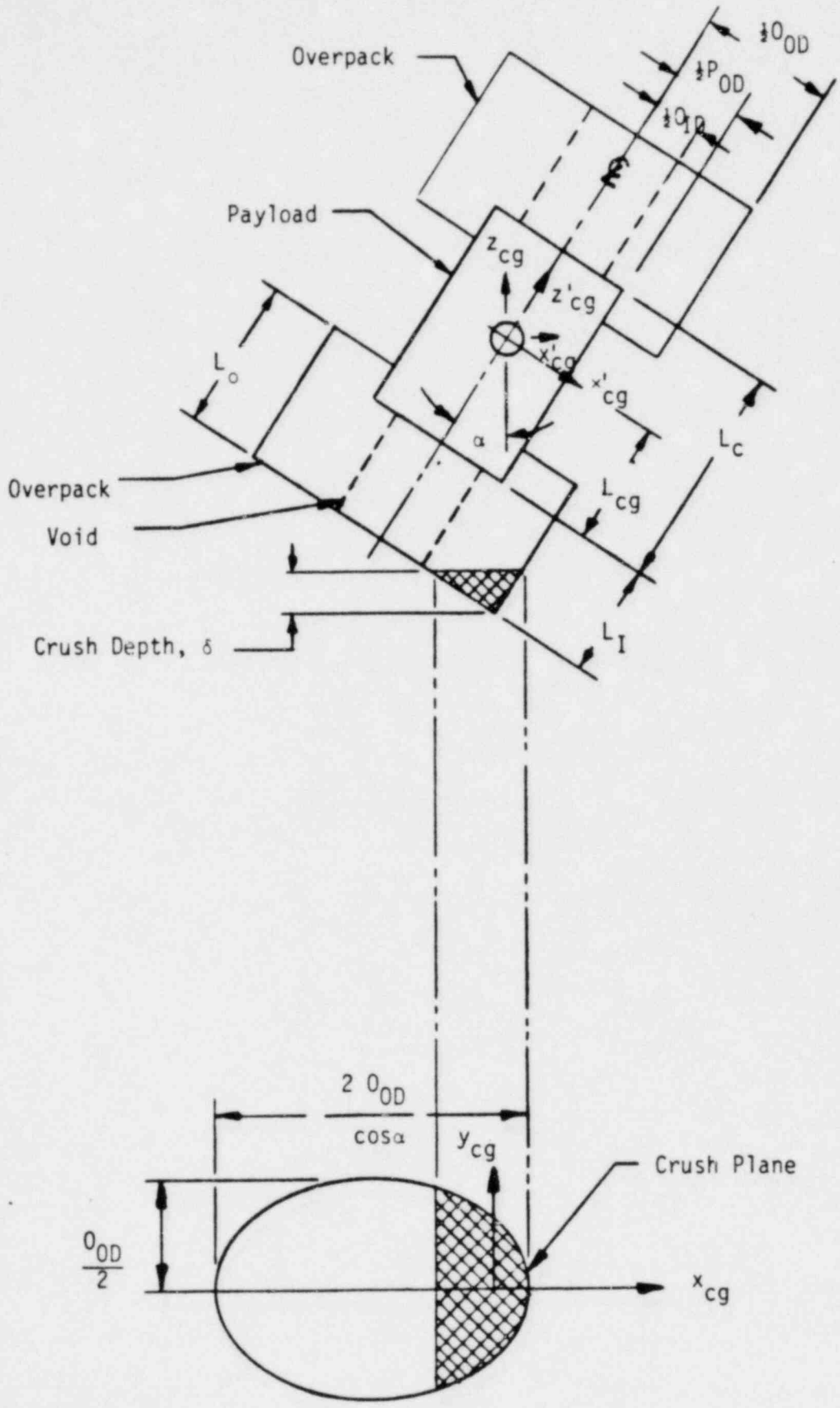

Figure 2.10.1-2 CORNER DROP IMPACT GEOMETRY

Calculation of strain is somewhat more complex. In principal, the distance from point (x_{CG}, y_{CG}) in the crush plane to the payload CG is found and denoted, z_{IMP}. Similarly the distances to the undeformed external and internal overpack surfaces are found and denoted as z_{OUT} and z_{IN}, respectively. The strain represents deformation divided by original thickness or:

$$\varepsilon = \frac{z_{OUT} - z_{IMP}}{z_{OUT} - z_{IN}}$$

At any point (x_{CG}, y_{CG}), the calculation of z_{IN} may follow three branches, according to location. The three branches relate to the payload surface intercepted. They are:

- The Circular Bottom of the Payload
  The bottom of the payload cylinder describes an ellipse in the crush plane. If (x_{CG}, y_{CG}) is inside this ellipse, the point is considered "backed" by the bottom of the payload. An exception to this general statement is noted in the discussion of the "Unbacked Region" below.
- The Cylindrical Surface of the Payload
  The cylindrical surface of the payload describes a rectangular region (with elliptical ends) tangent to the payload bottom ellipse at its major axes. If (x_{CG}, y_{CG}) is outside the bottom ellipse, yet inside the rectangular region, the point is considered "backed" by the payload cylinder.
- Unbacked Regions
  Unbacked regions are of two forms - those associated with the cylindrical end void and those near the external surface of the overpack. The unbacked region associated with the end void is a point in the crush plane which lies within the ellipse defined by the void circle lying in the plane of the payload bottom. The unbacked region associated with points near the overpack extremities is defined by those points (x_{CG}, y_{CG}) where the y coordinate exceeds the radius of the payload volume or lies outside both the rectangular region and the bottom ellipse.

2.10.1.1 Overpack Deformation Behavior (continued)

The calculation of z_{OUT}, the distance to the outer undeformed overpack surface, may follow two branches. These branches correspond to intercepts with either the cylindrical surface of the overpack or the circular end of the overpack.

The analytics describing the geometry discussed above consist of the sequential application of a series of geometric transformations of surfaces described in the coordinates of the cylindrical package (x'_{CG}, y'_{CG}, z'_{CG}) to the projected coordinates, (x_{CG}, y_{CG}, z_{CG}) in the contact plane. The surfaces in package coordinates are:

- Overpack Cylinder

$$x'^2_{CG} + y'^2_{CG} = \frac{1}{4} O^2_{OD}$$

- Overpack Bottom Circle

$$x'^2_{CG} + y'^2_{CG} = \frac{1}{4} O^2_{OD}$$

$$z'_{CG} = -(LCG + L_I)$$

- Payload Cylinder

$$x'^2_{CG} + y'^2_{CG} = \frac{1}{4} P^2_{OD}$$

- Payload Bottom Circle

$$x'^2_{CG} + y'^2_{CG} = \frac{1}{4} P^2_{OD}$$

$$z'_{CG} = -L_{CG}$$

- Void Circle at Payload

$$x'^2_{CG} + y'^2_{CG} = \frac{1}{4} O^2_{ID}$$

$$z'_{CG} = -L_{CG}$$

2.10.1.1 Overpack Deformation Behavior (continued)

- Void Circle at Overpack Exterior

$$x'^2_{CG} + y'^2_{CG} = \frac{1}{4} O^2_{ID}$$

$$z'_{CG} = - (L_{CG} + L_I)$$

2.10.1.2 Verification of Drop Load Analyses The verification of Chem-Nuclear's drop load analyses took two forms:

(1) Comparison of analytically predicted deformations with measured deformation of the overpacks of the CNS 1-13CII cask (test results are reported in the CNS 1-13CII SAR, NRC Docket No. 71-9152/B), and

(2) Comparison of the results of Chem-Nuclear's analysis with those obtained by Nuclear Packaging, Inc., for their previously validated and well-accepted analysis as used in licensing the CNSI 1-13CII cask.

The results of these validation comparisons are shown in the Table 2.10.1-1.

2.10.1.3 Finite Element Analysis The stress analyses of the cask for thermal, pressure, and drop conditions were done using ANSYS finite element models. The loads applied were taken from the impact and thermal analyses described elsewhere in this document. The geometry of the cask was modeled using axisymmetric harmonic elements, so as to allow the non-axisymmetric loading conditions which occur in the side and corner drop analyses. The loads were applied as nodal forces, elemental pressures, nodal and elemental temperatures, and whole-body accelerations.

(1) Harmonic Elements

In ANSYS, harmonic elements are elements having axisymmetric geometry with the capability of non-axisymmetric loading. These elements allow a less complex model than would be required for a full three-dimensional analysis while allowing realistic loading conditions.

DROP ORIENTATION AND HEIGHT	DROP TEST RESULTS	CNSI 1-13CII ANALYSIS RESULTS		CHEM-NUCLEAR ANALYSIS RESULTS	
	DEFLECTION	DEFLECTION	ACCELERATION	DEFLECTION	ACCELERATION
End - 2 ft.	N/A	0.69 in.	62.2 g	0.81 in.	60.4 g
End - 30 ft.	4.46 in.	4.46 in.	95.56 g	4.37 in.	102.8 g
Side - 2 ft.	N/A	1.70 in.	28.3 g	1.91 in.	27.5 g
Side - 30 ft.	N/A	7.21 in.	137.4 g	7.59 in.	102.4 g
Corner - 2 ft.	N/A	5.94 in.	14.2 g	6.16 in.	12.6 g
Corner - 30 ft.	N/A	14.83 in.	79.27 g	15.32 in.	73.9 g

Table 2.10.1-1 Comparison of Results of Chem-Nuclear Analyses with Test Results and Previous Analyses.

The loads and responses are characterized by Fourier series coefficients, and the value of the loading or response function is found by summing the contributions from each of the terms in the series. Each of the terms is of the form $a_n \sin(n\theta)$ or $b_n \cos(n\theta)$, where a_n and b_n are the Fourier coefficients, n is a nonnegative integer and θ is the angular coordinate in the model. The ANSYS Preprocessor, PREP6, may be used to generate the Fourier coefficients for a known input function. The output function is found from the output coefficients for any value of θ by summing terms:

$$\text{OUTPUT}(\theta) = \sum_{n=0}^{n_{max}} a_n \sin(n\theta) + b_n \cos(n\theta)$$

Examples of output functions are stresses and deflections.

PREP6 will compute up to 24 coefficients. If the applied loading function is known to be either even or odd, the sine or cosine terms may be omitted. This allows the user to have 24 non-zero coefficients. Because the drop analyses have planar symmetry, and the model was constructed so that the plane of symmetry corresponds to θ equal to zero degrees, all loading functions have even symmetry. Axial and radial response functions also have even symmetry. Repsonse functions in the hoop direction have odd symmetry. Hence only the cosine terms are used in the applied loads and in computing the axial and radial response functions, while only sine terms are used for computing hoop response functions.

(2) Acceleration Forces

In the drop loading analyses, described elsewhere, a computation is made of the pressure (compressive stress) distribution over the surface of the cask. This pressure distribution is converted to a nodal force distribution by taking effective area-times-pressure products at intervals around the circumference for each node in the finite element model. Each node of the finite element model then has

a corresonding force distribution which is a function of θ. Each of these force distributions is then converted to a Fourier series using the ANSYS PREP6 Preprocessor utility to compute the Fourier coefficients. Additionally, to counterbalance these forces, a constant acceleration is applied to the cask. Thus, the analysis is quasi-static, with the peak dynamic load being conservatively modelled as a steady state load.

(3) Pressures

Pressures are applied as loads on the surfaces of the elements around the cask cavity.

(4) Temperatures

For the cases of 100°F and 130°F steady state thermal conditions, temperatures from the thermal analysis were applied as nodal temperatures. For the fire accident condition, temperatures of solid elements (STIF25) were applied as nodal temperatures and for the shell elements (STIF61) as element surface temperatures. Treating the shell elements in this manner created an analysis in which temperatures varied linearly across the thickness of the elements, but were constant along the length of each element. Thus, for shell elements, radial temperature gradients were accounted for by model discretization and by the formulation of the solution in each element, while axial gradients were accounted for by model discretization.

(5) Constraints

Nodes along the centerline are constrained from moving in the radial direction because the model geometry is axisymmetric. Additionally, although all applied forces are theoretically in balance, one node was constrained from moving in the axial direction. This maintained static equilibrium in the face of roundoff and other small numerical tolerances experienced in any numerical analysis. The value of the reaction force at this node was checked for each analysis to ensure that it was negligibly small.

2.10.1.3 Finite Element Analysis (continued)

(6) Lead Interfaces

For an accurate analysis, it is necessary to model lead slump behavior during the end drop and to develop the radial loads caused by the lead bearing against the cask steel shells. To accomplish these two goals, the ANSYS model was constructed in such a way that the lead was free to move axially without any support from the shells, but was constrained radially so that the lead would bear against the steel shells. Additionally, the lead was modelled to bear against the end closure in the axial direction at the impact end of the cask, but was free to move axially, and thus slump, at the non-impact end.

(7) Bolt Loads

because the geometry used to model the cask was axisymmetric, the bolts could not be explicitly modelled. However, line loads at the bolt circle radii were computed. Based on these line loads and the bolt spacing, the maximum bolt load for each load case was computed by multiplying the peak line load by the circumferential bolt spacing. This is conservative because the peak load occurs only at a single point on the bolt circle and may be shared between two bolts, whereas the analysis assumes that the peak load occurs over an arc equal in length to the spacing between bolts and centered on a single bolt.

2.10.1.4 Oblique Impact This section presents an analysis demonstrating that oblique impacts are not worst-case conditions for casks having length-to-diameter ratios less than 1.37. Figure 2.10.1-3 illustrates a cask of length, L, and weight, W, dropped at an angle, a, measured from a horizontal plane. No energy absorption is initially assumed from the impact limiter or cask during primary impact (first contact of the lower end of the cask with the unyielding surface). This assumption results in the worst case (greatest) impact velocity of the higher end of the cask.

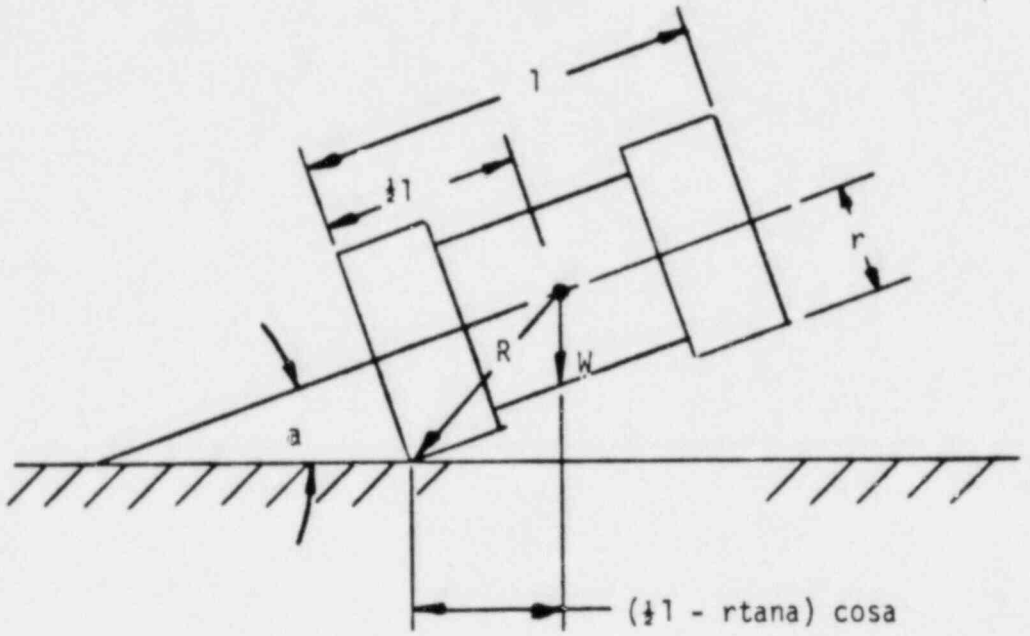

Figure 2.10.1-3 CASK ORIENTED FOR OBLIQUE DROP

2.10.1.4 Oblique Impact (continued)

The angular momentum before and after impact can be estimated based on the following assumptions:

- The impact point does not slide along the horizontal impact surface.
- The rotational inertia of the cask can be approximated assuming a uniform density solid cylinder; i.e.: $I_{CG} = \frac{1}{4} M (r^2 + \frac{1}{3} l^2)$.
- The gravitational acceleration of the cask is neglected after the initial impact.

Then, before impact,

$$L_1 = Mv_1 \left(\frac{1}{2} l - r \tan a \right) \cos a$$

and, after impact,

$$L_2 = I_i \omega_2$$

Where

L_1 = angular momentum before impact
M = mass of cask
v_1 = impact velocity
I_i = rotational inertia of cask about impact point
= $I_{CG} + Mk^2$

= $M \left(\frac{1}{4} r2 + \frac{1}{12} l^2 + k^2 \right)$

ω_2 = angular velocity of cask following impact

Since no moments are applied to the cask, angular momentum is conserved, and $L_1 = L_2$

$$Mv_1 \left(\frac{1}{2} l - r \tan a \right) \cos a = M \left(\frac{1}{4} r^2 + \frac{1}{12} l^2 + R^2 \right) \omega_2$$

2.10.1.4 Oblique Impact (continued)

Solving for angular velocity:

$$\omega_2 = v_1 \frac{(2\frac{1}{l} - r\tan a)\cos a}{\frac{1}{4}r^2 + \frac{1}{12}l^2 + R^2}$$

In general, maximum angular velocity occurs when the impact angle equals zero.

The velocity of the secondary impact is given by

$$v_s = l\omega_2$$

Then

$$V_s = v_1 l \frac{(\frac{1}{2}l - r\tan a)\cos a}{\frac{1}{4}r^2 + \frac{1}{12}l^2 + R^2}$$

The limiting case can be taken as that for which the secondary impact velocity equals the initial impact velocity for the worst case angular velocity. Then,

$$v_s = v_1 \quad \text{at } a = 0$$

$$\text{and } \frac{\frac{1}{2}l^2}{\frac{1}{4}r^2 + \frac{1}{12}l^2 + k^2} = 1$$

or

$$\frac{l^2}{r^2} = 7.5$$

implying that

$$\frac{l}{d} = 1.37$$

2.10.1.4 Oblique Impact (continued)

Thus, for length-to-diameter ratios greater than 1.37, slapdown impacts may be more severe than a normal side drop. Since this analysis very conservatively neglects any energy absorption for the initial impact, this ratio may be taken as a lower bound, below which one may safely assume that secondary impact will be less severe than side drop impacts. Since the CNS 8-120B package has a length-to-diameter ratio of 1.31, the oblique impact is less severe than the side drop. Cask stresses in an oblique drop will be less than those experienced during a side drop.

2.10.1.5 Thermal Analysis A thermal analysis of the cask was made using 100°F ambient temperature. The results of this analysis are combined with normal and accident conditions in accordance with NRC Regulatory Guide 7.8. The methods and assumptions of this analysis are fully described in Secion 3.0. This appendix presents a summary of pertinent results of that analysis.

Cask Temperatures, °F

	Inner Cavity	Lead Shield	Primary O-Ring	Secondary O-Ring	Outside Surface
Max.	151	138	138	141	151
Min.	132	132	138	141	132

Loads: 100°F Ambient
100W Payload
Insolation of 120 Btu/hr-ft^2

The resultant maximum internal pressure is 3.7 psig.

2.10.2 STARLYNE Learners Guide, Users Guide, Analysis System Summary

STARDYNE® LEARNERS GUIDE

STARDYNE (Version 3) is a user-oriented Structural Analysis System with many features. Included are automatic node and element generation to simplify input. Strong dynamic capabilities: transient, steady state, random and shock. Extensive static capability is complemented by nonlinear foundation analysis and gap and tension or compression-only analysis. STARDYNE has excellent documentation, proven reliability, many user options and good plotting capabilities.

In order to use the STARDYNE system the following documents are available:

(1) STARDYNE USER'S MANUAL (Required)
(2) STARDYNE JCL APPENDIX FOR YOUR COMPUTING SYSTEM (Required)
(3) STARDYNE LEARNERS GUIDE (Optional)

If information concerning STARDYNE is desired or if problems are encountered, the user is invited to make immediate contact with the Data Center STARDYNE Engineering Specialist or with the developers - System Development Corporation's STARDYNE Project Office.

- STARDYNE Project Office*
  System Development Corporation
  2500 Colorado Avenue
  Santa Monica, California 90406, U.S.A.
  Telephone: (213) 820-4111
  TWX: 910 343 6443
  TLX: 65-2358

  *STARDYNE Project Office Personnel

	Direct Telephone
Richard Rosen - Project Manager	(213) 453-5142
Richard Ragle - Associate Project Manager	(213) 453-5138
Raymond Curtis - Associate Project Manager	(213) 453-5168
Charles Bell - Engineering Verification	(213) 453-5167
Raymond Favignano - Computer Systems	(213) 453-5175
Sam Soule - Sales, Marketing, Consulting	(213) 453-5137

All questions relating to the STARDYNE Learners Guide should be addressed to the author, Charles Bell. This document should not be used with any STARDYNE User's Manual which was released prior to this date:

SEPTEMBER 1, 1979

STARDYNE® LEARNERS GUIDE

This document will present to the novice STARDYNE user a series of usage examples. Prior to using this manual, please read and become familiar with the STARDYNE User's Manual, Section A through page B-100. The pages in this manual, although in ascending order, are not necessarily in consecutive numerical order. This is to allow for future revisions and new pages.

TABLE OF CONTENTS

INTRODUCTION

The STARDYNE system of structural analysis programs is segmented into individual programs. A variety of static or dynamic analyses may be performed by using one or more of the individual programs in a coordinated series of computer runs.

The normal static analysis can usually be accomplished in one computer run, while the typical dynamic response analysis might take two or three computer runs. Data is transferred from one run to the next by saving output files on magnetic tape or on disc storage.

The STARDYNE programs are based on the finite element method. This method requires the analyst to place the structure within a three-dimensional frame. Pertinent points on the structure, called nodes, are given coordinates to identify their location within the framework. The nodes are connected by finite elements, with the choice of elements, depending on the shape and type of structure.

The reader should have the current STARDYNE User's Manual available, since each card shown in the examples is defined there. (The Manual page number is given in columns 73-80 of each example card.) The main feature of each example is the list of card images for the entire STARDYNE input deck. The only other cards required for the computer run, are the Job Control cards. These are shown in the STARDYNE JCL APPENDIX for your computing system. Only the Fixed Format type of input data is shown in the examples in this manual.

In addition to the list of card images, each example has a sketch of the model and several modeling details. The modeling details are not intended as a description of modeling technique, but rather as an explanation of STARDYNE input. Each example was designed to require a minimum size input deck, thereby reducing the amount of learning time for the various concepts.

DATA GENERATION

Described below are the two types of generation features included on many of the Fixed Format input cards. They are typically used during the input of node and element numbers. For example, see page B1-81.

(a) The FROM-TO is used to generate a sequence of element numbers, with a built-in increment of 1. For example, four beams are defined when

FROM = 5

TO = 8

When the input value of TO is blank, only 1 element is produced.

(b) The FROM-TO-INC is used to generate a sequence of nodes with a constant gap. The six node numbers 71, 77, 83, 89, 95, 101 are input when

FROM = 71

TO = 101

INC = 6

When TO is blank, the generation feature is turned off for the current card. Cards which generate a series of nodes or elements may be interspersed with single node/element cards.

LIMITATION FOR NODE AND ELEMENT NUMBERS

The maximum value for node numbers and element numbers are periodically increased. The maximums are listed in the STARDYNE User's Manual on page B-70. Since new editions of the Manual are spaced several years apart, more current values of maximums are given in the STARDYNE BULLETINS, which can be printed by accessing the STARDYNE BULLETIN program (STARBUL) with the JCL cards.

Both node and element numbers are assigned by the user. The numbers for the various types of elements do not have to be exclusive. That is, within the same model, there may be a Beam Number 10, a Quad Plate Number 10, and a Cube Number 10. (There is however an exception to this rule. Cubes and Wedges, which are entered in the same table, may not have the same numbers.)

Node and element numbers do not have to begin at 1; they may begin with any integer, and there may be gaps in the numbering system. For example, if there are 5 Triangular Plates in a model, they could be given the numbers

8, 22, 56, 88, 109

The computer run costs for some of the STARDYNE programs will be much higher if large gaps are in the node numbering system. During some phases of the solution these programs operate as if the number of nodes in the model is equal to the highest node number entered. In general, large gaps are to be discouraged.

DESCRIPTION OF THE STAR PROGRAM

STAR Program – Almost all of the applications of the STARDYNE system require STAR as the first step. It contains the following options:

(a) Geometry processing only, which is used for debugging and for developing a geometry data base.

(b) Static analysis.

(c) Mode shape and natural frequency determination (Dynamic Analysis).

The following files are written by STAR and are used for data transfer to other programs of the system. See Section R in the User's Manual.

(a) TAPE2 – this file consists of some bookkeeping tables and a copy of the input card images from the Structure Description card (page B1-73), to the ENDGEØM card (page B1-185).

(b) TAPE4 File 1 – the processed geometry data.

(c) TAPE4 File 2 – the results of either a static analysis, or a mode shape analysis.

STAR writes TAPE2 and TAPE4 File 1 automatically (provided no input errors cause the program to abort the job). The second file of TAPE4 has the deflections, or mode shapes, automatically written; other output quantities are written only when requested by the user - see the TAPE4G card, page B7-30. Several other files are output by STAR; please refer to page A-69 and page R-0.

A short description of the other programs in the STARDYNE system may be found in the STARDYNE User's Manual, pages A-52 through A-69.

STARDYNE (Version 3) is a user oriented Structural Analysis System with many features. Included are automatic node and element generation to simplify input. Strong dynamic capabilities: transient, steady state, random and shock. Extensive static capability is complemented by nonlinear foundation analysis and gap and tension or compression-only analysis. STARDYNE has excellent documentation, proven reliability, many user options and good plotting capabilities.

In order to use the STARDYNE system the following documents are available:

(1) STARDYNE USER'S MANUAL (REQUIRED)
(2) STARDYNE JCL APPENDIX FOR YOUR COMPUTING SYSTEM (REQUIRED)
(3) STARDYNE LEARNERS' GUIDE (OPTIONAL)

If information concerning STARDYNE is desired or if problems are encountered, the user is invited to make immediate contact with the Data Center STARDYNE Engineering Specialist or with the developers - System Development Corporation's STARDYNE Project Office.

- STARDYNE Project Office*
  System Development Corporation
  2500 Colorado Avenue
  Santa Monica, California 90406, U.S.A.
  Telephone: (213) 829-7511
  TWX: 910 343 6443
  TLX: 65-2358

  *STARDYNE Project Office Personnel

  Richard Rosen - Project Manager
  Richard Ragle - Associate Project Manager
  Raymond Curtis - Associate Project Manager
  Charles Bell - Engineering Verification
  Raymond Favignano - Computer Systems
  Sam Soule - Sales, Marketing, Consulting

(213) 615-1535 — 615-1535

Please see the section starting with page A - 52 for the list of personnel who are responsible for the individual STARDYNE program.

This manual should not be used with STARDYNE versions which were released prior to this date:

SEPTEMBER 1, 1979

STARDYNE MANUAL USAGE

Throughout this manual, outlined sections, such as this, are inserted to aid the user. They either contain important notes or refer the reader to appropriate sections of the manual.

The pages in this manual, although in ascending order, are not necessarily in consecutive numerical order (i.e., A-50, A-52, A-53). This is to allow for future revisions and new pages.

All first-time STARDYNE users, read all of Section A, Sections B, B1, M and JCL to get an overview of the STARDYNE system. The next step is to form the finite element representation of the structure. Turn to page B-100 for instructions concerning coding of your structural model.

The basic theoretical reference for the STARDYNE system is the 'STARDYNE Theoretical Manual', published by Control Data Corporation. Publication number 86616300.

[The terms STARDYNE, MRI/STARDYNE and SDC/STARDYNE are used interchangeably. However, STARDYNE is the preferred usage].

TABLE OF CONTENTS

STARDYNE ANALYSIS SYSTEM
SUMMARY

The STARDYNE Analysis System Consists of a series of compatible digital computer programs designed to analyze linear elastic structural models. The system encompasses the full range of static and dynamic analyses. These programs provide the analyst with a sophisticated, cost-effective, structural-dynamical analysis system.

The STARDYNE system can be used to evaluate a wide variety of static and dynamic problems:

- The static capability includes the computation of structural deformations and member loads and stresses caused by an arbitrary set of thermal, nodal applied loads and/or prescribed displacements.
- Utilizing either the direct integration or the normal mode techniques, dynamic response analyses can be performed for a wide range of loading conditions, including transient, steady-state harmonic, random and shock spectra excitation types. Dynamic response results can be presented as structural deformations (displacements, velocities, or accelerations), and/or internal member loads/stresses.

The data input and output formats (both numerical and graphical) have been prepared with one basic philosophy: to enable the user to obtain a meaningful solution in the most logical and straightforward manner possible while keeping the required data input as simple and minimal as practical. The programmed mathematical operations in the matrix decomposition, the eigenvalue-eigenvector extraction, and the error analysis, contain state-of-the-art innovations in the field of numerical analysis. A brief description of the finite element and normal mode analysis methods as they are implemented in STARDYNE is presented. Also included is a discussion on each of the major programs comprising the STARDYNE system.

THE FINITE ELEMENT, NORMAL MODE ANALYSIS METHOD

The basic concept of the "Finite Element" method is that every structure may be considered as a "mathematical" assemblage of individual structural components or elements. There must be a finite number of such elements, interconnected at a finite number of nodal points. The behavior of this finite element structural model will closely approximate the behavioral characteristics of the real structure.

STARDYNE ANALYSIS SYSTEM - SUMMARY - CONTINUED

Components of the Structural Model. The physical structure to be modeled must be described in a right-hand cartesian coordinate (global) system and is comprised of the "nodes" and "finite elements".

Nodes. The characteristics of the node point include position in space, movement in space (3 translation x,y,z and 3 rotation $\theta_x, \theta_y, \theta_z$) and connectivity to other nodes via the finite elements. Masses and external forces may be assigned to each node.

Finite Elements. The node points may be interconnected with finite elements in such a way as to realistically represent real physical structures. The most commonly used elements are shown on page A - 53, together with the nodal forces which can be transmitted through the element. The stiffness properties of each of these finite elements are defined in the "STARDYNE Theoretical Manual".

General Solution Procedure. The general solution procedure consists of stiffness matrix formulation, static analysis, eigenvalue/eigenvector determination, and dynamic response analysis.

Stiffness Matrix Formulation. The stiffness matrices of the individual finite elements are first computed and then transformed (if required) from its local coordinate formulation to a form relating to the global coordinate system. Finally, the individual element stiffnesses contributing to each nodal point are superimposed to obtain the total assemblage stiffness matrix $[K]$.

Static Analysis. During a static analysis, the equation

$$[K] \cdot \{\delta\} = \{P\}$$

where $[K]$ = the stiffness matrix
$\{\delta\}$ = the nodal displacement vector
$\{P\}$ = the applied nodal forces

may be solved to determine the nodal displacements and element internal forces and/or stresses given a set of applied nodal forces.

STARDYNE ANALYSIS SYSTEM - SUMMARY - CONTINUED

Eigenvalue/Eigenvector Analysis. The eigenvalues (natural frequencies) and eigenvectors (normal modes) of a structural system are determined by solving the equation

$$\omega^2 [m] \{q\} - [k] \{q\} = C$$

where $[m]$ = the mass matrix (assumed to be diagonal, ie, no mass coupling)

ω = the natural frequencies

$\{q\}$ = the normal modes.

Dynamic Response Analyses. Using the natural frequencies and normal modes together with the related mass and stiffness characteristics of the structure, appropriate equations of motion may be evaluated to determine structure response to dynamic loading.

PROGRAMS COMPRISING STARDYNE ANALYSIS SYSTEM

1. STAR (Project Engineer: Raymond Curtis)

The STAR program has two distinct functions. They are static load analysis and eigenvalue/eigenvector extraction. The static analysis and modal extraction phases are based on the "Stiffness Method" or "Displacement Method" and the answers are in the realm of "Small Displacement Theory".

A. Available Finite Modeling Elements

1. Beam and Pipe elements with shear stiffness in 3-D space.
2. Two Triangular Plate Elements (Thick plate and thin plate)
   a. Plate Bending
   b. Sandwich (Thick plate only)
   c. Inplane (constant strain)
   d. Shear Only (Thick plate only)
3. Quadrilateral Plate Element (Iso-parametric in-plane)
4. Infinitely Rigid Members
5. Springs, non-standard elements or substructures may be entered in numerical form, by direct alterations to the stiffness matrix.
6. Hexahedron (Cube) Solid Element (Iso-parametric)
7. Wedge Solid Element (Iso-parametric)
8. Tetrahedron Solid Element (constant strain)

STARDYNE ANALYSIS SYSTEM SUMMARY - CONTINUED

- Commonly Used Finite Elements

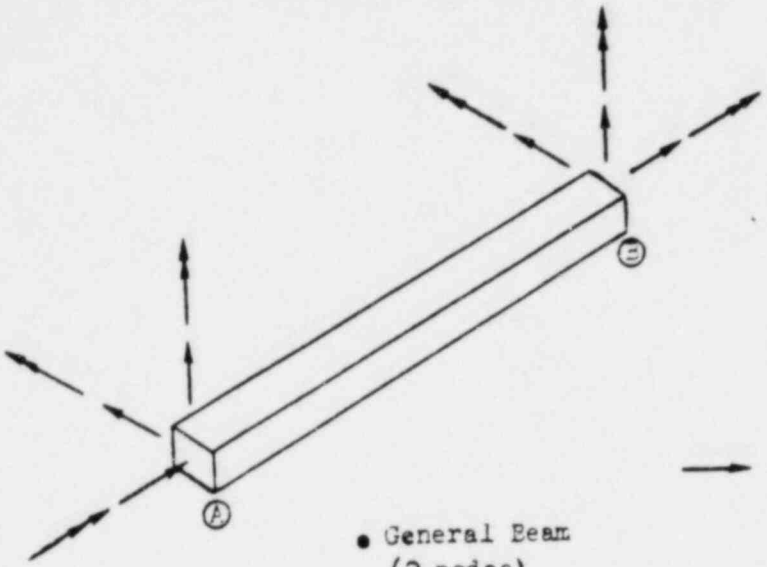

- General Beam (2 nodes)

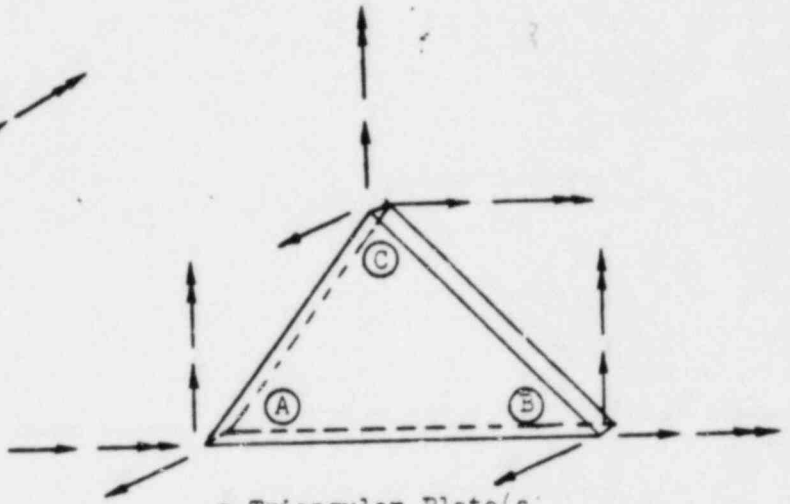

- Triangular Plate(s) (3 nodes)

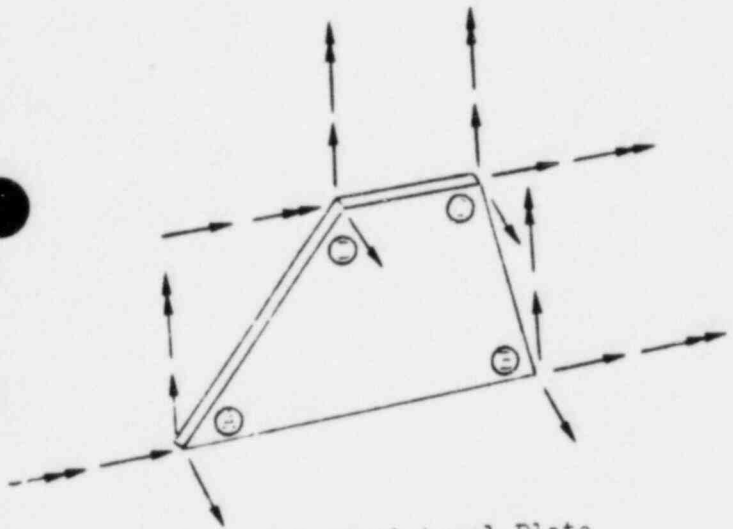

- Quadrilateral Plate (4 nodes)

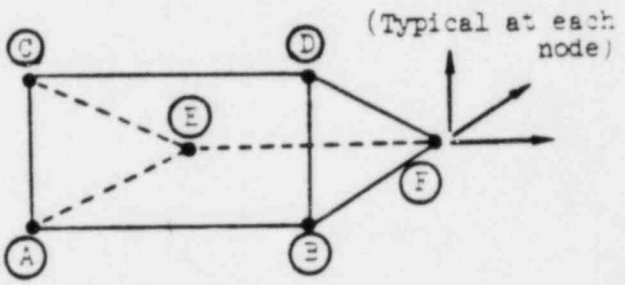

- Wedge Element (6 nodes)

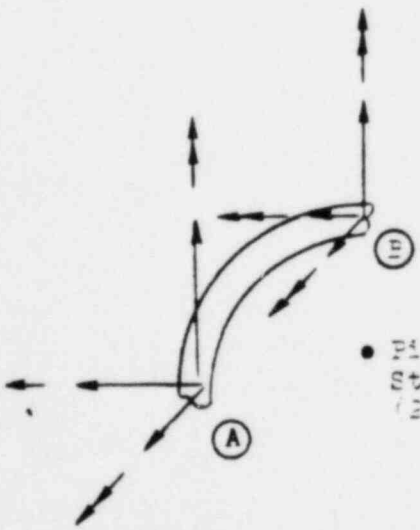

- Pipes-Curved and Straight (2 nodes)

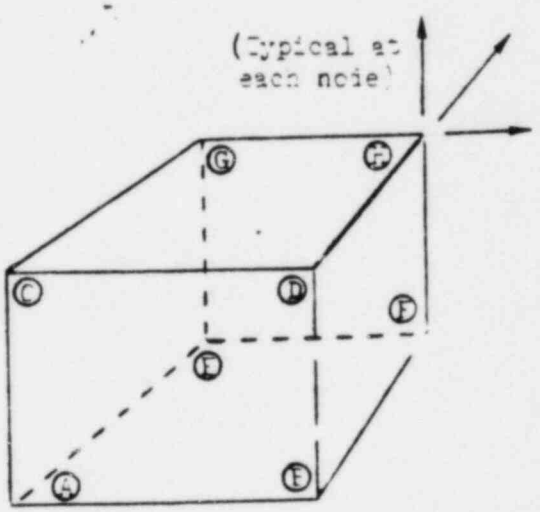

- General Six Sided Solid (Hexahedron) (8 nodes)

1. STAR - CONTINUED

B. Static Structural Analysis

1. Applied Nodal Loadings
2. Automated Thermal Analysis
3. Solutions of Free-Free Systems
4. Automated processing of psuedo-static load or displacement vectors as obtained from the dynamic response solutions
5. Element Loadings
6. Inertia Loadings
7. Combined Cases
8. Specified Displacements
9. Substructures

C. Extraction of Eigenvalues and Eigenvectors

1. Inverse Iterations Method for the eigenvalues within specified regions (uses full system weight vector)
2. Householder tri-diagonalization and Q-R extraction for reduced dynamic degrees of freedom - GUYAN reduction (usually used for truncated weight vector).
3. LANCZOS Modal Extraction Method (uses full system weight vector, no nodal limitations - this is a highly recommended method).

D. Output Section

STAR output processor phase computes element displacements, loads and stress; and nodal equilibrium check. Options are available to present the output in report form.

2. DYNRE1 (Project Engineer: Richard Ragle)

Transient response to imposed dynamic loadings are treated in DYNRE1 using the modal superposition technique. Input forcing functions may be in the form of forces, initial displacements, initial velocities and base accelerations. Output consists of nodal displacements, velocities, accelerations, element loads and stresses.

3. DYNRE2 (Project Engineer: Richard Ragle)

Steady state frequency response to steady state sinusoidal dynamic loadings are computed by DYNRE2. Input forcing functions may be in the form of distributed forces, base excitations (displacements, velocities or accelerations) and unit sinuscidal excitations (displacements, velocities, accelerations or forces) at specific nodes. Output consists of "relative" and "absolute" nodal responses and element loads and stresses.

4. DYNRE3 (Project Engineer: Richard Ragle)
Response of multi-degree-of-freedom linear elastic structural models subjected to stationary random dynamic loading. DYNRE3 will compute the RMS nodal responses, RMS element stresses and generate response power spectral density (PSD) curves for selected nodal degrees of freedom. Input forcing power spectrums are defined as shape of spectrum and type of spatial correlation.

5. DYNRE4 (Project Engineer: Richard Ragle)
Response of multi-degree-of-freedom, linear elastic models subjected to an arbitrarily oriented foundation shock input. The user may enter arbitrary shock spectra, shock spectra computed via DYNRE5, or call for some ratio of the 1940 El Centro (California) earthquake SPECTRA for any of the directions of motion. DYNRE4 will compute user specified combinations of ABSOLUTE and/or RSS and/or NRL sum and various NRC sum-summation techniques for nodal and/or element stress responses.

6. DYNRE5 (Project Engineer: Richard Ragle)
Computes shock spectrum values from a transient base acceleration time history digitized at equal or unequal time intervals. The user may specify frequencies at which shock spectrum values for displacement, velocity and acceleration will be computed, in turn for each value of damping entered.

7. DYNRE6 (Project Engineer: Raymond Curtis)
Computes the response of multi-degree-of-freedom structures subjected to transient dynamic loadings, using the direct integration technique. The model may also contain nonlinear one-dimensional springs.

8. PLØT3D (Project Engineer: Richard Ragle)
This program may be used to plot STAR finite element structural models. It enables the user to view the geometric structure in both the undeformed and deformed states. The deformations may be the result of a STATIC, Modal Extraction or a Dynamic Response solution.

9. CØNSTAR (Project Engineer: Raymond Curtis)
This program may be used to produce contour plots of stresses and displacements on surfaces composed of triangular and quadrilateral elements. In addition, the numerical response values may be printed directly on the plot.

10. WAVE4 (Project Engineer: Charles Bell)
This program may be used to compute hydrodynamic forces on the tubular and/or circular beam members contained in the submerged portion of a STAR model. The fluid forces can result from both wave motion and a steady current. The wave motion is defined by Stoke's 5th Order Theory.

11. SPRING (Project Engineer: Charles Bell)
This program may be used to determine the loads and deformations in a linear elastic structure supported by a nonlinear foundation, and subjected to general static loading.

12. NUBØP (Project Engineer: Richard Ragle)
This program may be used to consider bottom out, tension only, compression only members, etc., for the STAR STATICS problem.

13. NØDEXC
This program may be used to change node numbers of STAR substructure boundary data to match the boundary node numbers of the recipient math model. NØDEXC may be used on either the FORWARD or BACKWARD SUBSTRUCTURE PASS.

14. PØST (Project Engineer: Charles Bell)
This program may be used to combine the forces, stresses, and displacements from two (or more) previously computed load cases which are contained in the STAR TAPE4 format. In addition, POST will compute principal stresses, perform stress level searches and present the results either by node and element or by load case.

15. FACTØR
This program may be used to create new force and/or displacement vectors using combinations of these vectors entered in the STAR TAPE4 and/or DYNRE TAPE3 data file formats.

USER INFORMATION MANUAL (Originator/Editor: Richard Ragle)
If errors or ambiguities are found in this manual, please notify the Editor at once.

STARDYNE ANALYSIS SYSTEM SUMMARY - CONTINUED

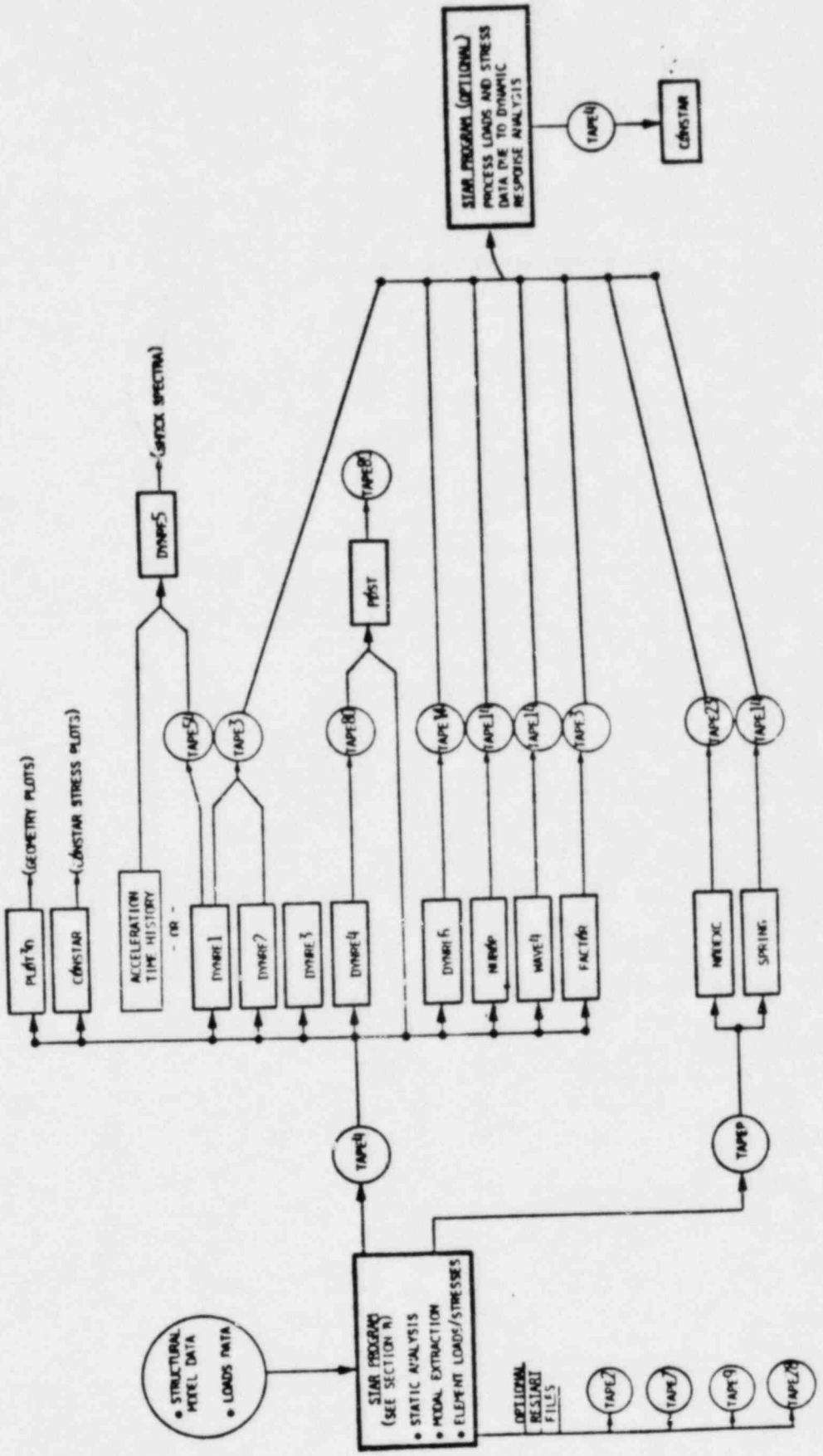

STARDYNE ANALYSIS SYSTEM SUMMARY

DATA CARD FORMATS

Every data card defines parameters which are required by the program. Each of these parameters must be input according to a specific format. The data card formats shown in this manual are of the following types:

a) "I" FORMAT, INTEGER (FIXED POINT)...I4,I7,3I4, etc. The value is to be input without a decimal point and packed to the right of the specified field. (Negative signs associated with INTEGER VARIABLES must also be righ-justified in the data field).

b) "F" FORMAT, REAL (FLOATING POINT)...F8.0,F20.3,6F8.0, etc. This format requires that the data be input with a decimal point; the number can appear anywhere in the field indicated. An "E" formatted number may be used in lieu of the "F" format. For example, the number "thirty million" could be entered in any of the following "F" or "E" formats: 30000000. , 30.E+06 , 30.E+6 , 30.E6 , 30.+6, 3.+7, etc. The "E" format exponent must be right-justified in the data field.

c) "A" FORMAT (ALPHANUMERIC)...A7,7A10, etc. This format indicates that certain alphabetic characters or title information must be entered in the appropriate fields.

d) "X" FORMAT...1X,4X, etc. This format indicates blanks (no data may be entered in these fields).

The following data card example demonstrates proper use of formats.

1	8	20	32	44	56	64	72	
BFRP	NØ	A	J	I2	I3	SF2	SF3	ID
(A4)	(I4)	(F12.0)	(F12.0)	(F12.0)	(F12.0)	(F8.0)	(F8.0)	

where:

NØ. = 13

A = 62.175

J = 2.17

I2 = .0000632174

I3 = 3.2817

SF2 = .437

SF3 = .833

The entries to the data card could be made as follows:

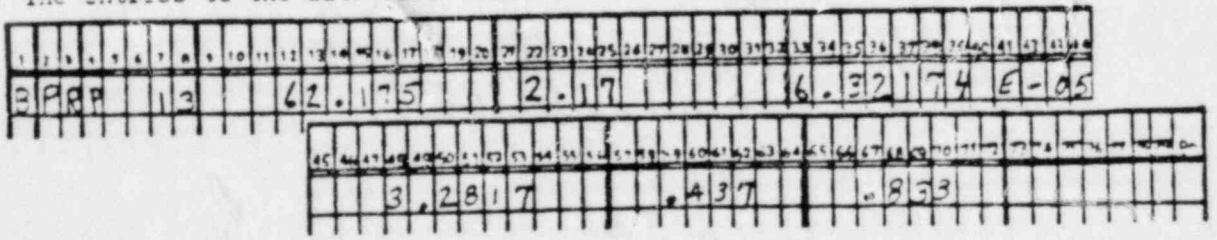

SPECIAL PURPOSE CARDS

Several 'special purpose' cards may be optionally entered at any place in the input decks of any of the STARDYNE programs. They will be printed in the 'card image' printout and ignored elsewhere. These formats are:

(1) DESCRIPTION CARD - This card is useful to identify specific sections of large input data decks.

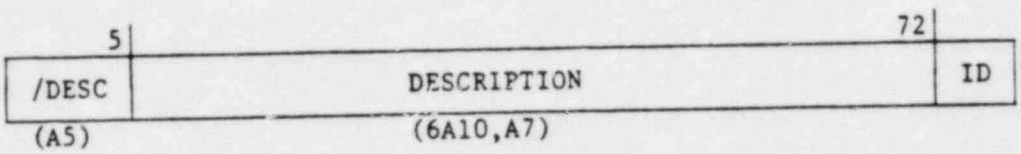

Punch /DESC in columns 1-5 of each card.

---

(2) *DECK card. In some instances it is desirable to use the CDC UPDATE utility program to maintain and alter large data decks.

OCTAL-DECIMAL CONVERSION

[FOR USE WITH THOSE OPERATING SYSTEMS WHICH REQUIRE A KNOWLEDGE OF OCTAL-DECIMAL CONVERSION]

OCTAL	DECIMAL
10	8
20	16
30	24
40	32
50	40
60	48
70	56
100	64
200	128
300	192
400	256
500	320
600	384
700	448
1000	512
2000	1024
3000	1536
4000	2048
5000	2560
6000	3072
7000	3584
10000	4096
20000	8192
30000	12288
40000	16384
50000	20480
60000	24576
70000	28672
100000	32768
200000	65536
300000	98304
400000	131072
500000	163840
600000	196608
700000	229376
1000000	262144
2000000	524288
3000000	786432
4000000	1048576
5000000	1310720
6000000	1572864
7000000	1835008
10000000	2097152

DECIMAL	OCTAL
10	12
20	24
30	36
40	50
50	62
60	74
70	106
80	120
90	132
100	144
200	310
300	454
400	620
500	764
600	1130
700	1274
800	1440
900	1604
1000	1750
2000	3720
3000	5670
4000	7640
5000	11610
6000	13560
7000	15530
8000	17500
9000	21450
10000	23420
20000	47040
30000	72460
40000	116100
50000	141520
60000	165140
70000	210560
80000	234200
90000	257620
100000	303240
200000	606500
300000	1111740
400000	1415200
500000	1720440
600000	2223700
700000	2627140

DECIMAL	OCTAL
800000	3032400
900000	3335640
1000000	3641100
2000000	7502200
3000000	13343300
4000000	17204400
5000000	23045500
6000000	26706600
7000000	32547700
8000000	36411000
9000000	42252100
10000000	46113200

ADDITION

	1	2	3	4	5	6	7
1	2	3	4	5	6	7	10
2	3	4	5	6	7	10	11
3	4	5	6	7	10	11	12
4	5	6	7	10	11	12	13
5	6	7	10	11	12	13	14
6	7	10	11	12	13	14	15
7	10	11	12	13	14	15	16

MULTIPLICATION

	1	2	3	4	5	6	7
1	1	2	3	4	5	6	7
2	2	4	6	10	12	14	16
3	3	6	11	14	17	22	25
4	4	10	14	20	24	30	34
5	5	12	17	24	31	36	43
6	6	14	22	30	36	44	52
7	7	16	25	34	43	52	61

The STAR program has two distinct functions; static load analysis and modal extraction.

1. Static Load Analysis

Once the structural model has been defined, the response to any general type of static load may be investigated. The program will determine the displacements of the system, as well as the internal forces and stresses for all the elements comprising the system. The solution may be obtained by a single model, or by sub-structuring techniques. It may be noted that a static load analysis may be performed on a free-free (unrestrained) structure provided the applied load case is self-equilibrating (see Section B2).

2. Modal Analysis

For any stiffness matrix and associated mass matrix, the program will extract the eigenvalues and eigenvectors in any desired frequency range. In addition, the program will compute the generalized weights, participation factors and internal forces/stresses on the elements associated with each eigenvector (see Sections B3, B4 and B5).

STAR PROGRAM FLOW DIAGRAM

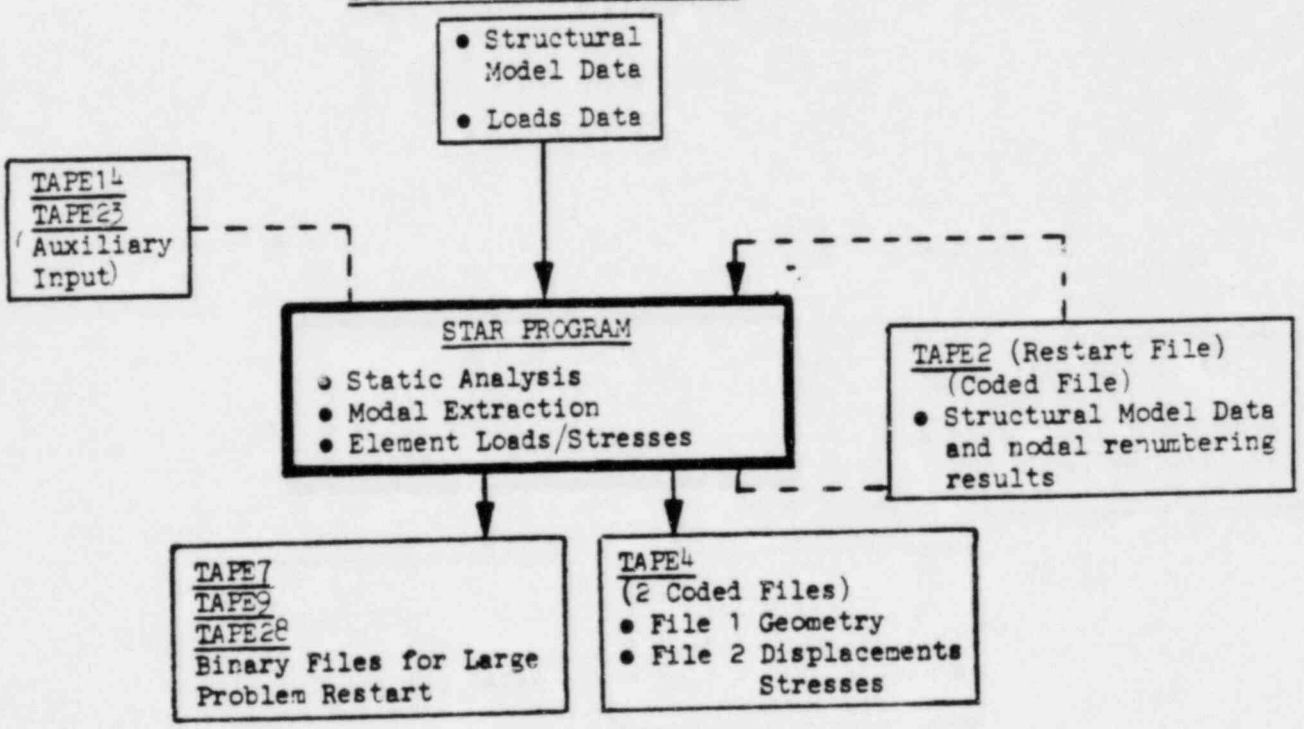

TABLE OF CONTENTS

JAN/80

The following maximums are allowable in STAR:
[Any changes in these values will be printed in the STAR bulletin.]

	STRUCTURE TYPE	
	6 DOF/NODE	3 DOF/NODE (TRANSLATION ONLY)
Number of Nodes and Maximum Node Number (Static)	4000*	4000*
Number of Nodes and Maximum Node Number (HQR)...	2500*	2500*
Dynamic DOF for HQR Modal Extraction (Pg. B3-10).	430	430
Number of Nodes and Maximum Node Number:		
• LANCZOS Modal Extraction (B5-5).....	4000*	4000*
• Inverse Iteration Extraction (B4-5).	1300*	1300*
Number of Beams (Rigid, Pinned, Elastic)+PIPES...	no limit	no limit
Number of Tri-Plates.....	no limit	no limit
Number of Quad-Plates.....	no limit	no limit
Number of Cubes + Wedges.....	no limit	no limit
Number of Tetrahedrons.....	no limit	no limit
Number of Elements into One Node.....	no limit	no limit
Number of Rigid Systems.....	no limit	none
Number of Nodes per Rigid System.....	no limit	none
Number of Rigid Bar Elements.....	no limit	none
Number of Static Load Cases.....	350	350
Number of Entries to Material Property Table.....	250	250
Number of Entries to Beam Property Table.....	999	999
Number of Nodes with Individual Reference Systems.....	no limit	no limit
Number of Individual Reference Systems.....	999	999
Matrix Bandwidth - Nodal.....	no limit	no limit
- d.o.f. (after renumbering; see page B-105).....	1985	1985
Substructure Matrix Reduction, maximum d.o.f....	20000	12000
• Maximum size of dependent system.....	19999	11999
• Number of Boundary d.o.f. if dependent system size is greater than zero.....	1500	1500

*VITAL NOTE!!: The maximum node number limits shown above are usually obtainable only if your computer's Operating System permits you to use in excess of 300,000 (OCTAL) words. Prior to coding any large model, you must examine the STARDYNE BULLETIN for the words of core required for the model and for instructions concerning the use of the CM parameter. (See page A-100 for a chart of OCTAL-DECIMAL conversions).

The DYNamic REsponse (DYNRE) programs have the following node number limits:

DYNRE1 = NO LIMIT
DYNRE2 = NO LIMIT
DYNRE3 = NO LIMIT
DYNRE4 = NO LIMIT
DYNRE5 = NO LIMIT
DYNRE6 = NO LIMIT

First-time STAR users should scan these 'INPUT NOTES'. If you are an experienced user, please turn to page B1 - 0.

A. RECOMMENDED GEOMETRY MODELING PROCEDURE

It is strongly advised that a small representation of the structural model be coded and solved prior to coding the actual model. This would resolve possible option and procedure problems in a more cost-effective manner.

The following order of operation is recommended for modeling and solving any structure in STAR.

1. Make nodal diagram of idealized structure (inspect limits, B-70).
2. Assign numbers to the node points, beams, plates and cubes.
3. Compute section properties, coordinates, element identifications, restraints, weights and/or Static Loads.
4. Code on data sheets.
5. Run STAR. The user may run STAR entirely in one run; however, on larger problems, it is advised to terminate the run after the geometry phase in order to check the running time estimates for the analysis types and to inspect the node/element table.
6. Read B2-20 for STATIC or pages B3-10 and/or B4-10 and/or B5-10 for Modal Extraction. Read the JCL APPENDIX for Job Control Card Information.
7. The program performs the following operations during the geometry phase:
   a) Checks whether data parameters exceed STAR capability.
   b) Checks for and flags duplicate and badly shaped elements.
   c) Checks for data inconsistencies.
   d) Element interconnectivity and property summation tables are printed which should be scanned to detect inadvertent omissions.
   e) Repeat feature is activated for repetitious data.
   f) The nodes are reordered internally to produce a minimum bandwidth. This does not affect the input data or the output data.
   g) Six scaled plots of the structural configuration as coded may be generated.
   h) The geometry input data deck is written onto TAPE2 for possible future use in STAR. In addition, TAPE4, file 1, the reformulated geometry data, is written for use by the dynamic response and post processor programs.

B. MATRIX REDUCTION AND NODE ORDERING CONSIDERATIONS

- In performing a Cholesky decomposition on the stiffness matrix, STARDYNE uses a proprietary algorithm which combines the best features of the wave front method operating in a bandwidth storage pattern. This technique has been fully optimized to provide an extremely cost effective solution. To further significantly reduce the problem cost STAR performs an automatic (invisible to the user) renumbering of the node numbers to minimize the matrix bandwidth.

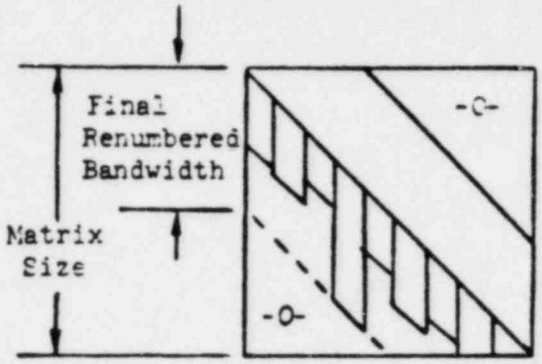

GLOBAL STIFFNESS MATRIX [K]

- WHAT IS BANDWIDTH?

The stiffness matrix nodal bandwidth is determined by the numerical difference between node numbers which define a particular structural element. If a node is "fully restrained" it need not be considered because restrained degrees of freedom (dof) do not appear in the Global Stiffness Matrix. Similarly, undefined nodes and dependent nodes of "Rigid Systems" do not contribute to the bandwidth.

Bandwidth example: A bar element coded between nodes 45 and 64, neither node being fully restrained, will cause a nodal band of (64-45) + 1 = 20. The automatic nodal renumbering seeks to exchange (or trade) node numbers internally until the minimum bandwidth is achieved.

- PLEASE NOTE!!!

When a structural model contains extreme stiffness mis-matches (i.e., very flexible structure attached to very stiff structure) ill-conditioning problems could arise during [K] matrix decomposition. On models of this type ill-conditioning may be minimized if the user assigns the lowest node numbers to the relatively most flexible section of the structure. Other types of structures can also benefit from proper selection of node numbers. For example, for a cantilever beam, free tip = node 1; for a tall building, top = node 1.

See special re-numbering card, page B1 - 74, if it is desired to revise the node ordering of 'problem' models which may have been coded the 'wrong' way (use NSTAGE = -3 option).

C. NODE ELEMENT INPUT DATA ORDERING CONSIDERATIONS - IMPORTANT!!!

Node and element numbers may have small gaps in the list of numbers defined and any number from one through the maximum may be used. The data is processed very inefficiently however, when very large "gaps" are left in node and element numbers. Within any node or element input table, the data may be entered in any order.

D. HEADER CARD IDENTIFICATION AND REPEAT FEATURES

All of the 'data tables' in STAR require one or more header words ('NØDE', 'NØDEG', 'CØNC', 'CØNCG', etc.) which serve to identify card formats within the table. A header word must start in the first column of the first card of the table. If desired, a header name may be entered on every card. If, however, a header field is blank on a subsequent card (header word not entered), the card format for the most recent previous header type coded will be assumed for that card. The weight (WGHT) input table, Page B1-93, is an exception to the above.

E. OPTIONAL INPUT FROM TAPE14 AND/OR TAPE23

The major part of the STAR Geometry and Static input sections are entered in the 'data table' format. Each of these data tables begins with the table name punched beginning in column 1 of the first card. Each table ends with a card which has END punched beginning in column 1. The data in any of the tables may be optionally read from a coded disc file by placing a table header card of the following form into the input deck at the point where the desired information is to be entered. DO NOT PUT THE 'END' CARD ON THE DISC FILE.

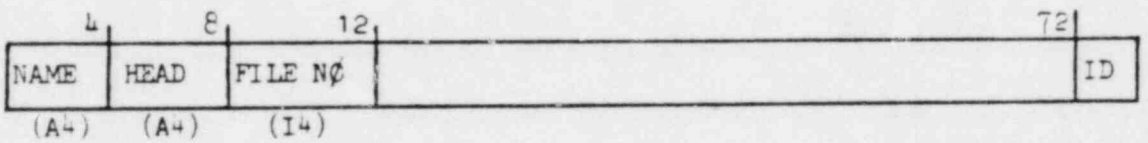

NAME = First four letters of table name.

HEAD = Punch the letters HEAD in columns 5-8.

FILE NØ = An integer disc file number from which additional card images will be read for this table. Reading will continue on this file until an END-OF-FILE mark is encountered. The next card read will be from the input file (User's data input card deck). The only two disc file numbers which are permitted are TAPE14 and TAPE23. FILE NØ can, therefore, be assigned values of 14 or 23 only.

Continued on the next page....

E. OPTIONAL INPUT FROM TAPE14 AND TAPE23 - Continued

The user must ensure that the 'data table' information has been transmitted in 'coded' format to the proper file. Several tables may be on this disc file, so long as they are separated by END-OF-FILE marks. The information must be positioned in the proper sequence to be read when the desired NAME-HEAD card is encountered. The table information may be placed on the file via Job Control Cards, prior to entry into the STAR program. NOTE: If BPRØP tables are entered via NAME-HEAD, they must be entered immediately prior to the BEAM table.

NAME-HEAD cards in the geometry deck will be written onto the 'card image' file, TAPE2. If TAPE2 is used for a re-start run, the disc files associated with the NAME-HEAD cards must be re-entered.

EXAMPLES OF DATA ENTRY ON AUXILIARY FILES TAPE14 AND TAPE23.

```
1           12                                          72
MADDHEAD    23
(Matrix alteration data is on TAPE23)
END

DISPHEAD    14
(Nodal displacement specification data is on TAPE14)
END

CONCHEAD    23
(Concentrated loads data is on TAPE23)
END
```

F. DATA TABLE 'FACTØR' CARD (OPTIONAL - The following card may be inserted in a 'data table' to cause subsequent cards in that table to be factored by a scalar multiplier. Only the appropriate values are multiplied by this factor. This card is convenient to convert data entered in one set of units to other units, etc.

```
4     8     12          22                                  72
NAME  FACT  ////////    FACTØR  ////////////////////////////  ID
(A4)  (A4)  (4X)        (F10.0)
```

NAME = First four letters of table name. Permissible tables: NØDE, MADD, WGHT, BMLØ, BMTE, TPTE, QPTE, CUTE, TETE, TPRS, QPRS, CØNC, DISP.

FACT = Punch FACT in columns 5-8.

FACTØR = A value which will factor the appropriate input data on the remaining cards of the input table or until another 'FACT' card is encountered. The Factor defaults to 1.0 at the beginning of each table. If FACTØR is entered as blank or 0.0, a value of 1.0 will be used.

NOTE: Data entered in the 'DECK' formats (page J-60) are not modified by this factor input (e.g., Boundary Force or Displacement vectors from STAR TAPEP outputs or 'SPRING' or 'NUBØP' TAPE14 force outputs.

H. SUMMARY OF STAR PROGRAM HEADER AND CONTROL CARDS

The STAR table header and control card names shown in this manual are summarized below for convenience. It should be noted that many names which appeared in earlier versions of the STAR manual are not in the list. The program will still recognize these names, however, provided that the table in which they originally appeared is entered entirely as described in the older manual.

START
PLØTS
RENUMB
MATLG
MATLG1
MATLG2
MATLHEAD
NØDE
NØDEG
NØDEFACT
NØDEGRD1
NØDEGRD2
NEWSYS
NØDEHEAD
ASYSG
ASYSHEAD
RESTG
RESTHEAD
WGHT
WGHTG
WGHTFACT
WGHTGEN
WGHTDECK
WGHTHEAD
BEAMG
BRECT
ELBØW
PIPEG
PIPET
BEAMHEAD
BPRØP1
BPRØP2
BPRØP3
BPRØP4
BPRØP5
BPRØP6
BPRØHEAD
TRIAB
TRIAHEAD
QUADB
QUADWARN
QUADHEAD
CUBEG
CUBEHEAD
WEDGE
WEDGHEAD
TETRG
TETRHEAD
MADDX
MADDFACT
MADDHEAD
MADDEL
ENDEL
MADDPRNT
BØUNG
BØUNGADD
BØUNHEAD
GUYAN
GUYANADD
GUYAHEAD
ENDGBØM
END
STATIC
TAPEHEAD
CTRL
BMTEMP
BMTEMPG
BMTEHEAD
BMTEFACT
TPTEMP
TPTEHEAD
TPTEFACT
QPTEMP
QPTEHEAD
QPTEFACT
CUTEMP
CUTEHEAD
CUTEFACT
TETEMP
TETEHEAD
TETEFACT
BMLØPRNT
BMLØAD
BMLØHEAD
BMLØFACT
TPRS
TPRSHEAD
TPRSFACT
QPRS
QPRSN
QPRSHEAD
QPRSFACT
CØNC
CØNCG
CØNCDECK
CØNCHEAD
CØNCFACT
CØNCGBL
DISPG
DISPGEN
DISPDECK
DISPHEAD
DISPFACT
ACCEL
FACTØR
FACTHEAD
END CASE
ALL DØNE
HQR
INVITR
DYNAMIC
ØPTION
ØUTPUT
MINVALUE
SEL-NØDE
SEL-BEAM
SEL-TRIA
SEL-QUAD
SEL-CUBE
SEL-TETR
TAPE4G
TAPE4GSEL
TITLE1
TITLE2
TITLE3
TITLE4
TITLE5
ENDMØDEL
TOLERANCE

STAR DECK SETUP DIAGRAM

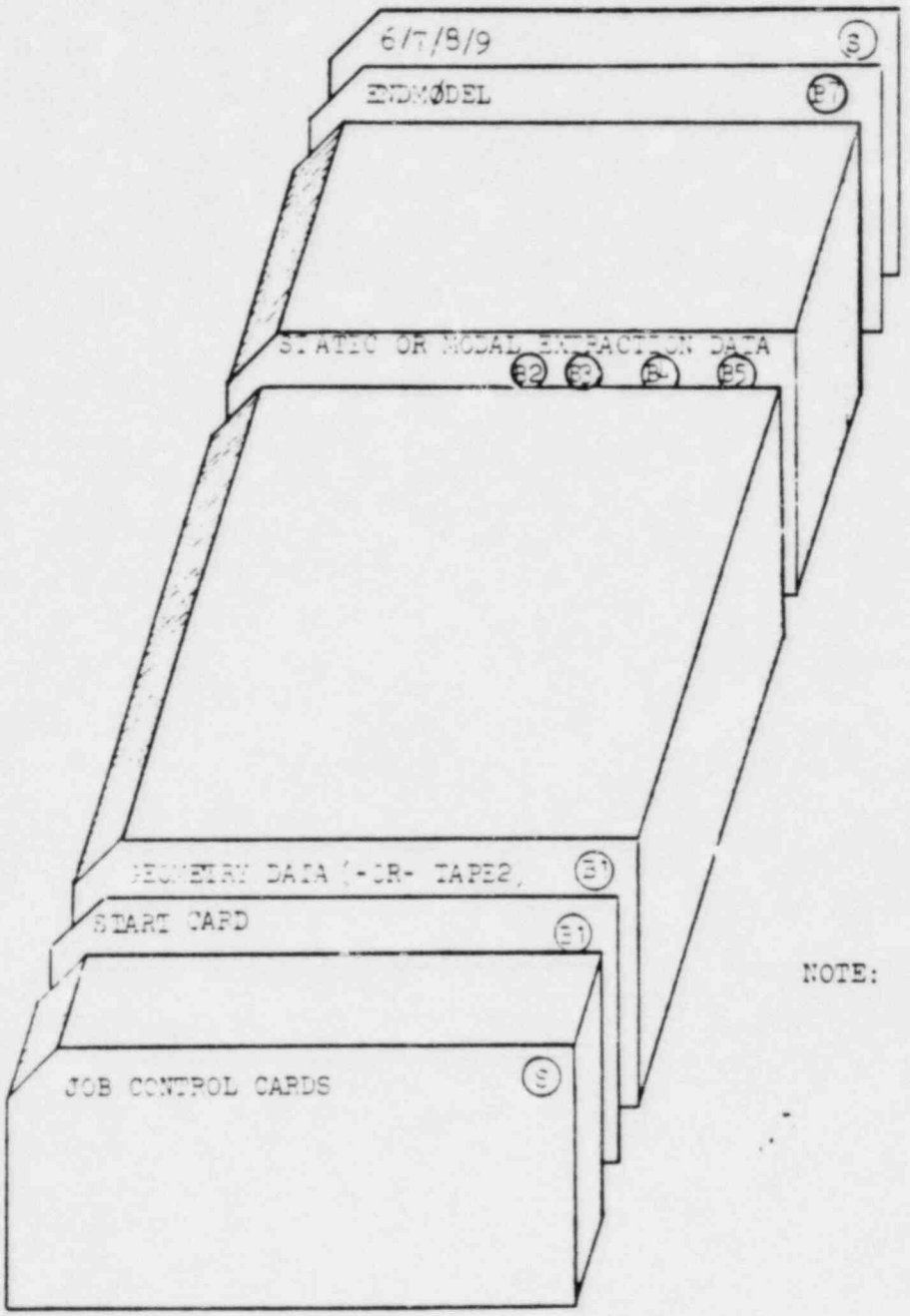

NOTE: Encircled letters refer to applicable sections of STARDYNE User's Manual

PISCES

Static and dynamic finite-difference codes based on computational methods developed to calculate nonlinear, large-amplitude responses of structures, fluid bodies, and solid media. The codes solve the fundamental partial differential equations on continuum mechanics expressed in the explicit finite difference form. PISCES provides solutions to problems including fluid-structure interaction, soil-structure interaction, hypervelocity particle impact and flow interaction. Batch

POSTEN/CNCGRD

Analyzes and designs continuous prismatic or nonprismatic slabs, girders, beams, waffle slabs, flat slabs with drop panels and flat plates with or without column capitals. Most designs conforming to American Concrete Institute (ACI) 318-77 standards are made in a single computer run. Includes continuous bents of up to 9 continuous spans plus cantilevers. Spans can have uniform load, up to 10 concentrated, 3 partial uniform and 3 partial triangular loads. Members can be prismatic or nonprismatic and of different shapes, including T, inverted T and I sections.

PS BASEPLATE

Analyzes flexible bolted baseplates in nuclear power plants in support of regulatory requirements. Pre-processor generates all input to STARDYNE/SPRING. Post-processor summarizes analysis results. Reduces engineer-hours required to perform baseplate analysis. Interactive.

SPSTRESS

Systems Professional Structural Engineering System Solver. Performs linear analysis on two- or three-dimensional elastic, statically loaded structures. Computes joint displacements, member end forces, and reactions for a structure. Input includes makeup, type and orientation of all members, position and magnitude of all applied loads, displacements and distortions. SGEN and STRCHK can also be used with SPSTRESS. SGEN generates input data for SPSTRESS, and STRCHK checks steel beam and column sections against member output from a previous SPSTRESS run for their ability to handle applied loads in accordance with American Institute of Steel Construction specifications. Batch and interactive.

STARDYNE

Finite element static and dynamic structural analysis. A STARDYNE static analysis will predict the stresses and deflections resulting from pressure, temperature, concentrated forces and enforced displacements. Dynamic analysis will predict the node displacements, velocities, accelerations, element forces and stresses from transient, harmonic, random or shock excitations. STARDYNE is user oriented, containing automatic node and element generation features that reduce the effort required to generate input. Plots of the original model and deformed structural shapes help the user evaluate results. Contour plots show surface stress for two-dimensional elements. The program creates time histories of element forces and stresses, and of node displacements, velocities, and accelerations. The RRESTAR preprocessor allows users to enter free-format input through an interactive terminal. Batch and interactive.

STRCHK

Uses the results of SPSTRESS frame analysis program to investigate a preselected steel beam or column. Each run automatically retrieves up to three independent loading conditions, and modifies and combines each with the others using load factors chosen by the user. Batch and interactive.

STRU-PAK

A library of 31 structural analysis programs designed for small, individual problems and for components or selected portions of larger structures. The library is organized according to 10 categories: general, section properties, beams, columns, frames/trusses, rings, plates, shells, dynamic analysis, springs and miscellaneous. Interactive, batch (partial)

SYSTEMS PROFESSIONAL

A library of 28 structural design programs for the building construction industry. Updated to the latest requirements of accepted building codes, such as AISC and ACI, these programs can be used to design individual structural components or to analyze entire framing systems. Programs are divided into concrete, steel, masonry, wood and general analysis. Interactive.

SPACE4

Service: APEX/SI, UCS/CRAY

Access Mode: Remote batch

Support Level: 3

Documentation:
Engineering Catalog
SPACINF, SPC4INF
SPACE4 Manual, $7.50
Digital Analysis Consultants
7460 Girard Avenue
La Jolla, California 92037
(714) 459-3373

VALUE-PRICED

SPACE4 performs linear elastic analysis of two- or three-dimensional structures that may be treated as assemblages of line members and/or panels.

STAAD-III

Service: APEX/SI, UCS/CRAY

Access Mode: Interactive, remote batch

Support Level: 3

Documentation:
Engineering Catalog
STDINFO
STAAD-III Reference Manual, $7.50
Research Engineers
P.O. Box 2706
Cherry Hill, New Jersey 08034
(609) 482-0900

VALUE-PRICED

This program analyzes and designs a two- or three-dimensional framed structure of any size.

STARDYNE®

Service: NOS/BE

Access Mode: Remote batch

Support Level: 3

Documentation:
Engineering Catalog
STARDYNE User's Manual, $22.50
STARDYNE Learners Guide, $12.50
STARDYNE Static Substructure Guide, $7.50

System Development Corporation
2500 Colorado Avenue
Santa Monica, California 90406
(213) 820-4111

VALUE-PRICED

STARDYNE performs static analysis, substructure analysis, seismic analysis, piping system analysis, and dynamic response analysis on any specified structure.

STRAN

Service: APEX/SI

Access Mode: Remote batch

Support Level: 3

Documentation:
Engineering Catalog
Synercom Technology, Inc.
500 Corporate Drive
Sugar Land, Texas 77478
(713) 491-5000

VALUE-PRICED

STRAN performs a linear analysis of large space frames using the substructures approach to the stiffness matrix method.

2.10.3 ANSYS Information

ANSYS

For the solution of a wide variety of problems in the areas of structural, heat transfer, thermal-fluid flow, thermoelectricity, and wave motion analysis, ANSYS is widely known for its linear and nonlinear capabilities. Using the finite element method to solve these and other problems, ANSYS is distinguished by its extensive user-oriented features and operational reliability. The program is offered to UIS clients on a value-priced basis on the APEX/SL Service and the CRAY-1S computer. It was developed and is supported by Swanson Analysis Systems, Inc., of Houston, Pennsylvania.

Among the many analytic tools that ANSYS provides are choice of analysis types, material behaviors, nonlinear options, loading conditions, and solution procedures, as well as a comprehensive element library. Graphic displays and both time-sharing and remote batch processing environments are at your disposal.

Types of Analysis

ANSYS provides you with access to its various capabilities through the following eight types of analysis.

Static analysis is used to solve for displacements, strains, stresses, and forces in structures under applied loads. Elastic, plastic, creep, and swelling material behaviors are available. In addition, stress stiffening and large deflection effects may be included. Such bilinear elements as interfaces (with or without friction) and cables can also be used.

With **Eigenvalue buckling**, ANSYS calculates critical loads and buckling mode shapes for linear bifurcating buckling, based on a previous static analysis.

Mode frequency analysis solves for natural frequencies and mode shapes of a structure. Stresses and displacements may be obtained by using the spectrum analysis option with a displacement, velocity, acceleration, or force spectrum.

For determining the time-history solution of the response of a structure to a known force, pressure, and/or displacement-forcing function, **nonlinear transient dynamic** analysis is used. Stiffness, mass, and damping matrices vary with time, and may be functions of the displacements. Among others, friction, plasticity, and large deflection nonlinearities may be included.

Linear transient dynamic analysis, used to determine the time-history solution of the response of a linear elastic structure to a known forcing function, contains a quasi-linear option that includes interfaces (gaps) with the structure or to the ground.

Harmonic response analysis evaluates the steady-state response of a linear elastic structure to a set of harmonic loads of known frequency and amplitude. ANSYS prints the complex displacements or amplitudes and phase angles. Stresses may be calculated at both specified frequencies and phase angles.

For the solution of the steady-state or transient temperature distribution in a body. ANSYS uses **heat transfer** analysis. Besides conduction and convection, radiation and internal heat generation may be included. The calculated temperature distribution may then be used as input to a structural analysis.

Substructures analysis assembles a group of linear elements into one "element" (a superelement) to be used in another ANSYS analysis. You will find this type of analysis particularly valuable when you wish to isolate the linear portion of a structure with an iterative solution.

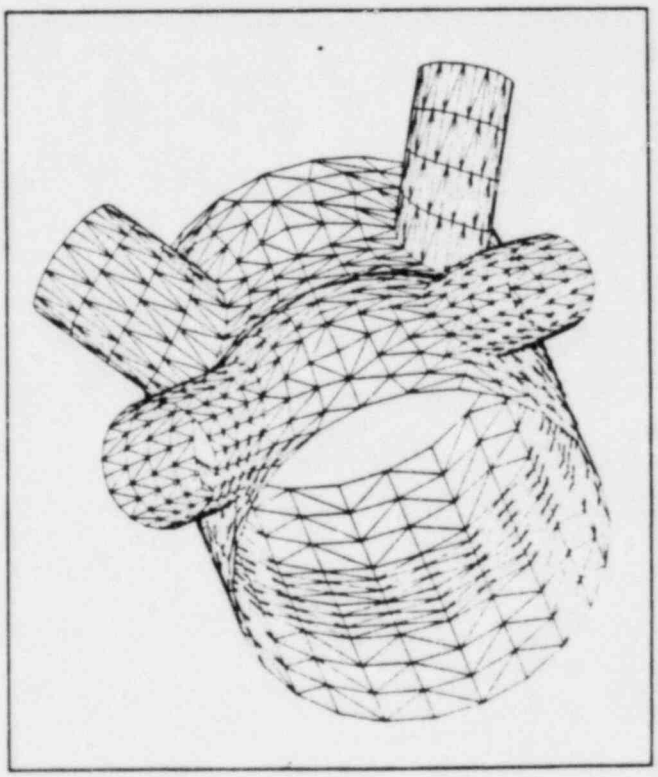

6MB67 582

Material Behaviors

All the elements of ANSYS include isotropic material behavior. In addition, you may use orthotropic material properties with all plane and solid elastic structural elements, and with all heat transfer elements. An elastic structural element allows user input of a complete material matrix for general anisotropic behavior.

ANSYS' elastic material properties may be functions of temperature. Temperature-dependent property input includes the following features:

- ☐ Curvefitting (4th order) to tabular property data
- ☐ Linear interpolation with tabular property data
- ☐ Temperature-dependent emissivity
- ☐ Temperature-dependent film coefficients
- ☐ Nonlinear properties (stress-strain curves) described at up to five different temperatures

Nonlinear material properties can be included in static or nonlinear transient dynamic analyses. For plasticity, stress-strain curves can be any of the following:

- ☐ Virgin stress-strain
- ☐ Bilinear kinematic hardening
- ☐ 10th-cycle empirical hardening

ANSYS also includes an option to model nonlinear elastic material behavior, in which more than ten primary and secondary laws are available.

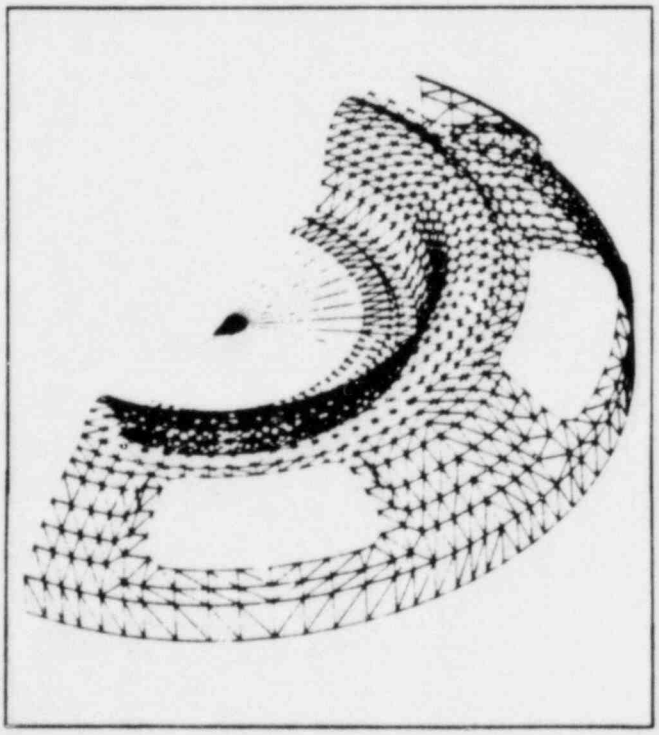

Nonlinear Options

ANSYS offers an impressive choice of nonlinear options, including geometric nonlinearities (large deflection, large rotation, and stress stiffening), special nonlinear elements, and nonlinear material behavior.

You can use large deflection analysis for both static and dynamic problems. ANSYS makes geometry modifications at the end of each load increment, and provides stress stiffening and large rotation effects for most of the elements in the library.

A number of special-purpose elements in ANSYS facilitate modeling nonlinear behavior, all of which are available in static or dynamic analysis. The **cable element** carries tension or compression only, and is useful for modeling suspension bridges or television and radio towers. A **crack-tip element** is available for fracture mechanics work. **Interface elements** (with or without friction) transmit load in compression only; they are especially useful for modeling such contact surfaces as gear teeth or threaded connectors. ANSYS also includes a three-dimensional solid element (with or without reinforcing material), a control element, and a nonlinear force-deflection curve element.

Loading Conditions

For structural analyses, loading inputs include nodal forces and moments, body forces, displacements, pressures, and temperatures. You may apply structural constraints in a user-defined coordinate system. In dynamic analyses, these loads can be random, sinusoidal, or arbitrary functions of time.

Loading inputs for heat transfer analyses include fluid convective heating, internal heat generation, radiation, and known temperatures or heat flows.

Solution Procedures

Four major solution procedures are available with ANSYS, as follows:

- ☐ Wavefront technique solves the system of simultaneous linear equations developed by the matrix displacement method.
- ☐ Guyan reduction creates a set of degrees-of-freedom (which is a subset of the total degrees-of-freedom in a structure); this subset is used to characterize the response of the structure.
- ☐ Jacobi and subspace iteration let you select the Jacobi technique for eigenvalue extraction, or subspace iteration to extract the first *n* modes.
- ☐ Transient analyses make use of an implicit numerical iteration in each time step.

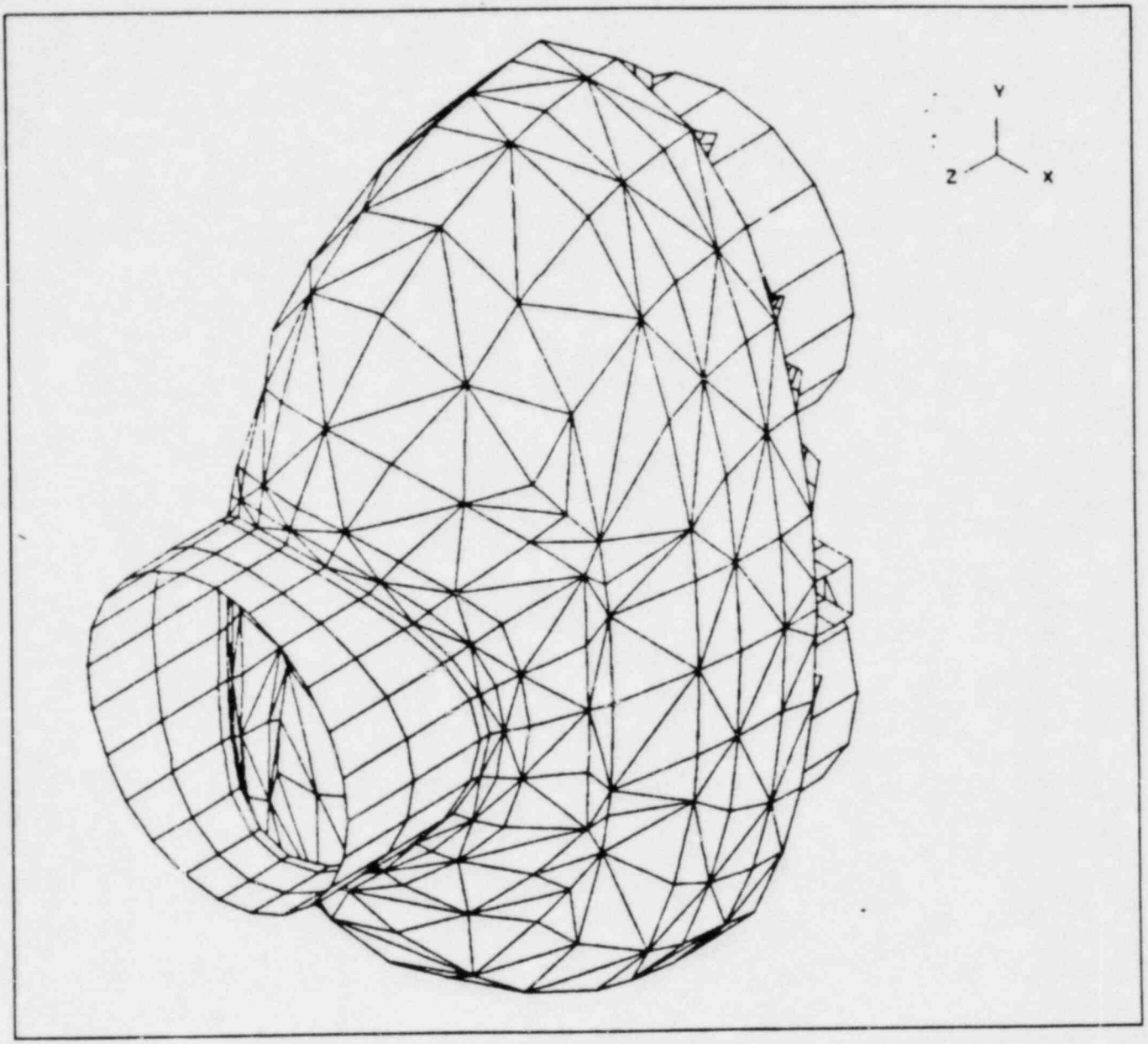

The ANSYS Element Library

ANSYS offers one of the most comprehensive element libraries available, containing more than 60 structural and heat transfer elements.

Structural element types include:

- ☐ Spars
- ☐ Beams
- ☐ Pipes
- ☐ Elbows
- ☐ Tees
- ☐ Plane and axisymmetric membranes
- ☐ Plates
- ☐ Solids

Additional structural elements include masses, springs, dampers, sliding and gap interfaces, and cables, as well as arbitrary stiffness, mass, and damping matrices.

Heat transfer elements include:

- ☐ Conducting bars
- ☐ Shells
- ☐ Plates
- ☐ Solids
- ☐ Harmonically-loaded axisymmetric elements
- ☐ Radiation and convection links

All heat transfer elements have geometrically equivalent structural elements for thermal stress evaluation.

Graphic Displays

ANSYS contains an exceptionally wide range of pre- and postprocessing routines to generate model data, display models for visual verification, and manipulate output from the program. In addition to windowing and surface plotting capabilities, ANSYS offers shrinking, hidden line plots, and element, node, material, type, or member property numbering.

User-Oriented Features

All portions of the ANSYS program can be run in either an interactive or remote batch environment, using free-format input data. In fact, a stand-alone program called PREP, also developed by Swanson Analysis Systems, can be used to create an entire ANSYS input deck from an interactive terminal. The results can then be postprocessed after analysis. Moreover, ANSYS provides specialized capabilities for editing and file manipulation, as well as a restart option for saving intermediate results.

ANSYS offers wide-ranging features in one integrated package, and is fully documented in a set of manuals describing program operation, use, and conceptual and practical techniques. In addition, the developer gives training seminars, as well as workshops that provide users with hands-on experience. For additional information on the ANSYS program, please contact your UIS representative, or Swanson Analysis Systems, Inc., P.O. Box 65, Houston, Pennsylvania 15342.

2.10.4 References

1. Timoshenko, Stephen P. and James M. Gere, Theory of Elastic Stability, Second Edition, McGraw-Hill Book Company, 1961.

2. Baker, E.H., L. Kovalevsky and F.L. Rish, Structural Analysis of Shells, Robert E. Krieger Publishing Co, 1981.

3. Roark, Raymond J. and Warren C. Young, Formulas for Stress and Strain, Fifth Edition, McGraw-Hill Book Company, 1975.

4. Timoshenko, S. and S. Woinowsky-Krieger, Theory of Plates and Shells, Second Edition, McGraw-Hill Book Company, 1959.

5. Higdon, Ohlsen, Stiles, Weese, Mechanics of Materials, Second Edition, John Wiley and Sons, Inc. 1968.

6. Bickford, John H., An Introduction to the Design and Behavior of Bolted Joints, Marcel Dekker, Inc., 1981.

2.10.5 Computer Stress Analysis Output Microfiche

3.0 THERMAL EVALUATION

This chapter identifies and describes the principal thermal aspects of the CNS 8-120B cask package for safety and compliance with the performance requirements of 10 CFR 71.

3.1 Discussion

Thermal protection of the package is provided in four basic areas. These are the cylindrical shell (sides), top, bottom, and overpacks.

The cylindrical shell has three layers. The outer layer consists of a 1.50 inch thick carbon steel plate. This is followed by a 3.50 inch thickness of poured lead. Finally, the inner cavity liner is formed by a 0.75 inch thick carbon steel plate.

The top consists of two sections; a 3.5 inch thick carbon steel plate, which forms the inner layer, and a similar 3.5 inch thick carbon steel plate which forms the outer layer. Both are circular in shape, with a diameter equal to that of the cylindrical side shells. A circular secondary lid is centrally located on the top of the cask; it has a cross-section of two 3.5 inch thick plates, similar to the rest of the cask top section.

The bottom section consists of two 3.5 inch thick carbon steel plates, also circular in shape, and of a diameter equal to that of the cylindrical side shells. The bottom section is essentially one cross-section, with no openings or differences throughout the section.

The overpacks are large circular structures of polyurethane foam which are mounted on each end of the cask. Although primarily intended as mechanical impact limiters, they also function as thermal insulators.

For a pictorial view of the basic cask configuration, refer to Figure 3.1.1-1.

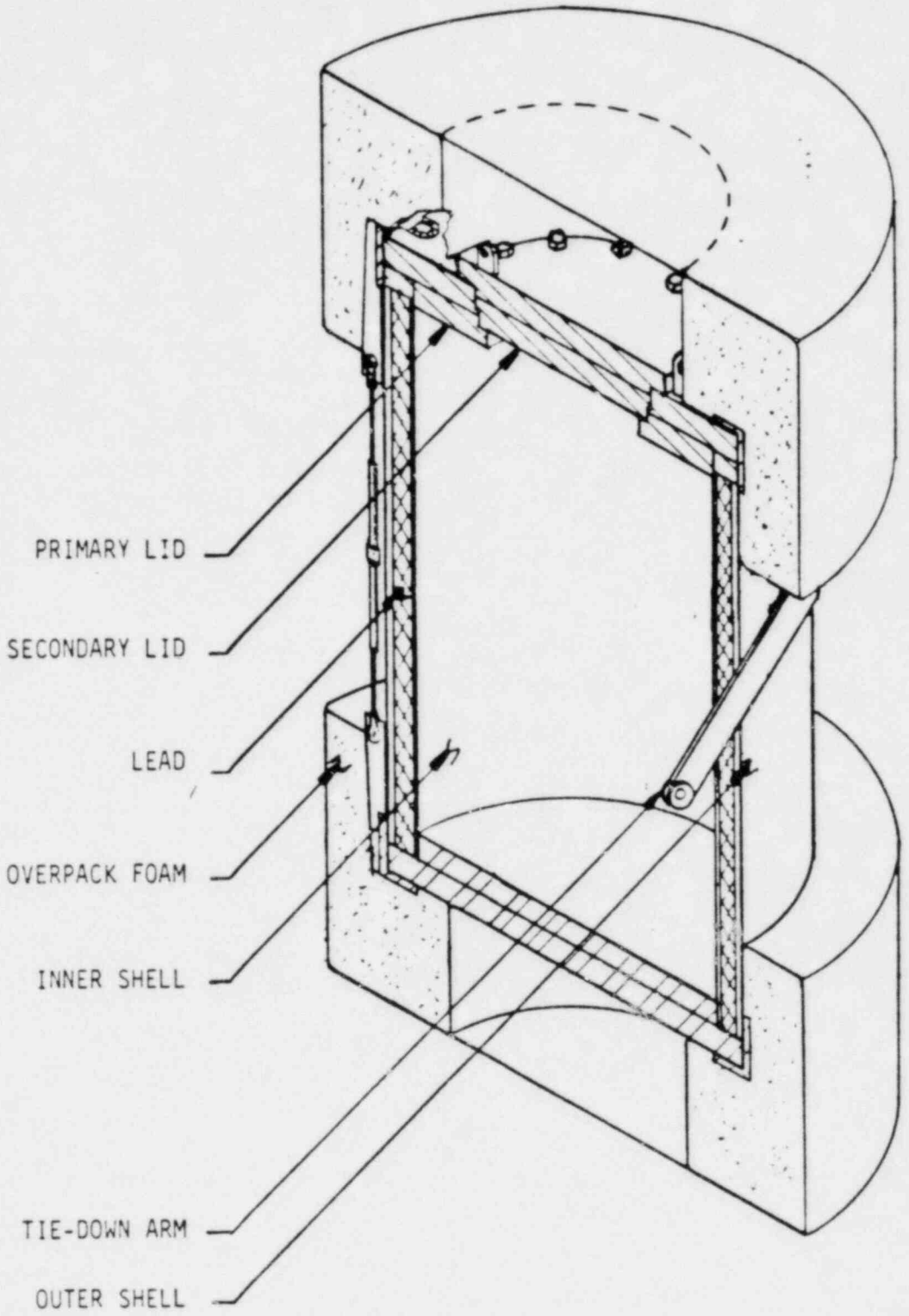

Figure 3.1.1-1 CASK SCHEMATIC

3.1.1 Normal Transport Conditions

The cask receives heat from two sources during normal transport conditions. These are decay heat from the waste payload and insolation.

The decay heat is conducted out of the cask package through the sides, top, and bottom. Heat is then dissipated to the outside environment by a combination of natural convection and radiation. Since the overpacks possess a very low thermal conductivity, the cask surface area covered by these is assumed not available for heat transfer to the environment.

The insolation load is considered to be a pure radiation load, and is also effective over the net exposed surface area only (that not covered by overpacks). Heat from the solar load is distributed throughout the cask by conduction.

3.1.2 Hypothetical Thermal Accident Conditions

Heat from the hypothetical fire is transferred to the outer steel shell plates by radiation.

Heat is distributed throughout the cask by conduction through the lead shielding layer and conduction through the inner steel plates.

The steel shell plates and the lead shielding will store heat during the period of the fire and, subsequent to the fire, will dissipate this heat to the surrounding environment by natural convection and radiation.

As previously mentioned, the outside surface area of the cask which is covered by the overpacks is considered not available for radiation input from the fire, or for the subsequent convection and radiation to the outside. However, the entire metallic mass of the cask contributes to its conductive behavior, and its attendant capability for storage of heat.

3.1.3 Results of Thermal Analysis

The cask has been evaluated for a decay heat of 100 watts. Steady-state analyses have been performed for this decay heat value at ambient air temperatures of 100°F and 130°F. In addition, a transient analysis has been performed for the hypothetical thermal accident conditions a 1475°F radiaiton environment with a 100°F ambient air temperature.

Important temperatures in the cask for both normal transport conditions and hypothetical thermal accident conditions are summarized below.

Normal Transport Conditions - Temperatures, °F

Ambient Outside Air		Inner Cavity	Lead Shield	Primary O-Ring	Secondary Lid Seals	Outside Surface
100°F	Max.	151	138	138	141	151
	Min.	132	132	138	141	132
130°F	Max.	177	164	165	168	177
	Min.	159	159	165	168	159

Hypothetical Thermal Accident Conditions - Temperatures, °F., Maximum *
Ambient Air Temperature = 100°F

Time		Inner Cavity	Lead Shield	Primary O-ring	Secondary Lid Seals	Outside Surface
At 1/2 hr. after thermal accident begins	Max.	342	252	142	209	612
	Min.	139	139	142	209	336
Within 10.0 hr. after thermal accident begins	Max.	360	359	220	224	612
	Min.	132	132	138	141	132

* includes heating due to decay heat and insolation.

The maximum value of the minimum cavity temperature was found to be 215°F.

Important conclusions derived from the above results include:

3.1.3 Results of Thermal Analysis (continued)

(1) The lead shield does not melt under hypothetical thermal accident conditions (maximum lead temperature = 359°F at the outside of the lead shield); $T_{\text{lead melt}} = 621°F$.

(2) The components of the closure system (primary o-ring seals, and secondary lid seals) are exposed to temperatures not in excess of 224°F. Silicone seals retain excellent sealing properties to temperatures exceeding 500°F.

(3) The maximum predicted temperature at any location within the cask cavity, at any time, is 360°F.

(4) The maximum pressure within the cask cavity is 6.7 psig under normal operating conditions and 19.2 psig under thermal accident conditions.

3.2 Summary of Thermal Properties of Materials.

Thermal material properties used for analyses were taken from several sources listed in Appendix 3.6.

For each material within the cask (i.e., carbon steel, lead) relevant material properties were selected. Density is assumed constant; however thermal properties such as specific heat and conductivity (which can vary significantly with temperature) are represented by tables which show how the particular property varies over the range of temperatures encountered. The tables are shown below:

Carbon Steel (Ref. 1)

Temperature	Specific Heat	Conductivity	Density
70°F	0.1033 Btu/lb_m -°F	35.1 Btu/hr-ft-°F	489 lb/ft^3
100	0.1053	34.7	
200	0.1121	33.6	
300	0.1177	32.3	
400	0.1234	30.9	
500	0.1278	29.5	
600	0.1322	28.0	
700	0.1381	26.6	
800	0.1452	25.2	
900	0.1535	23.8	
1000	0.1624	22.4	
1100	0.1710	20.9	
1200	0.1829	19.5	
1300	0.2045	18.0	
1400	0.4010	16.4	
1500	0.1982	15.7	

Lead (Ref. 3)

32°F	0.0306 Btu/lb_m -°F	20.3 Btu/hr-ft-°F	710 lb/ft^3
212	0.0315	19.3	
392	0.0325	18.2	
572	0.0335	17.2	
752	0.0328	--	

The emissivity of carbon steel was taken as 0.85 (Ref. 4) and the solar absorptivity was 0.40 (See discussion, Section 3.4.1.1)

3.3 Technical Specifications of Components

Not Applicable.

3.4 Thermal Evaluation for Normal Conditions of Transport.

3.4.1 Thermal Model

3.4.1.1 Analytical Model A steady state thermal analysis was performed in order to evaluate the cask during normal conditions of transport. Specific conditions and assumptions were as follows:

(1) 100 watts internal decay heat

(2) 300 Btu/hour-feet^2 solar load (ref. 4, page 130). This was the severest load, or ...gest day of the year. This was used in conjunction with a solar absorptivity of 0.40, to give a net solar load of 120 Btu/hour-feet^2.

The cask will be painted white; ref. 3, page 3-22 gives solar absorptivity for white painted surface as 0.26. Using 0.40 for the absorptivity lends conservatism to the solar heat load, inasmuch as this results in a higher thermal loading.

The maximum insolation given in Table 1, NRC Regulatory Guide 7.8 is:

(for curved surfaces) 1475 Btu/ft^2/12 hours = 122.9 Btu/hour-feet^2

This is comparable to the solar load of 120 Btu/hour-feet^2 which was used in the analysis.

(3) All radiation shape factors (F) have been assumed to be equal to 1.0, as virtually all heat emitted from one radiating surface is received by the next surface.

3.4.1.1 Analytical Model (contiued)

(4) Standard English units were used throughout the analysis. Units used:

Length: feet
Heat: Btu
Time: hour

The only exception to this is the watt, which is used to express decay heat. To obtain compatibility with other units used, the conversion 1 watt = 3.414 Btu/hour was used.

(5) Thermal mass and conductivity of the payload were ignored. This represents a conservative assumption.

(6) Convective heat transfer from the outside surface was modelled as natural convection from an upright cylinder for the sides of the cask:

For Vertical Plates or Cylinders (Ref. 2, p. 219)

$$h = 0.29\left(\frac{\Delta T}{L}\right)^{1/4}$$

h = Convective Heat Transfer Coefficient, BTU/hour - feet^2 - °F
ΔT = Temperature Difference, $T_{surface} - T_{ambient}$, °F
L = Major Dimension of Cylinder, feet

This is utilized in Conjunction with the total convective heat flow relation:

$Q = h A \Delta T$

Q = Heat flow, Btu/hour
A = Surface area, feet^2
ΔT = Temperature difference
$= T_{surface} - T_{ambient}$, °F

Convective heat transfer from the top and bottom sections was modelled in a similar fashion, except the equation for the convective heat transfer coefficient, h, was:

3.4.1.1 Analytical Model (contiued)

$$h = 0.27 \left(\frac{\Delta T}{L}\right)^{1/4} \qquad \text{(Ref.2, p.219)}$$

h = Convective Heat Transfer Coefficient
Btu/hour-feet^2-°F

ΔT = Temperature Difference
= $T_{surface} - T_{ambient}$, °F

L = Major dimension of plate, feet

Using the above asumptions, an analytical model was created which effectively modelled thermal behavior of the package. The package was divided into geometric segments. Each segment contained appropriate thermal resistances and thermal conductances as required.

This model was implemented using the MITAS-II software package. The program balanced the heat flow equations using a finite differencing algorithm. A graphical representation of the thermal network used in the analysis may be found as Figure 3.4.1-1.

Steady state analyses were performed for both 100°F and 130°F ambient air temperatures. The MITAS-II program determined when steady-state conditions were achieved by examining heat flows throughout the cask; when these stabilized within a small margin, the model was assumed to be steady state. The heat flow criterion used for this analysis was 100 Btu/hour; i.e., when all heat flows were within 100 Btu/hour of each other, steady-state conditions were assumed to exist.

3.4.1.2 Test Model Not Applicable

3.4.2 Maximum Temperatures

Maximum temperatures of the package for normal transport conditions are listed below:

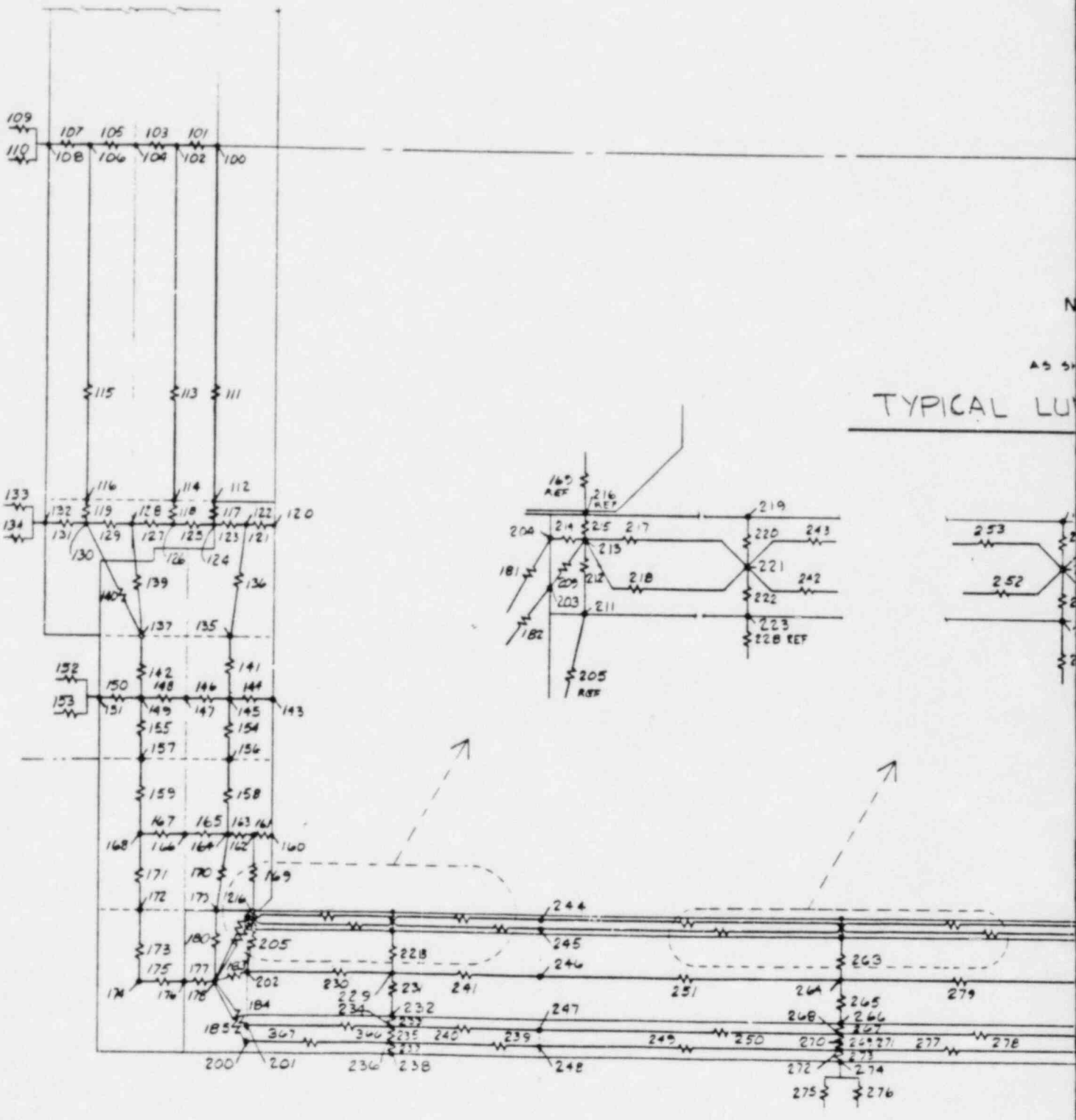

Figure 3.4.

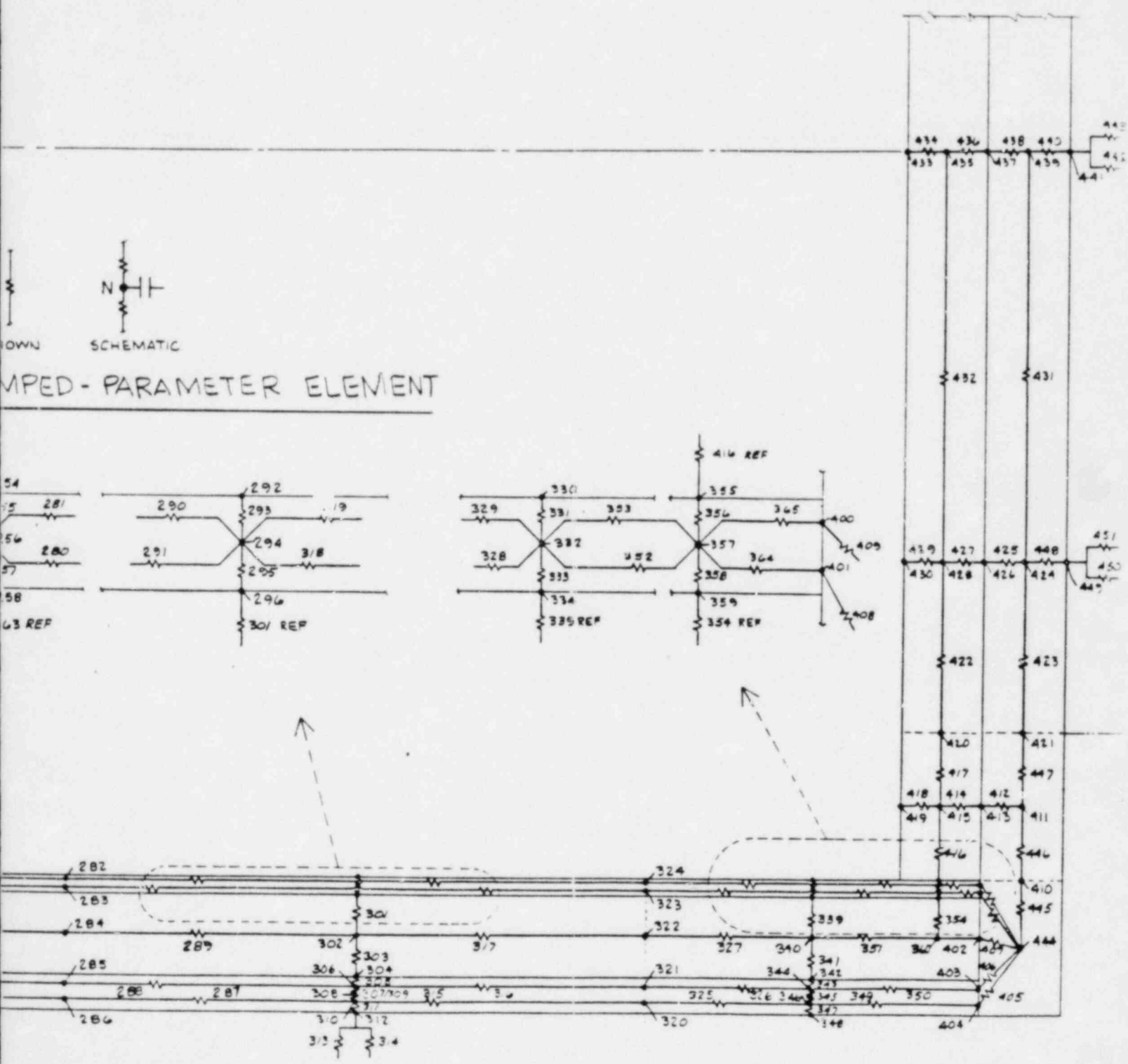
N
SCHEMATIC
MPED - PARAMETER ELEMENT
ETWORK SCHEMATIC

3.4.2 Maximum Temperatures (continued)

Outside Air Temperature	Inner Cavity	Lead Shield	Primary O-rings	Secondary Lid Seals	Outside Surface
100°F	151	138	138	141	151
130°F	177	164	165	168	177

3.4.3 Minimum Temperatures

Since the package can be moved without a payload, the minimum temperature obtainable at any point is the minimum ambient temperature of -40°F.

3.4.4 Maximum Internal Pressures

The cask will reach a maximum internal pressure of 6.7 psig for an ambient outside air temperature of 130°F. This pressure will be the worst internal pressure the cask will experience under steady-state thermal conditions. It is a function of the minimum internal temperature. Although the package is in a steady-state condition and balanced in regard to heat flows, different temperatures will exist throughout the package interior. For a discussion of package interior temperatures and their significance to internal pressure calculations, refer to Appendix 3.6.2.

The minimum interior temperature is 159°F for steady-state conditions with a 130°F ambient outside air temperature.

To find the maximum internal pressure, assume the cask is loaded at 70°F and 14.696 psia. From the saturated water tables (ref. 8, Page 456), the partial pressure of water is 0.3631 psia. Therefore, the partial pressure of air at 70°F is:

$$P_{atmos} - P_{water} = P_{air}$$

$$14.696 - 0.3631 = 14.333 \text{ psia} = P_{air}$$

From the saturated water tables, the partial (vapor) pressure of water at 159°F is 4.638 psia.

3.4.4 Maximum Internal Pressures (continued)

The partial pressure of air at 159°F may be found from the perfect gas law:

$$\frac{P_1}{T_1} = \frac{P_2}{T_2}$$

In this case, T_1 = 70°F, P_1 = 14.333 psia, T_2 = 159°F. However, the perfect gas relation requires all temperatures to be absolute temperatures.

$$\frac{14.333}{530} = \frac{P_2}{619}$$

P_1 = 14.333 psia
T_1 = 70°F = 530°R
T_2 = 159°F = 609°R

P_2 = 16.739 psia = partial pressure of air at 159°F.

The absolute pressure will be the sum of the partial pressures:

$$P_{absolute} = P_{water} + P_{air} = 4.638 + 16.739$$
$$= 21.378 \text{ psia. } (6.68 \text{ psig})$$

3.4.5 Maximum Thermal Stresses.

A comprehensive evaluation of package stresses for the 130°F ambient temperature condition is presented in Section 2.6.1. The analysis used a finite element model, described in Section 2.10.2.3, to assess stresses in the package. The results of that analysis are shown in Table 3.4.5.

3.4.6 Evaluation of Package Performance for Normal Conditions of Transport

The thermal behavior of the package is completely consistent with the allowables for all materials of construction. In addition, the maximum predicted temperature of the payload cavity, 177°F, is below the established service limit for silicone seals.

ELEMENT TYPE	STRESS TYPE (σ allow) (psi)		BASE PLATES		CASK BODY							PRIMARY LID		SECONDARY LID	
			INNER	OUTER	LOWER INNER	LOWER OUTER	MID INNER	MID OUTER	UPPER INNER	UPPER OUTER	BOLT RING	INNER	OUTER	INNER	OUTER
SHELL ELEMENT . STIF61	MEMBRANE 23100	ELEMENT			51	62	95	118	159	126					
		VALUE (psi)			4369	6427	4360	6166	4407	6054					
	MEMBRANE + BENDING 34650	ELEMENT			51	50	119	118	159	158					
		VALUE (psi)			6777	12034	4619	6315	16362	9844					
SOLID ELEMENT . STIF25	MEMBRANE 23100	ELEMENT	3-4	39-40							167-172	237	187	247	250
		VALUE (psi)	1554	7489							5310	590	1196	219	644
	MEMBRANE + BENDING 34650	ELEMENT	4	34							169	204	191	276	242
		VALUE (psi)	2787	9289							3424	1096	1214	479	1126

LOADING: 130° F Ambient + Pressure + 100 W Payload

Maximum Stress Intensities in Cask Regions

Table 3.4.5

3.5 Hypothetical Accident Thermal Evaluation

3.5.1 Thermal Model

For purposes of analyzing the package performance during the hypothetical thermal accident, a transient thermal analysis was conducted. This utilized the same thermal network model that was used for the steady state analysis; geometric segments, thermal resistances, and thermal capacitances were identical. Listed below are other conditions and assumptions which were included in this analysis:

- All conditions and assumptions named in Section 3.4, items 1 through 6.

- The hypothetical fire was modelled as a black body pure radiation source, at 1425°F. 10 CFR Part 71, Appendix B, states that modelling shall be that of a "standard" fire, in which, "the heat input to the package is not less than that which would result from exposure of the whole package to a radiation environment of 1475°F for 30 minutes with an emissivity coefficient of 0.9, assuming the surfaces of the package have an absorption coefficient of 0.8". Thus the exterior surface of the package, not covered by overpacks, can be assumed to possess an emissivity and absorptivity of 0.8. The emissive power of the hypothetical accident source is assumed equivalent to a grey body with an emissivity of 0.9 at a temperature of 1475°F. This is equivalent to a black body source with a temperature of 1424.71°F.

$$T_o = [\, E_o \, (T_o)^4 \,]^{1/4}$$

$$T_o = [(0.9)(1475 + 459)^4]^{1/4} - 459$$

$$T_o = 1424.71°F$$

3.5.1 Thermal Model (continued)

As part of the initial starting conditions, the package is brought to thermal steady state; the outside air temperature is 100°F, and the package may dissipate heat to the environment through both radiation and convection. At this point, the hypothetical thermal accident conditions are imposed on the package. This involves removing the convective dissipation and then applying the 1425°F radiation load to the exposed external surface of the package. The duration of this load is 1/2 hour. Following this, the convective dissipation is reapplied and the package is allowed to dissipate heat to the environment by both convection and radiation.

The analysis evaluated temperatures throughout the package, once every fifteen minutes, for a total period of 10.0 hours. Plots of temperature vs. time are shown in Figures 3.5.1-1 through 3.5.1-11.

It should be noted that initial temperatures within the package, for the transient analysis, are approximately 30°F higher than outside air temperatures. This is the result of assuming initial conditions to be those associated with a 100°F ambient atmosphere.

3.5.1.1 Analytical Model As previously stated, the package was thermally modelled by dividing it into specific geometric segments. Within each segment, nodes (thermal capacitances) and conductances (thermal resistances) were created to model thermal characteristics in both longitudinal and radial directions. These, in turn, were connected segment to segment. This reflected the way heat flows throughout the package. A graphical representation of the thermal network may be found as Figure 3.4.1-1.

3.5.2 Package Conditions and Environment

Free drop and puncture test damage do not measurably alter the thermal behavior of the package. Specifically, free drop damage only affects the geometry of the overpack. Since the net effect of the overpack is to enforce near adiabatic thermal boundary conditions on the package ends, any change to the thermal characteristics of the overpack is of modest second order proportions.

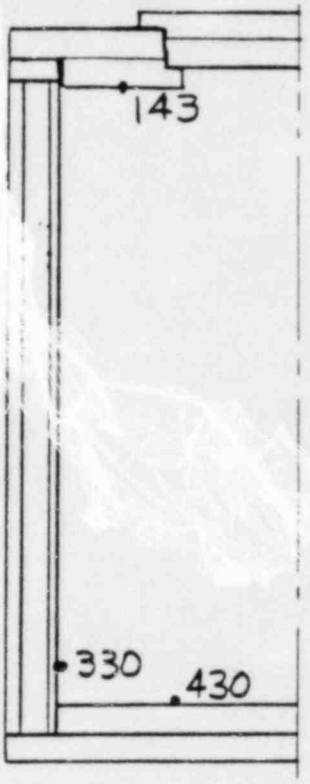
143
330
430

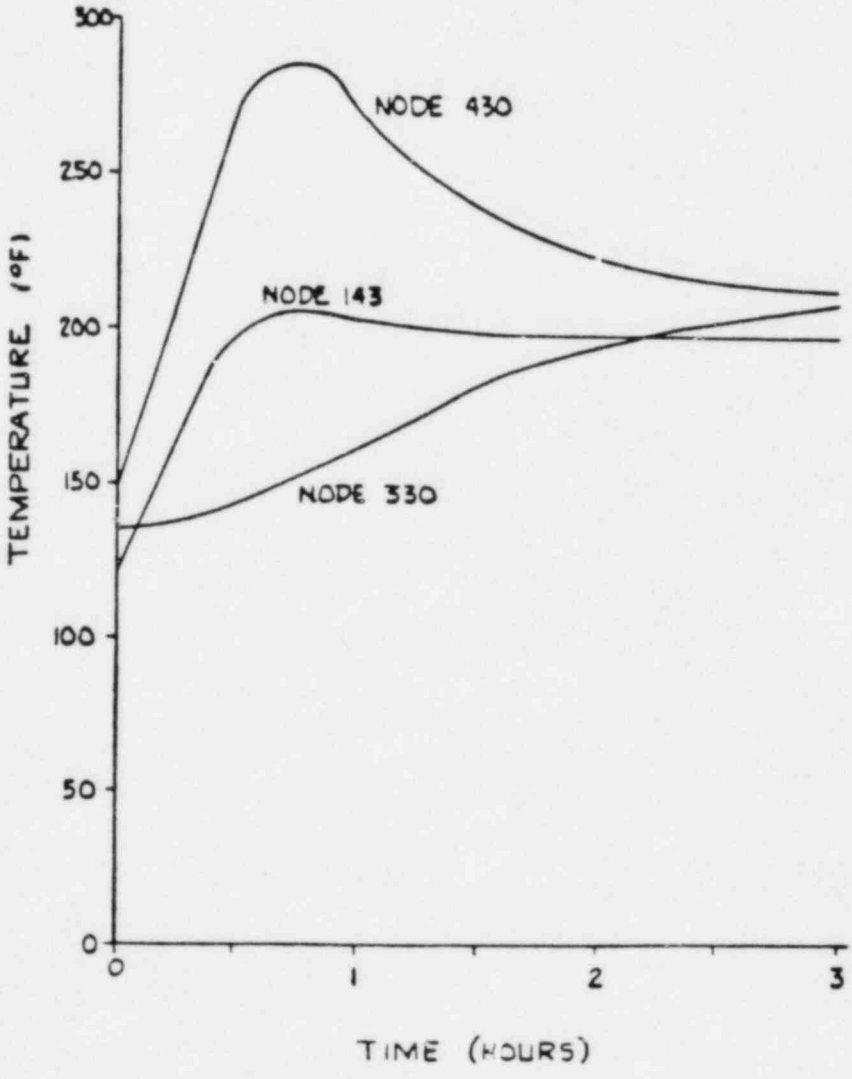
NODE 143, 330, 430
300
250
200
150
100
50
0
TEMPERATURE (°F)
NODE 430
NODE 143
NODE 330
0
1
2
3
TIME (HOURS)

Figure 3.5.1-1

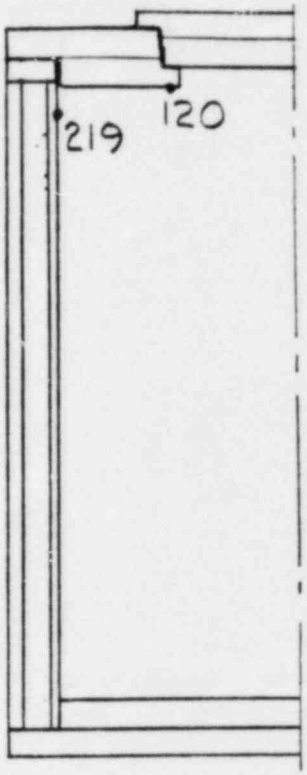
219
120

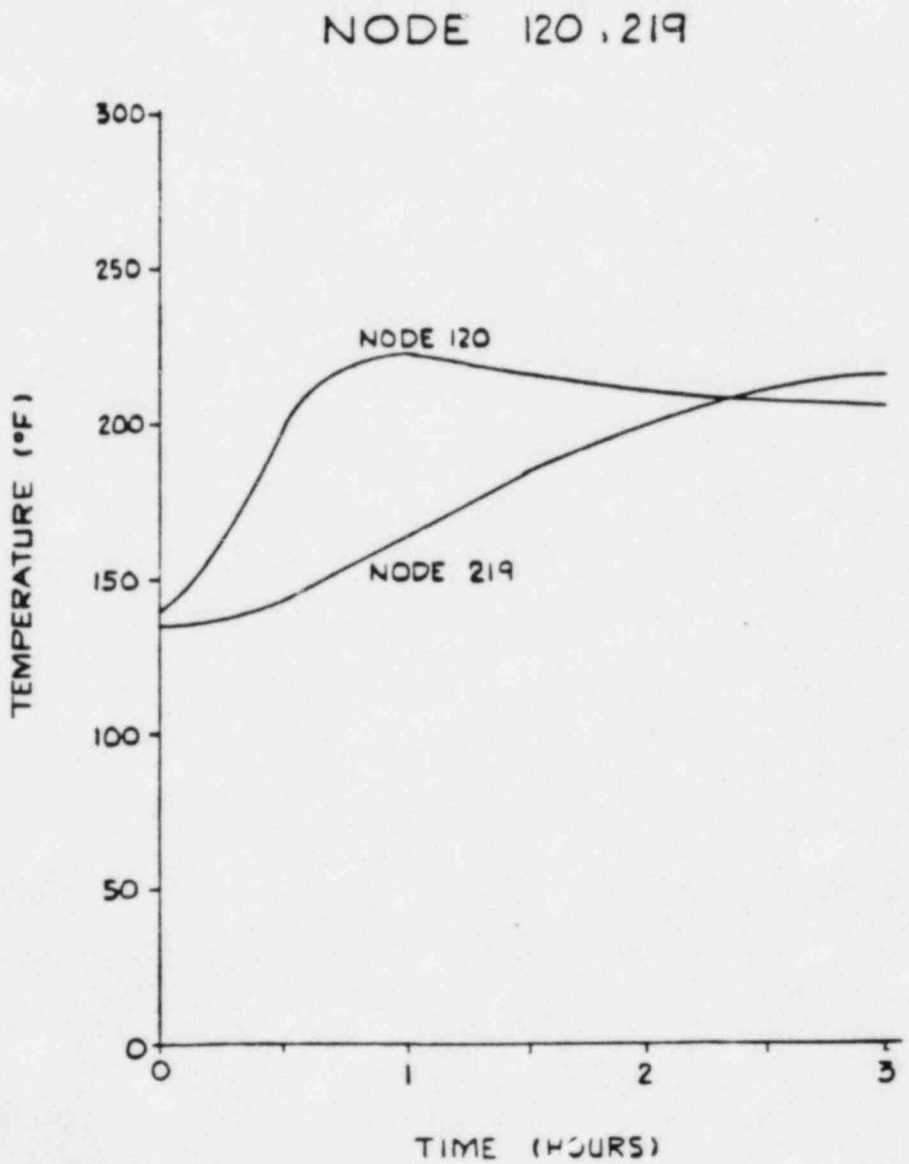
NODE 120, 219
300
250
200
150
100
50
0
TEMPERATURE (°F)
NODE 120
NODE 219
0
1
2
3
TIME (HOURS)

Figure 3.5.1-2

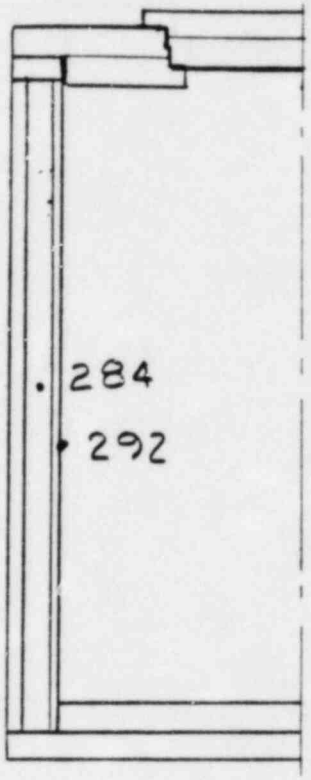
284
292

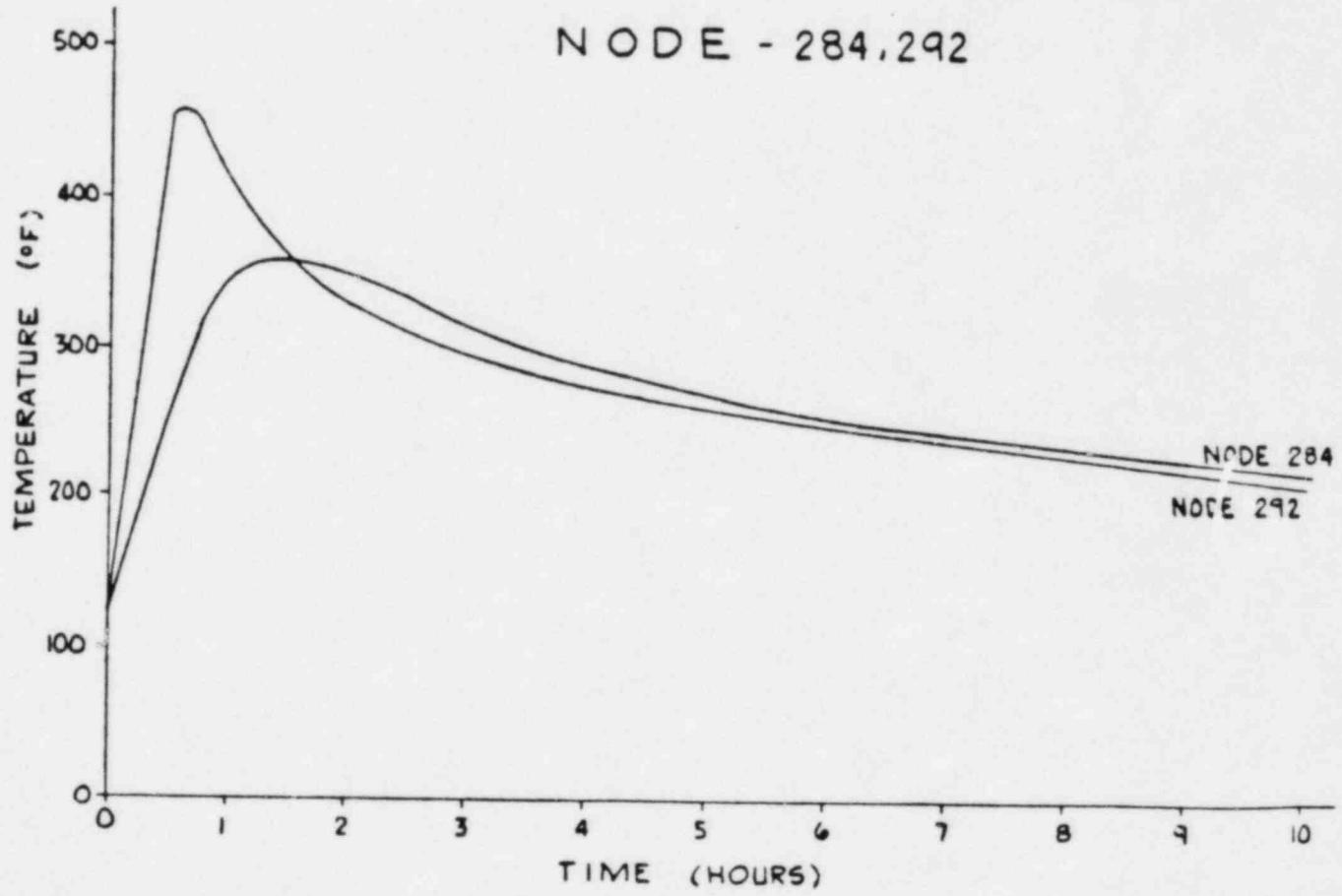
NODE - 284,292
TEMPERATURE (°F)
500
400
300
200
100
0
0
1
2
3
4
5
6
7
8
9
10
TIME (HOURS)
NODE 284
NODE 292

Figure 3.5.1-3

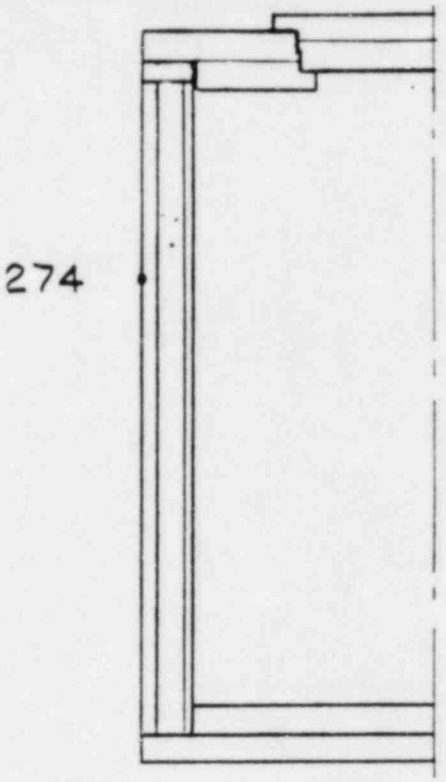
274

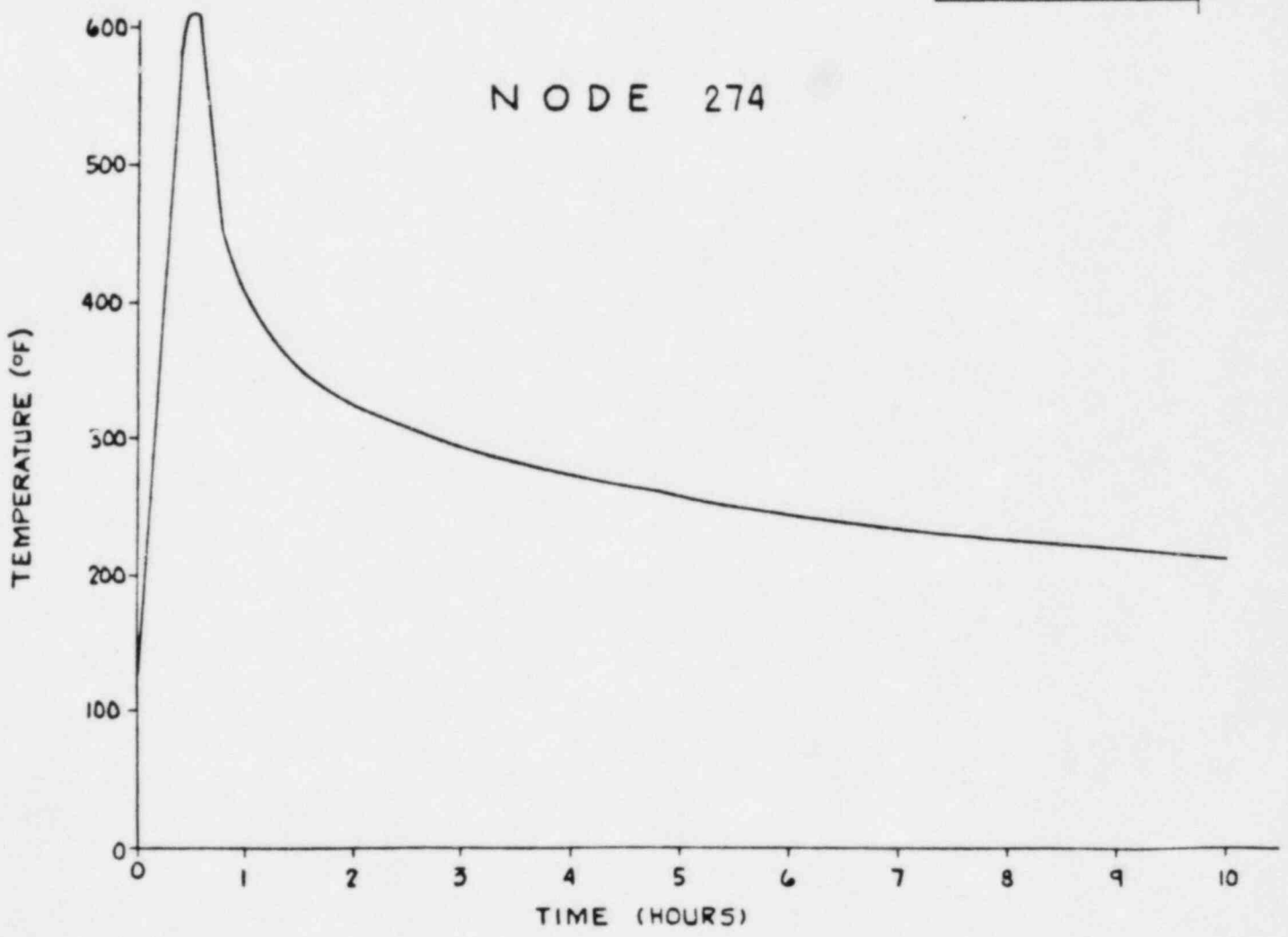
NODE 274
TEMPERATURE (°F)
600
500
400
300
200
100
0
0
1
2
3
4
5
6
7
8
9
10
TIME (HOURS)

Figure 3.5.1-4

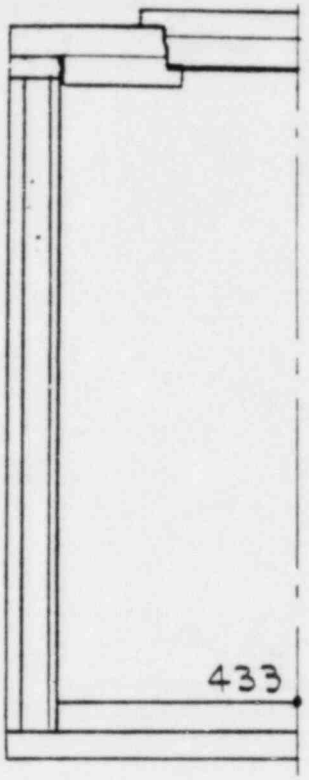
433

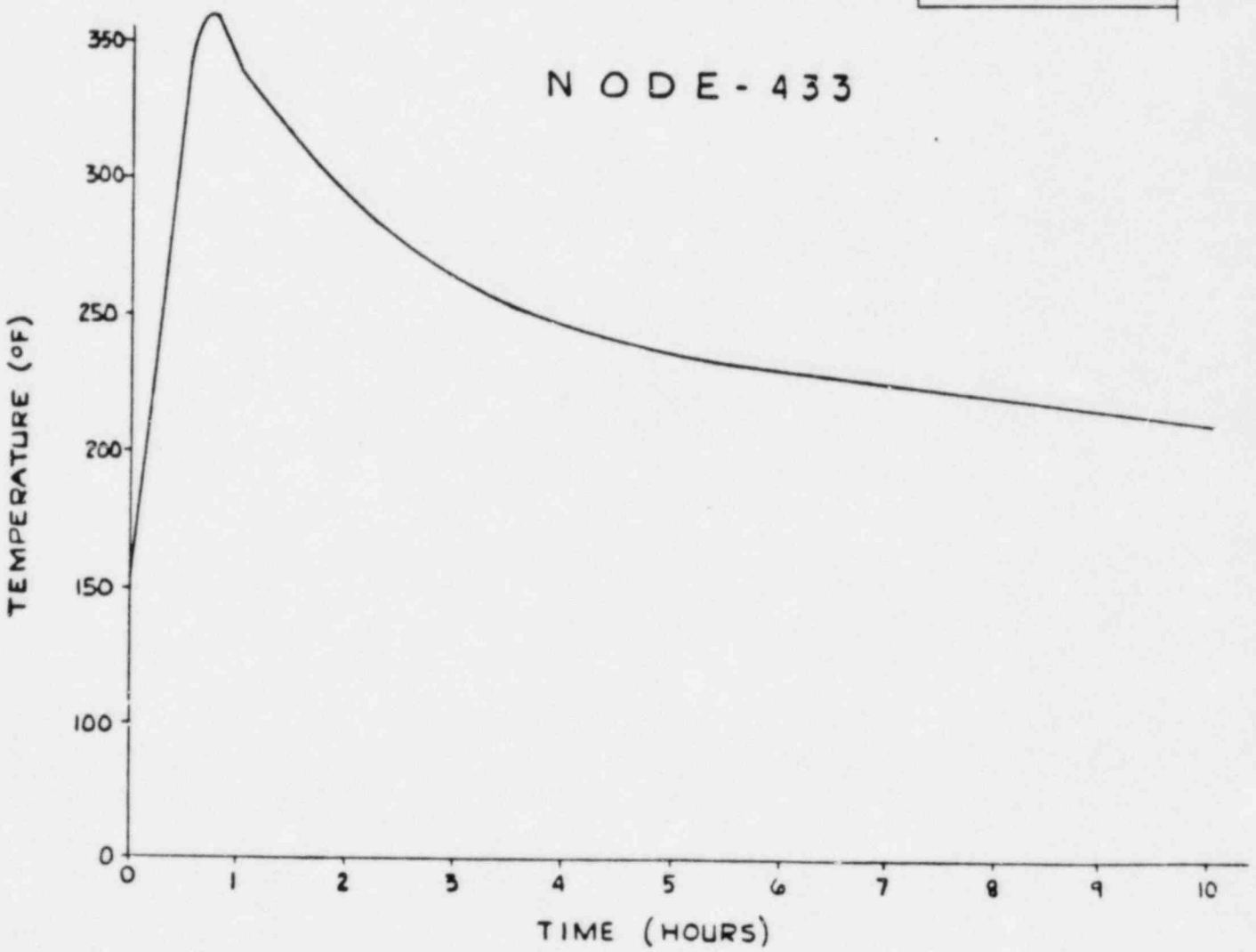
NODE-433
TEMPERATURE (°F)
350
300
250
200
150
100
0
0
1
2
3
4
5
6
7
8
9
10
TIME (HOURS)

Figure 3.5.1-5

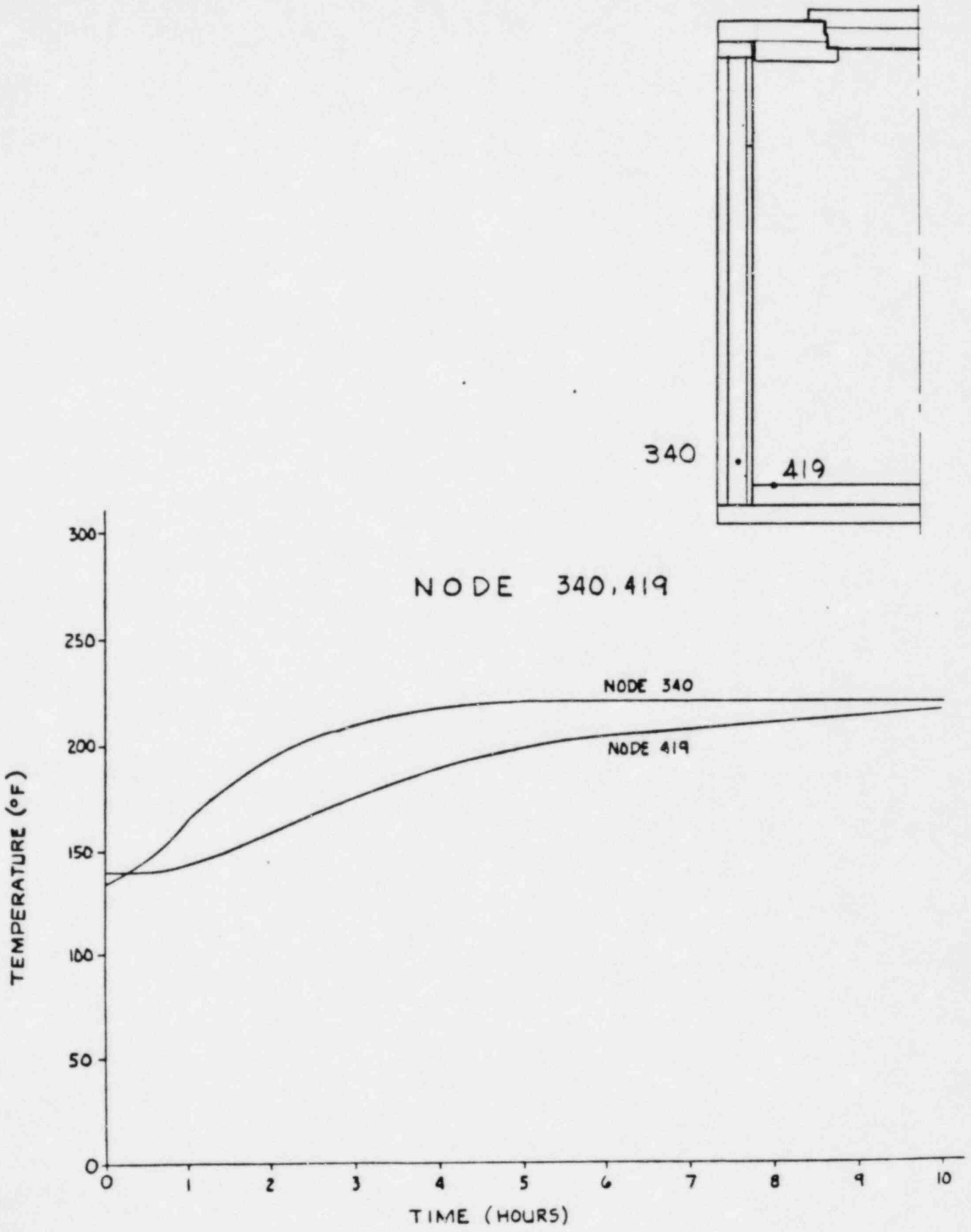
340
419
NODE 340,419
300
250
200
150
100
50
0
NODE 340
NODE 419
TEMPERATURE (°F)
0
1
2
3
4
5
6
7
8
9
10
TIME (HOURS)

Figure 3.5.1-6

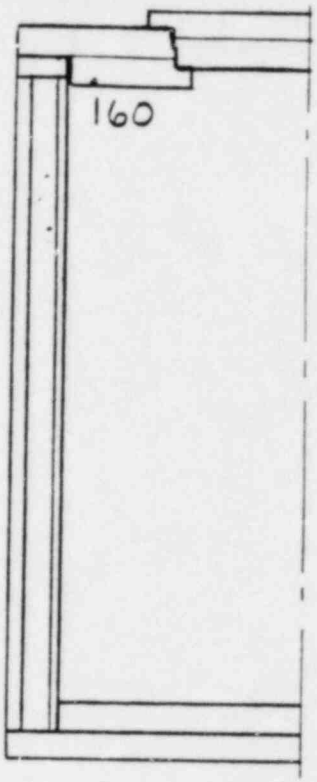
160

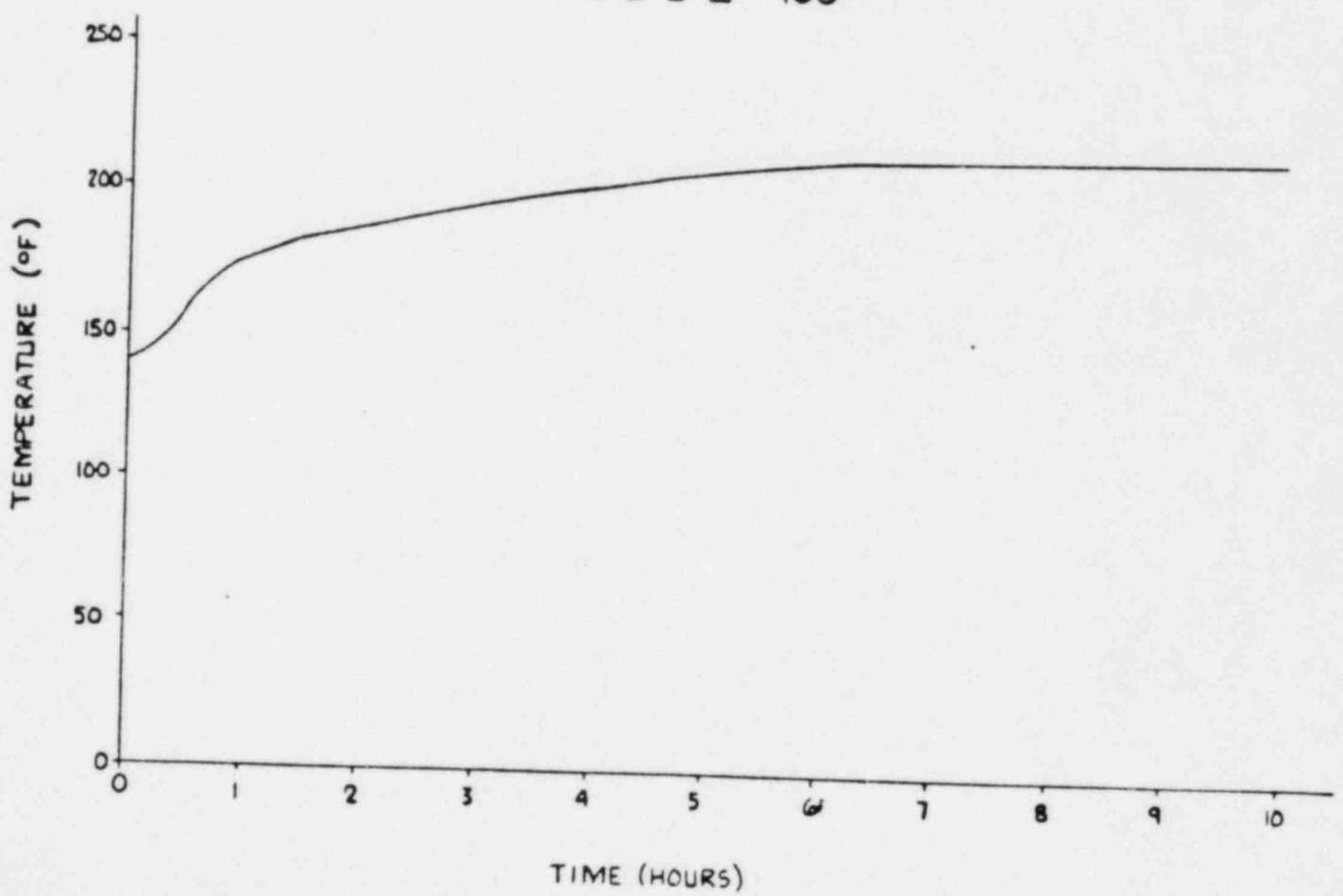
NODE 160
TEMPERATURE (°F)
250
200
150
100
50
0
0
1
2
3
4
5
6
7
8
9
10
TIME (HOURS)

Figure 3.5.1-7

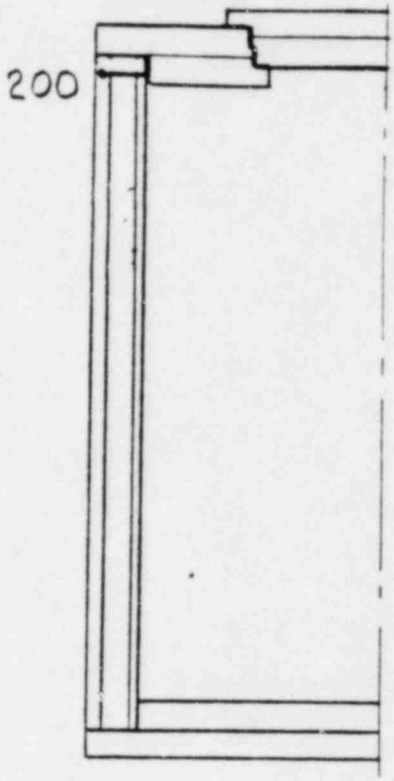
200

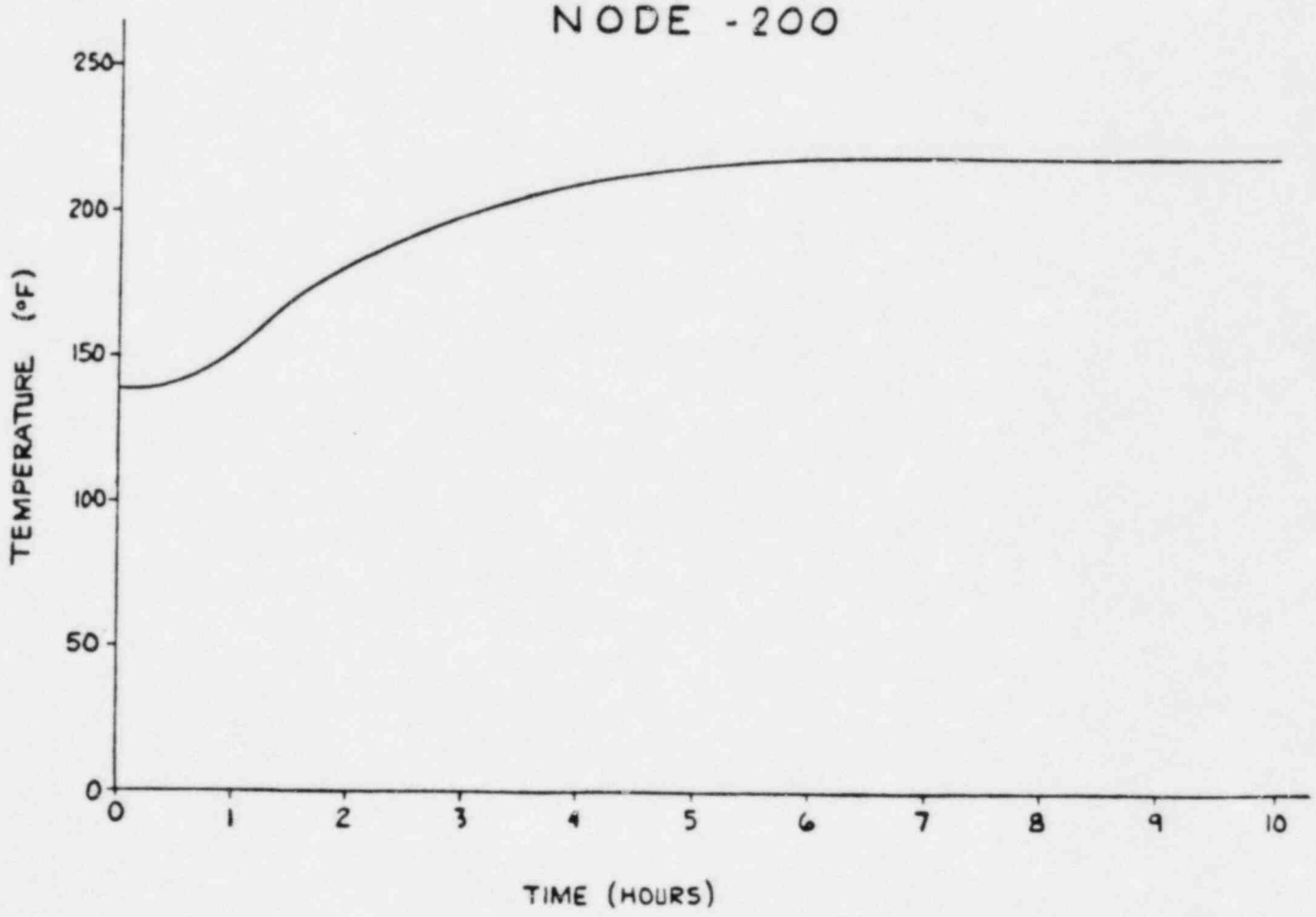
NODE -200
250
200
150
100
50
0
TEMPERATURE (°F)
0
1
2
3
4
5
6
7
8
9
10
TIME (HOURS)

Figure 3.5.1-8

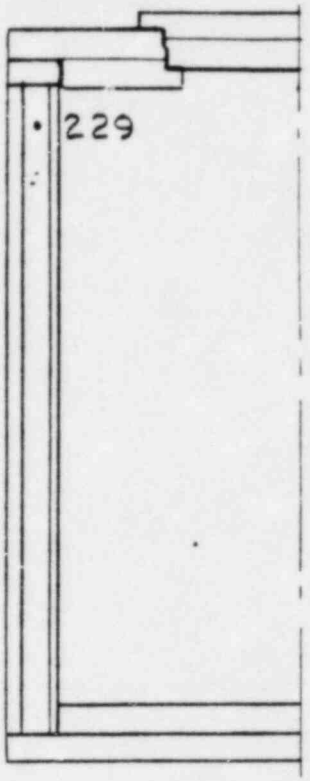
229

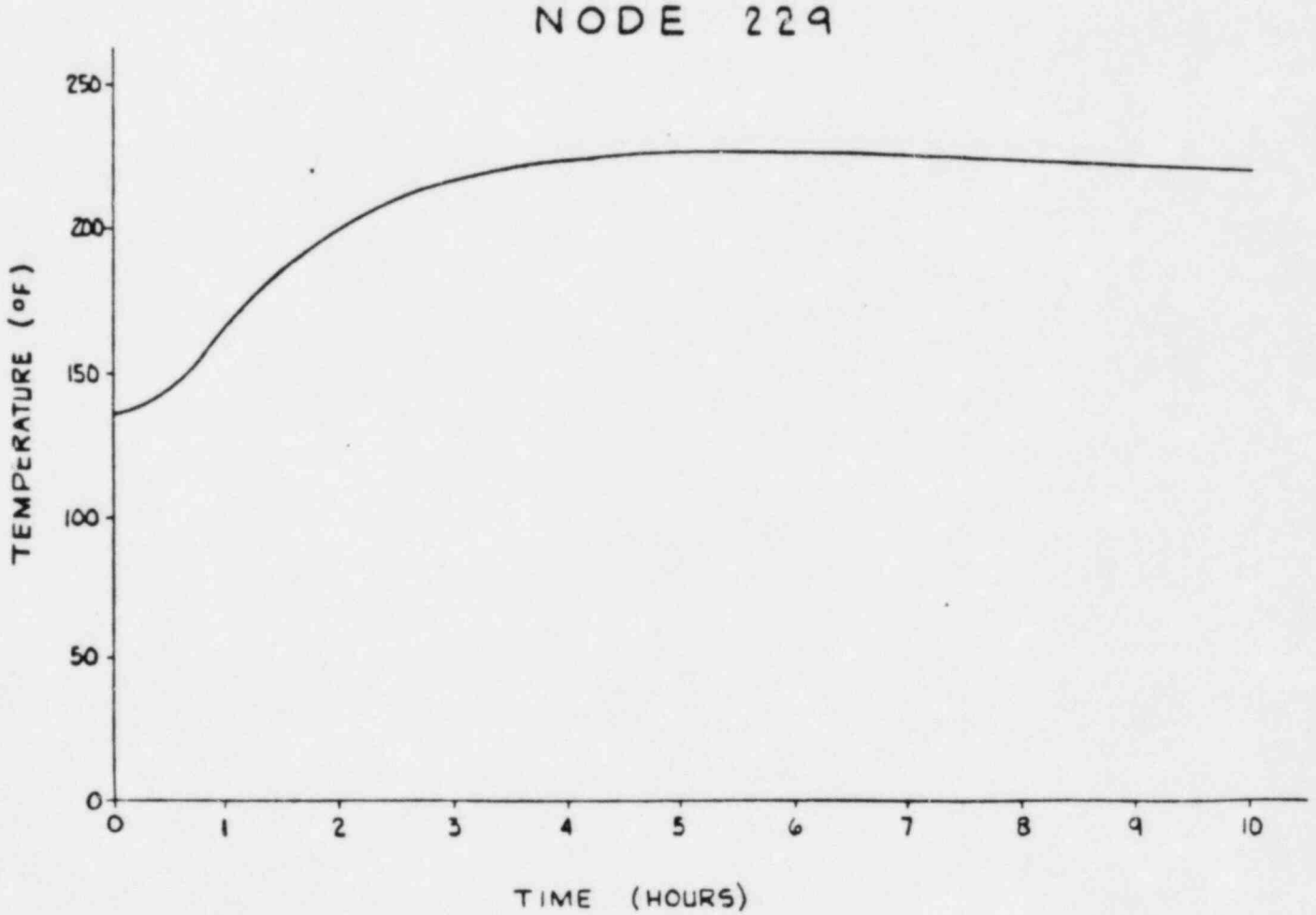
NODE 229
TEMPERATURE (°F)
250
200
150
100
50
0
0
1
2
3
4
5
6
7
8
9
10
TIME (HOURS)

Figure 3.5.1-9

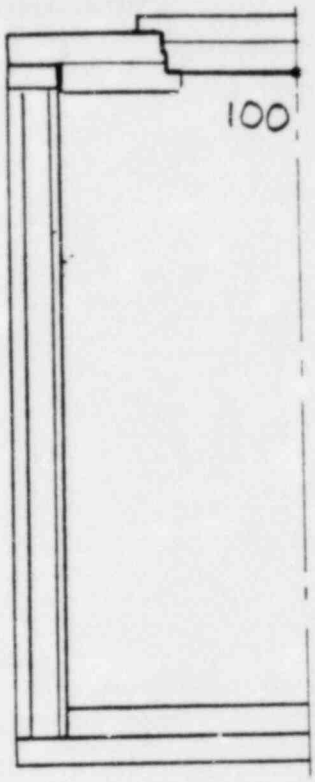

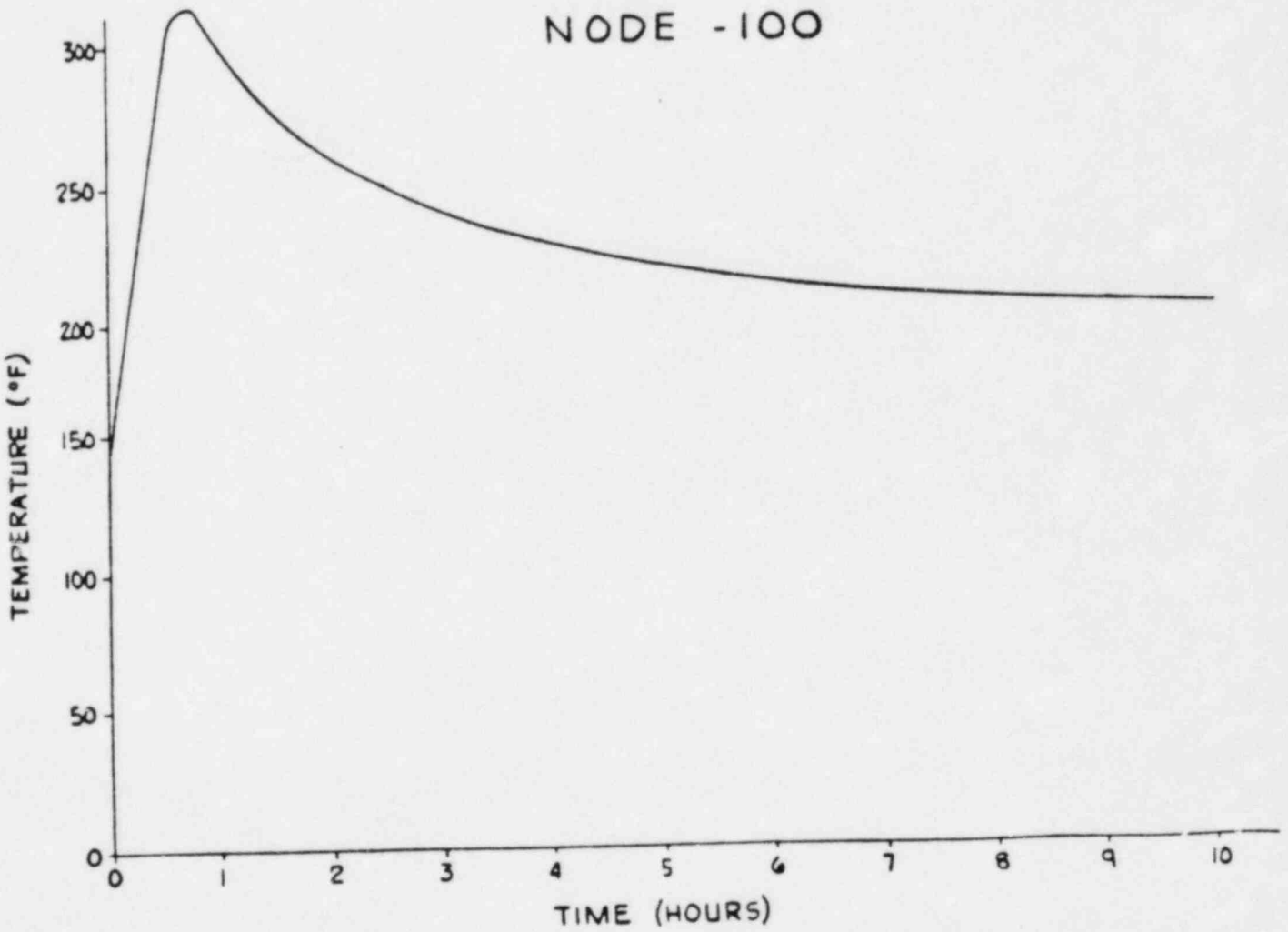

Figure 3.5.1-10

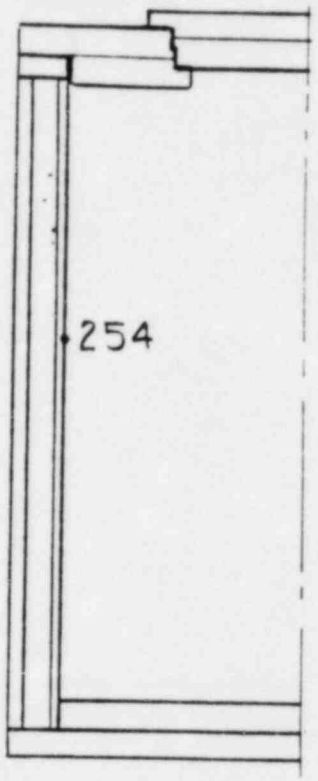

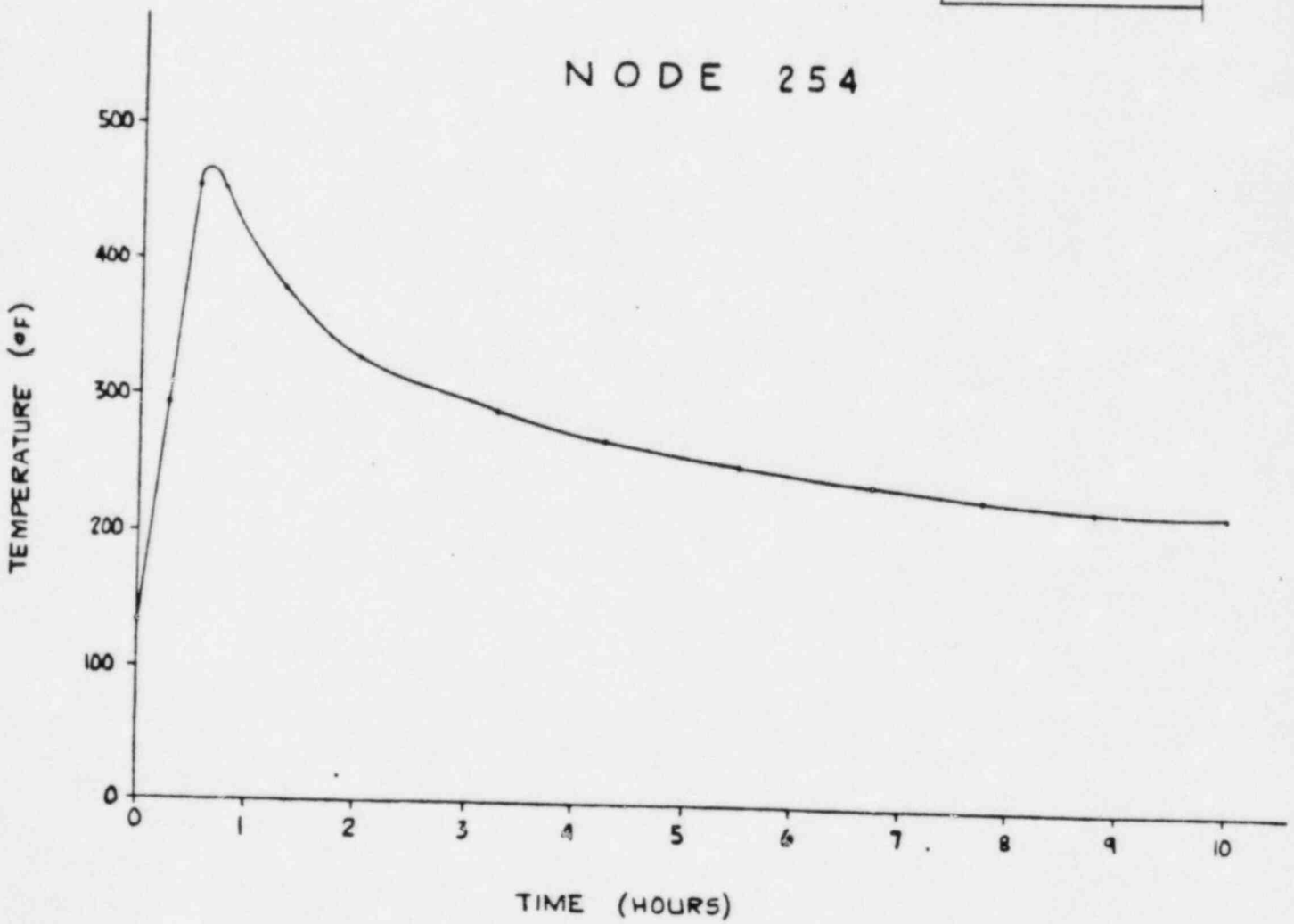

Figure 3.5.1-11

3.5.3 Package Temperatures

Results of the transient thermal analysis are as follows:

Temperatures
Ambient Air Temperature = 100°F

Time	Lowest Temp. within cavity	Highest Temp. within cavity	Lead mid-point	Primary O-Ring	Secondary Lid seal
at T=1/2 hr	139	342	184	142	209
at T=3/4 hr	141	360	213	149	225
at T = 10 hr	215	215	219	214	205

Temperature vs. time plots for selected locations within the cask may be found as Figures 3.5.1-1 through 3.5.1-11.

3.5.4 Maximum Internal Pressures

The cask will reach a maximum internal pressure of 19.2 psig as a result of the hypothetical thermal accident.

The maximum pressure experienced by the cask will be a function of the maximum value of the minimum interior temperature. This temperature, 215°F, is reached 10.0 hours after the beginning of the hypothetical thermal accident. For a discussion of the significance of this temperature in determining internal pressures, please refer to Appendix 3.6.2.

3.5.4 Maximum Internal Pressures (continued)

To find the maximum internal pressure, assume the cask is initially loaded at 70°F, and 14.696 psia. From the saturated water tables (ref.8, page 456), the partial pressure of water at 70°F is 0.3631 psia. Therefore, the partial pressure of air at 70°F is:

$$P_{atmosphere} - P_{water} = P_{air}$$

$$14.696 - 0.3631 = 14.333 \text{ psia} = P_{air}$$

From the saturated water tables, the partial (vapor) pressure of water, at 215°F, is 15.655 psia. The partial pressure of air at 215°F may be found from the perfect gas law:

$$\frac{P_1}{T_1} = \frac{P_2}{T_2}$$

In this case, $T_1 = 70°F$, $P_1 = 14.333$ psia, $T_2 = 215°F$. However the perfect gas relation requires all temperatures to be absolute temperatures.

$$\frac{14.333}{530} = \frac{P_2}{675}$$

$P_1 = 14.333$ psia
$T_1 = 70°F = 530°R$
$T_2 = 215°F = 675°R$

$P_2 = 18.254$ psia = partial pressure of air, at 215°F.

The absolute pressure will be the sum of the partial pressures:

$$P_{absolute} = P_{water} + P_{air} = 15.655 + 18.254 = 33.9 \text{ psia}$$

33.9 psia - 14.69 = 19.21 psig.

3.5.5 Maximum Thermal Stresses

A comprehensive evaluation of package stresses during the fire accident conditions is presented in Section 2.7.3. The analysis used an axisymmetric finite element model, described in Section 2.10.1.3, to assess stresses due to the thermal and pressure loads on the package. The results of that analysis are shown in Table 3.5.5

3.5.6 Evaluation of Package Performance for the Hypothetical Accident Thermal Conditions

The thermal behavior of the package is completely consistent with the allowables for all materials of construction. In particular, the maximum predicted temperature of the payload cavity, 360°F, is well below the established service limit of 500°F for silicone seals.

3.6 Appendix

3.6.1 List of References

(1) ASME Boiler and Pressure Vessel Code, Section III, 1980

(2) Holman, J.P. Heat Transfer, McGraw-Hill, 1977

(3) Rohsenow and Hartnett, Handbook of Heat Transfer, McGraw-Hill, 1973

(4) Shappert, L.D. "Cask Designer's Handbook", ORNL NSIC-66, Oak Ridge National Laboratory, 1970

(5) MITAS-II User's Manual, CDC Cybernet Services, Control Data Corp.

(6) Packaging of Radioactive Materials for Transport and Transportation of Radioactive Materials Under Certain Conditions, Code of Federal Regulations, Title 10, Part 71, January 1, 1981

(7) Mark's Standard Handbook for Mechanical Engineers, 8th Edition, McGraw-Hill, 1978

(8) Reynolds, William C., Thermodynamics, Second Edition, McGraw-Hill, 1968.

Element Type	Stess Type (σ allow) (psi)		Base Plates		Cask Body							Primary Lid		Secondary Lid	
			Inner	Outer	Lower Inner	Lower Outer	Mid Inner	Mid Outer	Upper Inner	Upper Outer	Bolt Ring	Inner	Outer	Inner	Outer
Shell Element . STIF61	Membrane (49000)	Element			59	46	91	122	159	126					
		Value (psi)			24121	16736	29374	12394	24185	13666					
	Membrane + Bending (70000)	Element			59	66	91	122	159	126					
		Value (psi)			31306	22476	30180	19269	47385	22218					
Solid Element . STIF25	Membrane (49000)	Element	27-28	33-34							167-172	244-245	181	277	250
		Value (psi)	26295	29632							26000	10543	15423	15796	11366
	Membrane + Bending (70000)	Element	23	25							167	236	191	270	242
		Value (psi)	22025	41455							20066	12549	20939	10008	20758

LOADING: Thermal Accident: ½ hour after start of fire
Includes 100W payload & internal pressure
Maximum stress intensities in cask regions

Table 3.5.5

3.6.2 Significance of Minimum Temperatures in Calculation of Cask Internal Pressures

The maximum pressure developed within the package will be directly related to the minimum interior temperature at any given time. The behavior of residual moisture within the cask cavity can be characterized by evaporation from the hotter surfaces and condensation on the coolest surfaces. These two conflicting requirements will reach a state of equilibrium pressure equal to the saturated vapor pressure associated with the condensation temperature, which will be the minimum internal temperature of the cask.

If the cask is in a steady-state thermal condition, the temperature will be time-invariant for a given location (although temperatures will be different at different locations). In this case, there will be one minimum temperature within the cask, and this will be the significant parameter in determining internal cask pressure for the steady-state thermal condition.

If the cask is in a transient thermal state, as it is when it has undergone the hypothetical thermal accident, it will be necessary to find the maximum value of the minimum interior temperature. When a large thermal loading is imposed upon this cask (as in the case of the hypothetical thermal accident) it will heat up unevenly, with some locations heating faster then others. This is due to the fact that the thermal loading is applied through a partial area of the cask (the outside surface area not covered by overpacks), and because some regions of the cask have more thermal capacitance than others. Consequently, the minimum interior temperature will vary over time. Since the internal pressure is directly related to the minimum temperature, the maximum value of this minimum interior temperature must be found in order to find the maximum cask pressure.

4.0 CONTAINMENT

This chapter describes the containment configuration of the Model CNS8-120B Package for normal transport and hypothetical accident conditions.

4.1 Containment Boundary

4.1.1 Containment Vessel

The package containment vessel is defined as the inner shell of the shielded transport cask, together with the associated lid o-ring seals, and lid closure bolts. The inner shell of the cask, or containment vessel, consists of a right circular cylinder of 62 inches inner diameter and 75 inches inside height. The shell is fabricated of 3/4 inch thick carbon steel plate, ASTM A516-70. At the base, the cylindrical shell is attached to a primary circular end plate with full penetration welds. The primary lid is attached to the cask body with thirty-two (32) equally spaced 2-8 UN bolts. A secondary lid covers a 29 inch opening in the primary lid and is attached to the primary lid using twelve (12) equally spaced 2-8 UN bolts. See Section 4.1.4 for closure details.

4.1.2 Containment Penetration

There are four penetrations of the containment vessel. These are (1) an optional drain line; (2) a primary lid seal test port; (3) a secondary lid seal test port, and (4) a cask vent port located in the primary lid. Located at the cask base, the drain line consist of a 2 inch diameter steel rod, drilled to 0.75 inches diameter, penetrating into the second 3 1/2 inch layer of steel that forms the cask bottom. A 0.63 inch diameter hole, drilled at a right angle, opens on the side of the outer shell near the cask bottom. The two seal test ports penetrate to the space between the double seals on both the primary and secondary lids. A vent port penetrates the primary lid into the main cask cavity. All four penetrations are sealed with silicone Parker Stat-O-Seals or equivalent.

4.1.3 Welds and Seals

The containment vessel is fabricated using full penetration groove welds. All weld configurations are designed and fabricated to the intent of Section III of the ASME Boiler and Pressure Vessel Code. Seals are described in Sections 4.1.2 and 4.1.4.

4.1.4 Closure

The top (primary lid) closure consists of two 3 1/2 inch thick laminated plates, stepped to fit over and within the top edge of the cylindrical body. The lid is supported at the perimeter of the cylindrical body by 2 1/2 inch plate welded to the top of the inner and outer cylindrical body walls. This plate confines two (2) solid, high temperature silicone O-rings in machined grooves. Groove dimensions prevent overcompression of the O-rings by the closure bolt preload forces and hypothetical accident impact forces. The lid is attached to the cask body by thirty-two (32) equally spaced 2-8 UN bolts. These bolts are torqued to 500 ft-lbs. $\pm$ 10 percent (lubricated). The cask is fitted with a secondary lid of similar construction attached to the primary lid with twelve (12) equally space 2-8 UN bolts, fabricated of SAE Grade 8 material. The secondary lid is sealed wth two (2) solid, high temperature silicon O-rings in machined grooves.

The vent, test ports, and drain penetrations are sealed with Parker Stat-O-Seals which are used beneath the heads of the hex head cap screws at all locations. Table 4.1.4 gives the torque values for the cap screws.

TABLE 4.1.4 Bolt and Cap Screw Torque Requirements

LOCATIONS	SIZE	TORQUE VALUES ± 10 (Lubricated)	
		in-lbs	ft-lbs
Test Ports (2)	3/8 in.	144	12
Vent	1/2 in.	240	20
Drain	3/4 in.	960	80
Primary Lid	2-8 UN	---	500
Secondary Lid	2-8 UN	---	500

4.2 Containment Requirements For Normal Conditions Of Transport

4.2.1 Release of Radioactive Materials

The CNS 8-120b cask is designed to assure no release of radioactive material in excess of limits prescribed in N.R.C. Regulatory Guide 7.4, "Leakage Tests on Packages for the Shipment of Radioactive Materials," under normal conditions of transport.

The CNS 8-120B package is designed to accomodate a variety of payloads with differing contents. The package is fabricated for leak tightness (1) and tested such that the package gaseous leakage does not exceed 1×10^{-7} atm.cm^3/sec, at standard conditions as defined in ANSI N14.5-1977. To demonstrate leak tightness, the sensitivity of the leakage test procedure will be 5×10^{-8} atm.cm^3/s, or better.

---

(1) Leaktight level: A leakage rate of 10^{-7} atm.cm^3/s or less, based on dry air at 25^{0}C and for a pressure differential of 1 atm against a vacuum, of 10^2 atm or less is considered to represent leak tightness. (ANSI N 14.5-1977, Section 3, 3.7).

By use of a leak tight design, compliance of the CNS 8-120B package with the requirements of N.R.C. Regulatory Guide 7.4 is assured. In accordance with the Regulatory Position, Paragraph C of this guide, compliance of the CNS 8-120B package with the requirements of Section 71.35 of 10 CFR 71, for "no release of radioactive material from the containment vessel," Paragraph 71.35(a)(1), is demonstrated.

4.2.2 Pressurization of the Containment Vessel

Section 3.4.4 summarizes normal condition temperatures and pressures within the containment vessel. These pressures and associated temperatures are used to evaluate integrity of the CNS 8-120B package. None of these conditions reduce the effectiveness of the package containment.

4.2.3 Coolant Containment

Not applicable; there are no coolants in the CNS 8-120B package.

4.2.4 Coolant Loss

Not applicable; there are no coolants in the CNS 8-120B package.

4.3 Containment Requirements For The Hypothetical Accident Conditions

The following is an assessment of the packaging containment under the hypothetical accident conditions as a result of the analysis performed in Chapters 2.0 and 3.0. In summary, the containment vessel was not affected by these tests (see section 2.7).

4.3.1 Fission Gas Products

There are no fission gas product present.

4.3.2 Release of Radioactive Materials

The CNS 8-120B package is designed to assure no release of radioactive material in excess of limits prescribed in N.R.C. Regulatory Guide 7.4, "Leakage Tests on Packages for the Shipment of Radioactive Materials," under hypothetical accident conditions.

The CNS8-120B package is designed to accomodate a variety of payloads with differing contents. Provided the package is fabricated and tested to a leak-tight level (1) compliance of the CNS 8-120B package with the requirements of N.R.C Regulatory Guide 7.4 is assured. In accordance with the Regulatory Position, Paragraph C of this guide, compliance of the CNS8-120B package with the requirements of Section 71.36 (a)(2) of 10 CFR 71, for "no release of radioactive material from the containment vessel....exceeding specified limits" is demonstrated.

(1) Leak tight: A leakage rate of 10^{-7} atm.cm^3/s or less, based on dry air at 25^{o}c and for a pressure differential of 1 atm against a vacuum of 10^{-2} atm or less is considered to represent leaktightness. (ANSI N 14.5-1977, Section 3, 3.7).

5.0 SHIELDING EVALUATION

5.1 Discussion and Results

5.1.1 Operating Design

The CNS 8-120b will be operated such that the contents in the cask will not create a dose rate exceeding 200 mrem./hr. on the cask surface, or 10 mrem./hr. at six feet from the cask surface.

The package shielding must be sufficient to satisfy the condition of 10 CFR Part 71, paragraph 71.36(a)(1) for the hypothetical accident conditions. Any shielding loss resulting from the 30 foot drop or the fire transient will not increase the external dose rate to more than 1000 mrem./hr.at 3 feet from the external surface of the cask.

5.1.2 Shielding Design Features

The cask side wall consists of an outer 1.5 inch thick steel shell surrounding 3.5 inches of lead and an inner containment shell wall of 0.75 inch thick steel. Total material shield thickness is 2.25 inches of steel and 3.5 inches of lead.

The primary cask lid consists of two layers of 3.5 inch thick steel, giving a total material shield thickness of 7.5 inches of steel. This lid closure, is made in a stepped configuration to eliminate radiation streaming at the lid/cask body interface.

A secondary lid is located at the center of the main lid, covering a 29.0 inch opening. The secondary lid is constructed of two 3.5 inch steel plates with multiple steps machined in the secondary lid. These match steps in the primary lid, eliminating radiation streaming pathways.

5.1.3 Maximum Dose Rate Calculations

Table 5.1.3-1 gives both normal and accident condition dose rates for a typical loading of the cask. The following assumptions were used to develop the values given in the table.

Table 5.1.3-1

SUMMARY OF MAXIMUM DOSE RATES (mrem/hr)

	Package Surface			3 Feet From Surface of Package		
	Side	Top	Bottom	Side	Top	Bottom
Normal Conditions						
	(1)			(1)		
gamma	105	200	200	2.1	5.7	5.7
neutron	0	0	0	0		
total	105	200	200	2.1	5.7	5.7
Hypothetical Accident Conditions						
gamma, neutron, total	same as for normal conditions shown above					
10 CFR 71 Limit	----	----	----	1000	1000	1000

5.1.3.1 Normal Conditions

(1) The source is modeled as a point source which can exist on any interior cask surface. The source is considered to be in contact with all inner cask surfaces at the same time.

5.1.3.2 Accident Conditions

(1) Lead slump (see Section 2.7.1.1) causes no increase in dose rate.

(2) The cask shielding configuration after a 30 foot drop and other accident tests is the same as before the drop.

---

(1) The lower reading on the side vs the top or bottom comes from the assumption of a steel buildup factor for the laminated side walls. The side walls and top/bottom have the same lead equivalent value based on Co-60 energies.

5.2 Source Specification

5.2.1 Gamma Source

The equivalent point source, assuming Co^{60} energies, is determined for the normal geometry. This equivalent source is then used to evaluate the effects of the hyptohetical accidents.

The point source is determined as follows:

$$\phi_\gamma = \frac{BS_o e^{-b_1}}{4 \pi r^2}$$

where,

ϕ_γ = Photon Flux, γ/cm^2 - sec

S_o = Equivalent Source, γ/s

$b_1 = \sum_i \mu_i t_i$

B = Buildup factor

r = distance from source to dose point

5.2.2 Neutron Source

There are no sources of neutron radiation in the radioactive materials carried in the CNS 8-120B cask.

5.3 Model Specification

5.3.1 Description of Radial and Axial Shielding Configuration

Description of the radial and axial shielding material models are shown in Figure 5.3.1-1.

RADIAL MODEL:

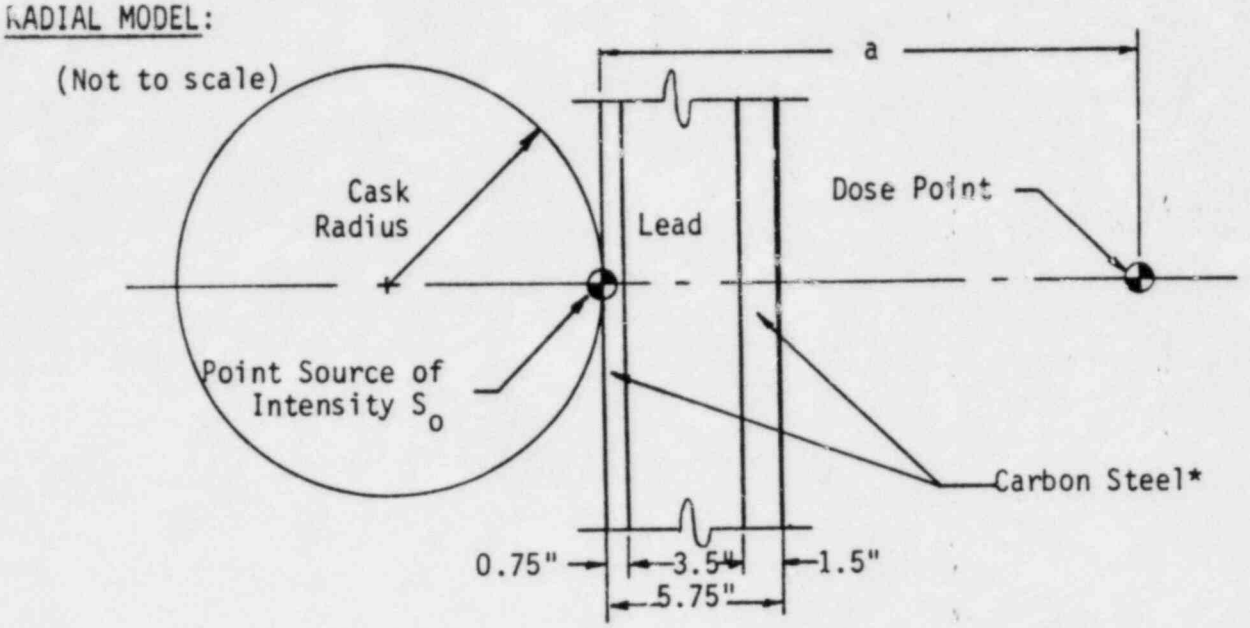

AXIAL MODEL:

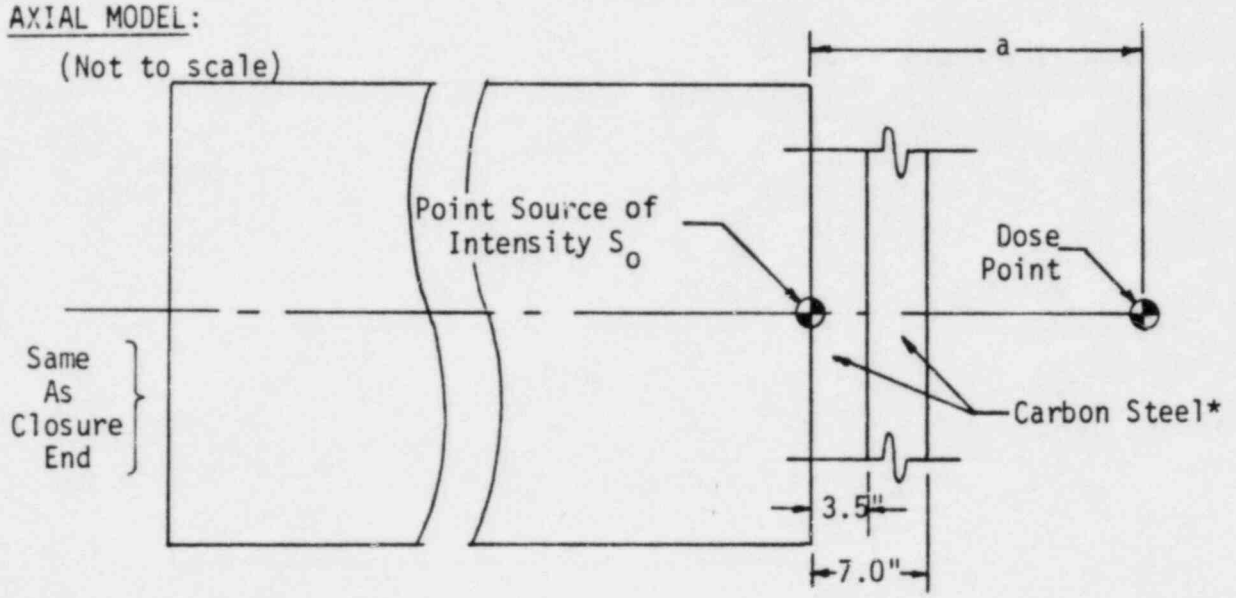

⇦ CASK BOTTOM

LID CLOSURE END ⇨

*Optional stainless steel liner not included

FIGURE 5.3.1-1 Radial and Axial Models- Shielding

5.3.2 Shield Region Densities

The mass densities for each material are shown in the table below.

TABLE 5.3.2 SHIELD REGION DENSITIES

MATERIAL	ELEMENT	DENSITY (g/cc)
Carbon Steel	Fe	7.86
Lead	Pb	11.34

5.4 Shielding Evaluation

5.4.1 Radial Model

The gamma radiation sources that correspond to regulatory dose rate limits for the cask in a radial direction were calculated assuming a point source. This gives the most conservative approach and allows for the wide variety of source geometries that could be encountered transporting irradiated non-fuel components. The dose model used for this calculation is shown in Figure 5.3.1-1.

The point source is determined as follows:

$$\phi_\gamma = KB \frac{S_o}{4\pi a^2} e^{-b_1}$$

where ϕ_γ = Photon Flux, γ/cm^2-sec

K = Flux to dose conversion = $2.4 \times 10^{-6} \frac{R/hr.}{\phi_\gamma}$ for Co-60

S_o = Equivalent source, γ/sec

$b_1 = \Sigma_i \mu_i t_i$

B = Buildup factor

a = Distance from source to dose point, cm

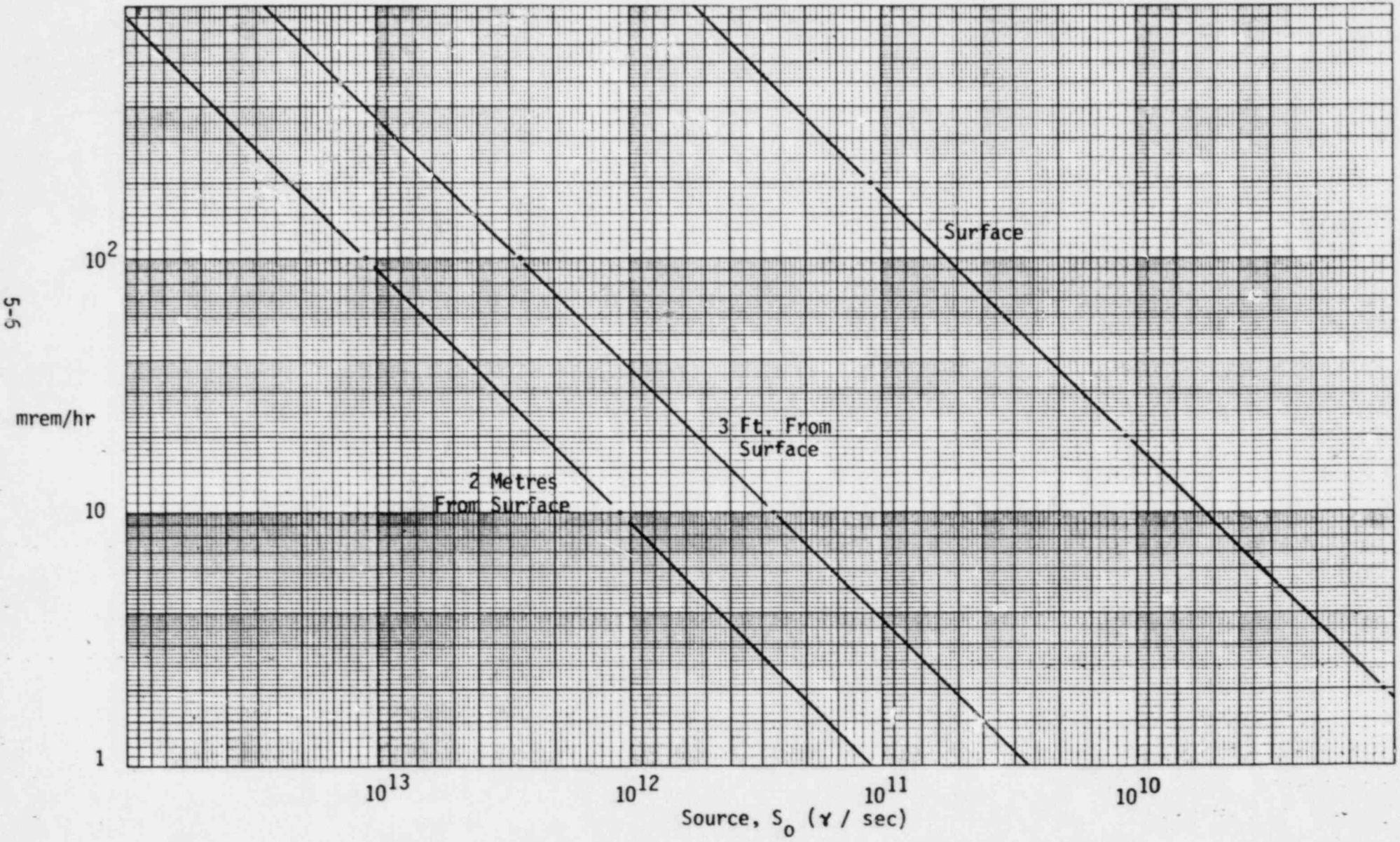

FIGURE 5.4.1-1 Dose Rate vs. Source Strength- Side of Cask

through the side of the cask, the following values are used:

Lead: $t = 3.5$ inches $= 8.9$ cm, $\mu/\rho = 0.0600 \frac{cm^2}{g}$

$\mu = 0.684\ cm^{-1}$

Steel: $t = 2.25$ inches $= 5.7$ cm, $\mu/\rho = 0.0515 \frac{cm^2}{g}$

$\mu = 0.415\ cm^{-1}$

Giving: $b_1 = 8.5$

the buildup factor is taken for iron to represent the laminated shield.

Therefore: $B = 11.5$

Two dose rates will be considered:

$D_1 = 10$ mrem/hr, where a = 15cm (5.75 inches) + 200cm = 215 cm
This gives:

$$S_o = \frac{D_1}{KBe^{-b_1}} (4\pi a^2) \qquad \text{(see 5.2.1)}$$

$$= \frac{0.01\ \text{Rem/hr}\ (4\pi)(215^2)}{(2.3 \times 10^{-6})(11.5)(2 \times 10^{-4})}$$

$$S_o = 1.1 \times 10^{12} \frac{\gamma}{sec}$$

and,

$D_2 = 200$ mrem/hr, where a = 5.75 inches = 15cm

which gives:

$$S_o = \frac{0.2\ \text{rem/hr}\ (4\pi)(15^2)}{(2.3 \times 10^{-6})(11.5)(2 \times 10^{-4})}$$

$$S_o = 1.1 \times 10^{11}\ \gamma/sec.$$

The dose rates at 3 and 6 feet from the side surfaces of the CNS 8-120b are shown in Figure 5.4.1-1 for various source strengths.

5.4.2 Axial Model

The gamma radiation sources that correspond to regulatory dose rate limits for the cask in an axial direction were calculated assuming a point source. This gives the most conservative approach and allows for the wide variety of source geometries that could be encountered transporting irradiated non-fuel components. The dose model used for this calculation is shown in Figure 5.3.1-1.

The point source is determined as follows:

$$\phi_\gamma = KB \frac{S_o}{4\pi a^2} e^{-b_1}$$

where ϕ_γ = Photon Flux, γ/cm^2-sec

K = Flux to dose conversion = $2.3 \times 10^{-6} \frac{R/hr.}{\phi_\gamma}$ for Co-60

S_o = Equivalent source, γ/sec

$b_1 = \Sigma_i \mu_i t_i$

B = Buildup factor

a = Distance from source to dose point, cm

Through the top of bottom of the cask, the following values are used:

Lead: None present

Steel: t = 7.0 inches = 17.8 cm, μ/p = 0.0600

$\mu = 0.415\ cm^{-1}$

Giving: $b_1 = 7.4$

the buildup factor, taken for steel is:

$B = 10$

Two dose rates will be considered:

D_1 = 10 mrem/hr, where a = 17.8 cm (5.75") + 200cm = 218 cm

which gives,

$$S_o = \frac{D_1}{KBe^{-b_1}}(4\pi a^2) \qquad \text{(see 5.2.1)}$$

$$= \frac{0.01 \text{ Rem/hr } (4\pi)(218^2)}{(2.3 \times .0^{-6})(10)(6.1 \times 10^{-4})}$$

$$S_o = 4.3 \times 10^{11} \frac{\gamma}{sec}$$

and,

D_2 = 200 mrem/hr, where a = 7.0 inches = 17.8cm

which gives:

$$S_o = \frac{0.2 \text{ rem/hr } (4\pi)(17.8^2)}{(2.3x10^{-6})(1))(6.1x10^{-4})}$$

$$S_o = 5.7 \times 10^{10} \gamma/sec.$$

The dose rates at the surface of the top or bottom of the cask and at 3 and 6 feet from the surfaces are shown in Figure 5.4.2-1 for various source strengths.

5.4.3 Accident Conditions

The cask shielding must be able to limit the dose rate to 1 Rem/hr at three feet from any surface of the cask after the cask goes through the accident conditions (i.e. fire, 30 foot drop test, etc.).

As the cask shielding is not reduced under the accident conditions, radiation levels will be the same before and after the aacident. This gives a dose of 5.7mrem/hr at 3 feet from the surface of the cask, a factor of 175 times below

$$(\frac{1000 \text{ mrem/hr}}{5.7 \text{ mrem/hr}} = 175)$$

the dose rate limit of 1.0 Rem/hr 3 feet from the package surface after an accident.

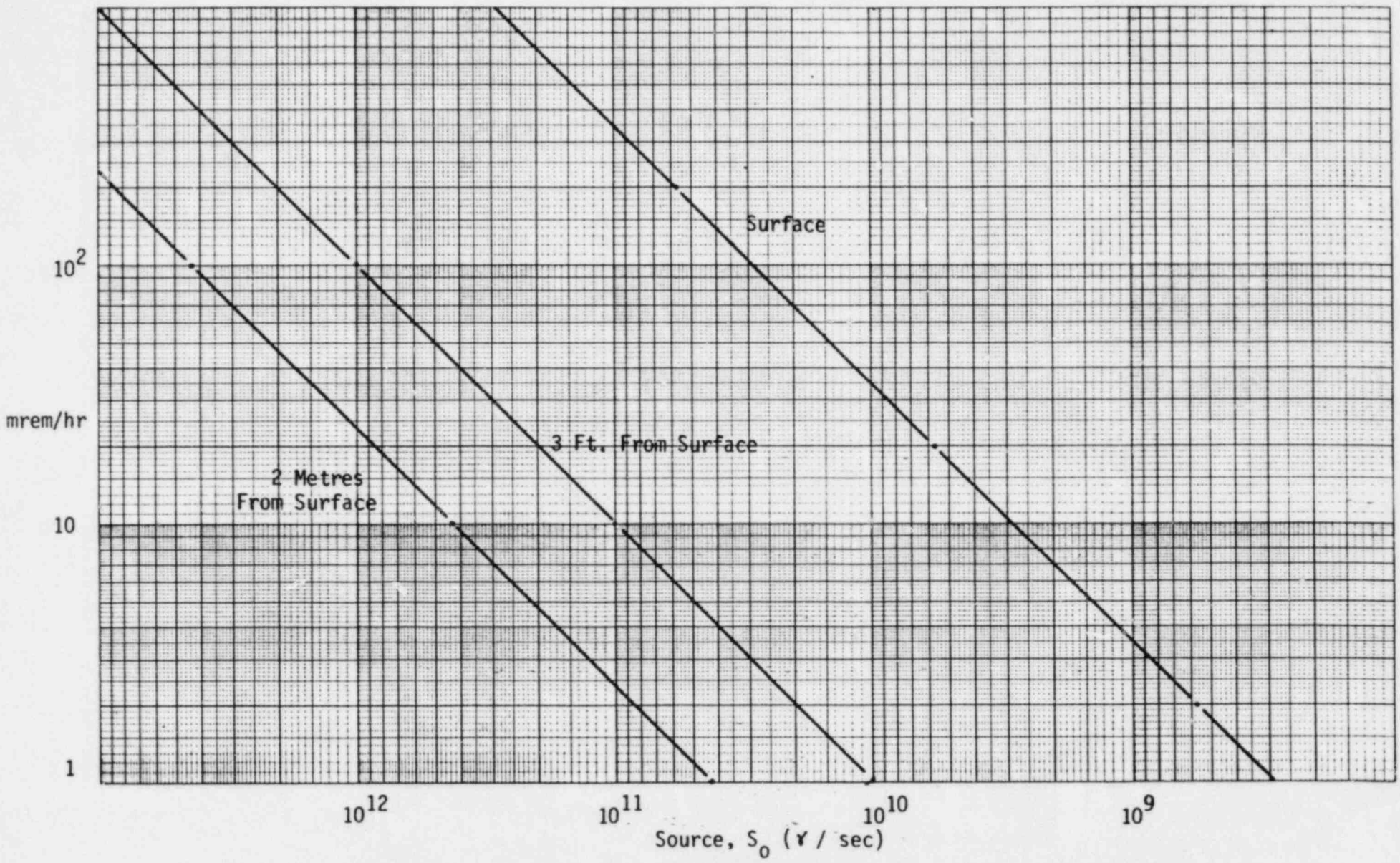

FIGURE 5.4.2-1 Dose Rate vs. Source Strength- Top/Bottom of Cask

6.0 CRITICALITY EVALUATION

The section is not applicable to the 8-120B cask as it is not intended to be used to transport fissile constituents.

7.0 OPERATING PROCEDURE

This chapter describes the general procedure for loading and unloading of the CNS 8-120B Cask.

7.1 Procedure for Loading the Package

7.1.1 Loosen and disconnect ratchet binders from upper overpack.

7.1.2 Using suitable lifting equipment, remove upper overpack assembly. Care should be exercised to prevent damage to overpack during handling and storage.

7.1.3 Determine if cask must be removed fom trailer for loading purposes. To remove cask from trailer:

7.1.3.1 Disconnect cask to trailer tie-down equipment.

7.1.3.2 Attach cask lifting ears and torque bolts to 200 ft-lbs ± 20 ft-lbs lubricated.

7.1.3.3 Using suitable lifting equipmemt, remove cask from trailer and the lower overpack and place cask in level loading position.

7.1.4 Loosen and remove the thirty-two (32) bolts which secure the primary lid to cask body.

7.1.5 Remove primary lid from cask body using suitable lifting equipment. Care should be taken during lid handling operations to prevent damage to cask or lid seal surfaces.

7.1.6 Inspect cask interior for damage or loose materials. Clean and inspect seal surfaces. Replace seals when defects or damage is noted which may preclude proper sealing.

NOTE: When seals are replaced verification leak testing is required as specified in section 8.2.

7.1.7 Place disposable liner, drums or other containers into cask, shoring or bracing as necessary to restrict movement of contents during normal transport.

7.1.8 Clean and inspect lid seal surfaces.

7.1.9 Replace and secure lid to cask body using the thirty-two (32) lid bolts torqued to 500 ft-lbs ± 50 ft-lbs lubricated.

7.1.10 If cask has been removed from trailer, proceed as follows to return cask to trailer:

7.1.10.1 Using suitable lifting equipment, lift and position cask into lower overpack on trailer in the same orientation as removed.

7.1.10.2 Unbolt and remove cask lifting ears.

7.1.10.3 Reconnect cask to trailer using tie-down equipment.

7.1.11 Using suitable lifting equipment, lift, inspect for damage and install upper overpack assembly on cask in the same orientation as removed.

7.1.12 Attach and hand tighten ratchet binders between upper and lower overpack assemblies.

7.1.13 Cover lift lugs as required.

7.1.14 Install anti-tamper seals to the designated ratchet binder.

7.1.15 Inspect cask for proper placards and labeling.

7.1.16 Complete required shipping documentation.

7.2 Procedure for Unloading Package

7.2.1 Move the unopened package to an appropriate level unloading area.

7.2.2 Perform an external examination of the unopened package. Record any significant observations.

7.2.3 Remove anti-tamper seals.

7.2.4 Loosen and disconnect ratchet binders from the upper overpack assembly.

7.2.5 Remove upper overpack assembly using caution not to damage the cask or overpack assembly.

7.2.6 If cask must be removed from trailer, refer to steps 7.1.3.

7.2.7 Loosen and remove the thirty-two (32) primary lid bolts.

7.2.8 Using suitable lifting equipment, lift lid from cask using care during handling operations to prevent damage to cask and lid seal surfaces.

7.2.9 Remove contents to disposal area.

7.2.10 Assemble package in accordance with loading procedure (7.1.8 through 7.1.16).

7.3 Preparation of Empty Packages for Transport

The model CNS 8-120B cask requires no special transport preparation when empty. Loading and unloading procedures outlined in this chapter shall be followed as applicable for empty packages.

NOTE: Each package user will be supplied with a complete, detailed operating procedure for use with the package.

8.0 ACCEPTANCE TESTS AND MAINTENANCE

8.1 Acceptance Test

Prior to the first use of the CNS 8-120B package, the following tests and evaluations will be performed.

8.1.1 Visual Examination

The package will be examined visually for any adverse conditions in materials or fabrication using applicable codes, standards and drawings.

8.1.2 Structural Tests

8.1.2.1 Testing of the lifting devices attached to the package, primary and secondary lids shall be accomplished to meet the standards of 10 CFR 71.31.

8.1.2.2 Visual examinations during fabrication will identify the integrity of structural welding and proper fabrication techniques.

8.1.3 Leak Tests(1)

The package will be subjected to a Fabrication Verification leak test prior to first use. This test will provide an evaluation of all seals for the containment boundary. Test procedure sensitivity will be established for detection of any leak greater than 1×10^{-7} atm.cm^3/sec (Section 4.4.10.). Any condition which results in a leakage rate in excess of 1×10^{-7} atm.cm^3/sec. will be corrected.

---

(1) ANSI N14.5 American National Standard for Leakage Tests on Packages for Shipment of Radioactive Materials.

8.1.4 Component Tests

8.1.4.1 Valves, Rupture Discs, and Fluid Transport Devices The package has no valves or penetrations into the containment boundary except the vent and drain lines. The vent and drain seals are verified during leak testing. No additional component testing will be performed with the exception of mechanical tests performed on materials used in package fabrication.

8.1.4.2 Gaskets Gaskets and seals will be procured and examined in accordance with the CNSI Quality Assurance Program. Leak testing of the package will be the final acceptance for gaskets after installation.

8.1.5 Tests for Shielding Integrity

Shielding integrity of the package will be verified by gamma scan or gamma probe methods to assure package is free of significant voids in the poured lead shield annulus. Voids resulting in shield loss in excess of 10 percent shall not be acceptable.

8.1.6 Thermal Acceptance Tests

No thermal acceptance testing will be performed on the CNS 8-120B package. Refer to the Thermal Evaluation, Section 3.0 of this report.

8.2 Maintenance Program

CNSI is committed to an ongoing preventative maintenance program for all shipping packages. The 8-120B package will be subjected to routine and periodic inspections and tests as outlined in this section and CNSI approved procedures.

8.2.1 Structural and Pressure Tests

Routine visual examinations will be performed to detect damage or defects significant to package condition. Exterior stencils, nameplates, seals and bolts will be verified in place.

8.2.2 Leak Tests (1)

8.2.2.1 Periodic leak testing shall be performed after the third use and within a 12-month period prior to use. The leak test procedure shall be equivalent to the Fabrication Verification Test with adequate sensitivity to detect a leak exceeding 1×10^{-7} atm.cm^3/sec. Conditions exceeding a leak rate as stated shall be corrected prior to continued use of package.

8.2.2.2 Assembly verification leak testing will be accomplished as part of preparation for each actual shipment when package is used for greater than Type A quantities or each three months whichever occurs first. This test will verify proper assembly procedures have been met and closure lids have been properly installed. The procedure for assembly verification leak test will pressurize the area through the installed test ports, testing the outer O-ring of each lid. The leak test sensitivity shall be adequate to detect any leak greater than 1×10^{-3} atm.cm^3/sec.

(1) ANSI N14.5 American National Standard for Leakage Tests on Packages for Shipment of Radioactive Materials.

8.2.3 Subsystem Maintenance

The CNS 8-120B package contains no subsystem assemblies.

8.2.4 Valves, Rupture Discs, and Gaskets on Containment Vessel

As a minimum, all seals will be replaced prior to the annual leak test. specified in 8.2.2.1.

8.2.5 Shielding

No shielding tests will be performed after acceptance testing unless damage has required repairs affecting shield integrity. Any shield testing which might be required would be in accordance with the original criteria specified in Section 8.1.5.